IN VIVO DISSECTION OF THE ROLE OF THE UBIQUITIN PROTEASOME SYSTEM IN THE PATHOGENESIS OF PRION DISEASE

A thesis submitted to the University College London for the degree of Doctor of Philosophy

Julie Moonga BSc (Hons), MSc

Institute of Neurology

University College London

London

DECLARATION STATEMENT

I, Julie Moonga declare that the work presented in this thesis in my own. Where information has been derived from other sources, I confirm that this has been indicated in the thesis.

Julie Moonga

ACKNOWLEDGEMENTS

I would like to extend my heartfelt thanks to my primary supervisor Professor Sarah Tabrizi. Without her tireless efforts, extraordinary knowledge and guidance, this project would not have been possible. Also, my sincere thanks to Dr. Ralph Andre who co-supervised this project, and coordinated my day-to-day experiments. Thank you for proofreading my thesis.

I would like to thank the BSF staff at Wakefield Street for assisting me with my animal colony and animal experiments. Special thanks are due to the Histology Team of the MRC Prion Unit for training me and allowing me to use their facility. I would like to thank some present and past members of the Tabrizi lab "Team Tabrizi" Dr. Rob Goold, Dr. Pela Deriziotis, Dr. Kerry Kerrington, Anna Magnusson, Dr. Samira Rabbanian, Chris McKinnon, Ulrike Traeger and Lucianne Dobson for their assistance and inspiration.

Throughout the course of my PhD there have been a core group of people who helped me stay focused, I could not have managed this far without their support. I would like to thank my friend and mentor Dr. Emmanuel Asante, who was instrumental and encouraging in my moving forward with this PhD when things were tough. Thank you for your input and for proofreading my thesis. Doctor Oke Avwenagha, for her words of wisdom when I needed a listening ear.

I would also like to acknowledge, the people who have made the biggest impact on my scientific career. Professor Terry Ann Krulwich, for encouraging me to follow a career in neuroscience. Professor Stephen Salton, my former supervisor for many years of support and encouragement.

I owe everything to my dear husband Choongo, for his unyielding love and support.

“Character cannot be developed in ease and quiet. Only through experience of trial and suffering can the soul be strengthened, ambition inspired, and success achieved”.

Helen Keller

For my mother

À quoi sert la vie si les enfants n'en font pas plus que leurs pères.

To Noli,

ABSTRACT

Prion diseases comprise a group of fatal neurodegenerative disorders caused by the conformational re-arrangement of a normal host-encoded prion protein, PrP^{C}, to an abnormal infectious isoform, PrP^{Sc}. Currently, the precise cellular mechanism(s) of prion-mediated neurodegeneration remain unclear. However, increasing evidence suggests a role for the ubiquitin proteasome system (UPS) in prion disease pathogenesis, with a direct functional impairment of the 26S proteasome leading to the accumulation of UPS substrates in the brains of prion-infected mice. The UPS functions to regulate the targeted degradation of intracellular proteins and maintain cellular proteostasis. Alterations in proteasome proteolysis have been shown to contribute to the build up of proteins associated with aging and dysregulation of the UPS has been linked to several neurodegenerative diseases. The principal aim of this thesis was to characterise the progression of UPS dysfunction *in vivo* in the brains of prion-infected mice using a ubiquitin-GFP reporter mouse model. Using the Ub^{G76V}-GFP transgenic mouse model, UPS dysfunction was observed in the brain early in the prion disease incubation period, before key hallmarks of disease pathology were observed. The accumulation of Ub-GFP reporter coincided with markers of prion disease neuropathology, such as PrP^{Sc} deposition and extensive astrogliosis. The majority of cells in which the Ub-GFP reporter was observed in the thalamus appeared to be astrocytes, suggesting that altered proteolysis and reactive astrocyte pathology may be linked. Ubiquitin levels were increased significantly in the brains of prion infected mice, while 26S proteasome peptidase activity was reduced. Behavioural abnormalities and motor skills deficits were also observed in prion-infected Ub^{G76V}-GFP mice, which may correlate to neuronal loss and/or synaptic dysfunction associated with impairment of the UPS machinery. Collectively, the data presented in this thesis provide evidence of an early and potentially important role for UPS dysfunction in prion disease pathogenesis.

Table of contents

List of Figures

List of Tables

ABREVIATION LIST

°C – degrees Celsius

Å – angstrom

Ab – antibody

Aβ – amyloid-β peptide

AD – Alzheimer's disease

AEBSF – 4-(2-aminoethyl) benzenesulphonyl fluoride

AF – Alexa Fluor

ALS – amyotrophic lateral sclerosis

AP – alkaline phosphate

APOE – apolipoprotein E

APP – amyloid precursor protein

Ar – argon

Atg – autophagy-related

ATP – adenosine 5'-triphosphate

ATPase – ATP hydrolyzing enzyme

BCA – bicinchoninic acid

bp – base pairs

Bip – immunoglobulin heavy chain binding protein

BSA – bovine serum albumin

BSE – bovine spongiform encephalopathy

cDNA – complementary deoxyribose nucleic acid

CHIP – C-terminus of the Hsc70 interacting protein

CJD – Creutzfeld Jakob disease

cm –centimeter

CMV – cytomegalovirus

CNS – central nervous system

CP – core particle

CWD – chronic wasting disease

Da – Dalton

DAB – diaminobenzidine

dH_20 – distilled water

ddH_20 – de-ionised distilled water

DNA – deoxyribonucleic acid

dNTP – deoxynucleotide triphosphates

DRM – detergent resistant membrane

DTT – dithiotreitol

DUB – deubiquitylating enzyme

E1 – ubiquitin activating enzyme

E2 – ubiquitin conjugating enzyme

E3 –ubiquitin ligating enzyme

E4 –chain elongation factor

ECL – enhanced chemiluminescence

EDTA – ethylene diamine tetra-acetic acid

EPOX – epoxomicin

ER – endoplasmic reticulum

ERAD – ER associated degradation

FCS – fetal calf serum

FFI – Fatal familial insomnia

FITC – fluorescein isothiocyanate

FVB – Friend Virus B-type (mouse)

FP – fluorescent protein

FSE – Feline spongiform encephalopathy

g – gravity (acceleration due to)

g – gram

GFAP – glial fibrillary acidic protein

GFP – green fluorescent protein

grp – glucose-regulated protein

GSS – Gerstmann-Straussler-Scheinker syndrome

hr – hour(s)

HD – Huntington's disease

HEPES – 4-(2-hydroxyethyl)-1-piperazineethanesulfonic acid

HeNe – helium-neon

HRP – horseradish peroxidase

Hsp – heat shock protein

Hsc70 – heat shock chaperone 70

Hz – hertz

IHC – immunohistochemistry

IPD – inherited prion disease

kDa – kiloDalton

KD – knock-down

KO – knockout

LAC – lactacystin

LTP – long term potentiation

M – molar

M - methionine

mg – milligrams

MHC – major histocompatibility complex

min – minute(s)

ml – milliliters

mm – millimeter

mM – millimolar

mRNA – messenger ribonucleic acid

MW – molecular weight

NCAM – neural cell adhesion molecule

ng - nanogram

NGS – normal goat serum

NMR – nuclear magnetic resonance

ORF – open reading frame

PAGE – polyacrylamide gel electrophoresis

PBS – phosphate buffered saline

PBS-T – phosphate buffered saline with 0.5% Tween

PCR – polymerase chain reaction

PD – Parkinson's disease

PFA – paraformaldehyde

pH – hydrogen ion concentration

PIPLC – phosphatidylinositol-specific phospholipase C

PK – proteinase K

PLL – poly-L-lysine

PMCA – protein misfolding cyclic amplification

PMSF – phenylmethylsuphonyl fluoride

PRNP – prion protein gene (human)

Prnp – prion protein gene (mouse)

PrP – prion protein

PrP^{C} – cellular prion protein

PrP^{Sc} – disease-associated scrapie prion protein

PSD – postsynaptic density

PVDF – polyvinylidene difluoride

RML – Rocky Mountain laboratory

RNA – ribonucleic acid

RNase – ribonuclease

RNAi – RNA interference

ROS – reactive oxygen species

RP – regulatory particle

rpm – revolutions per minute

RT – room temperature

SCA – scrapie cell assay

sCJD – sporadic Creutzfeldt-Jakob disease

SD – standard deviation

SDS – sodium dodecyl sulphate

sec – second(s)

s – second(s

SD – standard deviation

SNAP – synaptosomal-associated protein

SUMO – small ubiquitin-related modifier

SOD – superoxide dismutase

TBS – tris buffered saline

TBS-T – tris-buffered saline with 0.5% Tween-20

TCA – trichloroacetic acid

TME – transmissible mink encephalopathy

TSE – transmissible spongiform encephalopathy

U – units

Ub – ubiquitin

UBP – ubiquitin-specific processing protease

UDP - ubiquitin-like domain

UBL – ubiquitin-like protein

UCH – ubiquitin C-terminal hydrolase

UFD – ubiquitin fusion degradation

UPR – unfolded protein response

UPS – ubiquitin proteasome system

UV – ultraviolet

v/v – volume per volume

vCJD – variant Creutzfeldt-Jakob disease

WT – wild-type

w/v – weight per volume

µg – micrograms

µl – microlitres

µM – micromolar

1 INTRODUCTION

Prion diseases, or transmissible spongiform encephalopathies (TSEs), comprise a group of fatal and untreatable neurodegenerative diseases that affect humans (e.g., Creutzfeldt-Jacob disease) and various other mammals (e.g., bovine spongiform encephalopathy). Prion diseases can be transmitted naturally or experimentally by inoculation, dietary exposure or by contact with infectious tissue. Although a number of prion diseases have been identified in various mammals, including humans, they are believed to be caused by a single protein (Prusiner et *al*., 1991). Prion diseases are grouped together on the basis of their distinct neuropathological characteristics, as well as various clinical symptoms. Mammalian prions are characterized by their ability to cause fatal degeneration of the central nervous system (CNS). Biologically, the normal prion protein, PrP^{C} (C for cellular), undergoes a post-translational conformational change to the abnormal prion protein PrP^{Sc} (Sc denotes scrapie). A major conformational difference exists between the isoforms: PrP^{C} has a predominantly alpha–helical structure, whereas PrP^{Sc} is largely β-sheet in content. The altered structure of the protein is very stable and accumulates in infected tissue causing cell death and tissue damage. Prion diseases have incubation periods (the latent period from point of infection to appearance of the first sign of clinical disease) of months to several years, depending on the type of prion disease.

1.1 Prion diseases in animals

Scrapie, an endemic brain disease of sheep and goats, is known to have been first described in Europe in the 18th century, although it was not known to be infectious at the time. Scrapie is often considered to be the prototypic prion disease. A number of other mammals, however, develop prion diseases, including chronic wasting disease (CWD) in mule deer and elk, and bovine spongiform encephalopathy (BSE) in cattle. The clinical manifestation of animal prion diseases is characterised by the loss of motor control, paralysis and muscle wasting, which together ultimately lead to death. Other animal prion diseases such as transmissible mink encephalopathy (TME) have also been reported (**Table 1.1)**.

1.1.1 Scrapie

Scrapie is a fatal, sub-acute, progressive disease found in sheep and goats. Animals affected by scrapie have been recognised by shepherds for many centuries. The name scrapie corresponds to the unusual condition of the disease where the suffering animal scrapes itself up against walls or fences to alleviate itchiness caused by the disease However, for many years the disorder was regarded as an inherited, degenerative disease of the brain and spinal cord. The various symptoms of scrapie include hyperexcitability, itching, tremors, gait disorders, and loss of fur and skin damage due to scraping. The first report of scrapie being transmissible from one individual sheep to another was in the 1930s, with an incubation period of one year (Cuillé and Chelle, 1936). The transmissibility of scrapie was comprehensively demonstrated in 1943, when Scottish sheep were accidently inoculated against a common virus using infected material from a scrapie sick animal (Gordon, 1946). The natural mode of transmission of scrapie and the relative role of genetic susceptibility to the disease are long-standing areas of research, but are not yet fully understood (Parry, 1979).

1.1.2 Bovine spongiform encephalopathy (BSE)

Bovine spongiform encephalopathy (BSE), also known as “mad cow disease”, is a disease in cattle that was first observed as an epidemic in the 1980s, mainly in the UK (Wilesmith et *al*., 1988; Anderson et *al*., 1996). BSE was reported to be caused by processed animal feed, such as bone meal, containing rendered remains of scrapie affected sheep being fed to dairy cattle (Wilesmith et *al*., 1991; Wilesmith et *al*., 1988). The incidence of BSE assumed epidemic proportion within a very short period of time, with thousands of animals becoming affected (Wilesmith et *al*., 1988; Anderson et *al*., 1996). Since the outbreak in the UK, BSE cases have been reported in many other countries across the world, including the USA, Canada and Japan. The disease is characterised neuropathologically by spongiform change, neuronal loss and astrogliosis, which comprise the core characteristics of prion diseases (Wells et *al*., 1987). Clinical symptoms include changes in temperament, sensitivity to light and sound, as well as various movement disorders. The incidence of BSE in Australia and New Zealand, which are free of scrapie, is similar to that in the UK where scrapie in sheep is endemic. As an alternative explanation, the origins of BSE may lie in some sporadic cases that arose by chance to trigger the epidemic (Weissmann and Aguzzi, 1997).

1.1.3 Chronic wasting disease (CWD)

Chronic wasting disease (CWD) is a scrapie-like disease of unknown origin, found in North American wild and captive cervids, including mule deer, Rocky Mountain elk and captive mule (Sigurdson and Aguzzi, 2006). The disease ranges in duration from a few days to a few weeks from the initial onset of symptoms, which can include weight loss and excessive drinking (Williams, 2005; Williams and Miller, 2002). Experimentally, evidence confirms the presence of neuronal vacuolation (William and Young, 1980), aggregation of PrP in the CNS, as well as lymphoid tissues damage in affected animals (Browning et *al*., 2004). It is thought to be transmitted in a manner similar to scrapie, via saliva and blood

(Miller and William 2003; Mathiason et *a*l., 2006). However, the route of transmission is not clear and there is no evidence for CWD transmission to humans.

1.1.4 Transmissible mink encephalopathy (TME)

Transmissible mink encephalopathy (TME) is an animal prion disease seen in farmed mink. It has similar characteristics to the CWD found in elk and mule deer, and its occurrence is thought to have originated from being fed the meat of scrapie-infected sheep (Marsh et *al*., 1991; Marsh, 1992). Symptoms of TME include loss of muscle coordination and aggression. Following onset, the animal dies within a few weeks. Recent studies have reported similarities between TME and BSE in a mouse model (Baron et *al*., 2007).

1.1.5 Other animal prion diseases

Other animal prion diseases such as feline spongiform encephalopathy (FSE) have been reported. FSE has been reported in domestic and captive wild cats, predominantly in the UK (Leggett et *al*., 1990). Other TSEs have been reported in species such as kudu. Similarly to FSE, these diseases have been reported to exert similar characteristics to BSE and may have been caused by a BSE-like strain transmitted through feeding on contaminated material from cattle (Bruce et *al*., 1994; Collinge et *al*., 1996b).

Table 1.1 Prion diseases in animals

Host	Disease
Sheep and Goat	Scrapie
Mule deer, elk	Chronic Wasting Disease
Cattle	Bovine Spongiform Encephalopathy
Mink	Transmissible Mink Encephalopathy
Cat	Feline Spongiform Encephalopathy
Tiger, Cheater, Kudu	Other Transmissible Spongiform Encephalopathy

1.2 Human prion diseases

Humans are susceptible to several prion diseases, amongst which are Creutzfeldt-Jakob disease (CJD), Gerstmann-Straussler-Scheinker disease (GSS), fatal familial insomnia (FFI) and kuru (**Table 1.2**). Human prion diseases are rare neurodegenerative disorders, but are invariably fatal. They are characterised by the accumulation of aggregated and abnormally folded protease resistant PrP^{Sc}. Most manifestations of prion diseases in humans share a common non-inflammatory pathological process that is largely restricted to the CNS and includes deposits of PrP^{Sc} in the form of diffuse plaques (**Figure 1.3**).

General neuropathological characteristics of human prion disease include spongiform degeneration, gliosis and severe neuronal loss (Collinge and Palmer, 1992), which ultimately lead the brain to degenerate resulting in a progressive decline in cognitive and motor function. Human prion diseases have been classified as occurring as inherited, sporadic and acquired forms, with a further sub-classification according to certain

molecular criteria (Wadsworth and Collinge, 2007). Most cases of human prion disease occur sporadically, but hereditary, iatrogenic and dietary transmission can also occur. There has been a considerable interest in the disease following the identification of new variant (v)CJD, and the demonstration through transmission studies that vCJD is caused by the same prion strain as that causing BSE (Weissmann and Aguzzi, 1997; Mallucci and Collinge, 2004). With recent reports of blood-borne transmission (Wroe and Pal, 2006), prion diseases remain in the spotlight due to public health concerns. Particular attention has focused on the development of therapeutic agents and a diagnostic test (Miller and Williams, 2003; Mathiason et *al*., 2006).

1.2.1 Sporadic Creutzfeldt-Jakob disease (sCJD)

Sporadic CJD (sCJD) is a rapidly progressive multifocal dementing disease with neurological features that include cerebellar ataxia, neuropsychiatric symptoms and myoclonus (Brown et *al*., 1984; Collins et *al*., 2006). sCJD makes up 85% of all recognized human prion disease, with an incidence of about 1.2 per million per year and an apparently random distribution (Caramelli et *al*., 2006). This is possibly an underestimate, since prion disease can sometimes be misdiagnosed and confused with other neurological disorders. Onset usually occurs from 45-75 years of age, with a peak age of onset between 60-65 years. Rapid clinical progression usually leads to death within weeks or months. The median duration of illness in sCJD is four months with, 14 % of cases having illness duration of a year or more, and 5 % of cases surviving greater than twenty years. Possible causes of sCJD are spontaneous production of PrP^{Sc} via rare stochastic events, somatic mutation of the PrP-encoding gene (*PRNP*), or some unidentified environmental exposure. Reports on a two-case control study suggested prior surgery as a risk factor for sCJD, therefore raising the possibility of some sCJD being classified as an acquired illness (Collins et *al*., 1999; Ward et *al*., 2002).

Much clinical heterogeneity exists within sCJD, especially at symptom onset where particular focal deficits may be present. For instance, an isolated progressive cerebellar syndrome is observed in approximately 10% of cases, or an isolated progressive visual disturbance culminating with cortical blindness known as the Heidenhain's variant is also sometimes reported (Collinge et *al*., 1996; Hill et *al*., 1999). The various clinical phenotypes associated with sCJD make it prone to misdiagnosis. The most difficult differential diagnosis of sCJD is the rapidly progressive feature, which can also be a characteristic of Alzheimer's disease (AD), with cases misdiagnosed as sCJD in several series (Zerr et *al*., 2000; Tschampa et *al*., 2001). Definitive diagnosis of sCJD is achieved through neuropathological examination of the brain at autopsy. Cerebral imaging is important in excluding other diagnoses, but more recently imaging analysis of sCJD revealed a combination of cortical and basal ganglia signal change on magnetic resonance imaging (MRI) to have a diagnosis sensitivity of greater than 90% (Young et *al*., 2005). MRI is able to reveal changes in the density of deep grey nuclei (Di Rocco, et *al*., 1993). Pathologically, PrP amyloid plaques are not typically present in sCJD. However, diffuse or synaptic PrP^{Sc} deposits are often present. PrP deposits are usually confirmed by immunohistochemistry (IHC) (Budka, 2003). The differential diagnosis also includes dementia with Lewis bodies, lymphoma and multiple cerebral infarctions (Poser et *al*., 1999; Steinhoff et *al*., 2004).

1.2.2 Acquired prion diseases

Acquired prion diseases in humans include kuru, iatrogenic CJD and vCJD. Kuru arose in the mid-20^{th} century as an epidemic disease in localised parts of Papua New Guinea and is associated with exposure to prions during cannibalistic mortuary feasts. Iatrogenic exposure occurs through accidental exposure to human prions through medical or surgical procedures, most frequently through implantation of dura mater or through administration of growth hormone derived from the pituitary glands of human cadavers (Brown et *al*., 1992). Variant CJD has been shown through strain-typing studies and

transmission studies in transgenic mice to be caused by the same prion strain as that causing BSE (Parchi et *al*., 1999; Hill et *al*., 2003).

Kuru

Kuru was the first disorder in humans to be shown to be a transmissible prion disease. It was brought to prominence in the 1950s during pivotal descriptions of the disease in the Fore tribal people in the highlands of Papua New Guinea. It reached epidemic proportions among the Fore ethnic group in the remote mountainous areas in which they lived (Mead et *al*., 2003; Gajdusek et *al*., 1966; Gajdusek et *al*., 1957). Kuru means shivering or trembling in the Fore language, but is also known as "laughing disease" due to the facial grimaces it causes. Kuru is a sub-acute, fatal disease associated with cerebellar degeneration. It is a progressive ataxic syndrome with late dementia and other neurologic impairments. It is neuropathologically characterised by non-inflammatory loss of neurons, gliosis, spongiform change and accumulation of abnormal protease-resistant PrP^{Sc} plaques (Collinge et *al*., 2006; Mead et *al*., 2003).

A remarkable characteristic of kuru is its association with the practice of ritual mortuary cannibalism as a sign of respect for deceased loved ones. The rites involved grinding up the brain into a pale Grey soup, which was heated and eaten as a sign of respect and mourning for deceased relatives (Alpers, 1987). Studies of the Fore tribe showed that kuru transmission was more common amongst women and children, as they ate the highly infectious tissue of the CNS, while the men ate relatively safe tissue such as muscle. Kuru has gradually disappeared over the past 60 years since the practice of mortuary feasting ceased following a ban by the Australian government. Cases of Kuru since this ban in the 1950s represent not new infections, but rather long incubation periods of infections before the ban (Lindenbaum, 1979). That kuru could be a human prion disease was noted on the basis of similarities in the epidemiology, clinical course and histopathological features of kuru and scrapie. This led to the suggestion that the

transmission of kuru should be attempted (Collinge et *al*., 2006), prompting the successful experimental transmission of kuru to non-human primates (Gajdusek et *al*., 1966)

Iatrogenic CJD

Iatrogenic CJD is usually referred to as CJD despite having a prominent cerebral syndrome more reminiscent of kuru (Wadsworth and Collinge, 2007). Transmission may occur by one of a number of routes involving the use of inadequately sterilised neurosurgical instruments due to the high heat resistance of the infectious prion agent. The acquired sources of such infection are through medical procedures such as neurosurgery, growth hormone injections, and dura mater and corneal transplants, as well as the use of gonadotrophin derived from the pituitary gland from cadavers (Brown et *al*., 1992; Brown et *al*., 2000). Contaminated surgical instruments have been shown to remain infectious two years after their reported sterilization (Brown et *al*., 1992; Brown et *al*., 2000). Over a hundred people have acquired CJD from injections of human growth hormone or human gonadotropins, prepared from pooled pituitary glands that inadvertently included glands taken from humans with sCJD (Collinge, 1999; Wadsworth et *al*., 2001; Peden et *al*., 2005).

Variant CJD (vCJD)

In 1995, a new human prion disease in humans resembling CJD, but showing clinically distinct traits, was reported in teenage patients with manifest clinical signs (Will et *al*., 1996; Collinge and Rossor, 1996). Concerns about cross-species transmission of BSE resulting from its epidemic in cattle lead to the establishment in the UK of a National Surveillance Unit for CJD, in 1990. Although no cases were noted during the first four years of monitoring the disease, twenty two cases of vCJD were reported between 1994 and 1997. These patients were typically younger than those with more familiar forms CJD, with prominent early psychiatric and behavioural manifestations, and persistent paraesthesias and dysaesthesias. Cerebellar ataxia uniformly develops and the course of the disease is

prolonged. These new cases of a previously unrecognised prion disease were termed new variant CJD (vCJD) (Collinge et *al*., 1996b; Hill et *al*., 1997; Bruce et *al*., 1997; Asante et *al*., 2002). Although rare, further cases in young adults were discovered, with their post-mortem brain histology showing a consistent and unique neuropathological appearance of prominent and diffuse PrP^{Sc} plaques reminiscent of kuru. Other symptoms of vCJD include anxiety, depression, persistent pain in the limb/face, withdrawal and behavioural changes with progression of the disease, with dementia developing thereafter (Peden et *al*., 2006).

Direct experimental evidence from molecular analysis of prion strain types, transmission studies in transgenic and wild-type mice, and clinical and neuropathological correlates, collectively revealed that the disease was caused by the same prion strain as that causing BSE in cattle (Collinge et *al*., 1996b; Hill et *al*., 1997; Bruce et *al*., 1997; Asante et *al*., 2002). Intracerebral inoculation of BSE material into primates produced a disease pathologically similar to vCJD (Lasmezas et *al*., 1996). In addition, analysis of proteolysis and glycosylation patterns showed identical patterns for BSE and vCJD (Collinge et *al*., 1996a). Therefore, vCJD poses a serious potential public health threat. Evidence that the causative agents of vCJD and BSE were the same, distinct from the patterns associated with sporadic and iatrogenic disease (Hill and Desbruslais, 1997), raised the possibility that an epidemic could occur in the UK and other countries as a result of dietary or other routes of exposure (Ghani et *al*., 1999; Collinge , 1999).

1.2.3 Inherited human prion diseases

Around 10-15 percent of prion diseases in humans are inherited, occurring due to pathogenic autosomal dominant mutations in the *PRNP* gene (Masters et al., 1981; Windl et *al*., 1999). The human *PRNP* gene is located on the short (p) arm of chromosome 20 between the end (terminus) of the arm and position 12, from base pair 4,615,068 to base pair 4,630, 233 (**Figure 1.2**). The first report of *PRNP* mutations described insertion and missense mutations found in families with a prominence of dominant inherited

neurodegenerative disease (Owen et *al*., 1989; Hsiao et *al*., 1989). Over thirty different pathogenic mutations have since been recognised, with point mutations leading to amino acid substitution, a premature stop codon, or insertion of additional octapeptide repeats.

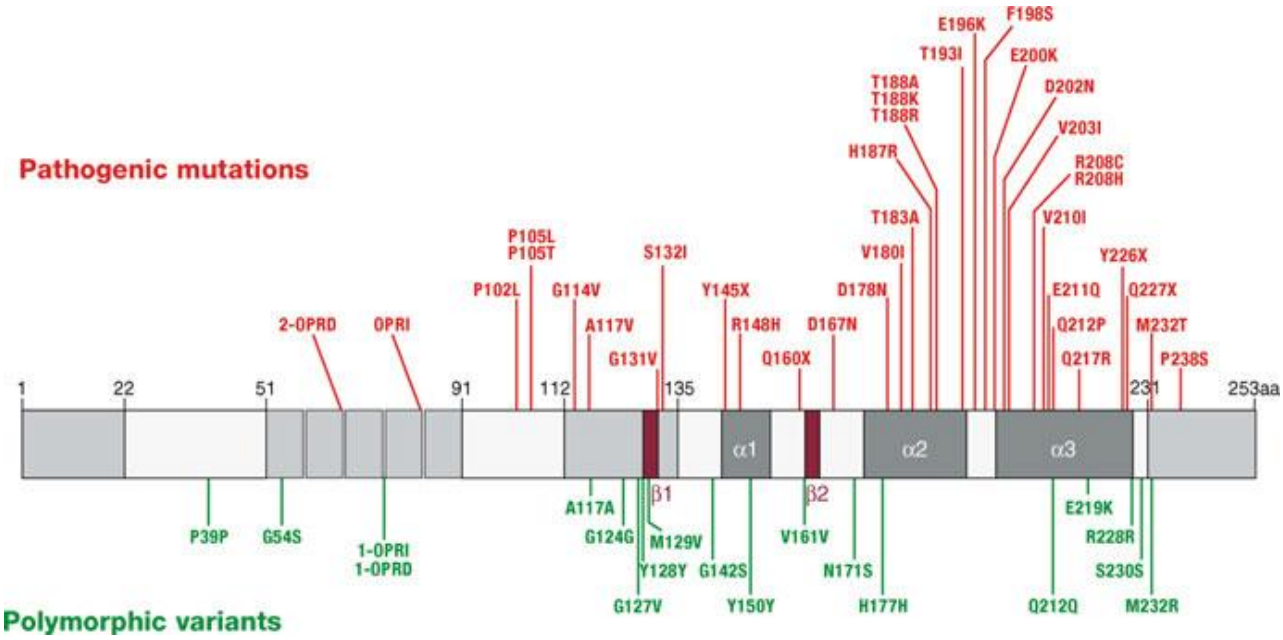

Figure 1.1 Mutations and polymorphisms in the PRNP cDNA.

Diagram of the human prion protein gene showing the octapeptide (51-91). Pathogenic mutations associated with inherited prion disease are shown above the gene (red), while non-synonymous polymorphisms and synonymous polymorphisms are shown below the gene (green). A polymorphism at codon 129 methionine (M) versus valine (V) is a common mutation in European populations, while a polymorphism at codon 219 glutamic acid (E) versus lysine (K) is common in Japanese populations[1].

[1] *Adapted from Llyod et al., 2011.*

Analysis of the *PRNP* gene has allowed for a clear pre-symptomatic diagnosis of inherited prion diseases (Collinge, 2005). There are many clinical symptoms manifested depending on the type of mutation involved, as well as a variety of neuropathological features (Chapman et *al*., 1993; Barbanti et *al*., 1996; Wadsworth et *al*., 2006). It is important to note that a single *PRNP* mutation can elicit different phenotypes, highlighting the role of epigenetic factors in prion disease pathogenesis. Although it is unclear how the *PRNP* mutations cause disease, many hypotheses have been postulated (Peden et *al*., 2004). The most common one is a tendency of the mutated PrP^{C} to spontaneously form abnormal infectious PrP^{Sc} (**Section 1.7**). Other studies report that the pathogenesis of inherited prion diseases may be due to a change in the thermodynamic stability of the mutated PrP (Riek et *al*., 1998; Swietnicki et *al*., 1998).

Familial CJD (fCJD)

Between 10 and 15 percent of persons with CJD have a family history consistent with an autosomal dominant inheritance of the disease. Most of these point mutations, deletions or insertions are found in the coding sequence of the gene for PrP on the short arm of chromosome 20. More than 20 mutations in this gene have been described that are associated with phenotypes mimicking typical CJD or induce distinctive progressive diseases with spongiform changes in the nervous system (Johnson and Gibbs, 1998). In general, familial CJD has an early age of onset and a more protracted course than sporadic disease. The typical electroencephalographic changes are often missing and the 14-3-3 protein is not detected in cerebral fluid in about half of cases (Zerr et *al*., 1998). The neuropathological changes may vary in topographic distribution and in the prevalence of amyloid plaques, but the essential changes of vacuolization of neural cells with gliosis and neuronal loss are generally present. The most common mutation leading to the typical clinical and pathological findings of CJD is at codon 200. Clusters of disease among Libyan Jew in Israel, in a region of Slovakia, and in Chile are all explained by this mutation (Goldfarb et *al*., 1991).

Gerstmann-Straussler Scheinker disease (GSS)

GSS, first described in the early 20th century, is a distinct autosomal dominant prion disease. Phenotypic variability is a major feature with a median range of onset of 50 years of age (range 25-70 years) and a median duration of 4 years (Barbanti et *al*., 1996). The traditional GSS phenotype is a slowly progressive ataxia resulting later in dementia (Kretzschmar et *al*., 1992). Although dementia is less common in GSS, the disease course lasts several years until death. The histological hallmark is the presence of the multicentric amyloid plaques. GSS is most commonly associated with the P102L mutation in the *PRNP* gene, in which a proline is replaced by a leucine residue at position 102. It can also be associated with a valine instead of an alanine residue at position 117 (A117V).

Fatal Familial Insomnia (FFI)

FFI is a progressive and untreatable insomnia disorder, first described in 1986. It is an autosomal dominant inherited sleep disorder, associated with particularly prominent cortical astrocytosis (Collinge and Palmer, 1997). Early thalamic generation of FFI and related disorders produces the distressing symptom complex of progressive insomnia with late dementia. People with this rare disorder have inherited a *PRNP* gene with an asparagine residue instead of aspartic acid encoded at position 178 (D178N).

Table 1.2 Neuropathological criteria for diagnosis of human prion diseases[2].

Prion disease	Criteria
CJD *Sporadic* *Iatrogenic* *Familial*	Spongiform encephalopathy in cerebral and/or cerebellar cortex and/or subcortical grey matter; and/or encephalopathy with PrP immunoreactivity (plaque and/or diffuse synaptic and/or patchy/peri-vacuolar types
vCJD	Spongiform encephalopathy with abundant PrP deposition, particularly multiple fibrillary PrP plaques surrounded by a halo of spongiform vacuoles ('florid') and other PrP plaques, and amorphous pericellular and perivascular PrP deposits especially prominent in the cerebellar molecular layer
GSS	Encephalo(myelo)pathy with multicentric PrP plaques
FFI	Thalamic degeneration with variably spongiform change in the cerebrum
Kuru	Spongiform encephalopathy in the Fore population in Papua New Guinea

1.3 Prion disease genetics

Most inherited human prion diseases, as described above, are associated with mutations in the *PRNP* gene. However, *PRNP* polymorphisms can also influence the conformational change of the protein to influence sporadic and acquired forms of the disease. In particular, homozygosity at amino acid position 129 of human PrP predisposes

[2] ***From the world Health Organisation, http://www.WHO.int***

an individual to acquired and sporadic CJD. Individuals can be either homozygous for methionine (M) or valine (M) at this codon, or heterozygous. The influence of codon 129 is seen, for example, in patients with a D178N mutation and a methionine at position 129 who will go on to develop FFI, whereas family members with a valine at 129 in addition to the D178N mutation will develop familial CJD (Gambetti et *al*., 1995; Goldfarb et *al*., 1992) (**Figure 1.1**).

The codon 129 genotype also has a profound effect on the incubation period of and susceptibility to kuru, with the MM genotype having the shortest incubation period, followed by VV homozygotes (Lee et *al*., 2001). MV heterozygotes are the most resistant genotype, having been reported to show incubation times greater than fifty years (Collinge et *al*., 2006). Several families previously exposed to mortuary feasts have been studied and elderly women survivors who were monitored are predominantly *PRNP* codon 129 heterozygotes (Lee et *al*., 2001; Mead et *al.*, 2003). It is notable that *PRNP* codon 129 homozygotes have been essentially eliminated in the Fore population, as kuru imposed a strong balancing selection. The polymorphism at codon 129 appears to be the main genetic risk factor for vCJD (Mead et *al*., 2009), with every case genotyped being homozygous for methionine at codon 129 apart from a recent case report of vCJD in an individual heterozygous for *PRNP* codon 129 (Kaski et *al*., 2009). This particular case highlights the further potential of clinically silent cases of vCJD in the UK population. There is a marked genetic susceptibility to sCJD, with most cases occurring in homozygotes of methionine (M) or valine (V) at codon 129 of the *PRNP* gene; MV heterozygotes appear to be relatively protected from developing sCJD (Palmer et *al*., 1991). Moreover, genetic studies have revealed polymorphisms upstream of exon 1 of the *PRNP* gene (Mead et *al*., 2001) and in the 5' UTR (Vollmert et *al*., 2006), that are reported to be associated with sCJD.

One possibility of a genetic explanation for these mutations could be that they enhance the rate of spontaneous conversion of PrP^{C} to PrP^{Sc}, permitting disease manifestation within the lifetime of an individual. This suggests that some sporadic incidents of prion disease can be accounted for by somatic mutations of the *PRNP* gene, which is an alternative explanation that these mutations confer susceptibility to infection. It has been known that some breeds of sheep in the UK have specific genotypes that confer resistance to sheep scrapie and these sheep are resistant to BSE as well (Weissmann and Aguzzi, 1997).

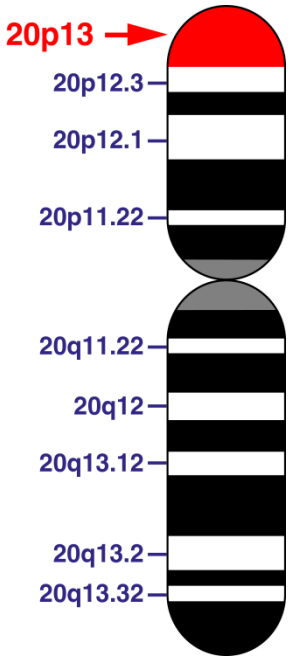

Figure 1.2 The PRNP gene.

The human *PRNP* gene is located on the short (p) arm of chromosome 20 between the end (terminus) of the arm and position 12, from base pair 4,615,068 to base pair 4,630, 233.

1.4 Prion disease neuropathology

Prion diseases are diagnosed clinically at post-mortem by histopathological examination of brain tissue: neuropathological assessment of the structural changes in the CNS has been the mainstay in diagnosis of human prion diseases for many years. Histological analyses of both human and animal tissue shows that prion diseases cause a variety of neurological damage in the CNS resulting in neuronal cell death and brain atrophy (Kubler et *al*., 2003). The neuropathology of human prion diseases is characterised by four features: spongiform change, neuronal loss, astrogliosis and amyloid plaque formation, though the last feature is not always present. However, different prion diseases often have unique neuropathological features (Budka, 2003) (**Figure 1.3, 1.4**). For instance, vCJD is characterised by markedly increased accumulation of PrP^{Sc} in the brain and an accumulation of discrete plaques surrounded by prominent spongiosis (Will et *al*., 1996; Collinge and Rossor, 1996)**.** In most human prion disease cases, the histologically distinctive vacuoles can appear in any layer of the cerebral cortex and may become confluent resulting in substantial distortion of the cortical network cytoarchitecture. Most cases of CJD are usually accompanied by spongiform change in the basal ganglia, thalamus, and cerebellar cortex. However, it is also recognized that these changes are enormously variable both from case to case, and within different parts of the CNS in individual cases.

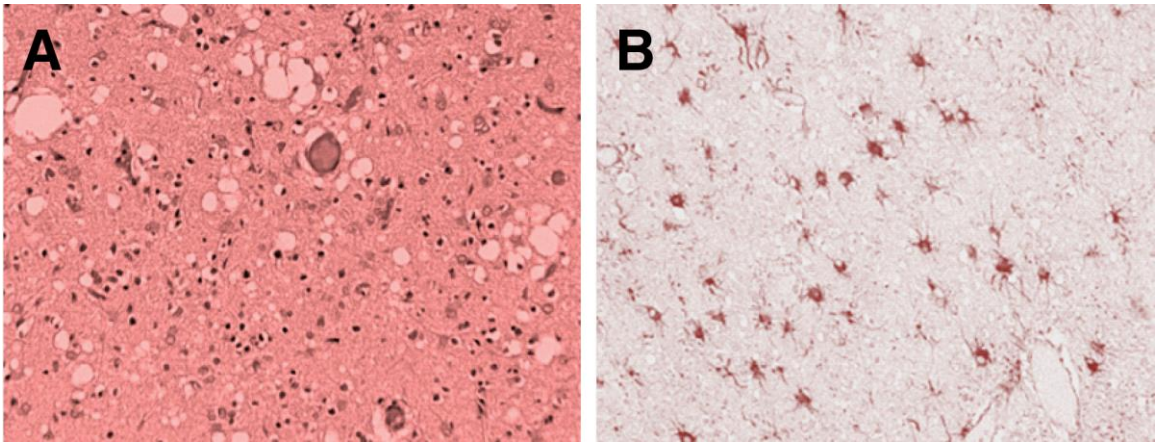

Figure 1.3. Characterisation of disease-related spongiosis and gliosis in human prion disease.

(**A**) Spongiform changes in the cerebellum comprise multiple small vacuoles in the molecular layer which usually do not appear confluent. Spongiform change in most brain regions is accompanied by neuronal loss and gliosis involving both astrocytes and microglia. The tissue was stained for Glial Fibrillary Acidic Protein (GFAP). (**B**) Microglial hypertrophy and hyperplasia occur in a widespread distribution within the CNS in CJD, and microglia are also implicated in the pathogenesis of PrP plaques. Immunocytochemistry studies in both human and animal prion diseases have demonstrated that microglial cells are intimately involved in PrP plaque formation, and may perhaps play a role in the processing of PrP into an amyloid structure. The tissue was stained with haematoxylin and eosin (H&E).

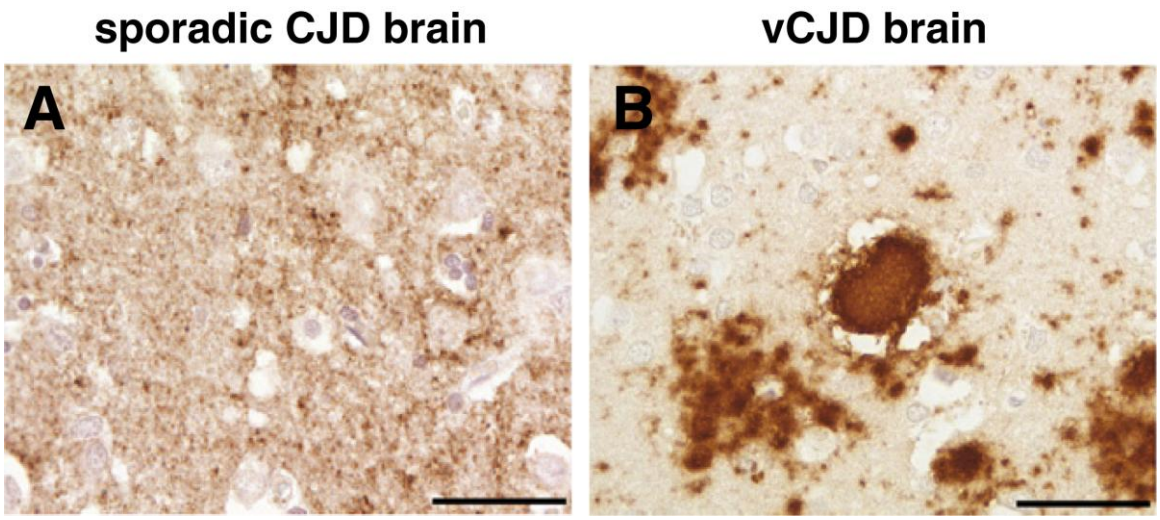

Figure 1.4 Characterisation of disease-related PrP in human prion disease.
Brain sections from sporadic CJD (**A**) and variant CJD (**B**) showing abnormal PrP accumulation following immunohistochemistry using anti-PrP monoclonal antibody, ICSM35. Abnormal PrP deposition in sCJD most commonly present itself as diffuse, synaptic staining, whereas vCJD brain is distinguished by the presence of florid plaques consisting of a round amyloid core surrounded by a ring of spongiform vacuoles[3]. Scale bars: 50 µm.

1.5 Prion disease transmission

Prion disease transmission occurs naturally through peripheral routes, either orally or trans-cutaneously. They can be transmitted through direct inoculation into the brain, or a closely related organ such as the eye (Johnson and Gibbs, 1998). CJD cases occurring after growth hormone injection show transmission via the bloodstream (Brown et *al*., 1992). Scrapie prions injected into limbs are able travel along peripheral nerves to the CNS (Kimberlin and Walker, 1980).

[3] *Adapted from Wadsworth et al., 2010.*

Several lines of evidence suggest an involvement of the lymphoid system in the early stages of acquired prion disease. In particular, the spleen and lymph nodes have been demonstrated to be the first sites of the PrP^{Sc} replication after infection by peripheral routes (Hilton et *al*., 2002). Indeed, splenectomy and other methods that reduce peripheral lymphoid structures delay clinical manifestations following infection (Hilton et *al*., 2002). Diagnostic tests for scrapie based on detecting PrP in tonsillar tissue of infected sheep and goats have been developed (Van Keulen et *al*., 1996; Schreuder et *al*., 1996). The presence of PrP in peripheral lymphoid tissue can be observed on the surface of follicular dendritic cells (Muramoto et *al*., 1992), suggesting that transport by immune cells, such as macrophages or lymphocytes, could be important. However, the role of the immune system in this group of diseases is not well understood (Aguzzi and Calella, 2009; Brandner et *al*., 1999).

In BSE, infected animals showed that infectivity is virtually restricted to the nervous system, with only low infectivity in the lymph nodes and spleen (Brown et *al*., 1994). Muscle tissue seems to be relatively free of infectivity, even though PrP^{C} is expressed in skeletal muscle (DeArmond, 2004; DeArmond et *al*., 1996). In lambs exposed to scrapie-infected flocks, infectivity is first found at about one year of age in the lymphatic tissues and intestines, suggesting transmission by way of the alimentary tract. Infectivity in the brain is found at about two years of age, and infectivity slowly increases in the brain, with resultant spongiform changes and clinical disease during the subsequent year. In studies with mice infected with prions by sub-cutaneous inoculation, infectivity was found first in the lymphatics and spleen, and later in the brain (Eklund et *al*., 1967). Other studies have shown infectivity has been found in the blood of experimentally infected rodents (Kuroda et *al*., 1983). In addition, the presence of differentiated B cells appears important for invasion of the nervous system of the mouse after intraperitoneal inoculation (Klein et *al*., 1997). In all affected species, infectivity is greatest in brain tissue, but is also present in some peripheral tissues. The route of entry of the pathogen, infectivity of blood and tissue

at different stages of the infection, and variations between species and between the routes of inoculation of the nervous system, are central to many of the questions about the risk of prion infection.

1.6 The protein-only hypothesis of prion propagation

The prion protein-only hypothesis asserts that infectivity in prion diseases resides solely in a protein – a proteinaceous infectious particle, or prion. For many years, the nature of the infectious agent causing scrapie was subject to much debate. In particular, the scrapie infectious agent was known to be highly resistant to treatments that modify nucleic acids such as ultraviolet radiation and nucleases, but could be inactivated by exposure to compounds that destroy or denature proteins such as detergents (Alper et *al*., 1967; Alper et *al*., 1978; Prusiner 1982). In the 1960s, a physicist called J.S Griffith first raised the possibility that the material responsible for the transmission of prion diseases could be a protein that is able to replicate itself (Griffith, 1967). This hypothesis required that a protein with the ability to be infectious was purified and characterised. The work of Stanley Prusiner culminated in a partial purification protocol, involving ultracentrifugation and treatment with proteinase K, for a proteinaceous infectious agent (Prusiner et *al*., 1981). Further work by Prusiner and colleagues demonstrated the presence of a disease-associated protein as a component of the infectious agent, rather than a product of the disease (Bolton et *al*., 1982; Prusiner et *al*., 1982; Hope et *al*., 1986; Safar et *al*., 1990). The lack of a nucleic acid genome distinguishes prions from other infectious pathogen such as bacteria, fungi, viruses and viroids (Prusiner, 1982).

The initial purification protocols were adapted by the addition of a sucrose gradient step to isolate and identify the major constituent of infective fractions from hamster brain homogenates (Prusiner et *al*., 1982). Subsequent experimental data showed that the major constituent of infectivity was a 27-30 kDa protease-resistant protein, designated prion protein $(PrP)^{27\text{-}30}$ (**Figure 1.5**). A protein of similar size was identified in uninfected brain

tissue, but unlike the disease-associated protein, it was completely digested by proteinase K treatment (Bolton et *al*., 1982). Experimental evidence confirming that the purified protein was infectious came from the transmission of scrapie into Syrian golden hamsters (Prusiner et *al.*, 1980; Prusiner et *al*., 1982).

The successful purification of PrP led to the identification of its amino acid sequence, allowing further analysis of the protein and the production of anti-PrP antibodies (Bendheim et *al*., 1984). The protease-resistant protein fragment, $PrP^{27\text{-}30}$, was co-purified with scrapie infectivity in hamster brain, which allowed the molecular cloning and sequencing of PrP cDNA (Basler et *al*., 1986). Following the purification of the prion protein, the gene encoding PrP was identified. Amino acid sequencing of the N-terminus $PrP^{27\text{-}30}$ was used to derive a cDNA clone encoding a host protein, which subsequently demonstrated that $PrP^{27\text{-}30}$ was encoded by a chromosomal gene (Oesch et *al*., 1985; Basler et *al*., 1986). Several lines of research suggested that a normal host-encoded protein undergoes a post-translational modification to become an abnormal infectious form. There was no evidence to support the notion that the PrP encoding gene (*PRNP*) undergoes re-arrangement during disease or a genetic basis for alternative splicing of the gene transcript (Basler et *al*., 1986). Other studies demonstrated that the PrP mRNA does not increase during the course of prion disease (Oesch et *al*., 1985). Amino acid sequencing studies of the N-terminus of PrP^{C} and PrP^{Sc} revealed similarities between the two, suggesting that the observed differences are due to post-translational modifications (Turk et *al*., 1988).

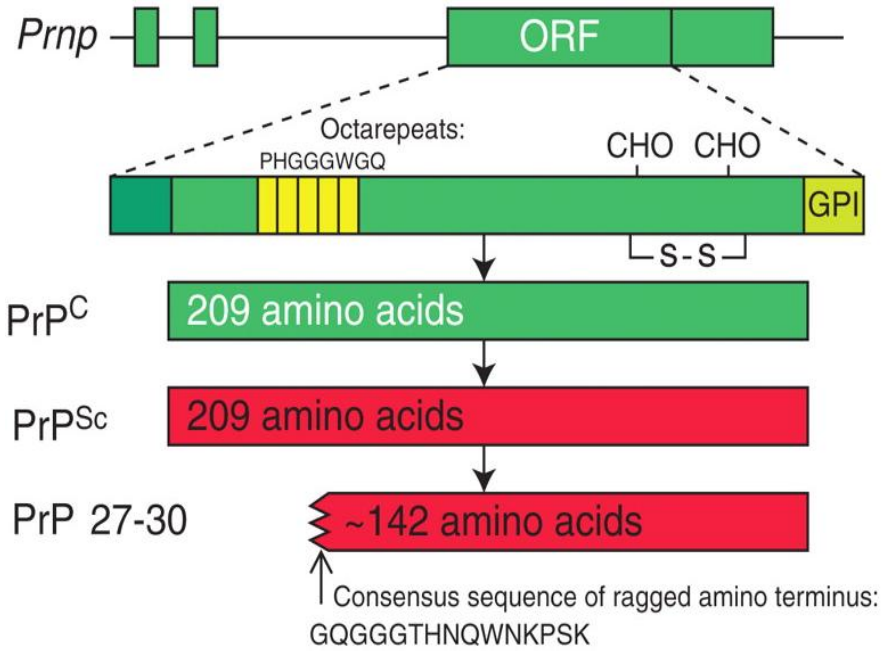

Figure 1.5 Prion protein isoforms.

Bar diagram of the hamster *Prnp* gene and PrP isoforms. The *Prnp* ORF encodes a protein of 254 residues, which is shortened to 209 residues during posttranslational processing. PrP^{sc} is an alternate conformation of PrP^{C} with identical primary structure. Limited PrP^{sc} cleaves the amino terminus and produces PrP 27-30, composed of approximately 142 residues[4].

The protein-only hypothesis was adapted, therefore, to suggest that infectivity arose from a single protein with an identical nucleic acid and amino acid sequence that could give rise to two conformations with exceedingly different properties. One is a normal cellular isoform (PrP^{C}), expressed in normal brain which is readily soluble and protease-sensitive; the other an abnormal scrapie-associated isoform (PrP^{Sc}) that accumulates in infected brain, is poorly soluble and partially protease-resistant, and is associated with infectious activity. Prions are, therefore, encoded by alterations in protein conformation rather than in nucleic acid or amino acid sequence (Cashman, 1997). Further evidence for this comes

[4] *Adapted from Colby and Prusiner, 2011. Cold Spring Harb Perpect Biol.*

from findings that inherited prion diseases are linked to mutations in the *PRNP* gene (Collinge, 2001), indicating that in these cases a genetic disease may be propagated in an infectious way.

The dependence of PrP^{Sc} generation on PrP^{C} has been demonstrated *in vivo* in PrP knockout mice, which are entirely resistant to scrapie (Sailer et *al*., 1994; Mallucci et *al*., 2002). This finding is supported by a study in a cell-free system (Kocisko et *al*., 1994). These observations demonstrate that host-encoded PrP^{C} is necessary for the disease (Pruisner et *al*., 1993). Studies in transgenic mice indicate that mutations in the *PRNP* gene or overexpression of PrP can lead to spontaneous spongiform changes (Prusiner, 1996). The protein-only hypothesis is now the most widely accepted model of prion propagation, and forms the basis of work to characterise the replication and transmission of the prion disease infectious agent (Prusiner, 1998; Abid and Soto, 2006; Tatzelt and Schatzl, 2007; Wadsworth and Collinge, 2007).

Unequivocal proof of the protein-only hypothesis is frequently suggested to reside in demonstrating the *in vitro* generation of infectious prions solely from PrP. *In vitro* replication of PrP^{Sc} was first demonstrated using an amplification system that used radio-labelled PrP^{C} (Kocisko et *al*., 1994), but this method was not successful in transmission barrier studies (Bessen et *al*., 1995; Raymond et *al*., 1997). A more recent method of amplification, a protein misfolding cycling amplification (PMCA) assay, has proven more successful (Castilla et *al*., 2005). Experiments using PMCA have been efficient in regards to amplification and infectivity, and have helped to demonstrate that infectious material can be produced in a cell-free system, leading to a scrapie–like disease when inoculated into mice (Supattapone, 2004; Castilla et *al*., 2005). In addition, it has been reported that synthetic prions that polymerise into fibrils *in vitro* have been shown to be infectious *in vivo* (Legname et *al*., 2004).

1.7 The prion protein (PrP)

1.7.1 PrP^C structure and function

The normal prion protein, PrP^C, is a host-encoded 250 amino acid glycoprotein that is widely expressed throughout the body. This 30-35-kDa protein is found abundantly in the neurons and glia of the brain, as well as in several peripheral tissues and leukocytes (Dodelet and Cashman, 1998; Harris, 1999; Aguzzi and Polymenidou, 2004). There is slight variation in the exact size of the protein in different species due to the number of octapeptide repeat region in the N-terminus of the protein (Stahl et *al*., 1990; Stahl et *al*., 1987). Most PrP^C molecules are normally localized on the cell surface, where they are attached to the lipid bilayer via a C-terminal, glycosylphosphatidylinositol (GPI) anchor (Stahl et *al*., 1990; Stahl et *al*., 1987).

Studies by Fourier Transform Infrared Spectroscopy (FTIR) and circular dichroism have demonstrated that PrP^C is predominantly α-helical as compared to PrP^{Sc}, which is rich in β-sheet (Gasset et *al*., 1993; Pan et *al*., 1993). It contains a globular domain with three alpha-helices and a two-stranded antiparallel beta-sheet, an NH2 terminal tail, and a short COOH terminal tail (Riek et *al*, 1997). PrP^C is divided into two distinct regions: one N-terminal region that is flexible and contains an octapeptide repeat domain and a C-terminal region which comprise 3- alpha helical structures and two anti-parallel beta sheet structures. The C-terminal domain of PrP^C is folded into alpha-helices that are stabilized by a single disulphide bond and nuclear magnetic resonance (NMR) revealed that it is monomeric (Riek et *al*, 1996). Studies into the C-terminus of PrP revealed a crystal structure that has three alpha-helices and a short anti-parallel beta-sheet (Knaus et *al*., 2001; Haire et *al*., 2004; Eghiaian et *al*., 2004). The octapeptide repeats have been shown to have tight binding sites for Cu^{2+} and Zn^{2+}, suggesting possible regulatory and signalling properties (Riek et *al*., 1998; Hosszu et *al*., 1999; Jackson et *al*., 2001). The N-terminus of

PrP^C contains an octapeptide repeat, which is thought to be involved in the cellular function of PrP^C.

Comparing the sequences of PrP^C from various mammalian species demonstrates that it is highly conserved (Damberger et *al*., 1995). However, its precise cellular function remains unknown. Possible suggestions have included copper binding, signal transduction, regulation of immune responses, synaptic functions and roles in apoptosis (Seidel and Engelhard, 2011; Haigh et *al*., 2010). As mentioned above, the N-terminal region of PrP^C containing the octapeptide repeats represents a high-affinity binding site for copper ions properties (Riek et *al*., 1998; Hosszu et *al*., 1999; Jackson et *al*., 2001). In addition, recent evidence suggests that copper imbalance is an early change during infection, suggesting PrP may have a role in copper transport or metabolism. PrP^C has been described to be a positive regulator of neural precursor proliferation during developmental and adult mammalian neurogenesis. Several lines of evidence have also suggested that PrP^C may exert a cytoprotective activity, particularly against internal or environmental stresses that initiate an apoptotic cascade (Roucou and LeBlanc, 2005; Roucou et *al*., 2004). Various studies suggest that PrP^C can activate transmembrane signaling pathways involved in several different phenomena, including neuronal survival, neurite outgrowth, and neurotoxicity (Westergard et *al*., 2007).

The biosynthetic pathway followed by PrP^C is similar to that of other membrane and secreted proteins, involving synthesis on ER-attached ribosomes, transit to the Golgi, followed by delivery to the cell surface. Since PrP^C is a GPI-anchored protein, the entire polypeptide chain is located on the extracytoplasmic face of the lipid bilayer, which is known to serve as molecular scaffolds for signal transduction (Tsui-Pierchala et *al*., 2002; Taylor and Hooper, 2007). Some of the protein is transferred to clathrin-coated pits where it is subject to constitutive endocytosis and recycling (Sunyach et *al*., 2003; Naslavsky et *al*., 1996; Shyng et *al*., 1994). PrP^C can be produced in three topological conformations: the normal plasma membrane GPI-anchored PrP^C; the transmembrane C-trans form (^{Ctm} PrP),

for which the C-terminus part is in the ER lumen; and a N-trans membrane (^{Ntm}PrP) for which the NH2-terminus is in the lumen (Crozet et *al*., 2008).

1.7.2 PrP^{Sc} structure

Studies comparing PrP^{Sc} and PrP^{C} reveal marked differences in their respective tertiary structure, with PrP^{Sc} containing a much higher percentage of β-pleated-sheet regions (~45%) as compared to PrP^{C} (~3%) (Gasset et *al*., 1993; Pan et *al*., 1993; DeArmond and Prusiner, 1995). This difference in tertiary structure causes PrP^{Sc} to have a high tendency to form aggregated, insoluble deposits (Prusiner, 1996; Riek et *al*., 1996). PrP^{Sc} is insoluble in non-ionic detergents and has a partial resistance to proteases. Only its N-terminus is readily cleaved, leaving a protease resistant core that retains infectivity (Riesner, 2003). The propensity of PrP^{Sc} to form aggregates correlates with its resistance to proteinase K digestion (Prusiner, 1996; Riek et *al*., 1996).

Distinguishing PrP^{Sc} from PrP^{C} relies on the differential mobility of the protein on SDS-PAGE and the partial resistance of PrP^{Sc} to proteinase K digestion (Parchi et *al*., 1996; Collinge et *al*., 1996b). Different prion strains, moreover, can exhibit different levels of proteinase K-resistance (Bessen and Marsh, 1994; Bessen and Marsh, 1992) and PrP^{Sc} glycosylation patterns (Khalili-Shirazi et *al*., 2005). For example, distinct ratios of the PrP^{Sc} domains glycoforms (di-, mono- and unglycosylated) have been reported when comparing several prion strains, and is clearly demonstrated by comparisons between the PrP^{Sc} associated with sCJD and vCJD prions in humans (Collinge et *al*., 1996a; Hill et *al*., 2003) (**Figure 1.6**). The C-terminus of PrP^{Sc} can be digested by cathepsin D, which liberates its GPI anchor, but leaves it retaining prion infectivity (Lewis et *al*., 2006). Indeed, it has been shown in transgenic mice expressing PrP lacking a GPI anchor can propagate prions (Chesebro et *al*., 2005), thereby suggesting that the GPI anchor is not a prerequisite component of the infectious prion. Unlike PrP^{C}, which is readily cleaved from membranes by treatment with phosphatidylinositol-specific phospholipase C (PIPLC) (Stahl et *al*., 1987),

PrP^{Sc} is resistant to such treatment (Caughey et *al*., 1990; Borchelt et *al*., 1993). This suggests a conformational change preventing accessibility of PIPLC.

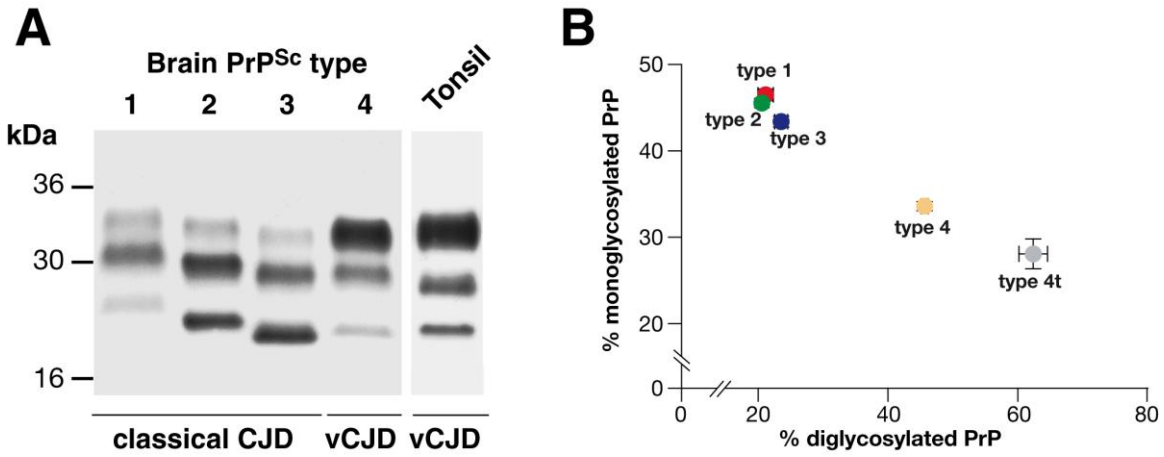

Figure 1.6 Distinct prion strain of Creutzfeldt-Jakob disease.

(**A**) Immunoblot of proteinase K digested brain homogenates using anti-PrP monoclonal antibody 3F4 showing PrP^{Sc} types 1-4 in human brain according to the London classification Types 1-3 PrP^{Sc} are seen in the brain of classical forms of CJD (either sporadic or iatrogenic CJD) and kuru, while type 4 PrP^{Sc} is uniquely seen in vCJD brain. (**B**) Relative proportion of di- and monoglycosylated PrP^{Sc} glycoforms following partial digestion with proteinase (K) in tonsil. The vCJD has a peripheral pathogenesis distinct from classical forms of CJD, with a prominent and uniform involvement of lymphoreticular tissues[5].

Further insights into the native conformation of PrP^{Sc} are hindered by its insolubility and aggregation state. Amyloid, defined as extracellular proteinaceous deposits with a cross β-sheet structure, is readily detected by reagents such as Congo Red (Pedersen et *al*., 2010). Protease resistant PrP^{Sc} has been shown *in vivo* to re-arrange into amyloids rods, which stain with the dye Congo red and show green-gold birefringence, the typical presentation of amyloids (Prusiner et *al*., 1983). PrP^{Sc} deposits can vary in size and morphology, and amyloid plaques have been identified in the brain tissue of animals

[5] *Adapted from Wadsworth and Collinge, 2011*

infected with scrapie (Merz et *al*., 1981). Studies using synthetic fibrils have provided clues on human prion diseases (Baskakov et *al*., 2002; Tattum et *al*., 2006). Studies have demonstrated that small PrP oligomers of 14-28 molecules are maximally infective compared to monomeric or fibrillar PrP (Silveira et *al*., 2005).

1.7.3 PrP^{Sc} conversion

The precise mechanisms of the conversion of PrP^{C} to PrP^{Sc} are not fully understood. PrP^{Sc} is suggested to act as a seed, providing a template for its own conversion from PrP^{C}. As this conversion event proceeds, small soluble aggregates are formed, which then become large insoluble deposits as the disease progresses. These PrP^{Sc} deposits accumulate in neural cells leading to disruption of their function and cell death. Current models propose that PrP fluctuates between its native PrP^{C} state and a series of conformations where the molecule self-associates to form a stable multimeric PrP^{Sc} molecule composed of misfolded monomers (Collinge, 2005). Studies using recombinant protein have shown that ß-sheet-rich PrP aggregation occurs until it reaches a critical size at which it remains stable (Prusiner, 1998). However, it is not clear whether such alternative conformational states of the protein are sufficient to adopt a PrP^{Sc}-like conformation that is infectious and causes disease. It has been reported that particular PrP^{Sc} molecules can only convert PrP^{C} of the same, or at least similar, primary structure. For example, yeast engineered to form two types of prions form two types of "pure" aggregates within the cell, suggesting that each type of prion finds and aggregates with others of its own type. In PrP, this requirement for "like-with-like" resides in a short sequence at its N-terminal (Wickner, 1997; Serio and Lindquist, 2000; Wickner et *al*., 2007).

The site of PrP conversion in the cell has been thought to either be the cell surface membrane or within the endocytic pathway. PrP^{Sc} is located at the membrane and is continuously recycled through endocytosis (DeArmond and Ironside, 1999**).** Recently, a unique cell system in which epitope-tagged PrP^{C} is expressed in a PrP knock-down

neuroblastoma cell line demonstrated that the initial site of PrP conversion is at the cell surface membrane, after which PrP^{Sc} is trafficked into the cell (Goold et *al*., 2011). This conversion of PrP^{C} to PrP^{Sc} at the cell membrane is extremely rapid following prion infection, with synthesis of PrP^{Sc} being observed within minutes of cells being exposed to infectious prions (Goold et *al*., 2011).

1.8 Prion strains and transmission barriers

Prion strains remain the most challenging phenomenon in prion biology. Different prion isolates often have different properties that remain consistent over repeated passages, and are referred to as strains. Distinct prion strains can be distinguished *in vivo* by differences in clinical signs, histological markers and incubation time (Morales et *al*., 2006). The possibility of distinct prion strains was first recognised in scrapie sick goats showing two different clinical syndromes, called "hyper" and "drowsy" (Pattison, 1965). Prion strains are defined as infectious isolates that when transmitted to identical host exhibit consistently distinct prion disease phenotypes (Aguzzi et *al*., 2007). The distinct pathologies and incubation periods in experimental animals associated with strains have been attributed to multiple forms of abnormal PrP folding (Telling, 1996). The existence of prion strains could be the underlying cause of the different forms of prion disease, each with their own incubation time and clinical severity (Bruce et *al*., 1991).

To comply with the criteria of the prion-only hypothesis of prion propagation, PrP^{Sc} needs to contain all the information necessary to encode strain formation (Hill and Collinge, 2003; Bruce, 1993). PrP^{Sc} encoded strain specificity was observed in the serial passage of two different strains of TME in hamsters, which demonstrated that they are associated with different physical and chemical properties of PrP^{Sc} (Bessen and Marsh, 1994; Bessen and Marsh, 1992). Prion strains can be propagated in lines of inbred mice with the same *PRNP* genotype (Scott et *al*., 1997), suggesting that strains are not encoded by differences

in the primary sequence of PrP. Strains most likely arise from alternative PrP^{Sc} conformations and glycosylation patterns (Bartz et *al*., 2000; Peretz et *al*., 2001; Morales et *al*., 2006). Indeed, distinct ratios of PrP^{Sc} glycoforms (di-, mono- and unglycosylated) are observed in different prion strains (Collinge et *al*, 2006; Hill et *al*, 2003) (**Figure 1.6)**.

Each prion strain is believed to have a precise set of biochemical characteristics in the infectious protein that is specifically linked to it. However, disease incubation times for a single prion isolate may vary when inoculated into different mouse strains (Collinge et *al*., 1996; Hill et *al*., 2003). This variation depends on the *PRNP* gene, suggesting some forms of PrP^{C} may be more easily converted to PrP^{Sc} than others. For example, BSE can be transmitted to a wide range of hosts, while maintaining specific characteristics after passage through an intermediate species. A combination of *PRNP* genotype and properties of the infectious strain influence the pattern of PrP^{Sc} deposition, and strain specific incubation times can be explained by differences in the relative efficiency of allotypic interactions that lead to conversion of PrP^{C} to PrP^{Sc} (Carlson et *al*., 1986).

Prions isolated from one animal species often have reduced infectivity to other species, and if infectious at all, often have a longer incubation time (Wadsworth and Collinge, 2007). This phenomenon is known as a species barrier. Species barriers exist for all prion diseases, and these barriers are more impenetrable in some species than in others. This manifests itself in cases where prions from species A are used to infect species B, and not all animals from species B develop the disease, or those that do present a prolonged and variable incubation time of the disease (Moore et *al*., 2005). Nonetheless, in some cases, on a secondary passage from species B to other members of the same species, all animals succumb to disease and display shorter and more consistent incubation times (**Figure 1.7)**.

The species barrier phenomenon is thought to depend on dissimilarities in PrP sequence and structure, thereby hindering the PrP conversion process (Palmer et *al*., 1991;

Chen and Gambetti, 2002; Vanik et *al*., 2004). Minor differences in sequence between species in the gene for PrP may determine the risk of spontaneous misconformation, and other sequence differences may determine the likelihood of disease crossing species barriers and explain the lack of phylogenetic order in transmission. For example, normal sequence differences could explain why scrapie can be transferred from sheep to mice but not pigs, or why bovine isoforms can cause degenerative disease in cats but not dogs, and why the disease may be spread to humans by beef products but not those from sheep.

Species barriers have been studied extensively in mice, including transgenic mice expressing human rather than mouse PrP. In contrast to their wild-type counterparts, transgenic human PrP-expressing mice readily succumb to disease after infection with sCJD prions (Collinge et *al*., 1995a). On the other hand, vCJD prions are able to infect both human PrP-expressing transgenic and wild-type mice (Hill et *al*., 1997; Bruce et *al*., 1997). Collectively, these studies highlight the fact that transmission barrier may be more suitable to describe transmissibility of prions strains instead of species barrier. Various models have been proposed to explain the transmission barrier (Hill and Collinge, 2003; Collinge and Clarke, 2007). Cross-species transmission remains a health concern founded on the emergence in the UK and later elsewhere of vCJD resulting from the consumption of BSE-infected material (Hill et *al*., 1997; Bruce et *al*., 1997*).*

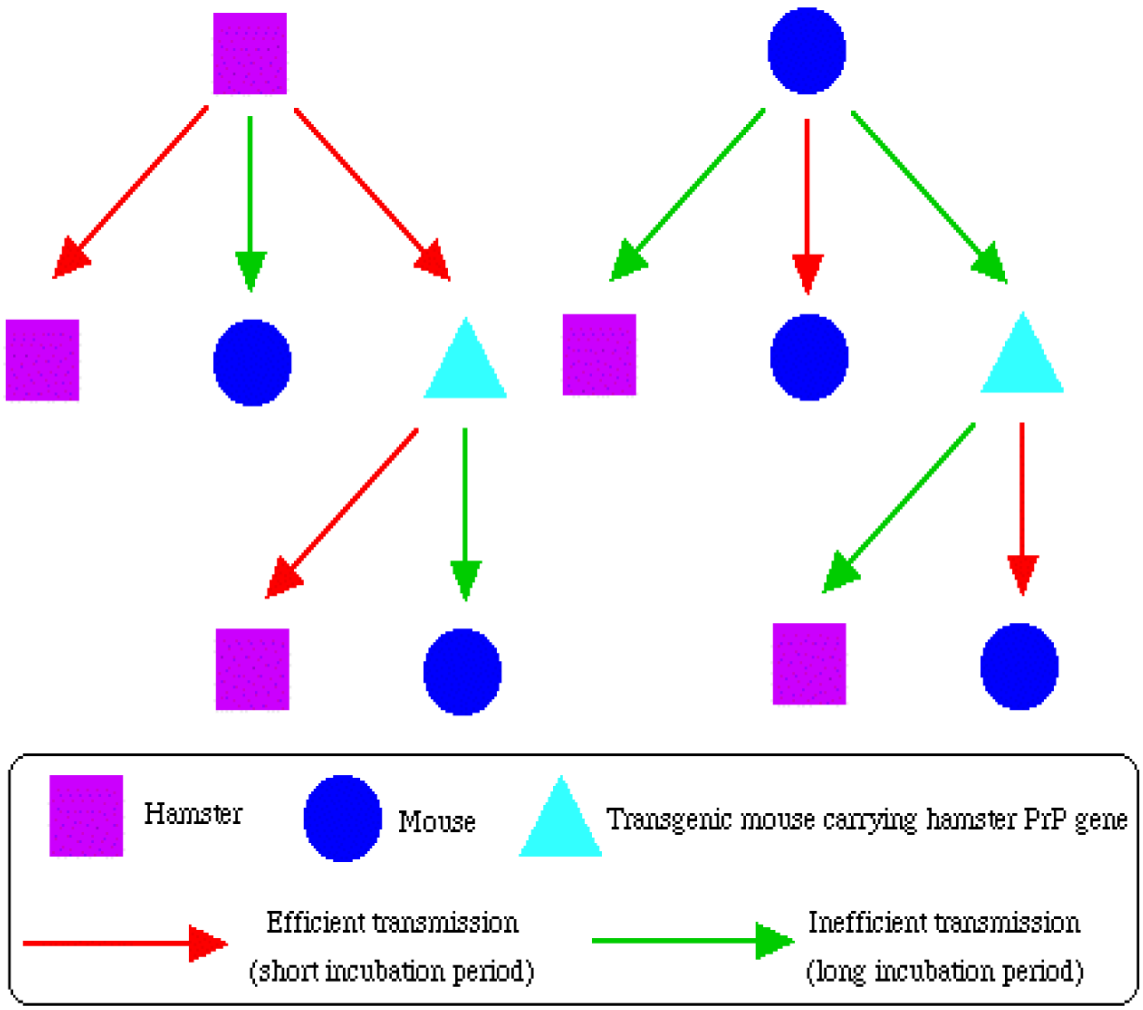

Figure 1.7 Schematic of prion transmission.

Susceptibility of a host to prion infection is co-determined by the prion inocula and the PrP gene. When prions are transmitted from one species to another disease develops only after a very long incubation period, if at all, but on serial passage in the new species the incubation time often decreases dramatically and then stabilizes. This species barrier can be overcome by introducing a PrP transgene from the prion donor i.e. hamster PrP^{Sc} but not murine PrP^{C} is a suitable substrate for conversion to hamster PrP^{Sc} by hamster prion.

1.9 Yeast prions

Non-mammalian prion proteins were discovered in the yeast, *Saccharomyces cerevisiae,* by Reed Wickner in the 1990s, who proposed that unexplained instances of cytoplasmic inheritance in yeast and other fungi were due to the same phenomenon that had been proposed to underlie mammalian prion diseases (Wickner, 1997; Serio and Lindquist, 2000; Wickner et *al*., 2007). Since then, the study of yeast prions has contributed significantly to a better understanding of mammalian prions. This is despite fungal prions not being associated with any known pathogenic state. These prions behave in a similar manner to the PrP protein, although they are generally not toxic to their hosts and may even confer an advantage through a form of a protein-based inheritance (Lindquist et *al*., 2003). A few molecules of a PrP^{Sc}-like form of the Sup35 protein, when introduced into yeast cells, converts the yeast cell's own Sup protein into prion aggregates.

Two yeast proteins, Sup35 and Ure2, can exist as either normal PrP^{C}-like forms or an abnormal PrP^{Sc} form. Studies of fungal prions have given strong support to the protein-only hypothesis for mammalian prions and it has been demonstrated *in vitro* that purified protein extracted from yeast cells with a prion state can convert the normal form of the protein into the abnormal form. In the case of the translation termination factor Sup35, the conformational conversion results in fibril formation and can be reproduced in a cell-free system (Glover et *al*., 1997). When introduced into normal yeast cells, the polymerised forms of Sup35 cause them to adopt the mutant, or {PSI+}, phenotype. Different forms of aggregates generated *in vitro* under specific conditions give rise to different phenotypes in the transformed yeast, demonstrating the link between protein conformation and phenotype (King and Diaz-Avalos, 2004). Collectively, these observations have shed considerable light on the mechanisms of conversion and propagation of mammalian PrP. The degree to which yeast prions are pathogenic in these organisms, or have evolved for other specific functions, remains an area of considerable interest.

1.10 Prion-mediated neurodegeneration

The mechanisms by which prions induce toxicity in neuronal cells are only partially understood. However, some studies support a cytosolic localisation for a small proportion of PrP^{Sc} in prion infected neuronal cells (**Figure 1.8**). In prion infected neuronal cells, toxicity is linked to a cytosolic localisation of a small proportion of PrP^{Sc} in aggresomes (Kristiansen et *al*., 2005). However, it is unclear how PrP^{Sc} oligomers traffic inside neurons and enter the cytosol resulting in UPS inhibition. Previous studies suggested that intracellular neuronal propagation of pathogenic PrP^{Sc} appears important in neurotoxicity (Brandner et *al*., 1996; Mallucci et *al*., 2003). Other studies have shown that various proteolytic stress condition can cause functional impairment of the UPS which result in cellular dysfunction and apoptosis (Lindsten et *al*., 2002)**.**

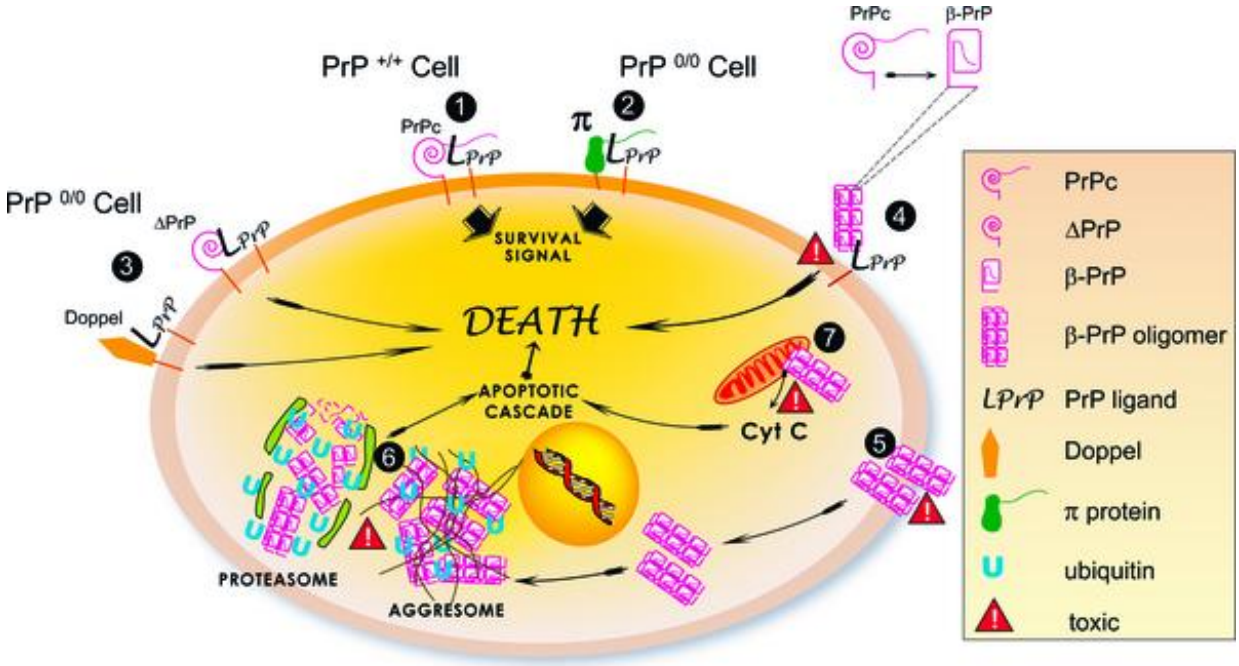

Figure 1.8 Model for the mechanism of oligomeric PrP-induced neurodegeneration.

(**1**) PrP interacts with its ligand LPrP on the cell surface to generate a signal necessary for cell survival. PrP binds to its natural ligand LPrP via its globular domain, while the interaction of the flexible N-terminus of PrP with LPrP triggers signal induction. (**2**) In a PrP knockout cell, n can replace PrP for both binding and signal tranduction. (**3**) In experimental models where truncated forms of PrP (ΔPrP) or Doppel (Dpl, a member of the PrP supergene family harboring partial sequence and structure similarity with PrP) are expressed on a $PrP^{0/0}$ background, binding of ΔPrP or Dpl to LPrP occurs, but not signal transduction in the absence of a complete N-terminus. Suppression of PrP or π signalling triggers cell death. (**4**) PrP oligomers present an altered interaction with LPrP. They bind, but do not trigger signal transduction, and thus by competition prevent PrP^{C} ($PrP^{+/+}$ cells) or π ($PrP^{0/0}$ cells) binding to LPrP, resulting in cell lethality. (**5**) The hydrophobic domain of PrP at the surface of the oligomers enhances their insertion in the cellular membrane. This leads to membrane dysfunction, and hypothetically to the formation of pore-like structures

inducing toxic signals. (**6**) At high intracellular concentration, PrP oligomers accumulate in the aggresome and saturate the proteasomal or other degradation pathways of the cell, leading to the generation of apoptotic signals. (**7**) The hydrophobic domain of PrP oligomers interact abnormally with mitochondrial membranes, leading to the release of cytochrome C (Cyt C) triggering the apoptotic cascade[6].

1.10.1 PrP^{C} loss of function vs. PrP^{Sc} gain of function

It is well established that both normal and pathological isoform of prion protein, PrP^{C} and PrP^{Sc} respectively, are involved in the development and progression of various forms of prion diseases. However, conflicting evidence is emerging with respect to the processing of abnormal PrP^{C}. Thus, the identification of physiological functions of PrP^{C} is crucial for understanding the pathology characteristics of prion diseases (**Figure 1.8**). Studies done by Bueler and colleagues revealed that PrP^{C} –null mice do not succumb to disease when inoculated with prions, instead, they reported that prion-infected heterozygous mice showed longer incubation times compared to WT mice, suggesting that PrP^{Sc} incubation time and disease progression are inversely related to PrP^{C} levels (Bueler et *al*., 1993). It is known that PrP^{C} is essential for the development of prion disease (Bueler et *al*., 1993). However, a loss of function of PrP^{C} is unlikely to be the cause of pathology since it was reported that neither embryonic mice nor adult knockout PrP mice results in neurodegeneration (Bueler et *al*., 1992; Manson et *al*., 1994; Mallucci et *al*., 2002). PrP^{C} has been reported to confer cytoprotection against the deleterious effects of the pro-apoptotic protein Bax (Bounhar et *al*., 2001). The truncated N-terminal of Bax has been shown to activate both Bax-dependent and independent neurotoxic pathways, suggesting a crucial region for putative cytoprotective activity of PrP^{C} (Li et *al*., 2007). In addition, primary neurons collected from PrP^{C} -null mice were shown to be more sensitive to oxidative stress compare to WT neurons (Brown et *al*., 1997; White et *al*., 1999). Moreover, cells exposed

[6] *Taken from Simoneau et al., 2007.*

to synthetic peptide treatment have been shown to result in microglia activation and the production of reactive oxygen species (ROS) (Combs et *al*., 1999). Synthetic peptide treatment has been used as a model for PrP^{Sc} (Forloni et *al*., 1993). Furthermore, another study reports that expression of N-terminally truncated PrP^{C} in PrP-null mice lead to a rapid degeneration of cerebellar neurons, which can be rescued by co-expression of WT PrP^{C} (Shmerling et *al*., 1998). Despite compelling evidence for conformational conversion in the course of prion diseases, it is still not clear what leads to the accumulation and toxicity of the pathological conformer and the gain-of-toxic-function hypothesis is not well understood.

1.10.2 Aberrant PrP^{C} trafficking

The physiological roles of the transmembrane forms of PrP are not clear. However, transgenic mice expressing transmenbrane form of PrP termed (^{Ctm}PrP) develop neurological symptoms and neuronal death that resembles certain prion disease. PrP^{C} is translocated to the ER due to the presence of the NH2-termianl peptide that is then cleaved into the ER lumen (**Figure 1.9**). Studies have suggested that PrP^{C} may be neuroprotective and atypical topology or aberrant PrP variants might be neurotoxic (Hegde et *al*., 1999; Hegde et *al*., 1998; Yedidia et *al*., 2001; Ma et *al*., 2002). Remarkably, following translocation in the ER, PrP^{C} can be synthesized with at least three topologies: a secreted form that reflects the main pathway for PrP^{C} synthesis in vivo, plus COOH- and NH2- terminal transmembrane forms, ^{Ctm}PrP and ^{Ntm}PrP, respectively, due to transmembrane insertion of hydrophobic pocket (Hegde et *al*., 1999; Hegde et *al*., 1998). The ^{Ctm}PrP was suggested to be toxic and cause neurodegeneration, and certain mutations appear to favour this conformer (Hegde et *al*., 1999; Hegde et *al*., 1998), although ^{Ctm}PrP appears not to be infectious when inoculated in reporter mice (Stewart et *al*., 2005). It was shown in vivo that the expression of PrP with the A117V mutation, which is linked to GSS, leads to neurodegeneration with a prion disease phenotype (Hegde et *al*., 1998). It was shown increased levels of ^{Ctm}PrP, but low levels of PrP^{Sc} accumulation, in the transgenic

mice carrying the AV117 mutation, as well as a patient (carrying the same mutation). In addition, it was shown that neurodegeneration in ^{Ctm}PrP transgenic mice depends on the co-expression of endogenous WT PrP^{C} (Stewart et *al*., 2005). It has been suggested that PrP^{C} accumulation in the cytosol may be neurotoxic (Ma et *al*., 2002). It is not clear why WT PrP^{C} is occasionally retained in the cytosol, nor whether it serves any physiological function or may be associated with pathogenesis. Indeed, in human primary neurons culture, cytosolic PrP^{C} is not toxic and may, instead have anti-apoptotic functions (Roucou et *al*., 2003). Significant variable amounts of cytosolic PrP^{C} usually detected after proteasome inhibition or overexpression of *PRNP* in neurons is still debatable. Under normal condition PrP^{C} in the cytosol would be degraded by the proteasome. However, following proteasome inhibition cytosolic PrP^{C} has been shown to aggregate, acquire partial resistance to proteases and ability to self-replicate (Ma and Lindquist, 2001; Ma and Lindquist, 2002; Cohen and Taraboulos, 2003). Furthermore, in the ER-associated degradation (ERAD) ER-resident proteins, in unassembled or misfolded forms, undergo retrograde transport to the cytosol, get ubiquitinated and are normally degraded by the proteasome (Meusser et *al*., 2005) (**Figure 1.9**). Misfolded, mutant and WT forms of PrP have been shown to be degraded by ERAD when proteasome inhibitors are present (Zanusso et *al*., 1999; Jin et *al*., 2000; Ma and Lindquist, 2001; Yedidia et *al*., 2001; Ma et *al*., 2002; Cohen and Taraboulos, 2003). Studies revealed evidence of ER stress and decreased translocation of nascent PrP during prion infection (Rane et *al*., 2008). It is suggested that PrP^{Sc} accumulation could cause ER stress, leading nascent PrP^{C} to retro-translocate to the cytosol, where putative toxic PrP molecules accumulate (Rane et *al*., 2008) (**Figure 1.9**). Although, cytosolic PrP has been attributed to ER re-translocation (Ma and Lindquist, 2002), others have found that cytosolic PrP^{C} contains NH2-terminal signal peptide, indicating that this subcellular location may be exclusively related to abortive translocation into the ER (Drisaldi et *al*., 2003; Fioriti et *al*., 2005; Campana et *al*., 2005).

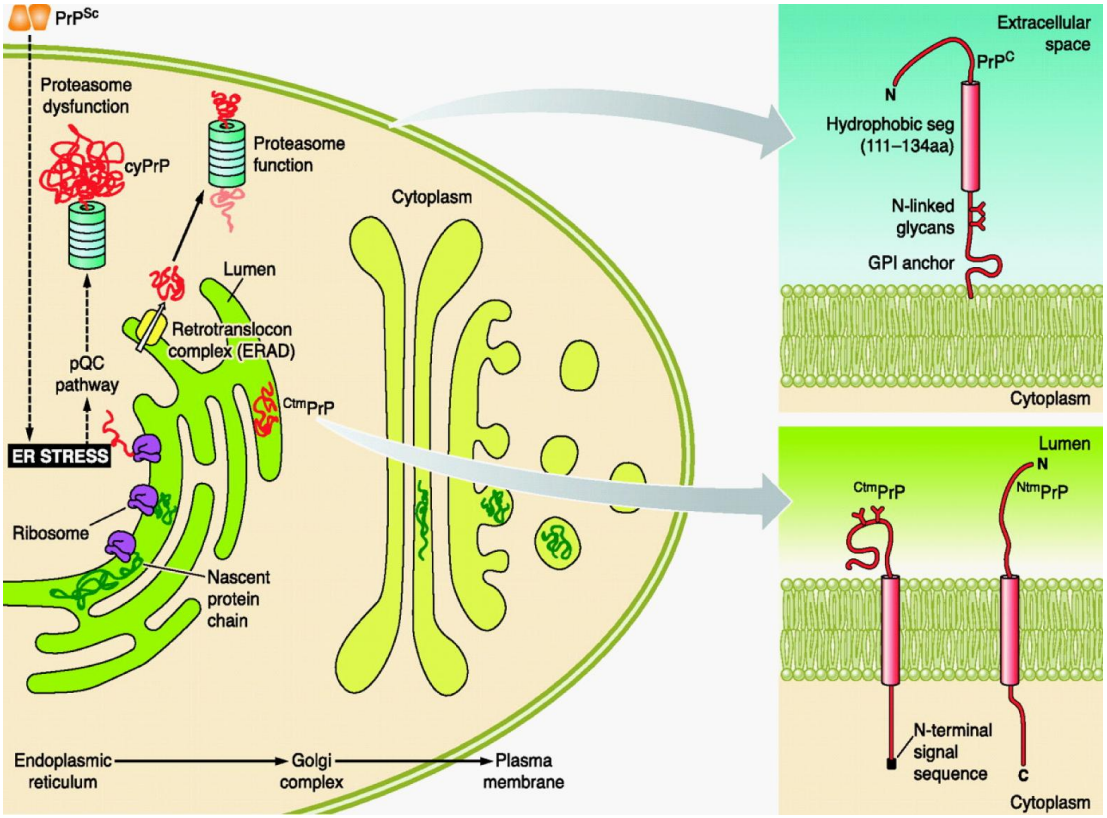

Figure 1.9 Toxicity mediated by abnormal topology or altered trafficking of PrP^C. The normal isoform of prion protein, PrP^C is synthesized, folded and glycosylated in the ER where its GPI anchor is added, before further modification in the Golgi complex. Mature PrP^C translocates to the outer leaflet of the transmembrane form, generated in the ER, which have their COOH, NH2 terminus in the ER lumen, respectively. Misfolded and aberrantly processed proteins which would normally be degraded by the proteasomes through the ER-associated degradation (ERAD) pathway, aggregate in the cytoplasm and cause cell death. Putative proteasomal inhibition or malfunction during prion disease would contribute to this route of toxicity. Induction of ER stress by PrP^{Sc} may lead to translocation of nascent PrP^C molecules to the cytosol for proteasomal degradation as a way to alleviate the overload of the ER (pQC pathway). However, this mechanism of

defence turns negative under chronic ER stress conditions, overwhelming the proteasome and leading to the cytosolic accumulation of potentially toxic PrP molecule[7].

1.10.3 Intermediate PrP species

There is evidence to suggest an implication of PrP^C -mediated signalling. However, the majority of signal transfers from PrP^C to intracellular compartment still remain unknown. The need for transmembrane signalling partners of PrP^C has been long recognized, there is evidence that PrP^C bind a variety of ligands, several of which may fulfill the requirement for a signalling intermediate and others may bridge PrP^C with further transmembrane partners. Studies in cell suggest that, rather than playing a specific role in a straightforward signalling pathway, PrP^C may serve as a scaffolding protein in multiple sets of poorly defined interactors at the cellular surface. It is likely that both the endogenous, as well as the ligand induced trafficking of PrP^C may strongly affect its functions according to the intermediate membrane environment (Roucou and LeBlanc, 2005; Roucou et *al*., 2004). Several basic features of PrP^C favour a dynamic scaffolding of multicomponent complexes. Distal to the lipid bilayer, specific PrP^C domain binds various proteins, glycosaminoglycans and metal ions (Hosszu et *al*., 1999; Jackson et *al*., 2001). Since the binding of domains of PrP^C are distinct for at least some of these ligands, and the affinity constants for confirmed ligand are variable, each cell likely interacts with a distinct set of partners through PrP^C, depending on both level of expression of the latter and the characteristics of intermediate microenvironment. A link between prion propagation and neurotoxicity has been suggested; A possible explanation is that PrP^{Sc} is itself inert, but toxicity resides in a smaller, labile oligomeric PrP species named PrP^L (for lethal), generated as an intermediate or side product during prion propagation (Hill et *al*., 2003; Hill and Collinge, 2003). It is suggested that neurotoxicity may require a critical PrP^L concentration that is reached during

[7] *Adapted from Aguzzi et al., 2009.*

conventional infections but the slower kinetic if increase in infective titre in the subclinically infected mice may not mean that toxic PrP^{L} levels are reached (Collinge, and Clarke, 2007).

1.10.4 Cellular aspects of prion toxicity

The means by which neuronal cells die following prion infection remain poorly understood. Many studies done on cell and animal models have highlighted the potential role of neuronal apoptosis in prion disease pathogenesis. Indeed, several studies done both *in vitro* and *in vivo* suggest the cause of cell death may be, in part, via apoptosis (Corsaro et *al*., 2012; Liberski et *al*., 2008; Liberski et *al*., 2005; Liberski et *al*., 2002; Thellung et *al*., 2000). Prion infection can induce apoptosis in primary neurons (Cronier et *al*., 2004), and treatment of primary cultures of various brain regions infected with the PrP peptide ($PrP^{106-126}$) has been shown to induce neuronal apoptosis (Forloni et *al*., 1993; Brown et *al*., 1994; Brown et *al*., 1996; Jobling et *al*., 1999; Thellung et *al*., 2000). Studies conducted *in vivo* in mice using the same $PrP^{106-126}$ peptide injected into the retina have also been shown to induce apoptosis (Ettaiche et *al*., 2000). However, the exact mechanism by which $PrP^{106-126}$ leads to apoptosis is unclear.

Alternative mechanisms of prion-induced toxicity include the production of reactive oxidative species (ROS) (Brown et *al*., 1996; Turnbull et *al*., 2003), or disruption of the mitochondrial membrane to cause release of cytochrome C and caspase activation (O'Donovan et *al*., 2001) (**Figure 1.10**). Early production of ROS and activation of caspase 3 may be caused by direct exposure of cells to $PrP^{106-126}$, with other pathways such as that of the c-Jun N-terminal kinase (JNK) also being involved (Carimalo et *al*., 2005). Activation of caspases such as caspase-12 has been detected in neuroblastoma cells treated with small amount of full-length PrP^{Sc} from scrapie infected mouse brain (Hetz et *al*., 2003). Prion infected neuronal cells have been shown to become apoptotic when exposed to mild

proteasome inhibition, with proteasome impairment resulting in the formation of cytosolic aggresomes that are associated with activation of caspases 3 and 8 (Kristiansen et *al*., 2005). Such have been shown also to have a higher sensitivity to oxidative stress as compared to uninfected cells (Milhavet et *al*., 2000). In addition, prion infection can alter the molecular mechanisms responsible for protection against oxidative stress, by decreasing superoxide dismutase (SOD) and glutathione levels (Milhavet et *al*., 2000) (**Figure 1.10)**.

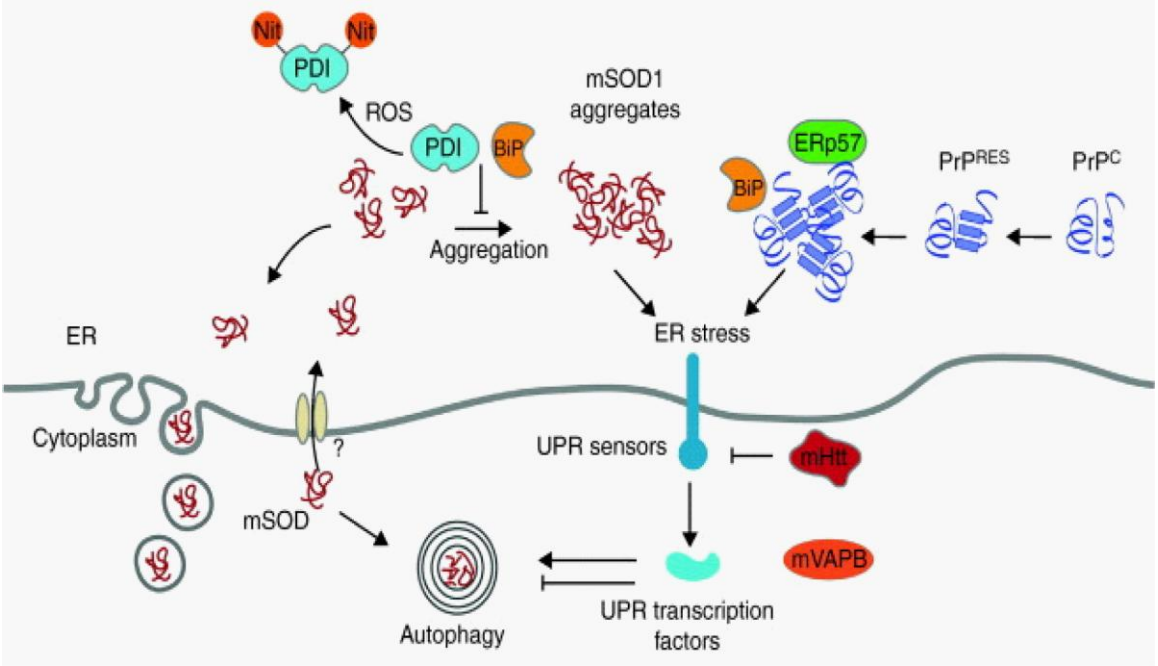

Figure 1.10 Mechanisms for apoptosis in prion mediated-neurotoxicity.

Misfolded PrP^{C} can contribute to ER stress. Excessive levels of misfolded proteins accumulate in the cytosol and might impair proteasome function either directly or indirectly by the incorporation of aggresomes. Under conditions of proteasome inhibition, cytoplasmic forms of PrP aggregates are generated; for example the retranslocation of PrPres from the lumen of the endocytic and lysosomal vesicles into cytosolic aggresome.

The ER is the major organelle for protein synthesis and regulation of intracellular trafficking. The activation of ER stress genes has been found to be significantly upregulated in prion pathogenesis. In particular, the ER stress chaperone GRP78/Bip which belongs to the ER-stress resident Hsp70 family has been found to play a central role in the unfolded protein response (UPR) (Hetz and Soto, 2006). Excess stress in the ER induces apoptosis, but the mechanism underlying this process in not yet clear. The release of ROS from chemokine-activated microglia cells could contribute to ER stress and/or the ERAD process by inactivation of ER chaperones such as GRP78 (Bip).

Recently, it has been demonstrated that prion propagation in the brain proceeds via two distinct phases: a silent clinical phase in which infectivity increases and then a plateau phase before clinical endpoint. This finding indicates that production of neurotoxic species is triggered when propagation of infectivity has been saturated. This subsequently leads to a switch in the auto-catalytic process producing two phases: firstly, an infectivity phase 1, and then secondly, a toxic pathway (phase 2) (Sandberg et *al*., 2011).

1.11 Therapeutic approaches in prion diseases

To date, there are no available cures, vaccines or treatments to halt or slow the course of prion diseases. The course of prion disease is alarmingly rapid compared with other neurodegenerative disorders. Overexpression of PrP increases the onset of disease in prion-infected transgenic mice (Mallucci et *al*., 2003; Mallucci et *al*., 2007). It follows, therefore, that agents that reduce PrP expression may delay the onset of prion disease pathogenesis. In particular, compounds that bind and stabilise the PrP conformation may be beneficial. Similarly, agents destabilising the PrP^{Sc} conformation may be effective. In this regard, several vaccines to amyloid plaques in Alzheimer's disease are in clinical trials and agents that interfere with the putative PrP^{C}-PrP^{Sc} interaction might be similarly

effective. Chemicals affecting the endocytosis, exocytosis, intracellular trafficking or degradation of PrP may also be effective.

A range of potential therapeutic compounds have been studied. These include Congo red, polyanionic compounds, amphotericin B, porphyrins and quinacrine, which have each been shown to reduce accumulation of PrP^{Sc} in prion infected cell models (Trevitt and Collinge, 2005). However, such models have not provided similarly stringent or reliable results *in vivo* (Aguzzi et *al*., 2001). Targeting endogenous PrP^{C} in mice with early prion infection has been shown to reverse spongiform change and prevent clinical symptoms, neuronal loss, and cognitive as well as behavioural deficits (Mallucci et *al*., 2003; Mallucci et *al*., 2007). The rise of RNA interference (RNAi) has been demonstrated to inhibit PrP^{C} expression in neuroblastoma cells (Tilly et *al*., 2003) and prevent PrP^{Sc} accumulation in prion-infected cells (Daude et *al*., 2003). Other studies have revealed prolonged survival in prion infected mice when a lentivirus-expressing shRNA that targets PrP is injected into the hippocampus (White et *al*., 2008).

Targeting the conversion of PrP^{C} to PrP^{Sc} has included the use of antibodies to bind to PrP^{C} and stabilise it against conversion (Enari et *al*., 2001; Heppner and Aguzzi, 2004; white et *al*., 2003; Aguzzi et *al*., 2001; Perez et *al*., 2001). Recently, anti-PrP antibodies capable of crossing the blood brain barrier and targeting cytosolic PrP have been described. However, administering large quantities anti-PrP antibodies into the CNS may be ineffective, as they have been shown to cause signs of neurodegeneration in mice (Solforosi et *al*., 2004). A different approach has made use of a cationic ligand tetrapyrrole (Fe III-TMPyP), which displays potent anti-prion activity, can bind to the human PrP^{C} via the C-terminus of PrP and potentially be used as therapeutic agent by preventing the conversion of PrP^{C} to its disease-associated form (Nicoll et *al*., 2010; Nicoll and Collinge, 2009).

Diagnosing the disease, or identifying potentially contaminated biofluids, is equally difficult. However, a standard steel binding assay (SSBA) has been developed, providing a

prototype blood test for detecting prion infection in the diagnosis of vCJD (Edgeworth et *al*., 2010). The assay has been shown to quantify solid binding matrix in the infected blood by the capture and direct immunodetection of surface-bound material. Such developments may prove critical in identifying patients with the disease, and preventing exposure to potentially infectious biological fluids or tissue by donation or during surgery.

1.12 The ubiquitin proteasome system (UPS)

One of the factors that determine the biological activities of proteins are their concentration, which in turn is controlled by a balance between their synthesis and degradation rates. Enzymes that carry out such reactions are called proteases and are part of a major mechanism by which cells regulate the concentration of particular proteins and degrade misfolded proteins. Regulation and degradation of intracellular protein is a tightly regulated process and is called collectively proteostasis. There are two main cellular degradation pathways: the UPS and autophagy. The UPS is a two-step mechanism that degrades intracellular proteins (**Figure 1.11**). Proteins are first targeted for degradation by attachment of ubiquitin molecules, which are then recognized by a protease complex, the 26S proteasome (Reinstein and Ciechanover, 2006). Autophagy involves the degradation of protein complexes and intracellular organelles as mediated by a cell's lysosomes. Autophagy involves formation of double-membrane bound structures known as autophagic vesicles. These vesicles then fuse with lysosomes and their contents are degraded by lysosomal hydrolases. Autophagy-mediated degradation is generally considered to involve low specificity in substrate recognition (Rubinsztein, 2006).

The UPS was discovered more than thirty years ago, but recently the field has rapidly expanded and gained the scientific interest that reflects its paramount role in cell biology and neuronal disorders. The UPS regulates degradation of cytosolic and nuclear proteins that occurs in the process of cell survival. In eukaryotes, the ubiquitination system often

serves as a triggering signal for degradation. It accounts for targeting selected proteins for degradation by tagging them with chains of a small heat stable protein, the adenosine triphosphate (ATP)-dependent proteolytic factor 1 (APF-1), which was later identified to be identical to the protein ubiquitin (Wilkinson et *al*., 1980). Hersko and Ciechanover, in the period of 1970 to 1980, found that ubiquitin could be conjugated to lysine residues of proteins in an energy-dependent process that required ATP (Hershko and Ciechanover, 1998. The ubiquitin modification of protein was followed by rapid degradation by an energy-requiring protease (Harper et *al*., 1997). The groups of enzymes required for accomplishing ubiquitin conjugation include a ubiquitin activating enzyme (E1), the ubiquitin-conjugating enzymes (E2) and the ubiquitin ligases (E3) (**Figure 1.11)**. In a sequential manner, these enzymes collaborate to covalently conjugate ubiquitin first to the substrates and next to one of the lysine residues within the ubiquitin until a chain of conjugated ubiquitin is formed. This conjugated protein is recognised by the proteasome, resulting in degradation of the ubiquitinated protein (Hershko and Ciechanover, 1998; Hershko et *al*., 1983).

Ubiquitin is encoded by a multi-gene family where monomeric ubiquitin genes are C-terminally linked to a sequence encoding a ribosomal protein and multimeric ubiquitin genes that are encoded in a tandem repetitive manner. The number of ubiquitin moieties in the precursors and the nucleotide sequence can vary substantially among different eukaryotic species. However, the amino acid sequence shows variation only of three positions in the seventy six residue long protein, making ubiquitin one of the most conserved eukaryotic proteins (Jentsch et *al*., 1991; Glickman and Ciechanover, 2002). Yeast and human ubiquitin, for example, differ only at amino acid residue positions 19, 24 and 28 (Graham et *al*., 1989). Newly synthesized ubiquitin fusion proteins or multimeric ubiquitin precursor are post-translationally processed by ubiquitin C-terminal hydrolases (UCH) that recognize and cleave the last glycine residue of each ubiquitin moiety, releasing functional single ubiquitin units. The high expression levels and stability of ubiquitin,

combined with the fact that ubiquitin is recycled after being used to tag proteins for degradation, safeguards the nuclear and cytosolic expression levels that are required for a functional UPS. In general, ubiquitin molecules are attached to an internal lysine in the protein and successive addition of other ubiquitin molecule is added to synthesize the polyubiquitin chain (Ciechanover, 2003; Glickman and Ciechanover, 2002).

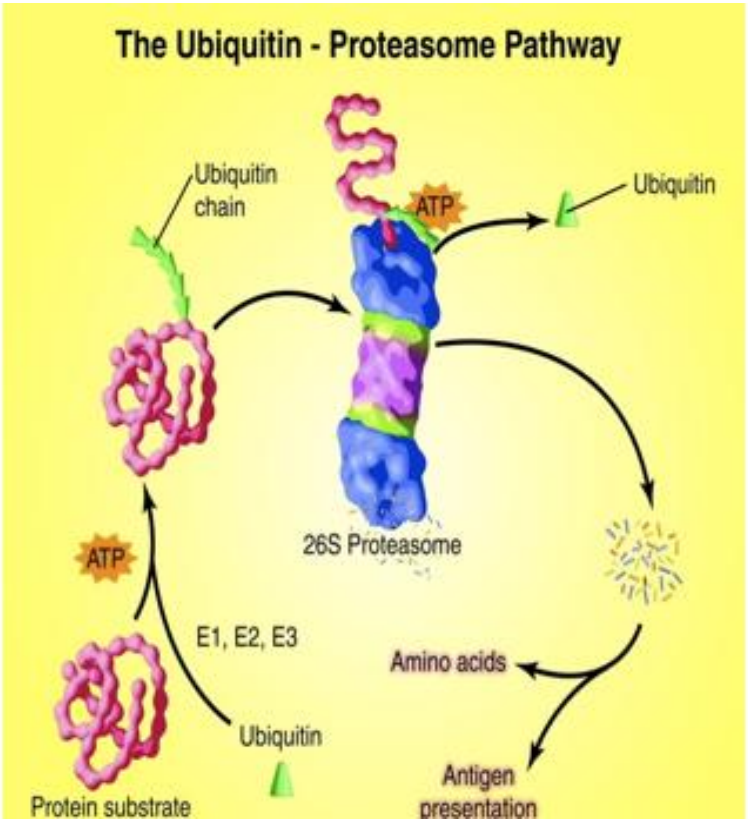

Figure 1.11 The ubiquitin proteasome pathway.

Ubiquitin is conjugated to proteins that are destined for degradation by an ATP-dependent process that involves three enzymes. A chain of five ubiquitin molecules attached to the protein substrate is sufficient for the complex to be recognized by the 26S proteasome. In addition to ATP-dependent reactions, ubiquitin is removed and the protein is linearized and injected into the central core of the proteasome, where it is digested to peptides. The

peptides are degraded to amino acids by peptidases in the cytoplasm or used in antigen presentation[8].

Two groups of proteins share sequence homology with ubiquitin: the ubiquitin-like proteins (UBL); and, proteins containing an ubiquitin–like domain (UDP) (Jentsch et *al*., 2000). UBLs like SUMO or Nedd8 can be conjugated to other proteins in a mode resembling ubiquitin modifications. Yet they do not target for degradation but fulfil roles such as inhibition of ubiquitination, regulation of protein trafficking and activation (Jones et *al*., 2002; Muller et *al*., 2001). The UDPs comprise a diverse family of proteins that have an uncleaveable ubiquitin-like domain most often located in their N-terminal part. It has been shown that ubiquitin-like domain can interact with the proteasome, but it is not believed that this interaction results in degradation.

1.12.1 Ubiquitination

Ubiquitination of a substrate is performed in a series of enzymatic steps that start with the ATP-dependent activation of ubiquitin by the formation of a thiol-ester linkage between its C-terminal glycine and an active site cysteine residue present within the ubiquitin-activating enzyme (E1). The ubiquitin is then transferred to a cysteine residue of a ubiquitin-conjugating enzyme (E2) enzyme, and then finally covalently linked by an isopeptide bond to the E-NH2 group of a lysine residue in the substrate, a process that is directed and catalysed by a substrate-specific ubiquitin ligase (E3) (**Figure 1.12**). Once the first ubiquitin is linked to the substrate, the procedure is repeated and additional ubiquitins are covalently linked by their C-terminal glycine 76 residue to specific lysine residues within the previous ubiquitin to eventually form a polyubiquitin chain. Long chains have higher affinity for binding to the proteasome, and a minimum of four ubiquitins are sufficient to serve as a recognition signal for degradation (Thrower et *al*., 2000).

[8] *Adapted from* Lecker et *al*., 2006.

Only one E1 enzyme has been described, deletion of the gene for which in yeast is lethal (McGrath et *al*., 1991). Mammalian cell lines expressing a temperature sensitive E1 tend to arrest in the G2 phase of the cell cycle and upregulate heat-shock proteins, indicating a strong stress response at non-permissive temperature (Finley et *al*., 1984; Ciechanover et *al*., 1984). The precise number of different E2 enzymes is not known, but estimations based on sequence homology suggest that over twenty E2 enzymes are encoded in the mammalian genome (Joazeiro and Weissman, 2000). The E2s are often small proteins identified by a characteristics core of around 15 kDa that contains the active site cysteine residues. Each E2 can interact with a number of different E3s, which comprises an even larger family of enzymes (**Figure 1.12)**. The E3s, which can be single proteins or consists of multi-protein complexes, are responsible for the specificity of the UPS, since they recognize the proteasome substrate through the presence of degradation signals (**section 1.12**). There are multiple interactions between these enzymes: a single substrate can be ubiquitinated by different E2s and E3s and a single E3 can ubiquitinate different substrates and interact with different E2s.

The E3s can be divided into three majors groups: the HECT (Homologues to E6-AP C-Terminus) domain family, the RING (Really Interesting New Gene) finger domain family, and the recently identified U-box ligases (Hatakeyama et *al*., 2001; Pickart, 2001). There are many fundamental differences in the enzymatic activities of these E3 families. Recently characterised U-box domains of E3s contain a conserved 70 amino acid long stretch identified in at least six mammalian proteins (Pickart, 2001). The domain is required for the E3 activity and also shares some structural similarities to the E3 RING finger domains (Aravind and Koonoin, 2000). The prototype U-box protein is the yeast Ufd2 protein, which contributes to ubiquitination of the ubiquitin fusion degradation (UFD) substrates (Koegl et *al*., 1999). CHIP (C-terminus of the Hsc70 interacting protein) is also a member of this group of E3s and together with the E3 parkin, promotes ubiquitination of the unfolded Pael receptor involved in Parkinson's disease (Imai et *al*., 2002). It is noteworthy that both Ufd2

and CHIP ubiquitinate substrates in concert with classic E3s and mainly promote elongation instead of initiation of the ubiquitin chain.

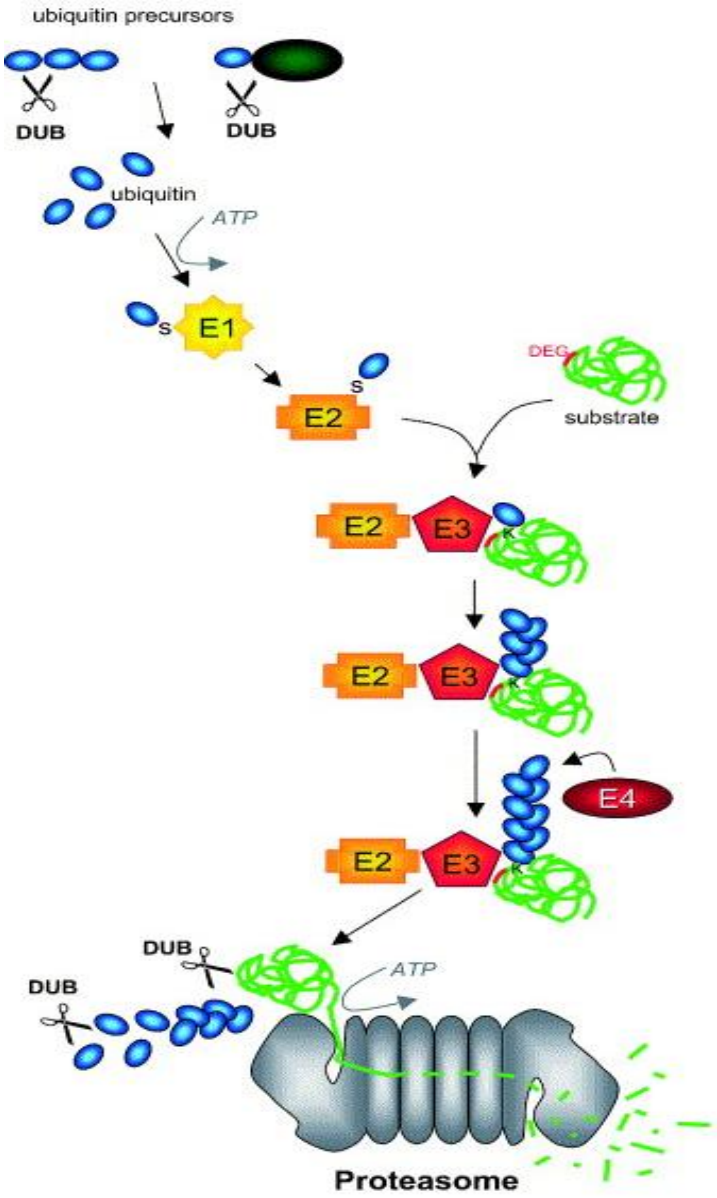

Figure 1.12 Overview of ubiquitination.

Ubiquitination is an enzymatic cascade involving an ubiquitin (Ub) - activating enzyme (E1), an Ub- conjugating enzyme (E2), and an Ub-ligase (E3). During ubiquitination, Ub is activated by the E1 Ub-activating enzyme and then transferred to an E2 Ub-conjugating

enzyme. The E3 Ub-ligase enzyme recognises and binds both the target substrate and the Ub-E2 enzyme and transfers UB to the target substrate. Ubiquitin is released as a single unit from its precursor forms through the cleavage by deubiquitination enzymes (DUBs). Ubiquitin is conjugated to proteins that are destined for degradation by an ATP-dependent process that involves three enzymes. A chain of five ubiquitin molecules attached to the protein substrate is sufficient for the complex to be recognized by the 26S proteasome. In addition to ATP-dependent reactions, ubiquitin is removed and the protein is linearized and injected into the central core of the proteasome, where it is digested to peptides. The peptides are degraded to amino acids by peptidases in the cytoplasm or used in antigen presentation. Activation of ubiquitin is an ATP-dependent process that result a thioelester linkage between ubiquitin and the enzymes[9].

The primary function of ubiquitination is to serve as a reusable selecting tag to sorting proteins that are destined for proteasomal degradation. Yet this is not its only function. Different modes of ubiquitination are involved in such diverse functions as DNA repair, protein activation and endocytosis. The different ubiquitination signals are a consequence of the various possibilities to build a lysine-linked chain (Pickart, 2000). Ubiquitin carries seven lysine residues at positions 6, 11, 27, 29, 33, 48 and 63, of which lysine 29, 48 and 63 linked chains have been identified *in vivo* (Gregori et *al*., 1990; Chau et *al*., 1989; Arnason and Ellison, 1994; Spence et *al*., 1995). The lysine 48-linked chain in which an isopeptide bond links the C-terminal glycine 76 residue of ubiquitin and the lysine 48 of the previous ubiquitin, are the conical signal for proteolysis by the UPS. Overexpression of ubiquitin, in which the lysine 48 is substituted for an arginine residue, is lethal in yeast (Finley et *al*., 1984). Though less common, lysine 29 linked ubiquitin chains can target a protein for degradation as well.

[9] *Adapted from Lindsten and Dantuma, 2003*.

Poly-ubiquitin lysine 48 chains target proteins to 26S proteasome-mediated degradation, whereas polyubiquitin chains formed via lysine 63 target proteins for other diverse cellular activities (Hicke, 1999; Lauwers et *al*., 2009). The level of membrane proteins are maintained by lysine 66 linked polyubiquitination, which functions as a signal for selective trafficking to the lysosomal lumen via multivescicular endosomal (MVE) or multivesicular body (MVB) degradation pathways (Raiborg and Stenmark, 2009). This process of endosomal sorting is dependent on ubiquitination of membrane protein, or "cargo". Ubiquitinated cargo is recognized by the endosomal sorting complex for transportation and recycling (Raiborg and Stenmark, 2009).

Regulation of the ubiquitination status of activators is critical in the control of transcription factor promoter function. The mechanism in which monoubiquitination balance is established with polyubiquitination and degradation has been the focus of intense investigation. Studies in yeast on Gal4-dependent genes first indicated that the 19S proteasomal ATPases bind to the Gal4 activation domain independently of both the non-ATPase 19S subunits and the 20S proteolytic core (Gonzalez et *al*., 2002). In 2007, Ferdous and colleagues demonstrated a non-proteolytic "destabilizing" function of the APIS (19S ATPase proteins independent of 20S) complex involving an ATP-dependent, rapid, and reversible disassociation of the transactivator-promoter complex, which was inhibited in the presence of mono-ubiquitin (Archer et *al*., 2008; Ferdous et *al*., 2001). Further studies have shown that mono-ubiquitination of transcription factors increase transactivation (Ferdous et *al*., 2007); however, the mechanisms involved in this process were unclear. Together, these studies shed light on the non-proteolytic and proteolytic role of ubiquitination.

1.12.2 Deubiquitination

Ubiquitination is a reversible protein modification process, as conjugated polyubiquitin can be removed and disassembled by the action of deubiquitination enzymes

(DUBs). DUBs comprise a large family of enzymes within the ubiquitin proteasome system. All DUBs are cysteine proteases with the exception of one recently discovered DUB within the proteasome that is a metalloprotease (Verma et *al*., 2002; Yao and Cohen, 2002). There are two groups of DUBS: UCHs and ubiquitin-specific processing proteases (UBP). The two classes have some common residues in their active sites, but besides that there is a poor sequence homology between them and other proteases. UCHs are typically small proteins that remove peptides fused to the C-terminus of ubiquitin while UBPs make up a more diverse family of proteins that are able to cleave isopeptide bonds between ubiquitin and lysine residues within a substrate or between ubiquitin in a polyubiquitin chain. DUBs play a vital role in maintaining a sufficient pool of free ubiquitin in the cell by processing the ubiquitin monomers from their precursors and by recycling polyubiquitin chains from substrates targeted for degradation (Chung and Baek, 1999; Wilkinson, 2004).

1.12.3 Proteasomes

Proteasomes are very abundant in the cellular cytosolic and nuclear compartment, accounting for up to 1% of total cellular protein (Baumeister et *al*., 1998). They can diffuse freely in the cytosol and the nucleus (Reits et *al*., 1997). They enter the nucleus through the nuclear pore complex, or they get entrapped within the nuclear compartment when the envelope is restored after cell division. In yeast, proteasomes are associated with the nuclear and ER membrane, and have an altered distribution during mitosis (Enenkel et *al*., 1998). Similar to lysosomes which degrade mostly extracellular proteins in a less selective manner, the proteasome controls its proteolytic activity through self-compartmentalisation of the responsive proteases.

The proteasome was first observed in 1968 by electron microscopy, but it took almost twenty years before Goldberg and colleagues renamed the prosome, as it was originally known (Schmid et *al*., 1984) to the proteasome, highlighting its pivotal role in intracellular degradation (Arrigo et *al*., 1988). In eukaryotic cells, the proteasome forms a

barrel shaped complex consisting of a 20S core particle with the proteolytic active sites facing inward to the lumen of the proteasome (**Figure 1.13**). The 20S core particle is located between two 19S regulatory particles, also called PA700, that serve as proteasomal gatekeepers and control entry and exit of proteins and peptides. Progressive degradation of proteins by the proteasome results in the production of peptides of various lengths. These peptides are further degraded by cytosolic peptidases, generating amino acids that can be reused in protein synthesis. In vertebrates, these peptides can also be translocated into the ER and loaded in major histocompatibility complex (MHC) class I molecules that are subsequently transported and displayed at the cell surface, a process known as antigen presentation (Rock and Goldberg, 1999). Since the proteasome degrades the majority of intracellular proteins, the presented peptides are representative of the total pool of proteins present within the cell. This pool also includes proteins that are derived from infectious agents and are consequently eliminated by cytotoxic T-cells. Antigen presentation is one of the fundamentals phenomena of the immune system and is of major importance for the host response to viral infection (Dantuma et *al*., 2002; Lorenzo et *al*., 2001).

The mammalian proteasome is unique in that it has three exchangeable proteolytic βsubunits that are induced in the presence of the cytokine IFNγ, which is produced by activated CD4 and CD8 positive T-cells and natural killer cells, and plays a major role in mobilizing the host defence against infectious pathogens. The β1, β2, and β5 subunits are exchanged into iβ1/LMP2, iβ2/MECL1 and iβ5/LMP7, respectively, resulting in the formation of the immunoproteasome complexes (Gaczynska et *al*., 1996). These modifications cause an altered preference of cleavage sites favouring the generation of peptides with hydrophobic C-termini and reducing the output of peptides with acidic C-termini. A peptide with hydrophobic C-terminus is more likely to be suitable for antigen presentation by MHC class I. The alteration of the cleavage specificity for the C-terminus is the most important for the proteasome (Serwold et *al*., 2002; Cascio et *al*., 2001).

1.12.4 The 20S core particle

The 20S proteasome consists of four heptameric rings, named α and β, forming the structure α-β-β-α. The two inner rings consist of seven β-subunits and contain three proteolytic activities each. The proteolytic active sites are located in the β1, β2 and β5 subunits of the core particle, facing into the proteolytic chamber of the proteasome (Dick et *al*., 1998). The β1 subunit displays post-glutamyl peptide hydrolysing (PGPH) activity, cleaving preferably after acidic amino acids. The β2 subunit has a trypsin-like activity, cleaving preferably after basic amino acids. The β5 subunit is responsible for the chymotrypsin-like activity, which cleaves preferably after hydrophobic amino acids (Arendt and Hochstrasser, 1997).

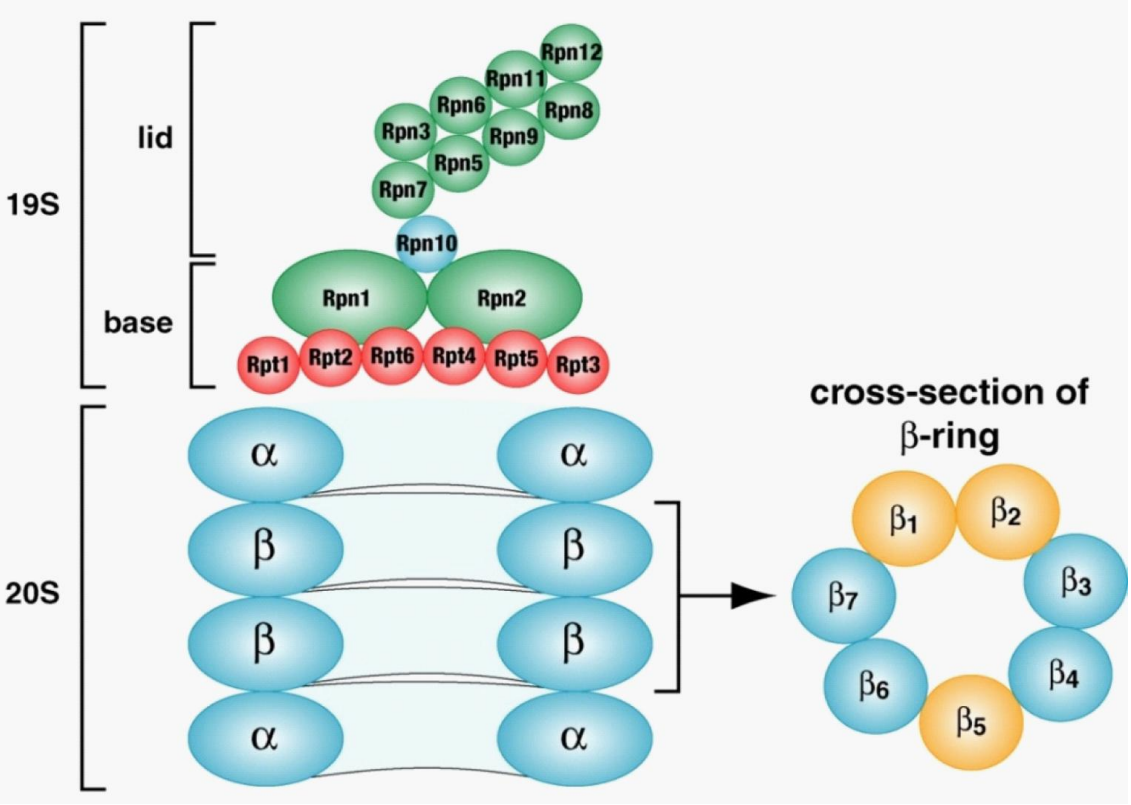

Figure 1.13 The 26S Proteasome in *Saccharomyces cerevisiae*

Schematic of the 26S proteasome in Saccharomyces cerevisiae, showing the 20S proteolytic core and one 19S regulatory particle. The ubiquitinated substrate binds to the 19S where the ubiquitin chain is removed. The 19S is composed of a "base" component and a "lid" component with nine non-ATPase subunits (Rpn3, Rpn5-9, Rpn11, Rpn12 andRpn15) in the lid and four non-ATPase (Rpn1, Rpn2, Rpn10 and Rpn13) and six ATPase subunits (Rpt1-6) in the base (shown in red). The C-termini of the ATPases dock into intersubunit pockets in the α-rings of the proteasome and open the gate for substrate hydrolysis by the 20S β subunits. Cross section of the β-ring reveals the positions of the caspase-like (β1), trypsin-like (β2) and chymotrypsin-like (β5) subunits (all shown in yellow). Polyubiquitinated proteins are tagged for degradation, recognized and unfolded by the 19S ATPases, and are

translocated to the 20S core. The 20S cleaves the protein into peptides and free ubiquitin is released[10].

1.12.5 Ubiquitin

All three catalytic sites are activated through cleavage of an N-terminal leader sequence that occurs during assembly of the proteasomal complex. The cleavage results in N-terminal threonine residues that exert the nucleophilic attacks on peptide bonds (Chen and Hoschtrasser, 1996). In addition, two less characterized proteolytic activities have been described, namely the "branched-chain amino acid preferring" (BrAAP) activity and the "small neutral amino acid preferring "(SNAAP) activity (Orlowski et a*l*., 1993). These additional activities are most likely accommodated by the already identified active β sites since the presence of additional proteases in the proteasome complex have been excluded by structural analysis (Groll et *al*., 1997), kinetic studies (Cardozo et *al*., 1999, McCormack et *al*., 1998) and site-directed mutagenesis (Dick et *al*., 1998). In the end the cleavage repertoire makes sure that virtually any peptide bond in a protein can be potentially digested, thus the active sites of the proteasome show how much broader specificity than their names reveal.

1.12.6 The 19S regulatory particle

The 19S proteasome regulates the entry of substrates targeted for degradation. It docks the 20S core protein and regulates the opening of a narrow hole of 10 Å (in diameter, a size that allows only unfolded protein to enter (Wenzel and Baumeister, 1995). The α-rings form the anterior chamber leading into the 20S, but without the association of the 19S regulatory protein with the N-termini of the α-subunits to serve as a plug to hold together the α3 subunits and keep the 20S core protein closed (Groll et *al*., 2003; Groll et *al*., 2000; Ciechanover, 2006; Ciechanover and Brundin, 2003). Electron microscopic

[10] *Adapted from Deriziotis and Tabrizi, 2008.*

studies revealed that the 19S regulatory particle is flexibly linked to the core protein and exerts wagging movement in an uncorrelated manner (Walz et *al*., 1998).

The 19S regulatory protein plays an important role in the recruitment of polyubiquitinated substrates, removal of polyubiquitin chains, as well as unfolding of protein substrates and their tethering into the 20S core chamber. The 19S regulatory protein can be subdivided into two sub-complexes, also known as the base and the lid. Using the nomenclature for mammalian proteasomes, the lid contains eight subunits: Rpn3, Rpn5, Rpn6, Rpn7, Rpn8, Rpn9, Rpn, and Rpn12 (**Figure 1.13)**. It has been suggested that the lid is required for proper protein degradation and substrate recognition. However, the precise role of the lid in the protein degradation pathway is unclear. Studies have also revealed some deubiquitination activity in the Rp11 subunit, suggesting that it is important for the removal of the ubiquitin chain prior to degradation (Verma et *al*., 2002; Yao and Cohen, 2002). The base of the regulatory protein contains nine subunits: Rpt1, Rpt2, Rpt3, Rpt4, Rpt5, Rpt6, Rpn1, Rpn2 and Rpn1 (**Figure 1.13)**. Rpt1-6 are ATPases associated with a variety of cellular activities (AAA), and form the ring entrance. AAA ATPases are known to be involved in protein remodelling and, in the context of the proteasome, it has been postulated that these subunits regulate unfolding and translocation of protein substrates into the proteolytically active chamber (Braun et *al*., 1999; Kohler et *al*., 2001). Rpt3 contains a polyubiquitin binding site that may be responsible for positioning the ubiquitinated substrate directly adjacent to the entrance (Lam et *al*., 2002). The two other base subunits, Rpn1 and Rpn2, are the largest subunits of the 19S regulatory particle and expose hydrophobic surfaces, possibly functioning as a scaffold for interacting proteins. Rpn1 has been shown in yeast to interact with UDP proteins such as Rad23 and Dsk2 (Elsasser et *al*., 2002).

1.12.7 The 11S regulatory particle

The formation of the immunoproteasome upon stimulation with IFNy stimulation involves the exchange of the 19S regulatory particle for another structure called termed the 11S regulatory particle or PA28 (Li and Rechsteiner, 2001). It has been shown that different complexes can be formed between the 20S core particle and either 19S or 11S regulatory particles (Tanahashi et *al*., 2000). Unlike the 19S particle, the 11S regulator contains two different types of subunits that form a hetero-hexameric ring structure that upon binding to the 20S is believed to open the entrance hole to the inner proteolytic chamber (Whitby et *al*., 2000). It has been shown that the *Drosophila* homologue of this regulator can modify the proteolytic activities of the proteasome (Masson et *al*., 2001).

1.13 The UPS and neurodegenerative disease

The UPS has been implicated in a range of neurodegenerative diseases, especially in conditions associated with the toxic accumulation of aberrant proteins that are prone to form potentially harmful aggregates. The importance of the UPS is highlighted by the direct relationship between onset of neurodegenerative diseases and perturbations in the UPS (Ciechanover and Schwartz, 2004; Rubinstzein, 2006). Many neurodegenerative disorders are characterised by the accumulation of ubiquitinated protein, suggesting that UPS dysfunction may play a prominent role in disease pathogenesis (Jung et *al*., 2009; Bedford et *al*., 2008). This accumulation of proteins may be caused by genetic or environmental factors, in combination with imbalances in anabolic and/or catabolic pathways in the cellular degradation system. Genetic mutation or environmental factors can lead to the production of proteins with different rates of degradation, or proteins with tendencies to form persistent cellular aggregates (**Figure 1.10).** Furthermore, disruption in gene expression also leads to accumulation of protein aggregates due to increased protein synthesis and reduced protein degradation by the 26S proteasome (Jung et *al*., 2009).

Intraneuronal aggregates contain ubiquitinated proteins and accumulation of these ubiquitinated aggregates is due to their impaired clearance by the proteasome.

UPS impairment is reported to be involved in aging, brain ischemia, Alzheimer's disease, Huntington's disease, Parkinson's disease and amyotrophic lateral sclerosis (ALS). Protein aggregation has recently been shown to directly impair the function of the UPS. Transient expression of two unrelated aggregation-prone proteins, a huntingtin fragment containing a pathogenic poly-glutamine repeat and a folding mutant of cystic fibrosis transmembrane conductance regulator, caused nearly complete inhibition of the UPS (Bennett et *al*., 2005; Bence et *al*., 2001). These data confirm a potential mechanism linking protein aggregation to cellular dysfunction and cell death. The link between the UPS and neurodegenerative diseases is further strengthened by observations that several mutations linked to neurodegenerative disease onset are found in genes that code for proteins involved in the UPS.

It has become increasingly evident that altered activities of the UPS are crucially involved in the pathophysiology of Huntington's disease, Parkinson's disease and spinocerebellar ataxia (Bence et *al*., 2001; Lindsten et *al*., 2002) (Ciechanover and Brundin, 2003). UPS impairment has also been studied in cell culture and animal models overexpressing mutant huntingtin protein (Lindsten et *al*., 2003) and consistent with data proposing a protective effect of aggregation due to sequestration of toxic species, treatment with a compound that increases inclusion formation prevents hungtingtin-mediated proteasome inhibition (Bodner et *al*., 2006). Global changes in the UPS were reported in HD, early in the disease course in both R6/2 transgenic model as well as in HD patient (Bennett et *al*., 2007), suggesting that impairment may be occurring at the level of ubiquitin turnover rather than impairment of proteolytic function. However, the lack of a reporter indicating UPS dysfunction in a Huntington's disease mouse model (R6/2) crossed to GFPu mice may be indicative of a more complicated relationship between overexpression of mutant polyglutamine proteins and UPS function (Bett et *al*., 2009).

Mutations in Parkin, encoding an ubiquitin-E3 ligase result in juvenile recessive PD (Dawson and Dawson, 2003). Decreased proteasome activity has been suggested as a cause of aggregation and Lewy body formation in Parkinson's disease. This hypothesis is supported by the observation that yeast models of Parkinson's disease are more susceptible to toxicity caused by α-synuclein, the major protein component of Lewy bodies, under conditions of low proteasome activity. Bedford et al reported data describing the link between the 26S proteasome dysfunction and the development of alpha-synuclein neuropathology (Bedford et *al*., 2008). In the study, they genetically ablated a critical 19S/PA700 subunit in the forebrain, and thus, prevented the formation of the 26S proteasome. A recent description of Usp14, a proteasome-associated deubiquitinating enzyme has been reported to inhibit the degradation of ubiquitin-protein conjugates in both *in vitro* and *in vivo* (Lee et *al*., 2011), suggesting that inhibition is mediated by the trimming of the ubiquitin chain on the substrate.

1.14 The UPS and prion diseases

Prion infection is known to cause neuronal loss in the brain, but the molecular basis of prion neurotoxicity remains unknown. Significant evidence exists as to the involvement of UPS dysfunction in the pathogenesis of prion disease. Study by Bedford and colleague, shows evidence of a dysfunction of the 26S proteasome in the development of alpha-synuclein neuropathology in genetic mouse model using the Cre/Ioxp system (Bedford et *al.*, 2008). Prion-infected cells are significantly more susceptible to apoptosis when treated with low levels of proteasome inhibition, accompanied by an accumulation of large cytosolic perinuclear PrP^{Sc} aggresomes (Kristiansen et *al*., 2005). Proteasomal activity is significantly decreased in prion-infected cells and in brain regions exhibiting significant neuropathology in prion-infected mice (Kristiansen et *al*., 2007). This finding established a solid link between UPS impairment and neurodegeneration associated with prion infection. Both PrP^{Sc} and recombinant forms of PrP containing large amounts of β-sheet structure inhibit the 26S proteasome directly *in vitro* (Kristiansen et *al*., 2007). Pre-incubation with

an anti-oligomer antibody or heat denaturation of PrP^{Sc} alleviates this inhibitory effect (Kristiansen et *al*., 2007). It has been reported that increased levels of ubiquitin conjugate, which correlate with decrease proteasome function accumulate in the brain of mice infected with prion (Kang et *al*., 2004). Most recently, Deriziotis and colleagues reported an accumulation of UPS substrate in prion infected mouse brains, suggesting impairment of the 26S proteasome (Andre and Tabrizi, 2012; Deriziotis et *al*., 2011). However, other studies by Quiaglio and colleagues revealed that transgenic mice expressing a non-infectious mutant form of PrP associated with certain inherited human prion diseases do not show UPS impairment (Quaglio et *al*., 2011).

1.15 The Ub^{G76V}-GFP reporter mouse model

In order to understand the precise role of the UPS under pathological conditions, the development of fluorescent-based reporters for monitoring the function of the pathway and quantifying proteolytic activities of substrate in mouse models is imperative. The major work of this thesis is based on a particular green fluorescent protein (GFP) proteasome substrate that allows monitoring of the UPS (Dantuma et *al*., 2000). GFP is a small soluble protein of 26 kDa that originates from the jellyfish *Aequorea victoria.* Well established in the literature, it does not have any known interacting partners is relatively well tolerated at high concentrations in mammalian cells, and is very stable (Tsien, 1998). The generation of the fluorescent reporter system in both cell line and transgenic model has made it possible to monitor the functionality of the UPS (Tsien, 1998). Furthermore, the development of fluorescent proteasome inhibitors has allowed specific labelling of proteasomes *in vitro* and *in vivo* (Dantuma et *al*., 2000). GFP reporters were initially characterized and used for studies in cellular systems but more recently development of a transgenic mouse model constitutively expressing the GFP reporter was developed. Subsequently, the use of these models has allowed the investigation of the effect of proteotoxic stress condition in the degradation of different proteasomal substrates (Verdoes et *al*., 2006; Menendez-Benito et *al*., 2005) and to gain insight into the

mechanisms contributing to the long-term accumulation of deleterious proteins during proteotoxic stress (Menendez-Benito et *al*., 2005).

The Ub^{G76V}-GFP proteasome substrates were generated by insertion of different N-end rule of UFD degron that converted GFP into a substrate of the UPS. Ubiquitin is recognised as a degradation signal leading to ubiquitylation within the ubiquitin moiety and subsequently lead to the degeneration of the UFD containing protein (Dantuma et *al*., 2000). Degradation of the substrates results in low basal fluorescence intensities, with pharmacological inhibition of the proteasome leading to the accumulation of GFP-fluorescent cells that can be monitored by fluorescence microscopy, flow cytometry and fluorimetry. Although the ubiquitination of GFP by the N-end rule and UFD degrons rely on different enzymes, both pathways converge at the level of the proteasome. This implies that these reporters cannot be used to test the individual catalytic activities of the proteasome, but rather monitor the general status of the UPS. The Ub^{G76V}-GFP reporters have proven their general applicability in several species including mammals (Dantuma et *al*., 2000, Lindsten et *al*., 2002; Myung et *al*., 2001; Verhoef et *al*., 2002) *Drosophiia* (Lundgren et *al*., 2003) and yeast (Heessen et *al*., 2003; Heessen et *al*., 2002).

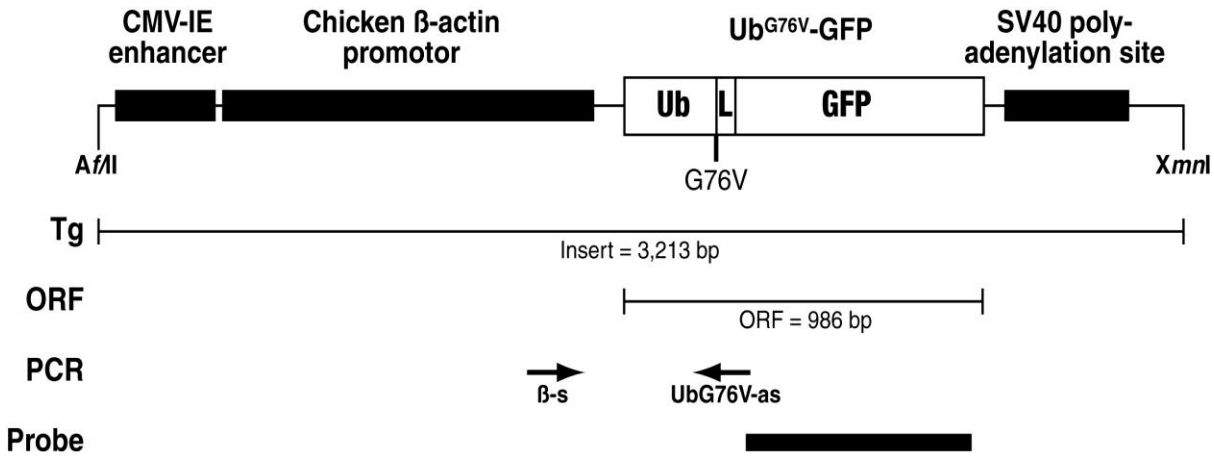

Figure 1.14 Generation of Ub^{G76V}-GFP transgenic mice.

For generation of N-end rule of substrates ubiquitin was cloned in frame with GFP so that cleavage by UCH exposes the amino acid on the N- terminus. Ubiquitin fused GFP is expressed in living cells. Upstream of the promoter, the GFP substrate is fused to a mutant ubiquitin moiety. GFP reporter mice were designed to study proteasome inhibition. The transgene has a Cytomegalo virus (CMV) early enhancer upstream and chicken beta actin promoter. Upstream of the promoter the GFP substrate is fused to a mutant ubiquitin.

The Ub^{G76V}-GFP reporter mouse model was generated from a chicken ß-actin promoter with a cytomegalovirus (CMV) immediate early enhancer, which is a promoter complex that is known to induce a constitutive expression (**Figure 1.14)** (Okabe et *al*., 1997). Indeed the transcript of the GFP reporter could be detected in all tissues examined (Lindsten et *al*., 2003). However, inhibition of proteolysis is required in order to detect the Ub^{G76V}-GFP protein. Studies in primary cultures of fibroblasts and other cells demonstrated a clear dose-dependent accumulation of the GFP reporter in response to inhibition treatment. The functionality of the reporter was also confirmed *in vivo* by intraperitoneal injections with the different proteasome inhibitors MG-132, MG-262 and epoxomicin (Lindsten et *al*., 2003). A dramatic accumulation of GFP occurred in the liver, which is in line with previous data showing that proteasome inhibitor treatment of drug-primed mice

induces hepatotoxicity in the form of accumulation of Mallory bodies (French et *al*., 2001). Other studies have been done on the generation of related reporter substrates. Bence and colleagues described a GFP reporter that is targeted through a short hydrophobic sequence (Bence et *al*., 2001), which was originally identified in a screen for degrons in yeast (Gilon et *al*., 1998).

The particular Ub^{G76V}-GFP construct was chosen based on its destabilizing and well tolerated effect in tissue culture. The Ub^{G76V}-GFP reporter mouse was the first *in vivo* model developed to investigate proteasomal degradation. It provides an excellent tool for studying the UPS in human disorders, especially neurodegenerative diseases characterized by pathologic accumulation of misfolded and aberrant proteins, which are potentially proteasome substrates. Previously, it has been shown that the functional analysis of the UPS can be accomplished by monitoring steady state levels of fluorescent reporter substrates (Salomons et *al*., 2005; Bence et *al*., 2001; Dantuma et *al*., 2000). The availability of the GFP reporter Ub^{G76V}-GFP reporter mouse model has been instrumental for the studies presented in this thesis, since it allowed a direct monitoring of the UPS dysfunction in *vivo* and neuro-pathological conditions associated with prion disease. The work described in this thesis shed light on understanding the role of UPS impairment in the pathogenesis of prion disease.

1.16 Aims

- To generate both lines of the Ub^{G76V}-GFP reporter mouse and characterize the Ub^{G76V}-GFP reporter in primary neurons;
- To investigate whether dysfunction of the ubiquitin- proteasome system (UPS) can be detected in RML prion infected Ub^{G76V}-GFP reporter mice;
- To sequentially monitor UPS impairment *in vivo* over the time-course of prion infection and determine whether it is an early or late event;
- To assess behavioural phenotype and motor skills deficits in the Ub^{G76V}-GFP reporter mice following RML prion infection.

2 MATERIALS AND METHODS

2.1 Ub^{G76V}-GFP reporter mice

Breeding pairs of Ub^{G76V}-GFP1 and Ub^{G76V}-GFP2 mice were provided by Professor Nico Dantuma at the Karolinska Center for Transgenic Technologies, Sweden (Lindsten et al., 2003). They were provided as hemizygotes that had been back-crossed for approximately 30 generations to a C57BL/6N background using both males and females. The mice were subsequently bred in-house at the MRC Prion Unit Biological Safety Facility (BSF).

2.1 Animal care

All work with animals conformed to United Kingdom legislation and institutional guidelines for animal welfare. The mice were housed at an appropriate temperature (22°C) in a light-controlled room (12-hr light/dark cycle), and kept in groups of four to six per cage. All animals had free access to food and water.

2.1.2 Genotyping

Mice were genotyped by PCR of genomic DNA isolated from ear biopsies taken from each individual animal. Ear biopsies were taken at three weeks of age. They were digested at 55°C overnight in a solution containing 49 µl Direct PCR lysis reagent (Viagen Biotech) and 1 µl proteinase K (PK) (21mg/ml) (Roche). The lysates containing genomic DNA were then incubated at 85°C for 45 min and briefly centrifuged.

PCR was performed on the genomic DNA using oligonucleotide primers specific to the Ub^{G76V}-GFP construct. A PCR stock solution was made containing 12.5 µl of 1x REDTaq ReadyMix PCR Reaction Mix with $MgCl_2$ (Sigma), and 1 µM each of the forward and reverse primers. The stock solution was added to individual reaction tubes, followed by the addition of 2 µL genomic DNA to a final volume of 25 µl of solution. The samples were

subjected to cycling temperatures of 94°C for 30 sec, 58°C for 30 sec and 72°C for 1 min, for 36 cycles. The PCR product was loaded onto a 1.25 % agarose gel or stored at 4 °C until ready for loading into gel.

Primers were designed using Primer Express software (Applied Biosystems). Ub^{G76V}-GFP primer sequences were: forward primer 5' CCT ACA GCT CCT GGG CAA CGT 3'; reverse primer 5' TCG ACC AAG CTT CCC CAC CAC 3'). β-actin primer sequences were: forward primer 5' ACC AGG GTG TGA TGG TGG GAA 3'; reverse primer 5' AGC CAG GTC CAG ACG CAG GAT 3').

Agarose gel electrophoresis was conducted using 1.25 % agarose in 1x TAE buffer, pH 8.0. Ethidium bromide was added to the mixture to visualise the gel. The mixture was poured into a mini-gel system with appropriate fitted combs (Thermo Fisher). Twenty five microlitres of PCR solution was loaded into each well. To confirm the 300 base pair size of the product, 10 µl of TrackIt 1000 bp DNA ladder (Sigma) was added to a single well. The gel was run at 90 volts for 20-25 min. The gel was examined on a BioRad Gel Doc 1000 imaging system under UV light to evaluate sample integrity. Gels were photographed and analysed using Quantity One software (BioRad).

2.2 Inoculation of mice with RML prions

2.2.1 Preparation of inocula

Inocula were made from homogenised brain tissue. Frozen brains were transferred to a Petri using clean a disposable forceps and 1 ml of sterile 1X PBS was added to the brain immediately. Homogenisation was done using a tissue RiboLyser (Eppendorf). Screw cap tubes filled with small clean ribolysing beads were weighed and samples were ribolysed at a speed of 6.5 for 45 seconds; 10 % (w/v) tissue homogenates were prepared.

2.2.2 Prion infection of mice

Mice were inoculated intracerebrally (ic) between the midline of the two hemispheres with 30 µl 1% (w/v) RML (Rocky Mountain Laboratories) brain homogenate, or 30 µl 1% (w/v) I7723 normal CD-1 brain homogenate as control. All mice were monitored on a daily basis and subsequently examined for clinical signs of scrapie-like disease.

2.2.3 Timed-culls of mice

Following inoculation, a series of timed culls were carried out at days 45, 85, 105, 125, 145 and 165 post-inoculation until end-stage disease. Early indicators for the onset of disease include erect ears, rigid tail, piloerection, ungroomed appearance and a hunched posture. However, a definitive diagnosis was not made until a confirmatory sign was seen, such as ataxia, limb paralysis, ruffled fur and generalised tremor. Animals were culled by an authorised **Schedule 1 procedure** (Animals Scientific Procedures Act 1986) using a sealed chamber with a rising concentration of CO_2 for 5 min, followed by confirmation of death by cervical dislocation.

2.2.4 Tissue handling and collection of samples

All procedures were carried out in a microbiological containment level III facility and strict safety protocols were followed. Tissue was harvested from animals immediately after they were culled. The brains were separated into right and left hemisphere. The left hemisphere was fixed into buffered formalin, whilst the right hemisphere was snapped-frozen in iced cold isopentane and stored at -80 ^{o}C.

2.3 Primary cell culture

Adult pregnant mice were culled at gestation day 16, as described above. An incision was made along the length of the abdomen and the surrounding skin dissected away to expose the embryonic sac. Individual embryos were removed and kept on ice. The head was removed from the embryo and pinned by the nose to a wax-filled Petri dish. Dissected cortices were then placed in a dish containing ice-cold medium NeuroBasal medium supplemented with B27 supplement, 1% 200 mM L-glutamine, 1% penicillin (5000 U/ml)/ streptomycin (5000 μg/ml) and 5% foetal bovine serum (FBS). Cortices were dissociated using a sterile surgical scalpel blade, then triturated through a series of three flamed glass pipettes with different diameters to produce a single-cell suspension. The suspension was allowed to settle by gravity for 1 min to reduce un-dispersed clumps. The supernatant was transferred into a fresh tube and centrifuged at 350 xg for 5 min. The resultant cell pellet was resuspended in pre-warmed culture medium, as above.

Culture plates, or glass coverslips placed in 6-well tissue culture plates, were coated with 1 % poly-L-lysine (1mg/ml) at room temperature for 10 min. Excess poly-lysine was then removed and the coverslips were washed three times in sterile water. The coverslips were left to dry in a sterile environment for at least 2 hr prior to use. Single cell suspensions were counted using a haemocytometer. The cells were seeded at a density of 1.125×10^5 cells cm^{-2} onto poly-L-lysine plated plates. Cultures were incubated at 37°C in a humidified, 5% CO_2 incubator. After two days of culture, the cultures were given a full media change and a half media change every 4-5 days thereafter.

2.4 Immunocytochemistry

Primary cortical neurons were fixed onto coverslips with 4 % paraformaldehyde (PFA) for 20 min at room temperature. They were washed three times with D-PBS and permeabilised at -20 °C with pre-cooled 100 % methanol for 15 min. They were then washed with 1x PBS and the cells were blocked with 10 % bovine serum albumin (BSA) (Sigma) for 1 hour at 37 °C. Coverslips were incubated for 1 h at 37 °C with primary antibodies diluted in 1x PBS (**see Appendix I**). Alexa-fluor secondary antibodies diluted into 1x PBS was added onto each coverslip and incubated for 1 hour at 37 °C in the dark. Following incubation, a series of three washes were carried out with 1X PBS. Coverslips were mounted onto Superfrost Plus slides (Thermo Fisher) using mounting medium (Dako) and left to dry in a cool dark place.

Confocal microscopy was used to obtain fluorescence images. The confocal microscope (Zeiss microscope LSM510 META) was equipped with 'plan-Apochromat' 63 x/1.40 Oil DIC objective and was controlled by Zeiss LSM software. Fluorescence was recorded at 488 nm using 30 mW Ar-laser for excitation or at 543 nm using 1 mW HeNE-laser for excitation. Zeiss Imersol™ was used as the imaging medium.

2.5 Immunohistochemistry

For histological studies, half-brains were fixed in buffered formalin for at least 72 hours and up to a maximum of seven days. The sections were dehydrated and then embedded in a paraffin block by the MRC Prion Unit Histology staff. Sagittal serial sections were obtained from each block, cut at a standard thickness of 3-5 µm. Sections were mounted on Superfrost slides (Thermo Fisher), and allowed to dry at room temperature for 2 hours and then overnight at 60 °C. For a list of the antibodies used, see **Appendix I**.

2.5.1 Immunostaining for PrP

For anti-PrP staining, sagittal sections were first de-waxed and re-hydrated through two washes with xylene and three washes with decreasing concentrations of ethanol. Sections were then washed in water and treated with 98 % formic acid for 5 min and boiled in EDTA-Tris-citrate buffer pH 7.8 for 25 min.

The buffer solution was transferred to the pressure cooker, the temperature was set on high (setting 10) and the buffer brought to boil. Sections were then placed in the boiling solution allowing full pressure to be reached in the cooker with the lid completely sealed. The heating time began only when full pressure was reached. After a constant jet of steam was emitted, the heat on the electric hotplate was reduced to setting 7 and the pressure in the cooker was released immediately; a timer was set for 3 min. After the cooker was depressurised, the electric hot plate was turned off. An additional 3 min was timed; the cooker was then transported to a nearby sink and put under cold running water.

Immunohistochemical staining was performed using a Ventana Medical Systems, USA. PrP deposition and distribution were visualised using an anti-PrP monoclonal antibody, ICSM35 (1:3000) (D-Gen), and a rabbit anti-mouse secondary antibody (Asante et *al*., 2002).

2.5.2 Immunostaining for GFP and ubiquitin

For GFP and ubiquitin stainings, the sections were not pre-treated; however, antigen retrieval was done through enzymatic digestion and standard citrate buffer. For primary antibody, either a rabbit polyclonal anti-GFP antibody (Invitrogen) was used, followed by a swine anti-rabbit secondary antibody (1:200). Intracellular ubiquitin deposits were detected using a monoclonal anti-ubiquitin antibody (1:10:000) (Santa Cruz, Biotechnology) and a rabbit anti-mouse secondary antibody was used after a treatment of a citrate buffer (MCC2) pH 6.

All immunohistochemistry was carried out using Ventana Discovery or Benchmark automated systems, following manufacturer's instructions (Ventana Medical Systems). Reagents supplied including a DAB Map kit designed for automated immunohistochemistry for detecting antigen localization in paraffin-embedded tissue section. The DAB Map Kit contains a series of antigen detection reagents such as diaminobenzidine (DAB), horse radish peroxidise (HRP), copper sulphate and inhibitor D for reducing endogenous peroxidise activity. An *i*View DAB Detection Kit was also used; it is an indirect biotin streptavidin system for detecting mouse IgG, mouse IgM and rabbit primary antibodies. The *i*View DAB Detection Kit contains; inhibitor (3 % hydrogen peroxide solution), SA-HRP (a conjugated streptavidin horseradish peroxidase, H_2O_2 (.04 %-.08% hydrogen peroxide in a phosphate buffer solution, DAB substrate; diaminobenzidine, copper sulphate. The *i*View DAB Detection Kit uses an indirect method to visualize specific antibodies bound to antigens by depositing a brown colour precipitate. Bluing reagent, a strong alkaline reagent help interpret the result as it blues the haematoxylin stained sections on the glass. Counterstains, haematoxylin and bluing reagent work through the combined effect of lithium ions for the staining of cellular nuclei. A signal amplification technique was used to enhance the sensitivity of GFP staining (Ventana Medical Systems).

2.5.3 Immunostaining for GFAP

Gliosis was detected with anti-glial fibrillary acidic protein (anti- GFAP) rabbit polyclonal antiserum (1:1000, Dako) at 42° C for 32 min using the Ventana automated immunohistochemical system Sections for GFAP were not pre-treated, but antigen retrieval was done with protease 3 and mild citrate buffer. The enzymatic digestion method involved a process of dewaxing, rehydration and rinsing the sections under running water. The slides were then re-equilibrated in mild or standard citrate buffer and incubated for 2 to 6 min protease level 1 or level (Ventana Medical Systems). Antigen retrieval was either done with a strong protease (protease 1), an alkaline protease solution for strong

enzymatic treatment (0.55 ±.1 acidic units/ml), or protease 3, a mild alkaline protease treatment (0.02 ±.0075 units/ml). Sections for GFAP staining were treated with protease 3.

The sections were counterstained with haematoxylin for 5 min and a bluing reagent was used as post-counterstain. A basic diaminobenzidine (DAB) detection kit was used according to the manufacturer's instruction (Ventana Medical Systems).

2.5.4 Immunostaining for NeuN and synaptophysin

For the labelling of neurons and synapses, sections were placed in a stainless steel tray, de-waxed and, re-hydrated through three washes of xylene, two washes of 100 % ethanol through one wash of 90 % and one wash of 70 % ethanol. The slides were then rinsed in cold running water. The slides were submerged in one litre of 1 M EDTA pH 7.8 and microwaved for a period of 25 min in maximum power. After the microwave treatment, the sections were washed in cold dH_20 before proceeding with immunostaining.

Either a monoclonal neuronal nuclei (NeuN) antibody was used (1:2000) (Chemicon) for 32 min or a monoclonal anti-synaptophysin (Zymed) was used and a rabbit anti-mouse secondary antibody (1:200) (Dako) using the Ventana automated system. To visualise neurons, basic diaminobenzidine detection system was used according to the manufacturer's instruction (Ventana Medical Systems, USA).

2.5.5 Light Microscopy

Light micrographs of histological areas of interest were taken using a light microscope (Zeiss), attached to a digital camera on an ImageView digital microscope. Images were analysed with the help of Professor Sebastian Brandner in the Department of Neuropathology at the UCL Institute of Neurology.

2.6 Immunoblotting

2.6.1 Preparation of homogenates

Tissue was homogenised in 100 mM Tris.HCl, pH 7.4, 300 mM NaCl, 4 mM EDTA, 1 % Triton-X-100, 1% deoxycholate using sequentially narrower syringe needles. Homogenates were treated with 50 U/ml benzonase for 20 min on ice. An aliquot was removed for protein assay to ensure equal loading. For PrP^{Sc} western blots, proteinase K was added to a final concentration of 50 μg/ml for 30 min at 37 °C. Samples were then centrifuged at 16,000 x*g* for 1 min to pellet cellular debris. Digestion was ended in samples by adding 8 mM AEBSF. An equal volume of 2 X reducing sample buffer was added to each sample (125 mM Tris, pH 6.8, 20 % glycerol, 0.05 % bromophenol blue, 4 % SDS), which were then boiled at 100 °C for 10 min prior to use or storage.

2.6.2 BCA protein assay

A bicinchoninic acid (BCA) protein assay reagent kit (Pierce) was used to detect and quantify the total of protein in tissue homogenate. The BCA assay is based on the ability of the protein to reduce Cu^{2+} to Cu^{+} in an alkaline environment. Protein standards were prepared with bovine serum albumin (BSA) in the same diluent as the unknown sample. A series of 0, 25, 50, 100, 150, 200 and 250 μg standards were used. Twenty five microliters of each standard or unknown sample was pipetted into a 96-well plate in triplicate. Two hundred μl BCA working reagent was then added to each well and mixed gently for 30 seconds follow by a 25 min incubation at 37^{o} C. The plate was analysed using a plate reader (Tecan), with the absorbance filter set at 570 nm.

2.6.3 SDS-Polyacrylamide gel electrophoresis (SDS-PAGE)

Samples in 1x reducing sample buffer were centrifuged at 16,000 x *g* for 1 min, briefly vortexed, and finally spun again at 16,000 x *g* for 1 min. Samples were loaded on to pre-cast 16% Tris-Glycine mini gels (Novex, Invitrogen). They were electrophoresed vertically in tris/glycine SDS running buffer (National Diagnostics) in X-Cell Mini-Cell system (Invitrogen) apparatus at 200 V for 90 min. Pre-stained Seeblue (Invitrogen) or Precision (BioRad) protein standards were used as a molecular weight marker.

2.6.4 Electroblotting

SDS-PAGE protein samples were transferred onto PVDF membrane (Immobilon). Membrane was pre-cut at the same size as the gels and pre-soaked in 100% methanol for 2 min to ensure even hydration prior to transfer. Proteins were transferred from the gel to the membrane in X-Cell II Blot modules (Invitrogen) and blotting buffer (National Diagnostics) at either 35 V for 90 min or 14 V overnight.

2.6.5 Dot blotting

Protein samples were prepared in 1x reducing samples buffer, as above. Fifteen micrograms of each sample was placed into a 96-well plate in triplicate and kept on ice. BioRad Bio-Dot microfiltration apparatus were assembled with a sheet of nitrocellulose membrane and 5-6 sheets of filter papers that had been pre-wetted in 1x TBS. A gasket was aligned above the support plate and placed over a vacuum reservoir, and the apparatus attached to a three-way flow valve. Samples were loaded into the 96-well frame of the Bio-Dot apparatus and incubated at room temperature for 30 min. The flow valve was then adjusted to apply a vacuum to draw any remaining sample on to the membrane. The membranes were washed under vacuum suction twice with 1x TBS, following which the membrane was removed from the apparatus.

2.6.6 Immunodetection

After electroblotting, membranes were transferred to an appropriately sized container and washed in either 1x PBS or 1x TBS. Blots were then blocked for 1 h at RT with gentle agitation using either 5 % non-fat milk powder (Marvel) diluted in 1x PBS-T (1x PBS, 0.5% Tween-20), or Li-Cor blocking buffer (Li-cor Biosciences) diluted in an equal volume of 1x PBS. Incubation with the appropriate primary antibody (see **Appendix I**) diluted in either 1 % non-fat milk or Li-Cor blocking buffer diluted in an equal volume of 1x PBS-T was done with gentle agitation overnight at 4^{o} C. The membranes were then washed in 1x PBS-T for a minimum of 45 min, changing the buffer five times. The membranes were incubated with an appropriate secondary antibody (see **Appendix I**), diluted in 1x PBS-T, for 45 min at room temperature. The membranes were then washed in 1x PBS-T for a minimum of 1 hr, changing the buffer ten times.

Detection of alkaline phosphatase bound antibody was performed using Tropix CDP-star (DAB) (Applied Biosystems), according to manufacturer's instructions. Excess reagents were poured off and the membranes were placed between acetate films and transferred to a photographic cassette. Biomax MR films (Kodak from Anachem) were developed using Kodak developer and fixer by hand or by using a Xograph imaging machine (Xograph Imaging Systems). Developed films were scanned using an Epson scanner for electronic format and densitometry of digital images was achieved by using ToolLab 1D Gel analysis software. Detection of LI-COR antibodies was done by scanning the membrane using the Odyssey Infrared Imaging System and software (Li-cor Biosciences). For stripping and re-probing of membranes, Re-Blot Plus Western Blot Strong Antibody Stripping Solution was used, following manufacturer's instructions (Millipore).

2.7 Fluorogenic assays for proteasome activity

A protocol was used as described previously (Berkers *et al.*, 2005; Dantuma *et al.*, 2000; Kisselev and Goldberg, 2005). Homogenates were prepared, as described above, in 50 mM Tris-HCl pH 7.4, 2 mM ATP, 5mM $MgCl_2$, 250 mM sucrose. A small aliquot was taken for protein content determination by BCA assay and 1 mM DTT was added to the remaining sample. To control for non-specific peptide hydrolysis, an aliquot of sample homogenate was incubated with the specific proteasome inhibitor 50 µM epoxomicin for 30 min at 37°C. Proteasomal activity was measured in 10 µg of protein incubated with 100 µM fluorogenic substrates (Ac-nLPnLD-AMC for caspase-like activity (Bachem); Suc-LLVY-AMC for chymotrypsin-like activity (Enzo Life Sciences); Boc-LRR-AMC for trypsin-like activity (Enzo Life Sciences), and 50 mM Tris.HCl pH 7.4, 5 mM $MgCl_2$, 2 mM ATP, 1 mM DTT, to a final volume of 100 µl. Samples were incubated for 1 hr at 37 °C and the release of 7-amino-4-methylcoumarin (AMC) was monitored continuously every minute at 360 nm excitation and 465 nm emission using a TECAN 96-well plate reader.

2.8 Behavioural assessments

Behavioural testing was performed on groups of fifteen age-matched Ub^{G76V}-GFP mice. Mice were grouped house prior to individual experiment and were monitor daily. Mice were inoculated soon after they were weaned; fifteen mice were inoculated with RML prions and fifteen mice were inoculated with control brain homogenate (CD1). Testing was initiated twenty days following inoculation. Mice were tested within a conserved ~3 hour time period in the morning. All protocols using these mice were first approved by the animal committee, and official approved procedures were followed for the care and use of these mice. Experimental room environment was kept constant between test sessions with respect to temperature humidity and light intensity.

2.8.1 Nesting

Testing was followed as described previously (Deacon et *al*., 2001). Ub^{G76V}-GFP mice were kept in groups of 4 or 5 mice per cage prior to testing. Nesting assessments were carried out for period of fourteen weeks, starting at day 20 post-inoculation. For an accurate assessment of nest building, the mice were single-housed for 24 hr and then regrouped after testing. Nesting material was placed in clean cages, positioned at the end of the cage opposite the mouth of the water bottle. A square compact nest was put into the cage. The following morning, an assessment of the nest was made, and a grade was given to each mouse base on the amount of material shredded, the neatness of the nest and the height of the nest. A grade of (1) = nestlet not touched (more than 90% intact); grade (2) = nestlet partially torn (50-90% remain intact); grade (3) = nestlet mostly shredded (less than 50 % remain intact); grade (4) = nestlet mostly torn and the material gathered into a flat nest; and grade (5) = nestlet nearly perfect, made into a crater with wall matching mouse body. Images were photographed of each scored nest.

2.8.2 Burrowing

Testing was followed as described previously (Deacon et *al*., 2001; White et *al*., 2008). Ub^{G76V}-GFP mice were housed individually for the duration of the burrowing assessment. A one-end closed opaque plastic tube (250 ml in length and 55 mm in diameter) was filled with 200 g of food pellets of normal food diet and placed into a clean cage. The cylindrical-shaped tube was left overnight for mice to burrow the pellet out. The next morning, assessment was made by measuring the weight of the pellets displaced from the tube.

2.8.3 Grip Strength

Grip strength apparatus were calibrated for each trial. Mice were lifted and held by the tail so that their forelimb could grasp a wire grip. The mice were then pulled backward by the tail with their posture parallel to the surface of the table until they release the grid. The peak force applied by the forelimbs of the mouse was recorded in g. Each mouse was tested three times, and the average value obtained. The mouse body weight was measured. The mean of the three grip-strength measurements was used against the body weight to obtain the grip measurement.

2.8.4 Rotarod

A rotarod apparatus (UGO Basile) with a rotating cylinder of 3 cm diameter was used, with assessments done for a period of ten weeks, starting at day 45 post-inoculation. Mice were placed on the stationary rod and allowed to become familiar with the environment for one minute before the rod motor was engaged. On each day of testing, each mouse was tested for three trials with a 10 min inter-test resting period. Mice were tested within a conserved 3 hr time period in the morning. Mice were trained for 3 consecutive days prior to the first official testing date by repeatedly placing the mice on the rod until they were able to remain on the rod. Each mouse was held by the tail and placed on the rotating (4 r.p.m.) rod in such a way to walk forward on it. After 5 s the rod was accelerated at a constant speed of 20 r.p.m./min and the speed and time at which the mouse fell off were noted. Each mouse received three trials per session. The mean speed for each mouse was taken and analysed.

2.9 Statistical analysis

Data were expressed as standard deviation (SD) and analysed by Student' T-test or Two-way ANOVA with Bonferroni post-test. Significance was expressed as follows: $P<0.05$*; $P<0.01$**; $P<0.001$***, unless otherwise specified **Appendix IV**.

3 GENERATION AND PRION INOCULATION OF Ub^{G76V}-GFP REPORTER MICE

3.1 BACKGROUND

The functional state of the UPS can be monitored by steady state levels of a fluorescent reporter substrate (Dantuma et *al*., 2000). The Ub^{G76V}-GFP construct comprises a form of ubiquitin (G76V) fused to the N-terminus of GFP. When expressed in cells, Ub^{G76V}-GFP is poly-ubiquitinated at both its lysine 29 and lysine 48 residues, under normal cellular conditions it is targeted for degradation by the 26S proteasome (Bence et *al*., 2001; Cheroni et *al*., 2009). Fluorescent reporters have been expressed to study the function of the UPS in cells (Lindsten et *al*., 2003). Such cell models can be maintained at a lower cost, are quick to work with and provide high volumes of data. However, unlike transgenic animals, cell lines do not necessarily provide a full picture of complex diseases, thereby, cannot be used to study tissue specific responses involving changes of the UPS. The Ub^{G76V}-GFP reporter transgene, consists of ubiquitin (G76V) protein substrates, has been applied to the generation of animal models for in-depth study of the UPS. In this thesis, the first transgenic mouse model (Ub^{G76V}-GFP reporter), based on the ubiquitous expression of (G76V) protein substrates, developed for monitoring UPS degradation *in vivo,* has been used.

This mouse model allows a direct monitoring of UPS dysfunction in mice inoculated with RML prions to determine its possible correlation with disease pathogenesis. The Ub^{G76V}-GFP reporter mouse is based on the constitutive expression of a Ub^{G76V} substrate, which was selected because of its half-life degradation rate and low toxicity in cell culture. The Ub^{G76V}-GFP reporter mouse model consists of a Ub^{G76V}-GFP transgene, expressed from a chicken β-actin promoter with a cytomegalovirus (CMV) immediate early enhancer from the pCCALL vector excised using *Sca*I and *Hind*III, and cloned blunt-ended in the *Nhe*I site

located upstream of the Ub^{G76V}-GFP open reading frame (Lindsten et *al*., 2003). High constitutive expression is normally detected in all tissues (Okabe et *al*., 1997). Other mouse models for monitoring the UPS function have been developed, one of them is based on xenografts of UFD-luciferase reporter-expressing human cell lines in nude mice (Berkers et *al*., 2005; Luker et *al*., 2003). The Ub^{G76V}-GFP reporter mice are available as two lines: Ub^{G76V}-GFP1 and Ub^{G76V}-GFP2. These lines were characterised for the presence of the transcript, which was seen in all examined tissues including lung, spleen, small intestine, muscle, heart, kidney, pancreas, liver, testis and brain (Lindsten et *al*., 2003). Since its development, the usage of the Ub^{G76V}-GFP reporter mice has increased as UPS dysfunction has been increasingly reported to be linked with different neurodegenerative diseases (Cheroni et *al*., 2009; Rubinsztein, 2006). Indeed, the Ub^{G76V}-GFP transgenic mouse model appears to be an excellent tool to monitor the functionality of the UPS *in vivo*.

Work in this chapter presents the breeding and characterisation of the two lines of the Ub^{G76V}-GFP reporter mice, Ub^{G76V}-GFP1 and Ub^{G76V}-GFP2. These mice were exposed to RML prions to check their susceptibility to prion infection in a manner, similar to that in their non-transgenic counterparts. Brain tissue from RML-infected Ub^{G76V}-GFP1 and Ub^{G76V}-GFP2 mice at end-stage disease was analysed for the presence of typical pathological markers of prion disease, PrP^{Sc} and GFAP. The presence of the Ub-GFP reporter was also investigated, thereby confirming previous observations using a different prion strain (Kristiansen et *al*., 2007), and the suitability of the model for use in investigating the UPS throughout the course of prion disease pathogenesis.

3.2 AIMS

- To breed Ub^{G76V}-GFP1 and Ub^{G76V}-GFP2 transgenic mice for subsequent study of the UPS.

- To confirm expression of the Ub-GFP reporter in these mice in response to inhibition of the UPS.

- To transmit RML prions to both Ub^{G76V}-GFP lines and confirm the onset of disease.

- To characterize the Ub^{G76V}-GFP1 reporter mice in primary neurons.

3.3 METHODS

Breeding pairs of Ub^{G76V}-GFP1 and Ub^{G76V}-GFP2 mice were provided by Professor Nico Dantuma at the Karolinska Center for Transgenic Technologies, Sweden. These mice had been backcrossed on to a C57Bl/6N background for at least thirty generations (Lindsten et *al*., 2003) and were maintained on this background in generating the animals for our experiments. The mice were genotyped by PCR with GFP-specific oligonucleotide primers of genomic DNA isolated from ear biopsies taken from each individual animal (**Section 2.1.2**). Confirmation of Ub-GFP reporter expression in these mice was obtained by establishing primary cortical neuronal cultures that were treated with proteasome inhibitors (**Section 2.3**).

Transgenic and control mice were inoculated i.c. with 30 µl 1% RML brain homogenate (designated I6201), or 30 µl 1% I7723 normal CD-1 mouse brain homogenate (designated I7723) as a control (**Section 2.2.2**). The mice were then culled at end-stage disease. This work was done in collaboration with Dr Ralph Andre and the MRC Prion Unit's Biological Services Facility (BSF) at Wakefield Street under project license number 70/6454.

3.4 RESULTS

3.4.1 Establishing the Ub^{G76V}-GFP reporter mouse colony

To establish stable colonies of the Ub^{G76V}-GFP reporter mice, a single breeding pair for each of the Ub^{G76V}-GFP1 and Ub^{G76V}-GFP2 lines was obtained from Professor Nico Dantuma at the Karolinska Center for Transgenic Technologies, Sweden. Using these breeding pairs, heterozygous Ub^{G76V}-GFP+/- mice and homozygous Ub^{G76V}-GFP-/- littermates were generated in an expected Mendelian fashion for further experimental use (**Figure 3.1**).

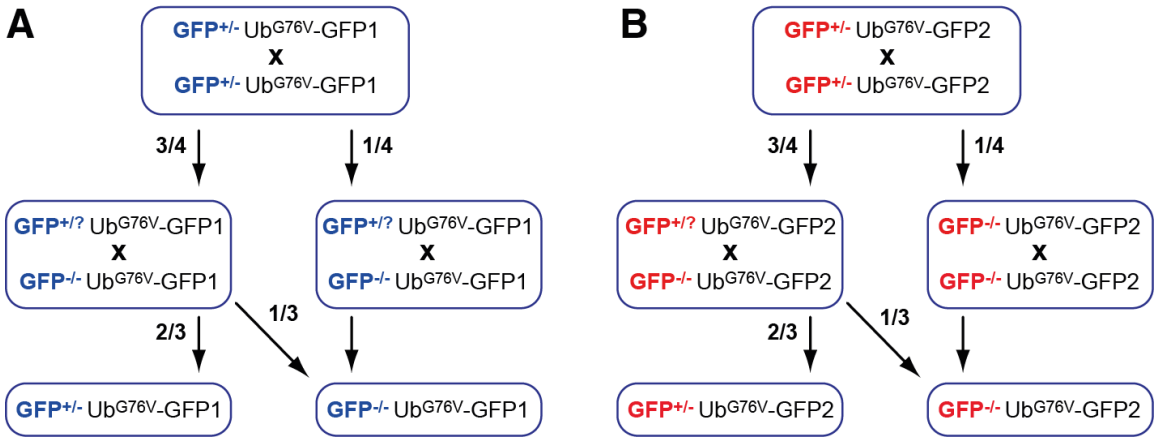

Figure 3.1 Breeding of the **Ub^{G76V}-GFP transgenic mice.**
Founders were backcrossed to C57BL/6N to produce Ub^{G76V}-GFP transgenic mice. Offspring were generated in an expected Mendelian fashion when heterozygous Ub^{G76V}-GFP mice were mated together. **(A)** Breeding plan for the ST5/Ub^{G76V}-GFP1 line. **(B)** Breeding plan for the ST5/Ub^{G76V}-GFP2 line.

3.4.2 Genotyping of the Ub^{G76V}-GFP1 and Ub^{G76V}-GFP2 mice

To identify Ub^{G76V}-GFP-positive mice, biopsies were taken from the ears of 5-6 week-old Ub^{G76V}-GFP progeny. Genomic DNA was analysed by PCR using primers to specifically detect the presence of the Ub^{G76V}-GFP transcript (**Section 2.1.2**). PCR products were analysed by agarose gel electrophoresis and Ub^{G76V}-GFP-positive animals were identified by the presence of a specific band of 300 base pair (bp) (**Figure 3.2**).

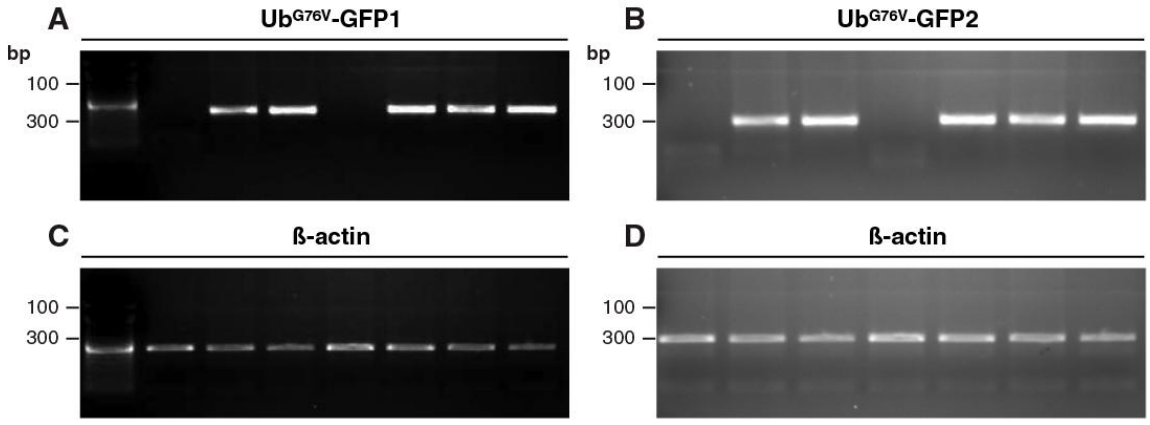

Figure 3.2 Genotyping of the Ub^{G76V}-GFP transgenic mice.

Genotyping of genomic DNA isolated from the Ub^{G76V}-GFP mice. The 300-bp PCR product identified Ub-GFP positive mice in the (**A**) Ub^{G76V}-GFP1 and (**C**) Ub^{G76V}-GFP2 lines. This method was not able to distinguish between heterozygous or homozygous Ub-GFP positive mice. (**B**, **D**) Primers specific for β-actin were used as a control in all PCR reactions.

3.4.3 Ub-GFP reporter expression in response to inhibition of the UPS in Ub^{G76V}-GFP primary cortical neurons

Accumulation of the Ub-GFP reporter was previously described in the Ub^{G76V}-GFP reporter mice (Lindsten et *al*., 2003). To validate the Ub^{G76V}-GFP transgenic mouse model, primary cortical neurons from embryonic E16 Ub^{G76V}-GFP1 mice were harvested and analysed by immunohistochemistry to detect the presence of the Ub-GFP reporter. Primary cortical neurons were treated with lactacystin, a proteasome inhibitor, at concentrations of 0.5 and 50 µM for 24 h. This treatment of lactacystin induced the accumulation of GFP in the neuronal cells, indicating the presence of the Ub-GFP reporter (**Figure 3.3**). Indeed, the primary cortical neurons responded to treatment with the proteasome inhibitor in a dose dependent manner as previously described (Lidnsten et *al*., 2003). The most intense Ub^{G76V}-GFP accumulation was observed in neurons treated with the highest concentration of lactacystin (**Figure 3.3 C**). This validated the functionality of the Ub-GFP reporter mouse model in detecting dysfunction of the cellular UPS machinery.

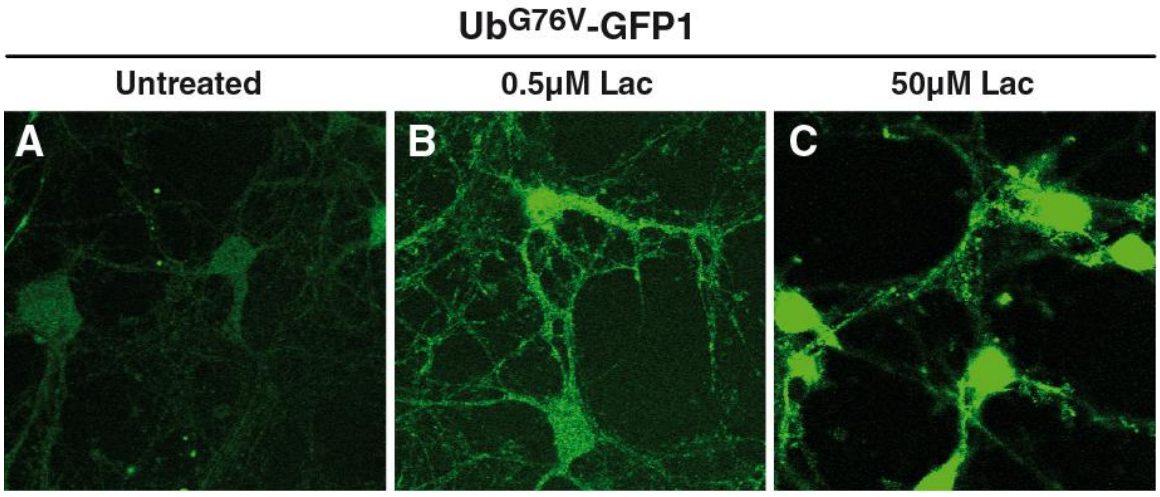

Figure 3.3 Functional characterisation of Ub^{G76V}-GFP expression in primary cortical neurons.

Primary cortical neurons were harvested from neonatal E16 Ub^{G76V}-GFP1 mice. The proteasome inhibitor, lactacystin, was used to treat the cells in order to monitor Ub-GFP accumulation resulting from the inhibited UPS degradation pathway. The cells were fixed and confocal immunofluorescence images were taken of primary cortical neurons treated with (**B**) 0.5 μM and (**C**) 50 μM lactacystin, as compared to (**A**) untreated controls. Increasing GFP fluorescence was observed with increasing concentrations of lactacystin. Fluorescent imaging were analysed with a confocal microscope (Zeiss).

3.4.4 Basal expression of the Ub^{G76V}-GFP reporter in primary cortical neurons from Ub^{G76V}-GFP1 mice.

In analysing the induction of the Ub^{G76V}-GFP reporter in the Ub^{G76V}-GFP1, some basal level of the Ub-GFP reporter was detected in non-lactacystin treated cells. This basal level of GFP was observed in Ub^{G76V}-GFP1 primary neurons that were co-immunostained for GFP and a neuronal marker, neurofilament (NF200) (**Figure 3.4**).

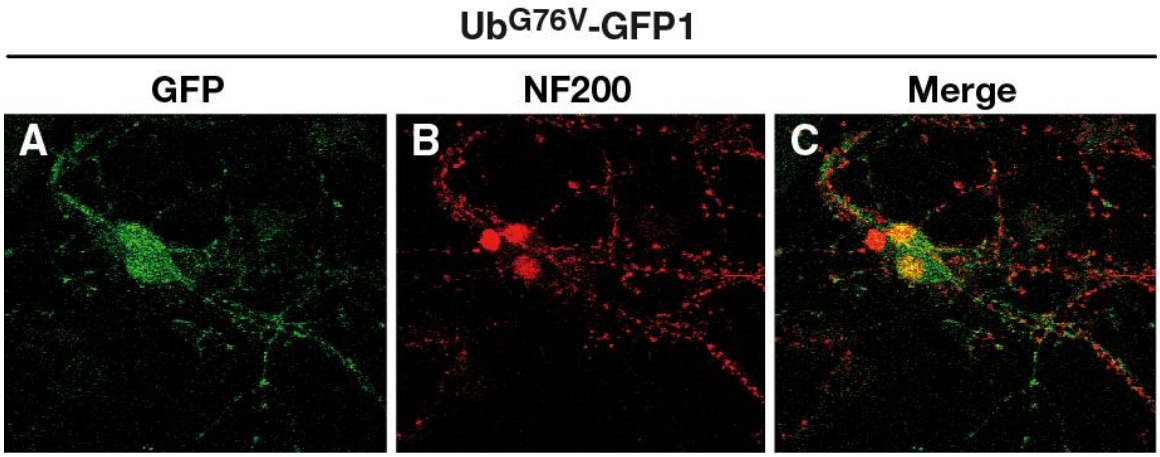

Figure 3.4 Basal expression of the Ub^{G76V}-GFP reporter in expression primary cortical neurons from Ub^{G76V}-GFP1 mice.

Primary cortical neurons were harvested from neonatal E16 Ub^{G76V}-GFP1 mice and fixed prior to immunocytochemistry. (**A**) Immunoreactivity using an anti-GFP antibody (Invitrogen) showed basal GFP expression in these cells. (**B, C**) The GFP-positive cells were positively identified as neurons as shown by co-localisation with neurofilament (NF200). Fluorescent imaging were analysed with a confocal microscope (Zeiss).

3.4.5 Inoculation of Ub^{G76V}-GFP reporter mice with RML prions

To monitor UPS impairment following prion infection, heterozygous Ub^{G76V}-GFP1+/- and Ub^{G76V}-GFP2+/- (henceforth termed Ub^{G76V}-GFP1 and Ub^{G76V}-GFP2, respectively) mice were inoculated with prions. Ub^{G76V}-GFP1+/- and Ub^{G76V}-GFP2+/- mice, along with Ub^{G76V}-GFP-/- littermate controls (termed Ub-GFP^{neg}), were inoculated with RML brain homogenate, or normal CD-1 brain homogenate as a control (**Section 2.2**). The mice were then monitored on a daily basis for sign of illness. Animals in the advanced stage of the disease showed the typical symptoms of inoculation with RML prions, including a ruffled coat due to poor grooming, erect ears, agitation, unusual gait and piloerection. As expected, the incubation period of the disease post-inoculation with RML prion was approximately 160 days (**Figure 3.5**). This incubation time period confirms previous incubation time observed in mice of the same C57Bl/6N strain (Llyod et *al*., 2001). Incubation period for the end-stage groups of the Ub^{G76V}-GFP1, Ub^{G76V}-GFP2 and Ub^{G76V}-GFP^{neg} mice were the same. This demonstrates that the Ub-GFP reporter itself does not influence the incubation period of RML prion infection in these mice. See **Appendix IV** for statistics report.

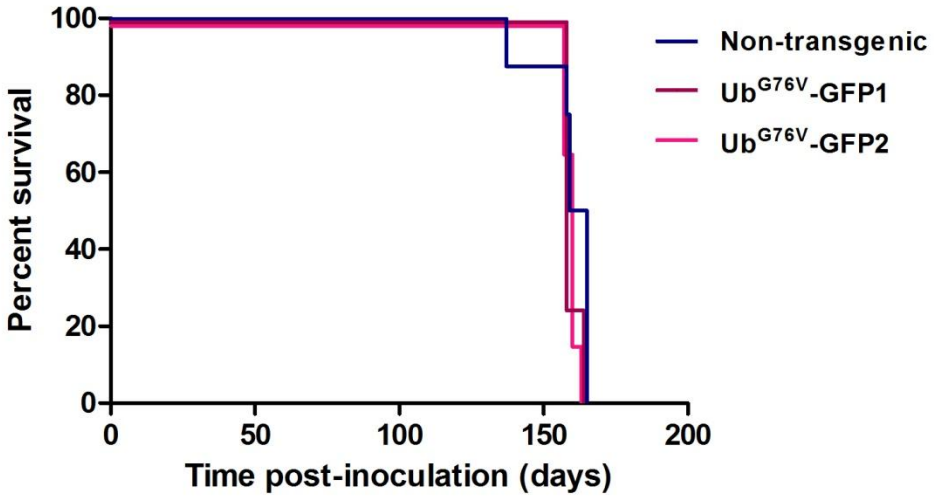

Figure 3.5 RML infected Ub^{G76V}-GFP mice succumb to disease at 160 days post-inoculation.

Groups of Ub^{G76V}-GFP1 (n=3) and Ub^{G76V}-GFP2 mice (n=5), alongside non-transgenic controls (n=8), were inoculated i.c with 30 µl of 1% RML-infected mouse brain homogenate. The x- axis shows the number of days post RML prion infection. The first observable signs of scrapie symptoms were seen at day 137 post-inoculation, with a mean incubation period to end-stage disease of 160.2 days. Non-transgenic (blue), Ub^{G76V}-GFP1 (red), Ub^{G76V}-GFP2 (pink). No differences in incubation period were observed between the groups of Ub^{G76V}-GFP1, Ub^{G76V}-GFP2 and non transgenic mice. See **Appendix IV.**

3.4.6 PrP^{Sc} accumulates in the brains of prion-infected Ub^{G76V}-GFP reporter mice.

To confirm that the brains of RML prion-infected Ub^{G76V}-GFP1 showed neuropathological features of prion infection, brain tissue was assessed by immunohistochemistry for the presence of formic acid resistant disease-associated PrP^{Sc}**.** Abnormal PrP^{Sc} deposits were detected in the brains of RML prion infected Ub^{G76V}-GFP

mice, and were seen throughout key neuropathological regions of the brain, including the thalamus, cortex and hippocampus, in both RML-infected Ub^{G76V}-GFP1 and Ub^{G76V}- GFP-/- mice (**Figure 3.6 A, B**)**.** No abnormal PrP^{Sc} was detected in non-infected littermate controls (**Figure 3.6 C**), and there were no differences in PrP^{Sc} accumulation or distribution between Ub^{G76V}-GFP1 and Ub^{G76V}- GFP-/- mice.

Parallel analyses were done in Ub^{G76V}-GFP2 mice. As expected, abnormal PrP^{Sc} deposits were detected throughout key neuropathological regions of the brain in both RML-infected Ub^{G76V}-GFP2 and Ub^{G76V}- GFP-/- mice (**Figure 3.7 A, B**), and no abnormal PrP^{Sc} was observed in non-infected littermate controls (**Figure 3.7 C**). No differences in PrP^{Sc} accumulation or distribution were seen between Ub^{G76V}-GFP2 and Ub^{G76V}- GFP-/- mice, or the Ub^{G76V}-GFP1 mice.

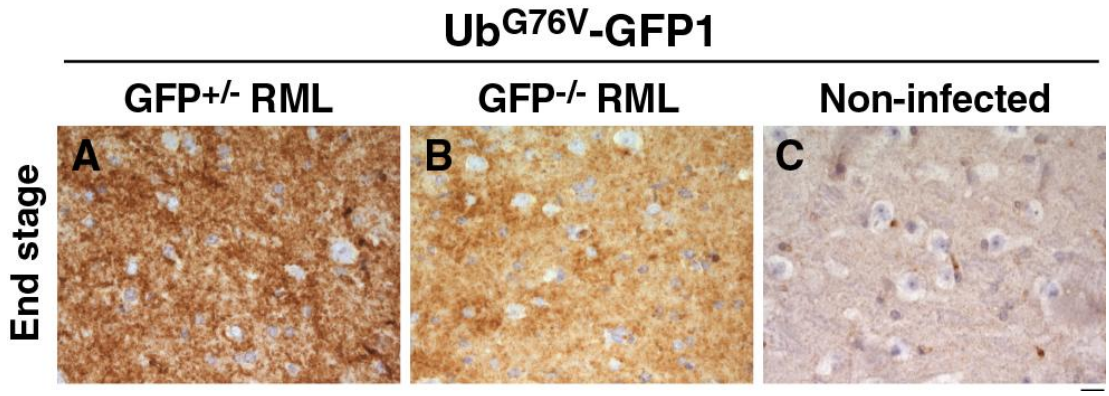

Figure 3.6 RML infected Ub^{G76V}-GFP1 mice accumulate PrP^{Sc} at end-stage disease. Ub^{G76V}-GFP1 mice (n=3) and non-transgenic controls (n=3) were inoculated i.c with 30 µl of 1% RML-infected mouse brain homogenate. Immunohistochemistry analysis was carried out on paraffin-embedded end-stage disease mouse brain tissue using the ICSM35 anti-PrP antibody. Significant deposition of formic acid-resistant PrP^{Sc} was observed throughout the brain in (A) Ub^{G76V}-GFP1 mice and (B) non-transgenic controls. (C) No PrP^{Sc} was observed in non-infected mice inoculated with control CD1 mouse brain homogenate. Images are taken of the thalamus, scale bar = 20 µm.

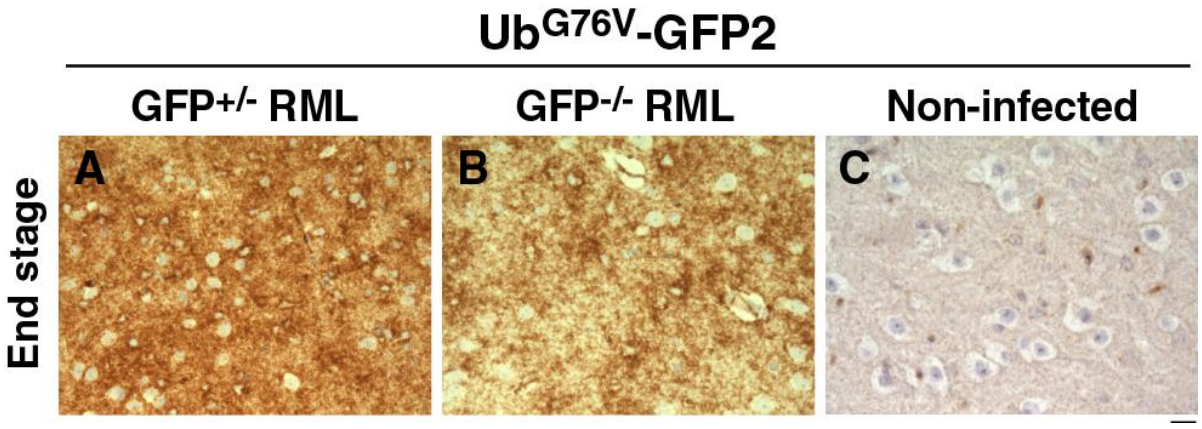

Figure 3.7 RML infected Ub^{G76V}-GFP2 mice accumulate PrP^{Sc} at end-stage disease. Ub^{G76V}-GFP2 mice (n=5) and non-transgenic controls (n=5) were inoculated i.c with 30 µl of 1% RML-infected mouse brain homogenate. Immunohistochemistry analysis was carried out on paraffin-embedded end-stage disease mouse brain tissue using the ICSM35 anti-PrP antibody. Significant deposition of formic acid-resistant PrP^{Sc} was observed throughout the brain in (A) Ub^{G76V}-GFP2 mice and (B) non-transgenic controls. (C) No PrP^{Sc} was observed in non-infected mice inoculated with control CD1 mouse brain homogenate. Images are taken of the thalamus, scale bar = 20 µm.

3.4.7 Gliosis increases in the brains of prion-infected Ub^{G76V}-GFP reporter mice.

To further investigate whether the Ub^{G76V}-GFP reporter mice demonstrate other typical hallmarks of prion disease pathology, brain tissue from both Ub^{G76V}-GFP1 and Ub^{G76V}-GFP2 mice were examined for the presence of astrocytic gliosis, a characteristic of neuropathological features in prion-infected brain tissue. GFAP is a well-established marker for astrocytes and was analysed by immunohistochemistry. The occurrence of gliosis was detected in the brains of prion-infected Ub^{G76V}-GFP1 mice (**Figure 3.8 A**), coinciding with the accumulation of PrP^{Sc} in the hippocampus, cortex, thalamus, cerebellum

and hypothalamus. This gliosis was similarly observed in the brain of RML prion-infected Ub^{G76V}-$GFP1^{neg}$ mice (**Figure 3.8 B**), but not in uninfected controls brain (**Figure 3.8 C**).

The same observations were made in RML-infected Ub^{G76V}-GFP2 mice. Gliosis was observed throughout key neuropathological regions of the brain in both RML-infected Ub^{G76V}-GFP2 and Ub^{G76V}-$GFP2^{neg}$ mice (**Figure 3.9 A, B)**, whereas increased gliosis was not observed in non-infected littermate controls **(Figure 3.9 C)**. No differences were observed in gliosis between Ub^{G76V}-GFP2 and Ub^{G76V}-GFP^{neg} mice.

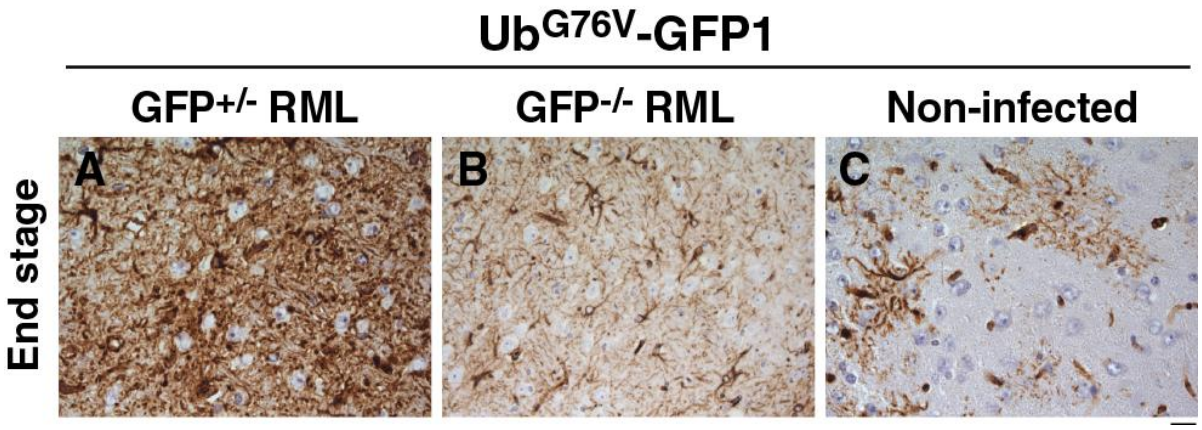

Figure 3.8 RML infected Ub^{G76V}-GFP1 mice demonstrate gliosis at end-stage disease.

Ub^{G76V}-GFP1 mice (n=3) and non-transgenic controls (n=3) were inoculated i.c with 30 µl of 1% RML-infected mouse brain homogenate. Immunohistochemistry was carried out on paraffin-embedded end-stage disease mouse brain tissue using an anti-GFAP antibody (Dako). Increased gliosis, a secondary neuropathological marker of prion disease pathology, was observed throughout the brain in (**A**) Ub^{G76V}-GFP1 mice and (**B**) non-transgenic controls. (**C**) Similar gliosis was not observed in non-infected mice inoculated with control CD1 mouse brain homogenate. Images are taken of the thalamus, scale bar = 20 µm.

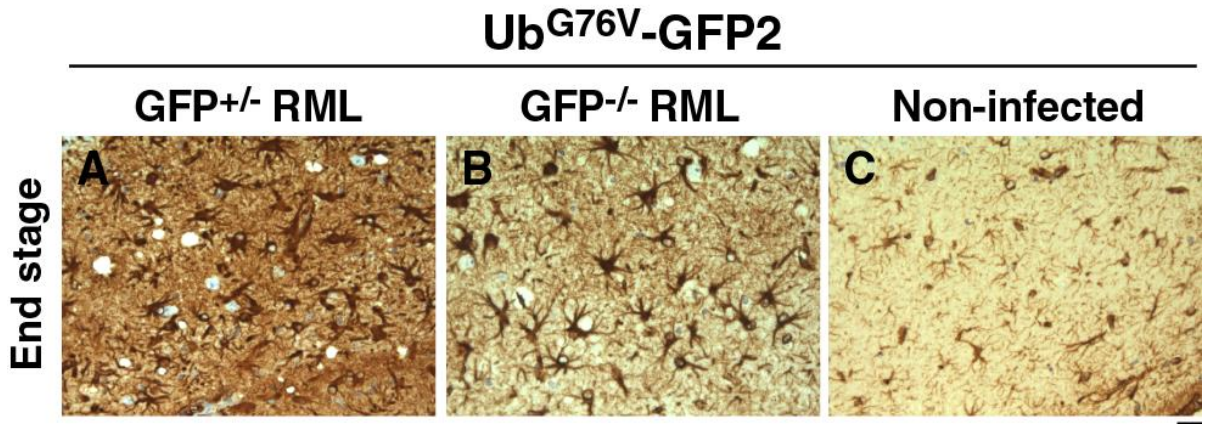

Figure 3.9 RML infected Ub^{G76V}-GFP2 mice demonstrate gliosis at end-stage disease.

Ub^{G76V}-GFP2 mice (n=5) and non-transgenic controls (n=5) were inoculated i.c with 30 µl of 1% RML-infected mouse brain homogenate. Immunohistochemistry was carried out on paraffin-embedded end-stage disease mouse brain tissue using an anti-GFAP antibody (Dako). Increased gliosis, a secondary neuropathological marker of prion disease pathology, was observed throughout the brain in (**A**) Ub^{G76V}-GFP2 mice and (**B**) non-transgenic controls. (**C**) Similar gliosis was not observed in non-infected mice inoculated with control CD1 mouse brain homogenate. Images are taken of the thalamus, scale bar = 20 µm.

3.4.8 Confirmation of GFP in 22 L prion infected Ub^{G76V}-GFP1 mice mouse brain

Accumulation of the Ub-GFP reporter was previously described (Lindsten et *al*., 2003) and recently, impairment of the Ub-GFP reporter was observed at end stage in Ub^{G76V}-GFP mice infected with 22L prion. It was shown that prion infection with 22L prion causes UPS impairment in end stage mice (Kristiansen et *al*., 2007).

To confirm and validate those previous findings, immunohistochemistry was done on brain sections of Ub^{G76V}-GFP1 mice infected with 22L prion, which were also used as positive control for the Ub^{G76V}-GFP mice infected with RML prion. Brain sections of 22L prion were assessed as described by Kristiansen and colleagues. GFP accumulation was observed in area of the thalamus as expected (**Figure 3.10 A**), no GFP was seen in mock-infected animals (**Figure 3.10 B**) or non-transgenic (**Figure 3.10 C**). Detection of the Ub-GFP reporter in the brains of these mice suggests that proteins accumulate as they are not degraded by the failing proteasome machinery, and that there is significant dysfunction in the activity of the UPS. This observation was as reported by Kristiansen and colleagues previously (Kristiansen et *al*., 2007).

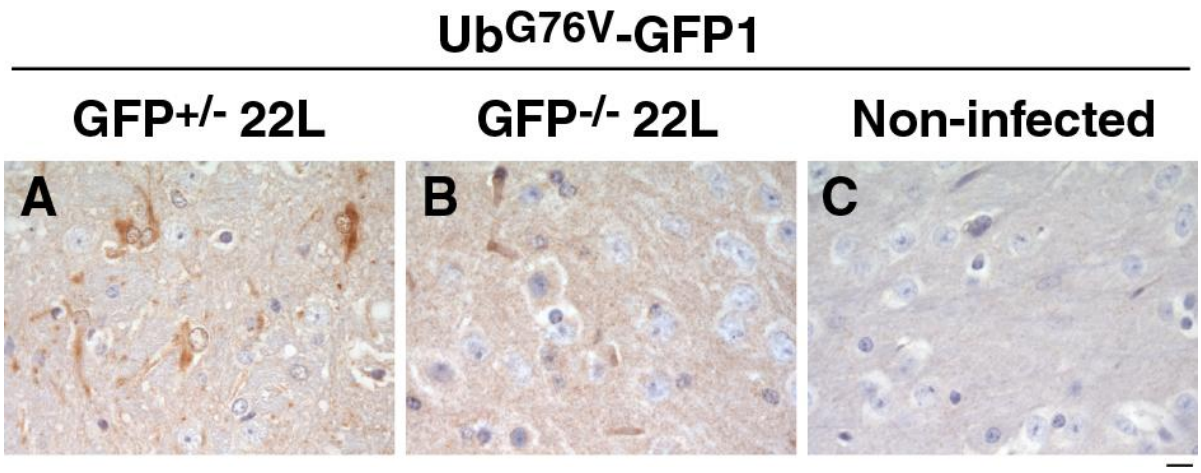

Figure 3.10 GFP accumulates in the brain of 22L prion infected Ub^{G76V}-GFP1 mice at end-stage disease.

Both Ub^{G76V}-GFP 1+/- (A) and Ub^{G76V}-GFP1-/- (B) were inoculated with 30 µl of 1% RML-infected 22 L prion, while Ub^{G76V}-GFP littermates (C), used as negative controls were inoculated with CD1 brain homogenate. Immunohistochemistry was done on paraffin sections using an anti-GFP antibody (Invitrogen). Scale bar = 20 µm. *22L prion infected brains embedded in paraffin were obtained from Prof. John Portis, Rocky Mountain Laboratories, USA*.

3.4.9 Ub-GFP reporter accumulates in the brains of prion-infected Ub^{G76V}-GFP reporter mice

To analyse the Ub^{G76V}-GFP reporter in RML prion-infected Ub^{G76V}-GFP reporter mice, brains tissue was assessed by immunohistochemistry for the presence of the Ub-GFP reporter. An anti-GFP antibody was used to confirm the presence of GFP in the brains of the Ub^{G76V}-GFP mice as they succumbed to disease.

In both Ub^{G76V}-GFP1 (**Figure 3.11**) and Ub^{G76V}-GFP2 (**Figure 3.12**) mice, GFP immunoreactivity was observed in the brains of the prion infected mice. This accumulation appeared to be restricted to the region of the thalamus. Importantly, the Ub-GFP reporter was not detected in the brains of either RML-infected Ub^{G76V}-GFP^{neg} mice, which lack expression of the reporter, or uninfected Ub^{G76V}-GFP mice (**Figures 3.11 B, C, & Figures 3.12 B, C**). This result demonstrates the accumulation of the Ub-GFP reporter substrate, indicating UPS dysfunction. This impairment is in this case specific to mice inoculated with prions, and that the anti-GFP immunoreactivity was specific to the presence of the Ub-GFP reporter. This finding confirms previous observations (Kristiansen et *al*, 2007), and indicates the suitability of the Ub^{G76V}-GFP model as means of monitoring UPS dysfunction throughout the pathogenic time-course of disease.

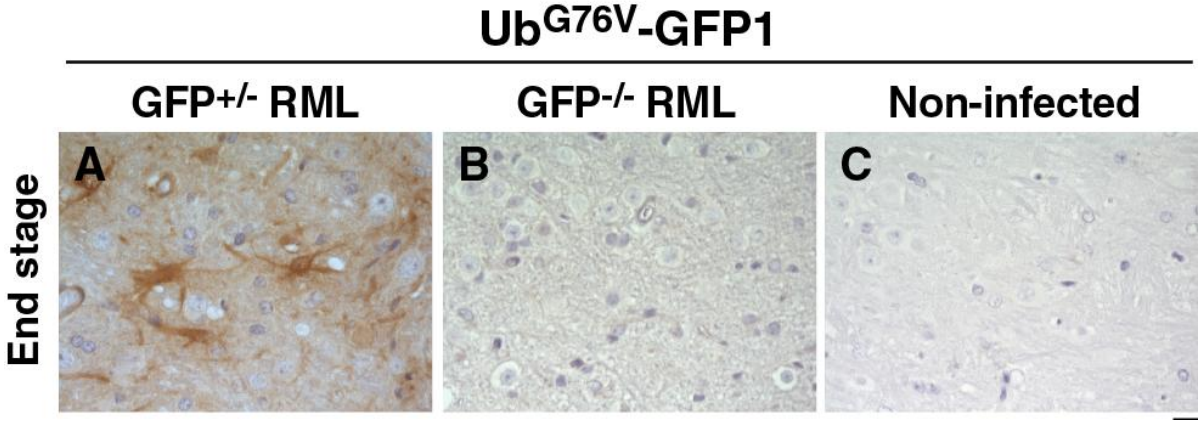

Figure 3.11 The Ub-GFP reporter accumulates in RML infected Ub^{G76V}-GFP1 mice at end-stage disease.

Ub^{G76V}-GFP1 mice (n=3) and non-transgenic controls (n=3) were inoculated i.c with 30 µl of 1% RML-infected mouse brain homogenate. Immunohistochemistry was carried out on paraffin-embedded end-stage disease mouse brain tissue using an anti-GFP antibody (Invitrogen). Accumulation of the Ub-GFP reporter was observed in the thalamus of (**A**)

Ub^{G76V}-GFP1 mice, but not in (**B**) non-transgenic controls or (**C**) non-infected mice inoculated with control CD1 mouse brain homogenate. Scale bar = 20 µm.

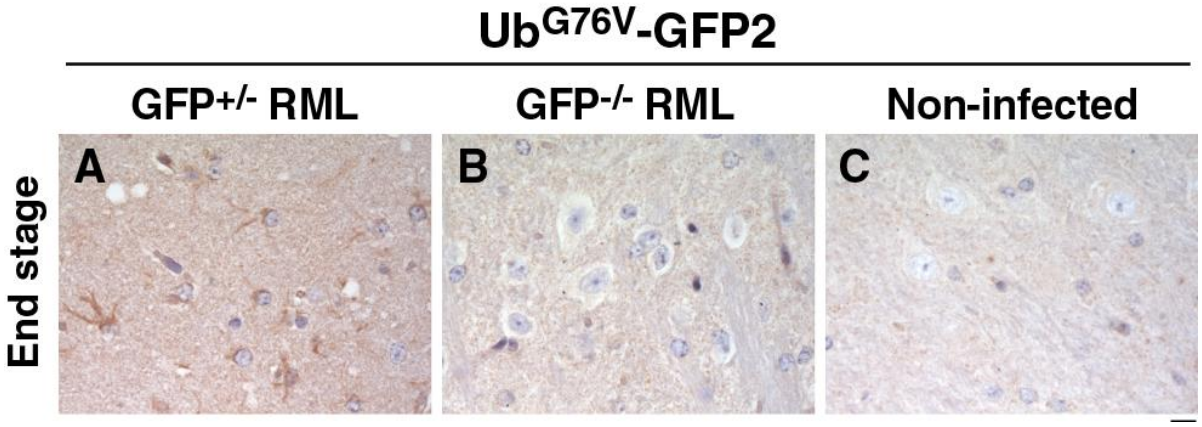

Figure 3.12 The Ub-GFP reporter accumulates in RML infected Ub^{G76V}-GFP2 mice at end-stage disease.

Ub^{G76V}-GFP2 mice (n=5) and non-transgenic controls (n=5) were inoculated i.c with 30 µl of 1% RML-infected mouse brain homogenate. Immunohistochemistry was carried out on paraffin-embedded end-stage disease mouse brain tissue using an anti-GFP antibody (Invitrogen). Accumulation of the Ub-GFP reporter was observed in the thalamus of (**A**) Ub^{G76V}-GFP2 mice, but not in (**B**) non-transgenic controls or (**C**) non-infected mice inoculated with control CD1 mouse brain homogenate. Scale bar = 20 µm.

3.5 DISCUSSION

Work presented here confirms the Ub^{G76V}-GFP reporter mice as a suitable model for monitoring UPS impairment following RML prion infection. In addition, validation and characterization of the Ub^{G76V}-GFP mice were done in primary cortical neurons. Neurons are particularly vulnerable during the progression of prion diseases (Mallucci et *al*., 2007; Mallucci et *al*., 2002), therefore it was important to confirm the functionality of the Ub^{G76V}-

GFP reporter in these cells. Cortical neurons isolated from the Ub^{G76V}-GFP mice brain were shown to have an accumulation of the Ub-GFP reporter in response to the inhibition of the UPS, as previously reported (Lindsten et *al*., 2003). This was achieved by treating the cells with lactacystin, a specific proteasome inhibitor. However, these neurons appeared to show, at least while being cultured *in vitro*, some basal level of Ub-GFP expression. The degree to which the Ub-GFP reporter can accumulate in non-neuronal cells, such as astrocytes, was not investigated at this point.

It was also important to demonstrate that the Ub^{G76V}-GFP mice are susceptible to infection with RML prions. Previous studies have shown the Ub^{G76V}-GFP mice are susceptible to 22L prions (Kristiansen et *al*, 2007). Therefore, to ascertain whether RML prion exerts similar effect, the Ub^{G76V}-GFP reporter mice were inoculated with RML prion in the same manner as previously done with 22L prion. Detection of the Ub^{G76V}-GFP reporter was observed in 22L prion-infected transgenic mouse brains, whereas no Ub^{G76V}-GFP accumulation in mice inoculated with normal brain or in 22L prion-infected non-transgenic littermates was seen (Kristiansen et *al*, 2007). Following inoculation of RML prion, the Ub^{G76V}-GFP mice succumbed to disease as would be expected. The incubation period until end stage disease of ~160 days was the same for the Ub^{G76V}-GFP1, Ub^{G76V}-GFP2 and Ub^{G76V}-GFP^{neg} mice. This demonstrates that expression of the Ub-GFP reporter itself does not influence the prion incubation period in these mice. Moreover, the incubation period observed was similar to previous observations of the C57Bl/6N background strain on which the Ub^{G76V}-GFP mice are based (Lloyd et *al*., 2001).

To investigate whether the Ub-GFP reporter displayed the neuropathological markers associated with prion disease at end stage disease, histological analyses of brain tissue isolated from the Ub^{G76V}-GFP mice were carried out. As expected, a widespread appearance of disease-associated PrP^{Sc}, accompanied by a marked astrocytosis and gliosis was observed throughout the brain, but more specifically in the region of the thalamus. No noticeable differences in staining of PrP^{Sc} or GFAP were observed between the Ub^{G76V}-

GFP1, Ub^{G76V}-GFP2 and Ub^{G76V}-GFP^{neg} mice, indicating that expression of the Ub-GFP reporter itself does not influence the prion-mediated neuropathology induced in these mice.

To confirm previous findings of GFP accumulation in 22L prion-infected Ub^{G76V}-GFP mice, similar detection methods were used. Analysis of the Ub-GFP reporter by anti-GFP immunoreactivity demonstrated that the UPS is impaired by RML prion at end stage disease, as was observed with 22L prion previously (Kristiansen et *al*., 2007). Moreover, positive staining was observed only in the Ub^{G76V}-GFP1 and Ub^{G76V}-GFP2 mice, with no such staining being detected in prion-infected Ub^{G76V}-GFP^{neg} mice. Indeed, this result confirms the specificity of the immunohistochemistry procedure used to detect the Ub-GFP reporter. Interestingly, the anti-GFP immunoreactivity was stronger in the prion-infected Ub^{G76V}-GFP1 mice than their Ub^{G76V}-GFP2 counterparts.

The variation in GFP staining between the two lines of the Ub^{G76V}-GFP reporter mice could be explained by the high basal level expression of the Ub-GFP substrate reported in the Ub^{G76V}-GFP1 mice (Lindsten et *al*., 2003). Similar variation was observed in the expression of the Ub^{G76V}-GFP transgene when double transgenic of ALS, (SOD1G93A) and Ub^{G76V}-GFP reporter mice were examined (Cheroni et *al*., 2009). Substantial differences were seen between the two transgenic lines of the reporter mice. The basal level GFP in the Ub^{G76V}-GFP1 were clearly detectable by immunostaining in both dorsal and ventral lumbar spinal cord, but no immunostaining was observed in the Ub^{G76V} GFP2 (Cheroni et *al*., 2009), suggesting the study Ub^{G76V}-GFP2 must be done in conjunction with the Ub^{G76V}-GFP1 transgenic mice. Using the proteasome inhibitor lactacystin, a significant accumulation of the Ub^{G76V}-GFP substrate was observed in cortical neurons, indicating impairment in the UPS machinery. This result was consistent with previous studies (Dantuma et *al*., 2000; Lindsten et *al*., 2003). The level of proteasome inhibition observed is likely to have severe consequences on neuronal viability.

Although the molecular basis of prion neurotoxicity is not yet clear, it is suggested that intracellular accumulation of disease-associated PrP^{Sc} is required for cytotoxicity. Previous studies support a cytosolic localization for a small proportion of PrP^{Sc} in prion infected neuronal cells in line with our previous data demonstrating toxic cytosolic PrP^{Sc} aggresomes (Kristiansen et *al*., 2005; Kristiansen et *al*., 2007). Granular deposits of disease-related PrP have been reported in cell body of neurons and CJD brains, suggesting the occurrence of intraneuronal prion aggregates (Kovacs and Budka, 2008). However, it is unclear how PrP^{Sc} oligomers traffic inside neurons and enter the cytosol to cause cell death. Other studies suggested that intracellular neuronal propagation of pathogenic PrP^{Sc} appears important in neurotoxicity (Brandner et *al*., 1996; Mallucci et *al*., 2003). However, it was shown that various proteolytic stress condition can cause functional impairment of the UPS which result in cellular dysfunction and apoptosis (Lindsten et *al*., 2002)**.**

PrP^{C} is essential for prion propagation and neurotoxicity (Bueler et *al*., 1993). However, some studies reveal that PrP^{C} knockout in adult mouse brain shows no overt phenotypic effect (Mallucci et *al*., 2002). Moreover, embryonic PrP^{C} knockout models demonstrate normal development and behaviour (Bueler et *al*., 1992; Manson et *al*.,1994). Therefore, PrP^{C} knockout studies effectively exclude loss of function of PrP^{C} in neurons as a significant mechanism in prion mediated neurodegeneration.

Down-regulation of PrP expression has been proposed as a possible therapy for prion disease, assuming prion expression is required for infection (Bueler et *al*., 1993) and the down-regulation of PrP expression can prolong disease incubation time (Manson et *al*., 1994; Prusiner et *al*., 1983). Studies by Mallucci and colleagues have shown the down-regulation of prion expression in mice can halt neuronal cell death and reverse the disease in the infected animal (Mallucci et *al*., 2007).

The pathogenesis of prion disease is likely to be multifactorial, but inhibition of the proteasome by pathogenic PrP is likely to result in neuronal perturbation and contribute to

neuronal loss (Ma and Lindquist, 2002). *In vivo* testing of the role of the UPS in neurodegeneration using the same Ub-GFP reporter mouse model as used here demonstrated that proteasome impairment does not contribute to pathogenesis in spinocerebellar ataxia 7 (SCA7) mice (Bowman et *al*., 2005). The Ub-GFP reporter does not accumulate when there is neuronal apoptosis *per se* and is only seen when there is a significant UPS dysfunction. Accumulation of the Ub^{G76V}-GFP reporter occurred only in prion infected mice brains and was associated with PrP^{Sc} deposition.

PrP^{C} accumulation in the cytoplasm by use of proteasome inhibitor is reported to be associated with neuronal cell death (Ma and Lindquist, 2002). However, the data are controversial with evidence both for (Ma et *al*., 2002; Heller et *al*., 2003; Rambold et *al*., 2006) and against (Drisaldi et *al*., 2003; Roucou et *al*., 2003; Fioriti et *al*., 2005). A major drawback of many studies on cytosolic PrP^{C} is the high levels of proteasome inhibition used, which may limit any physiological relevance in experiments *in vivo* (Ding et *al*., 2003). Importantly, for a prion disease such as CJD, the abnormal prion conformer PrP^{Sc} inhibits the 26S proteasome *in vitro*, while either preincubation with an oligomer antibody or heat denaturation of PrP^{Sc} alleviated this inhibitor effect (Kristiansen et *al*., 2007), indicating a specific effect (Kristiansen et *al*., 2007). Moreover, protesome activity also decreased in both cells exposed to prion-infected mouse brain homogenates and in brain region exhibiting significant prion neuropathology in mice infected with PrP^{Sc} (Kristiansen et *al*., 2007. This finding establishes a solid link between UPS impairment and neurodegeneration associated with prion infection.

Other studies have suggested both the full-length PrP^{Sc} (Hertz et *al*., 2003) and the short PrP peptides are toxic to cell *in vitro* (Forloni et *al*., 1993), and their relevance *in vivo* pathogenesis should be carefully investigated. However, strong evidence provided by several studies suggests PrP itself may not be the toxic component. For instance, it has been shown that PrP^{C} -null tissue can be in close proximity to PrP^{Sc} deposits without suffering deleterious effects (Brandner et *al*., 1996; Mallucci et *al*., 2003), and there is no

direct evidence to correlate between neuronal loss and PrP^{Sc} plaques in CJD brains (Parshi et *al*., 1996). As already mentioned, some have reported studies done on prion diseases in which PrP^{Sc} is barely detectable (Collinge et *al*., 1995; Lasmezas et *al*., 1997), and subclinical infection where high levels of PrP^{Sc} accumulate in the absence of clinical symptoms are recognized (Hill et *al*., 2000; Race et *al*., 2001; 2002; Hill and Collinge , 2003).

In vitro and *in vivo* experimental data presented in this chapter investigate Ub^{G76V}-GFP reporter mice following RML prion infection and confirm the model as suitable for monitoring the UPS dysfunction through the progression of prion disease (**presented in Chapter 4**).

3.6 SUMMARY

In this chapter, I present data, which characterize and validate the Ub^{G76V} -GFP mouse model for the purpose of the direct monitoring of the UPS dysfunction in the pathogenesis of prion diseases. Both Ub^{G76V} -GFP1 and Ub^{G76V} -GFP2 lines were generated and cross-bred in a C57BL6/N background to establish stable colonies. The Ub^{G76V} -GFP reporter was characterized in primary cortical neurons, and offspring were inoculated with RML strain prion. Both GFP reporter mice (Ub^{G76V}-GFP1 and Ub^{G76V}-GFP2) were generated to investigate the impairment of the UPS throughout the course of disease. To date, it is the first time the Ub^{G76V}-GFP reporter mice have been inoculated with RML strain prion and a time-course was designed not only to monitor disease progression, but to investigate UPS impairment at early stages of prion infection.

4 PRION INFECTION IMPAIRS THE UPS IN Ub^{G76V}-GFP REPORTER MICE

4.1 BACKGROUND

Aberrations in the UPS machinery have been implicated in the pathogenesis of many diseases, including a variety of neurodegenerative diseases (Ciechanover and Brundin, 2003), and significant evidence exists of UPS dysfunction contributing to those diseases (**Section 1.13).** Consequently, understanding the spatial and temporal activity of the UPS is important for understanding its exact role and function in a neurodegenerative disease such as prion disease. Indeed, previous research has provided evidence for the implication of the UPS in prion disease **(Section 1.14**). Studies in prion-infected mouse brain have shown a correlation between elevated levels of ubiquitin conjugates and reduced proteasome function (Kang et *al*., 2004), and functional impairment of the UPS in prion disease, leading to a potential role in disease pathogenesis has been described (Deriziotis & Tabrizi, 2008; Andre and Tabrizi, 2011).

Direct interaction has been demonstrated between β-sheet-rich PrP species similar to disease-associated PrP^{Sc} and the 20S core particle of the 26S proteasome (Deriziotis et *al*., 2011). These studies show that aggregated β-sheet-rich PrP oligomers inhibit the proteolytic activities of the 26S proteasome, in a manner that is specific to PrP in an aggregated non-native β-sheet form (Kristiansen et *al*., 2007). The extent to which these *in vitro* observations are recapitulated *in vivo* in prion infected animals has not been previously fully investigated. Dysfunction of the UPS has been observed before in prion-infected Ub^{G76V}-GFP mice, but the animals were analysed solely at end-stage disease (Kristiansen et *al*., 2007). As a result, little is known about whether such impairment occurs at an early stage in the time-course of the disease, or whether changes in UPS function after prion infection correlate with or even precede other aspects of cellular dysfunction as

the disease progresses. In this chapter, data is presented to address the *in vivo* time-course of UPS dysfunction in prion disease pathogenesis using both Ub^{G76V}-GFP Ub^{G76V}-GFP1 and Ub^{G76V}-GFP2 reporter mice (**Chapter 3**). Also investigated are other aspects of disease pathogenesis, including typical histopathological markers of prion disease such as disease-associated PrP^{Sc} and a marker of gliosis, GFAP.

4.2 AIMS

- To evaluate the functional status of the UPS through a time-course during the prion disease pathogenesis;

- To further clarify the relationship between UPS dysfunction and neuropathological markers of prion disease;

- To potentially correlate UPS dysfunction and ER stress during the course of prion disease.

4.3 METHODS

Mice were generated and genotyped, as described in Chapter 3. Heterozygous Ub^{G76V}-GFP1 and Ub^{G76V}-GFP2 mice, together with Ub^{G76V}-GFP^{neg} controls were bred. Mice were inoculated intracerebrally with either 30 µl 1% RML prion brain homogenate or 30µl 1% normal CD1 mouse brain homogenate as a control (**Section 2.2.2**). This was followed by a series of timed culls at days 45, 85, 105, 125 and 145 post-inoculation, and at end-stage disease (~160 days) (**Table 4.1**). At each time-point, one brain hemisphere was fixed for histological analysis and the other was frozen for biochemical studies. The presence of disease pathology was confirmed by immunohistochemical staining of PrP^{Sc} and GFAP, as shown in **chapter 3**.

Immunohistochemistry was performed using Ventana Medical Systems (**Section 2.5**). Western blots and/or dot blots were undertaken for PrP^{Sc} and ubiquitin. Fluorogenic assays were used to monitor the chymotrypsin-like activity of 26S proteasomes (**Section 2.8**). This work was done in collaboration with Dr Ralph Andre, MRC Prion Unit, UCL Institute of Neurology.

Data were expressed as standard deviation (SD) and analysed by Student T t-test. Significance was expressed as follows: *** p <0.001; ** p <0.01, * p <0.05. See **Appendix IV.**

Table 4.1 Ub^{G76V}-GFP mice were in inoculated in groups and culled at various time points thereafter.

Mouse type	Inocula	Day cull post inoculation
Ub^{G76V}-GFP1 +/-	I6201 RML i.c.	45,85,105,125,145,165
Ub^{G76V} -GFP1 +/-	I7723 normal i.c.	45,85,105,125,145,165
Ub^{G76V} -GFP1 -/-	I6201 RML i.c.	45,85,105,125,145,165
Ub^{G76V} -GFP1 -/-	I7723 normal i.c.	45,85,105,125,145,165
Ub^{G76V} -GFP2 +/-	I6201 RML i.c.	45,85,105,125,145,165
Ub^{G76V} -GFP2 +/-	I7723 normal i.c.	45,85,105,125,145,165
Ub^{G76V} -GFP2 -/-	I6201 RML i.c.	45,85,105,125,145,165
Ub^{G76V} -GFP2 -/-	I7723 normal i.c.	45,85,105,125,145,165

4.4 RESULTS

4.4.1 Ub-GFP is expressed in the brains of RML prion-infected Ub^{G76V}-GFP1 mice before the onset of clinical signs

To investigate the earliest time-point in which Ub^{G76V}-GFP reporter accumulates in RML prion infected mice, brain sections from Ub^{G76V}-GFP1 mice were analysed by immunohistochemistry. Accumulation of Ub-GFP was detected as early as day 85 in the thalamus of RML prion-infected Ub^{G76V}-GFP1 mice (**Figure 4.1**). This accumulation increased as the disease progressed. Ub-GFP was not observed in the brains of RML prion-infected Ub^{G76V}-GFP^{neg} mice or control inoculated animals (**Figure 4.1**). In addition, some Ub-GFP was observed in the cortex towards end stage disease, but the appearance of the reporter was largely restricted to the thalamus. By cellular morphology, it seemed that the majority of the cells in which the Ub-GFP reporter was observed in the thalamus were astrocytes, although some Ub-GFP in neurons was observed. Taken together, this data shows that UPS dysfunction occurs in the brains of prion-infected mice relatively early in disease progression, and before the onset of clinical signs.

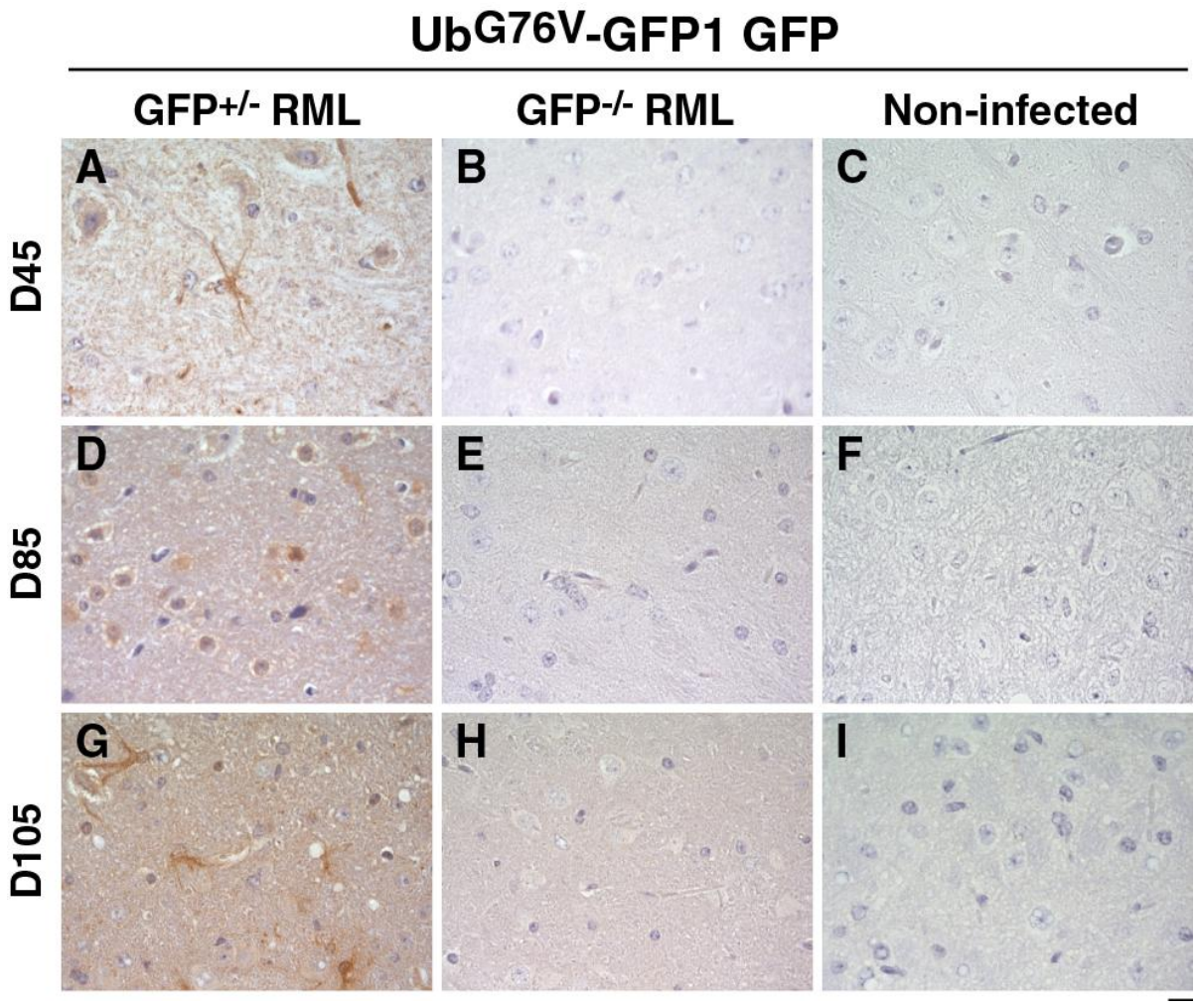

Figure 4.1 The Ub-GFP reporter accumulates in RML infected Ub^{G76V}-GFP1 mice at end-stage disease.

Ub^{G76V}-GFP1 mice (n=3) and non-transgenic controls (n=3) were inoculated i.c with 30 µl of 1% RML-infected mouse brain homogenates. Immunohistochemistry was carried out on paraffin-embedded mouse brain tissue using an anti-GFP antibody (Invitrogen). Accumulation of the Ub-GFP reporter was observed over time in the thalamus of Ub^{G76V}-GFP1 mice (**A, D, G, J, M, P**), but not in non-transgenic controls (**B, E, H, K, N, Q**) or non-infected mice inoculated with control CD1 mouse brain homogenate (**C, F, I, L, O, R**). Scale bar = 20 µm. **Continued overleaf.**

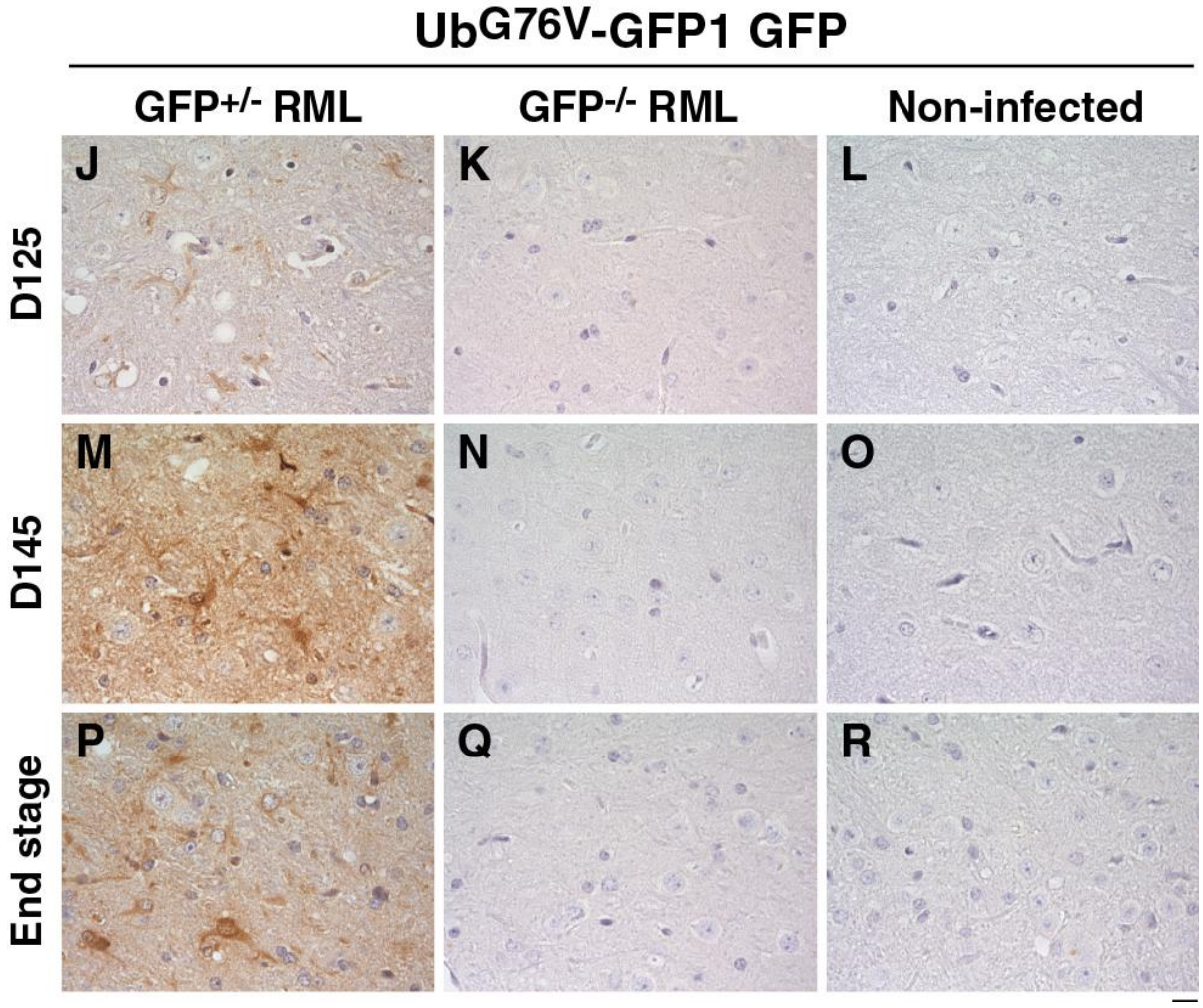

Figure 4.1(continued). The Ub-GFP reporter accumulates in RML infected Ub^{G76V}-GFP1 mice at end-stage disease.

4.4.2 Ub-GFP is expressed in the brains of prion-infected Ub^{G76V}-GFP2 mice before the onset of clinical signs

To verify whether similar accumulation of GFP could be observed in the Ub^{G76V}-GFP2 mice, brain sections were analysed in the same manner as the Ub^{G76V}-GFP1 reporter mice. Accumulation of the Ub-GFP was also observed in the thalamus of RML prion-infected Ub^{G76V}-GFP2 mice, although convincing stainings of GFP appeared to be from day 125 post-inoculation onwards (**Figure 4.2**). Ub-GFP was not observed in the brains of RML prion-infected Ub^{G76V}-GFP^{neg} mice or control inoculated animals. There were no differences in the histological or cellular patterns of the Ub-GFP accumulation between the Ub^{G76V}-GFP2 and the Ub^{G76V}-GFP1 mice. Collectively, this data shows that the two Ub^{G76V}-GFP lines behave similarly in response to prion infection. However, due to its apparent increased sensitivity to UPS impairment, the Ub^{G76V}-GFP1 line was chosen for use in the majority of further studies.

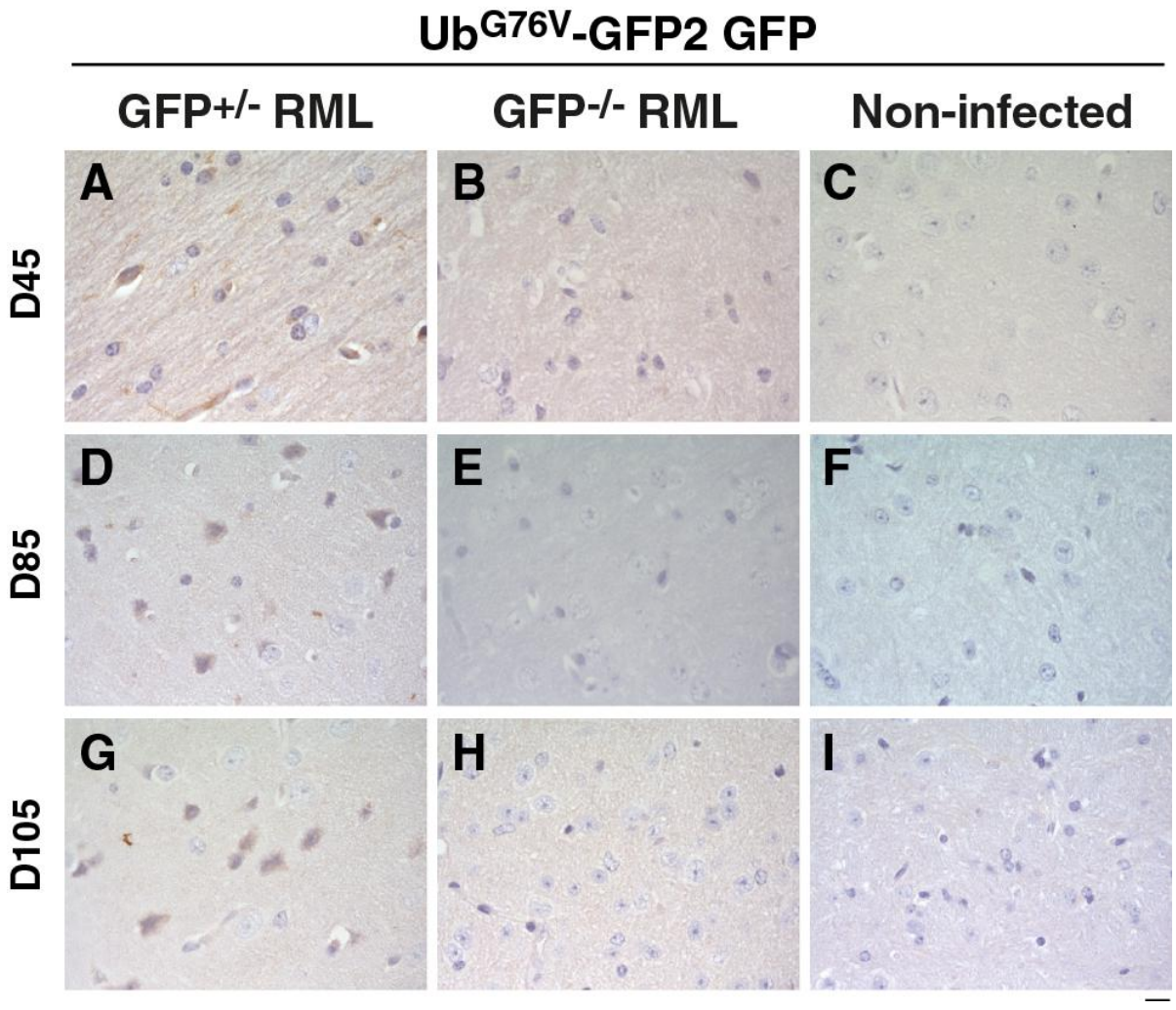

Figure 4.2 The Ub-GFP reporter accumulates in RML infected Ub^{G76V}-GFP2 mice at end-stage disease.

Ub^{G76V}-GFP2 mice (n=5) and non-transgenic controls (n=5) were inoculated i.c with 30 µl of 1% RML-infected mouse brain homogenates. Immunohistochemistry was carried out on paraffin-embedded mouse brain tissue using an anti-GFP antibody (Invitrogen). Accumulation of the Ub-GFP reporter was observed over time in the thalamus of (**A, D, G, J, M, P**) Ub^{G76V}-GFP2 mice, but not in non-transgenic controls (**B, E, H, K, N, Q**) non-infected mice inoculated with control CD1 mouse brain homogenate or (**C, F, I, L, O, R**). Scale bar = 20 µm. **Continued overleaf**.

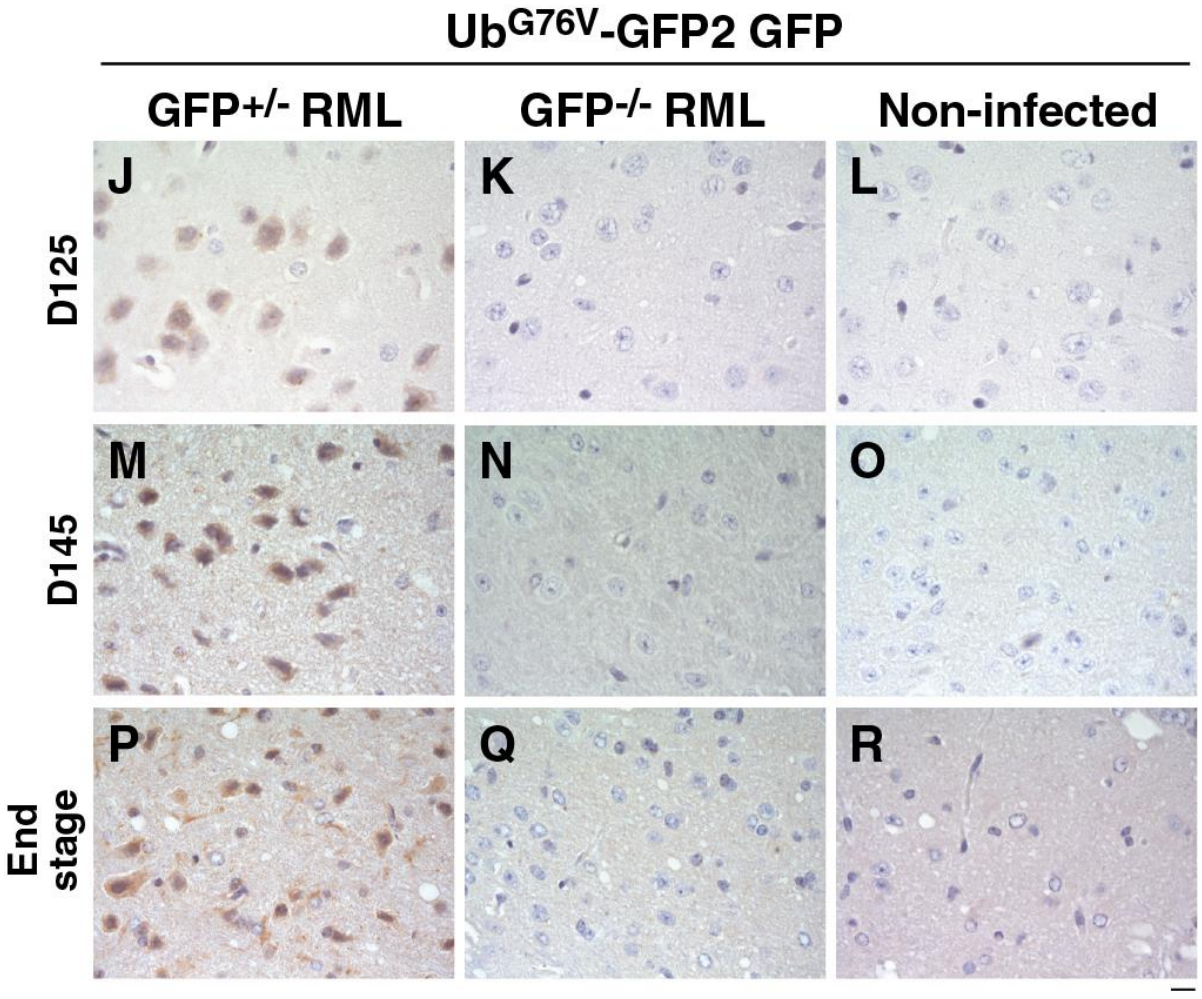

Figure 4.2 (continued). The Ub-GFP reporter accumulates in RML infected Ub^{G76V}-GFP2 mice at end-stage disease.

4.4.3 PrP^{Sc} deposition in the brains of RML prion-infected Ub^{G76V}-GFP1 mice

To determine whether PrP^{Sc} was present in RML prion-infected Ub^{G76V}-GFP1 mice, brain sections were analysed by immunohistochemistry. In the thalamus particularly where the Ub-GFP reporter could be detected from day 85 post-inoculation, significant amounts of disease-associated PrP^{Sc} deposition were observed (**Figure 4.3**). Similar levels of PrP^{Sc} were observed in RML-prion infected Ub^{G76V}-GFP^{neg}, indicating that the presence of the Ub-GFP reporter had no influence on the deposition of PrP^{Sc}. No PrP^{Sc} was detected in non-infected control mice. The concurrent appearance of PrP^{Sc} with the Ub-GFP reporter indicates that there may be a relationship between the two. It should be noted, however, that the deposition of PrP^{Sc} was far more widespread than the appearance of the Ub-GFP reporter, with PrP^{Sc} being readily observed in cortical, striatal and hypothalamic regions that are typically associated with RML prion neuropathology (**Figure 4.4**).

Furthermore, confirmation of the deposition of PrP^{Sc} was completed by Western blot analysis of protease K resistant material in 10% brain homogenates made from the RML prion-infected Ub^{G76V}-GFP1 mice. PrP^{Sc} was readily observed at later time-points, whereas a NaPTA precipitation of aggregated material was required to detect PrP^{Sc} at days 85-125 post-inoculation (**Figure 4.5)**. PrP^{Sc} was not observed at day 45 post-inoculation, in agreement with the immunohistochemistry analysis. Protease K-resistant PrP^{Sc} was not observed in the brains of non-infected control animals.

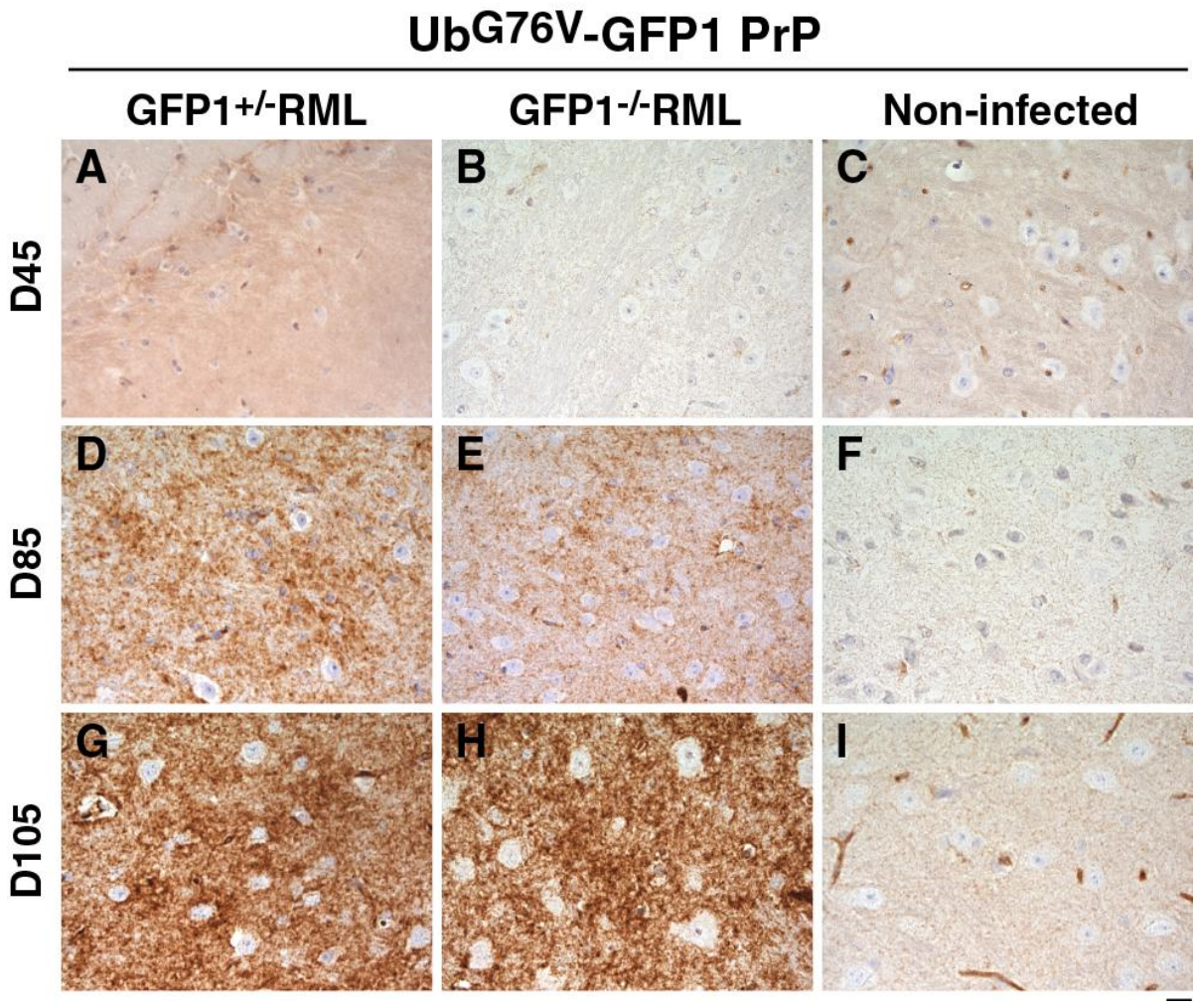

Figure 4.3 RML infected Ub^{G76V}-GFP1 mice accumulate PrP^{Sc} from day 85 post-inoculation through to end stage disease.

Ub^{G76V}-GFP1 mice (n=3) and non-transgenic controls (n=3) were inoculated i.c with 30 µl of 1% RML-infected mouse brain homogenates. Immunohistochemistry analysis was carried out on paraffin-embedded end-stage disease mouse brain tissue using the ICSM35 anti-PrP antibody. Significant deposition of formic acid-resistant PrP^{Sc} was observed throughout the brain in (**A, D, G, J, M, P**) Ub^{G76V}-GFP1 mice and non-transgenic controls (**B, E, H, K, N, Q**). No PrP^{Sc} was observed in non-infected mice inoculated with control CD1 mouse brain homogenate(**C, F, I, L, O, R**). Images are taken of the thalamus, scale bar = 20 µm.

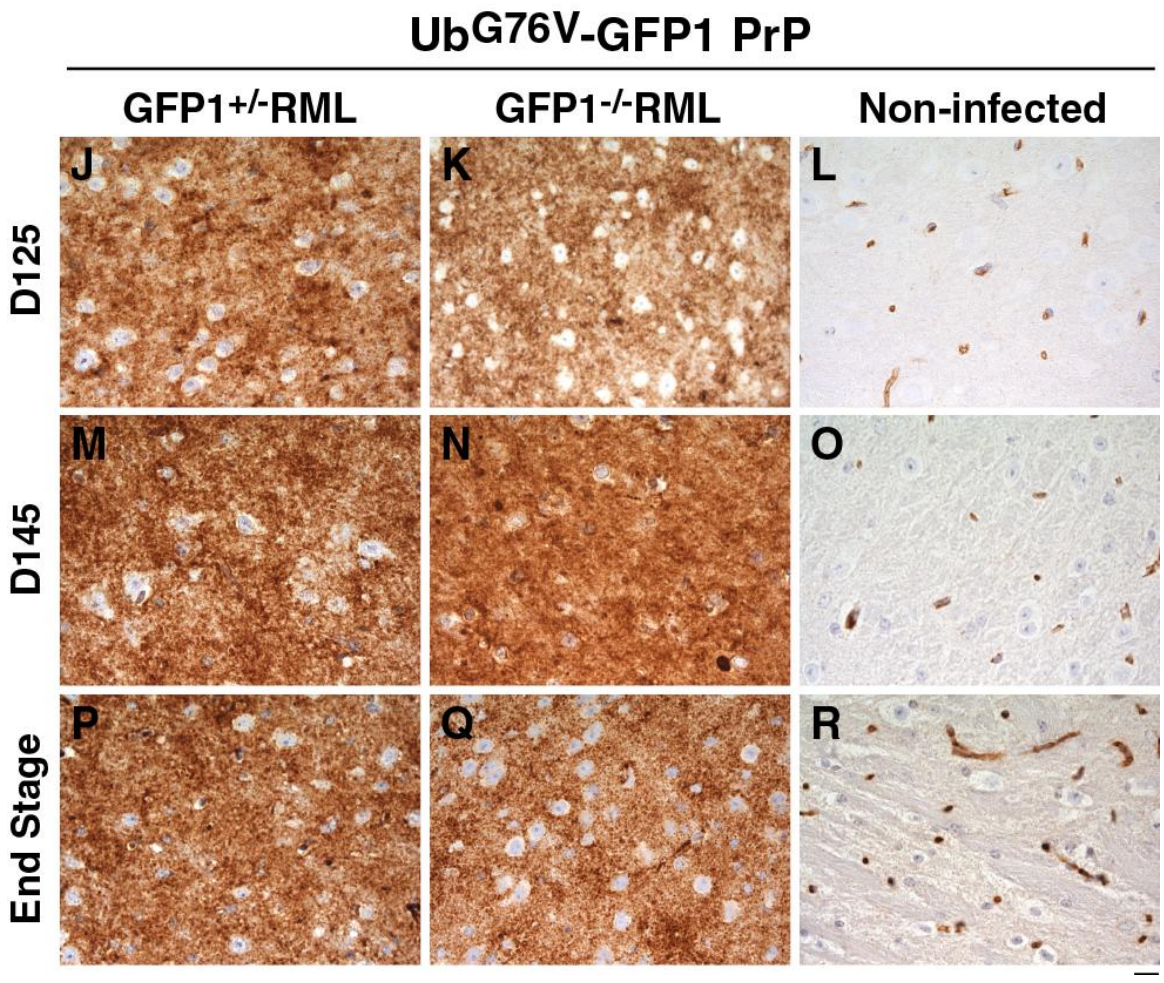

Figure 4.3 (continued). RML infected Ub^{G76V}-GFP1 mice accumulate PrP^{Sc} from day 85 post-inoculation through to end stage disease.

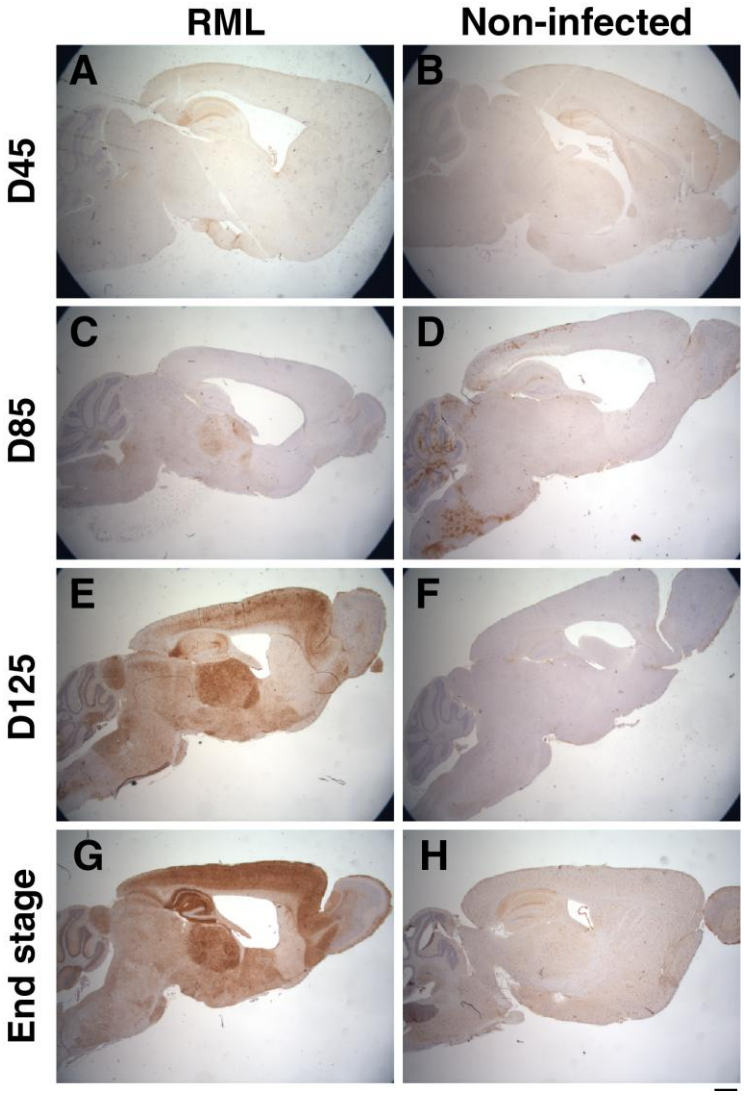

Figure 4.4 PrP^{Sc} deposition is widespread throughout the brain in RML infected Ub^{G76V}-GFP1 mice.

Ub^{G76V}-GFP1 mice (n=3) and non-transgenic controls (n=3) were inoculated i.c with 30 µl of 1% RML-infected mouse brain homogenates. Immunohistochemistry analysis was carried out on paraffin-embedded end-stage disease mouse brain tissue using the ICSM35 anti-PrP antibody. Significant deposition of formic acid-resistant PrP^{Sc} was observed throughout the brain in (**A, C, E, G**) Ub^{G76V}-GFP1 mice. No PrP^{Sc} was observed in non-infected mice inoculated with control CD1 mouse brain homogenate **(B, D, F, H)**. Scale bar = 1 mm.

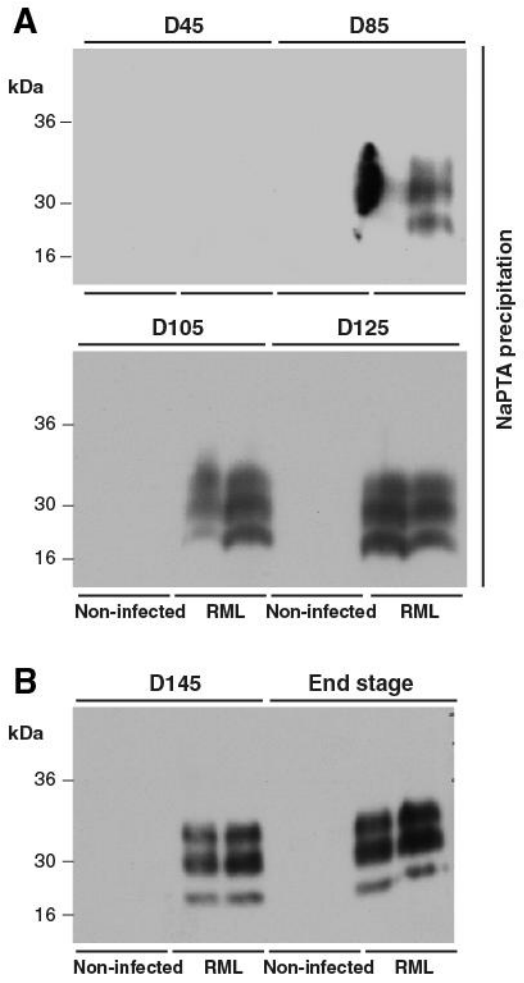

Figure 4.5 Immunoblot analysis of PrP^{Sc} expression in the brains of RML-prion-infected Ub^{G76V}-GFP1 mice.

Ub^{G76V}-GFP1 mice were inoculated with RML prions and culled at various time-points (days 45, 85, 105, 125, 145 and 165) post-inoculation. A 1% tissue homogenate was made for biochemical assay. (**A**) Samples obtained from the day 85, 105 and 125 groups required NaPTA precipitation prior to western blotting in order to observe a detectable PrP^{Sc} signal,(**B**) whereas as homogenates from days 145 and 165 produced a detectable signal without precipitation. Immunoblots were probed with the ICSM35 anti-PrP antibody.

4.4.4 Gliosis in the brains of RML prion-infected Ub^{G76V}-GFP1 mice

To directly assess neuropathological features of RML in the prion in Ub^{G76V}-GFP1 mice, brain sections were analysed by immunohistochemistry using a typical marker for gliosis. Extensive astrocytosis is a secondary marker of the onset of prion disease pathology, which can be readily detected by immunoreactivity of the specific astrocyte marker, GFAP. An increase in GFAP immunoreactivity was observed from day 85 post-inoculation onwards in the thalamus of RML prion-infected Ub^{G76V}-GFP1 mice (**Figure 4.6**), correlating to PrP^{Sc} deposits observed in the same time-point. This astrocytosis was also seen in Ub^{G76V}-GFP^{neg} mice, but not in non-infected controls. The increased GFAP expression was apparent throughout the brain (**Figure 4.7**). The concurrent appearance of prion disease-associated pathology with the Ub-GFP reporter indicates that there may be a relationship between the two in the earliest stages of pathogenesis.

Increasing evidence suggest that astrocyte pathology may contribute to a number of neurodegenerative disease mechanisms, including prion disease (Lepore et *al*., 2008; Wyss-Coray et *al*., 2003; Raeber et *al*., 1997). Astrogliosis is reported to be prominent, diffuse and intense throughout the affected CNS regions in CJD and other related prion disease, especially if clinical symptoms have been of long duration. Although this astrogliosis exhibit some characteristics of severe diffuse reactive astrogliosis, it is not clear whether astrocytes play an active role in prion replication and disease pathogenesis or whether astrogliosis is largely reactive to the disease process in other cell types (Kovacs and Budka, 2008).

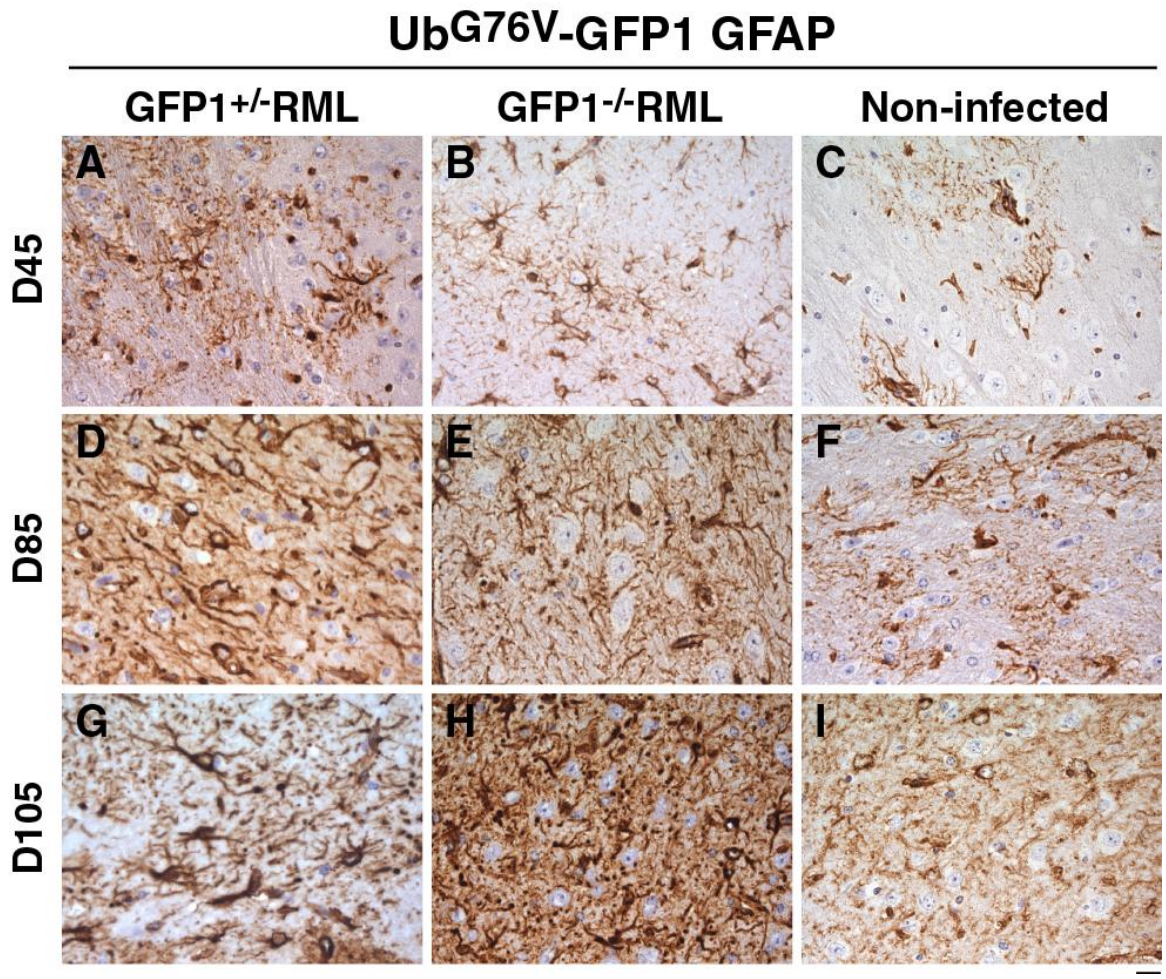

Figure 4.6 RML infected Ub^{G76V}-GFP1 mice exhibit increased astrocytosis from day 85 post-inoculation through to end stage disease.

Ub^{G76V}-GFP1 mice (n=3) and non-transgenic controls (n=3) were inoculated i.c with 30 µl of 1% RML-infected mouse brain homogenates. Immunohistochemistry was carried out on paraffin-embedded end-stage disease mouse brain tissue using an anti-GFAP antibody (Chemicon). Increased astrocytosis , a secondary neuropathological marker of prions disease pathology, was observed throughout the brain in (**A, D, G, J, M, P**) Ub^{G76V}-GFP1 mice and non-transgenic controls (**B, E, H, K, N, Q**). (**C-I;O-P**). Similar gliosis was not observed in non-infected mice inoculated with control CD1 mouse brain homogenate (**C, F, I, L, O, R**). Images are taken of the thalamus, scale bar = 20 µm.

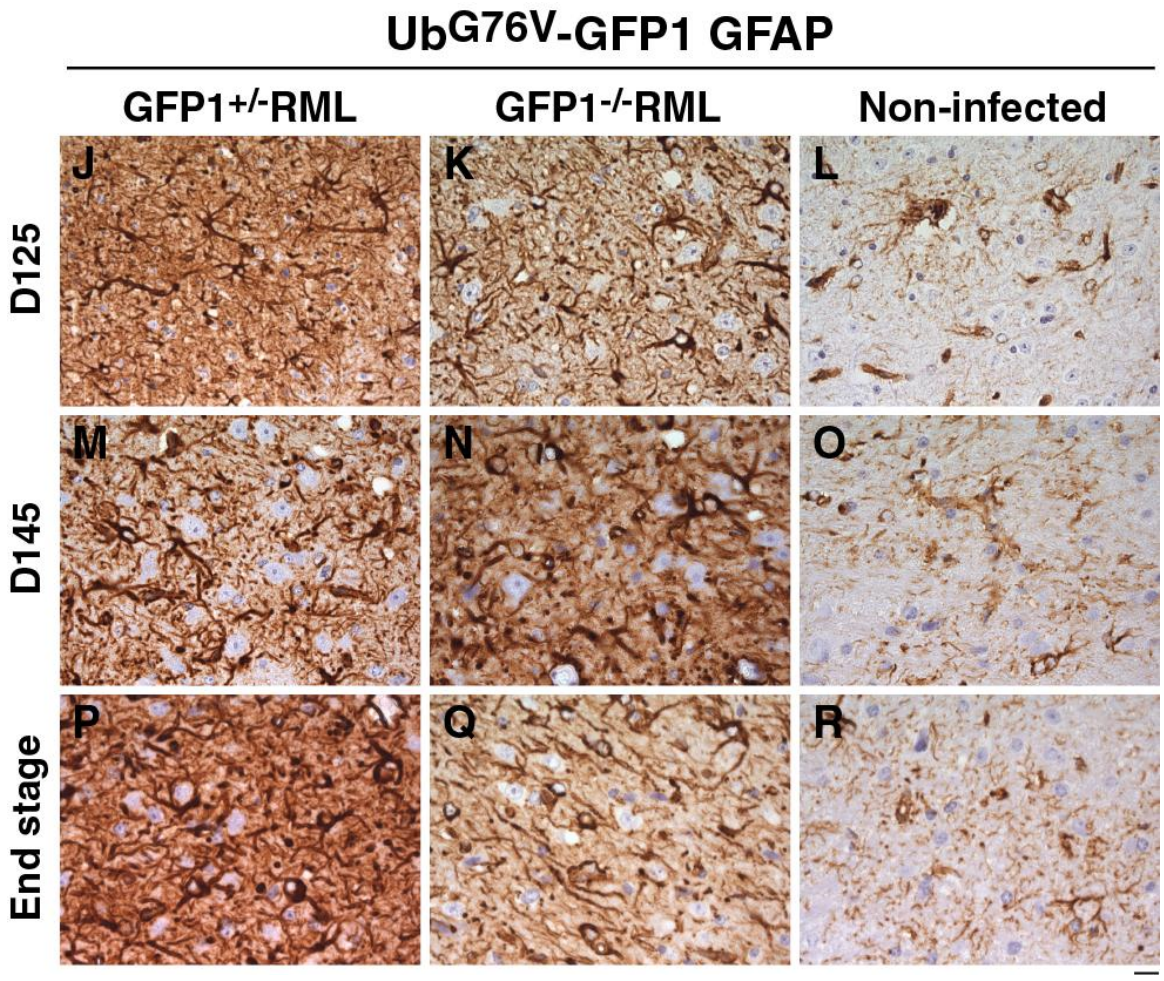

Figure 4.6 (continued). RML infected Ub^{G76V}-GFP1 mice exhibit increased astrocytosis from day 85 post-inoculation through to end stage disease.

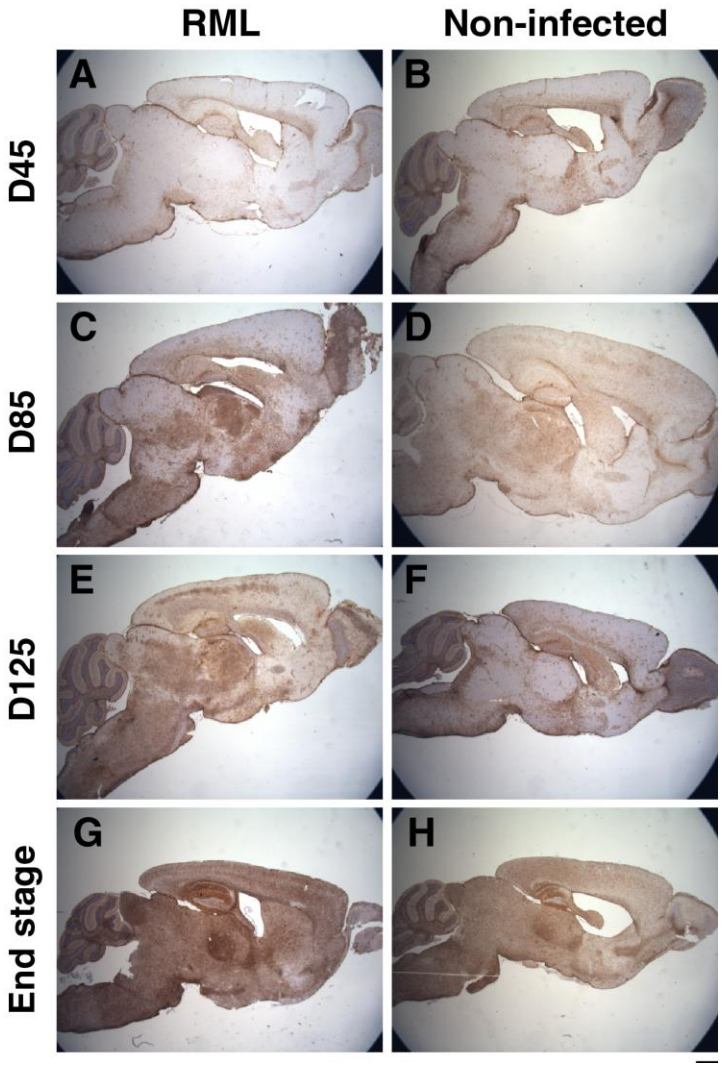

Figure 4.7 Astrocytosis is widespread throughout the brain in RML infected Ub^{G76V}-GFP1 mice.

Ub^{G76V}-GFP1 mice (n=3) and non-transgenic controls (n=3) were inoculated i.c with 30 µl of 1% RML-infected mouse brain homogenates. Immunohistochemistry was carried out on paraffin-embedded end-stage disease mouse brain tissue using an anti-GFAP antibody (Millipore). Increased astrocytosis, a secondary neuropathological marker of prions disease pathology, was observed throughout the brain in Ub^{G76V}-GFP1 mice **(A, C, E, G**). A lesser degree gliosis was observed in non-infected mice inoculated with control CD1 mouse brain homogenate (**B, D, F, H).** Scale bar = 1 mm.

4.4.4 Ubiquitin deposition in the brains of RML prion-infected Ub^{G76V}-GFP1 mice

To further clarify the relationship between prion infection and UPS dysfunction, immunohistochemistry was used to analyse ubiquitin deposition in the brains of RML prion-infected Ub^{G76V}-GFP1 reporter mice. Granular deposits of ubiquitin in the brain of end stage 22L prion-infected mice were previously reported (Kristiansen et *al*., 2007). Although discerning widespread changes in ubiquitin levels was proved difficult (**Figure 4.8**), similar granular ubiquitinated deposits as previously seen in the 22L prion infected mice were observed in the thalamus of the RML prion-infected Ub^{G76V}-GFP1 mice (**Figure 4.9**). This result provides some further evidence that the UPS machinery is impaired in the brains of prion infected mice.

Ubiquitin-protein conjugates within neurons have been previously reported in the brains of prion-infected mice, whereby intracellular ubiquitinated deposits were seen early and increased with disease progression (Lowe et *al*., 1992). Ubiquitin conjugates associated with pathological lesions have also been described in several neurodegenerative disorders. For example, In Parkinson's disease the level of the 26S proteasome and proteasome activity are reduced (Rubinsztein, 2006). However, a direct role of ubiquitinated proteins in those neurodegenerative diseases has not been established.

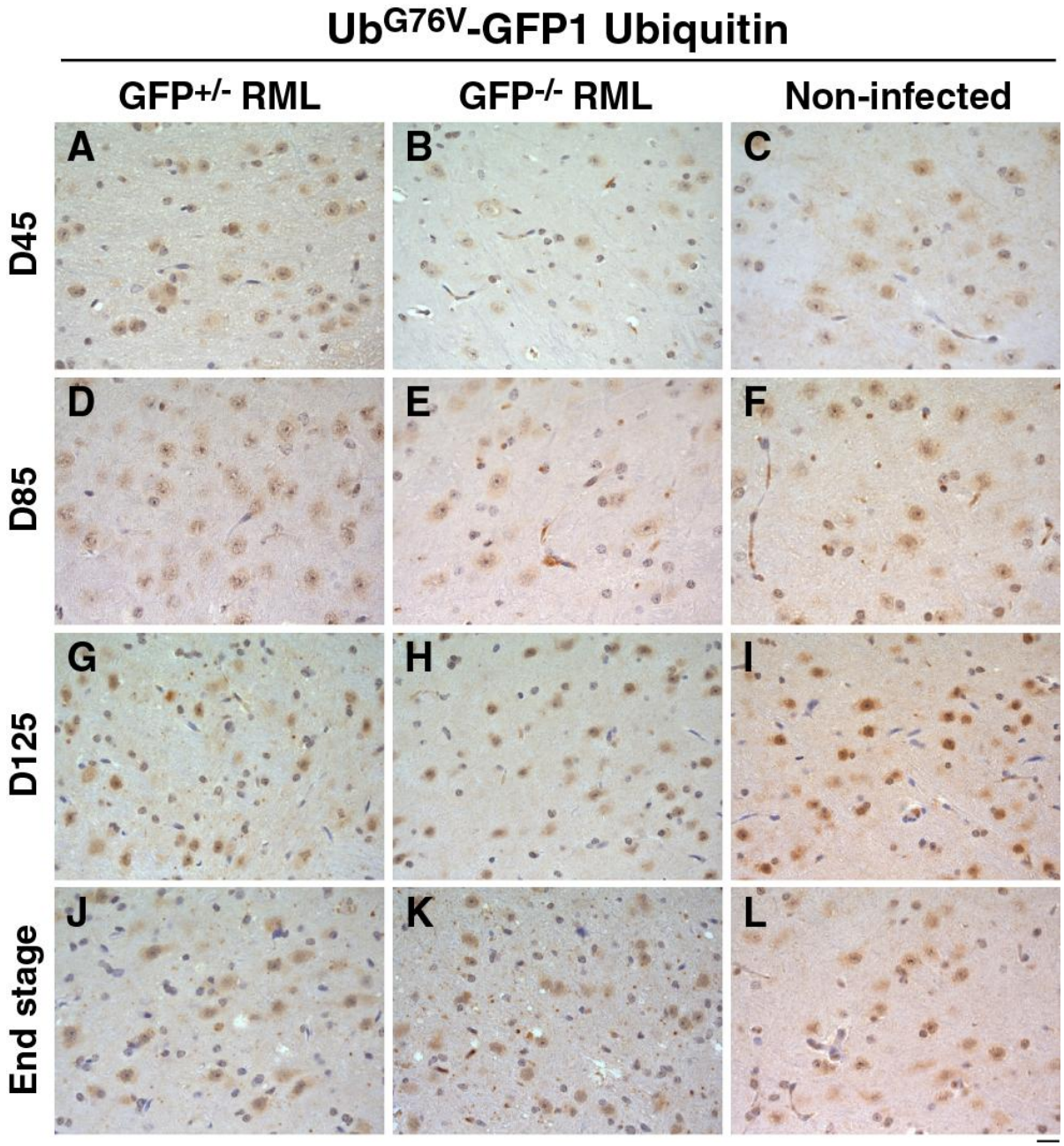

Figure 4.8 Prion infection causes some increase in the deposition of ubiquitinated proteins in Ub^{G76V}-GFP mice.

Ub^{G76V}-GFP1 mice (n=3) and non-transgenic controls (n=3) were inoculated i.c with 30 µl of 1% RML-infected mouse brain homogenates. Immunohistochemistry analysis was carried out on paraffin-embedded day 45, 85, 125 and 165 mouse brain tissue using an anti-

ubiquitin antibody (**Appendix I**). Ubiquitinated deposits were observed throughout the brain in Ub^{G76V}-GFP1 mice and non-transgenic controls. Images are taken of the thalamus, scale bar = 20 µm.

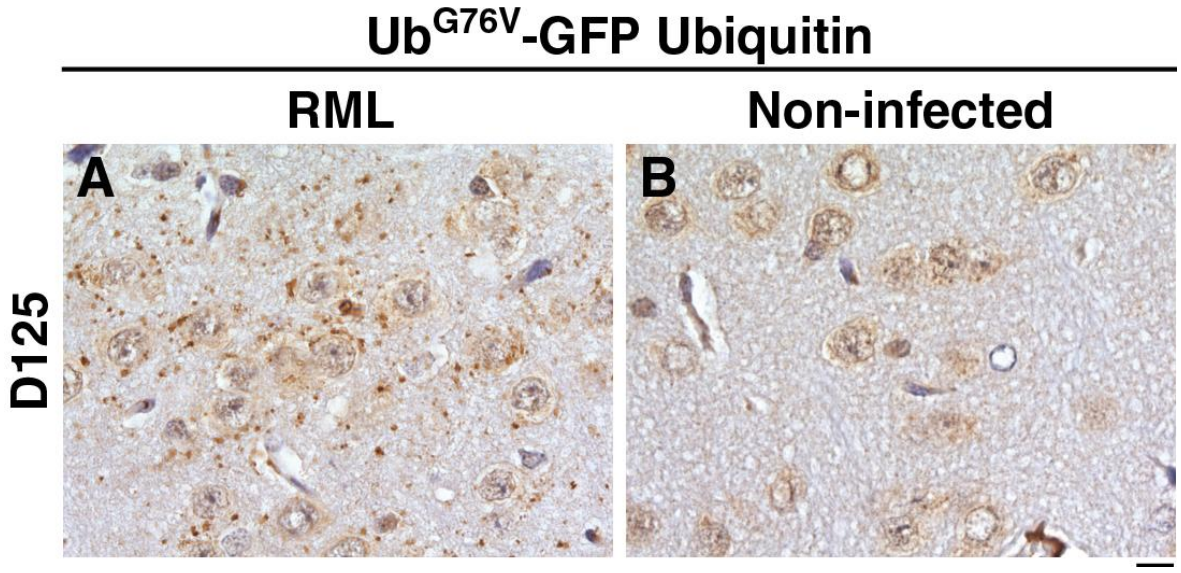

Figure 4.9 Ubiquitinated inclusions are observed in the thalamus of the brain in prion infected Ub^{G76V}-GFP mice.

Intracellular cytosolic granular ubiquitinated deposits is shown to accumulate at day 125 post RML prion infection in the brains of Ub^{G76V}-GFP1 reporter mice. These deposits could represent ubiquitinated-protein conjugates accumulate as they are not degraded by the failing proteasome. Immunohistochemistry analysis was carried out on paraffin-embedded day 125 on mouse brain tissue using an anti-ubiquitin antibody (Santa Cruz). Images are taken of the thalamus, scale bar = 20 µm.

In an attempt to quantify any differences in ubiquitin levels in the brains of RML prion-infected Ub^{G76V}-GFP1 mice, 10% homogenates were subjected to dot blot analysis. The data presented show that ubiquitin levels were significantly increased in the brains of RML prion infected mice from day 125 post-inoculation to end stage disease, as compared to their respective controls (**Figure 4.10**). Such differences were not observed at earlier time-points post-inoculation. Ubiquitin levels corresponded to differences in the poly-ubiquitin associated with accumulating UPS substrates, Western blots were carried out on the same samples (**Figure 4.11**). There was an increase in poly-ubiquitin level toward end stage disease in the RML prion infected mice brain. This result suggests that the differences on total ubiquitin levels could be ascribed to an accumulation of poly-ubiquitin associated with UPS dysfunction, rather than for example, differences in the expression level of non-conjugated monomeric ubiquitin. Student t-test. ***$p<0.001$, **$p<0.01$. For statistics report, see **Appendix IV.**

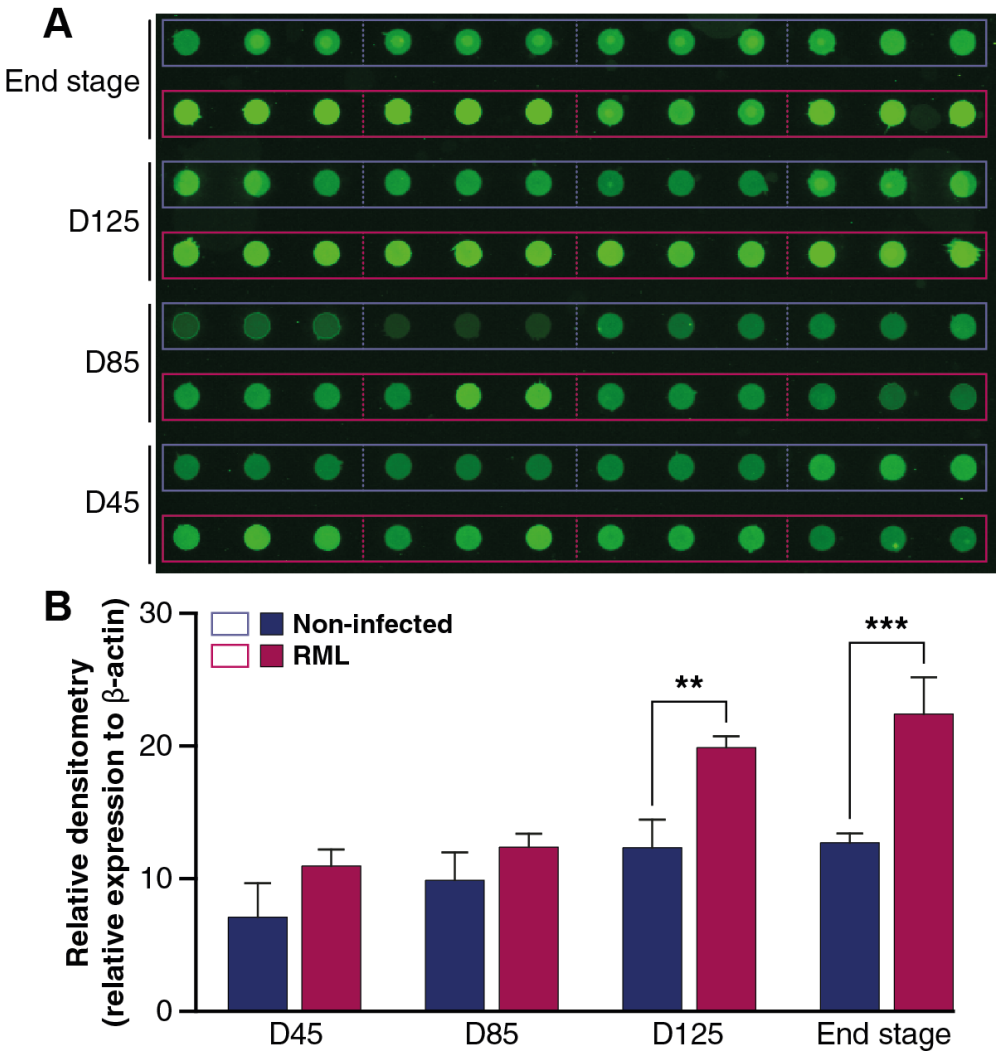

Figure 4.10 Total ubiquitin levels are increased in the brains of prion-infected Ub^{G76V}-GFP1 mice.

Ub^{G76V}-GFP1 mice were inoculated with RML prions and culled at various time-points (days 45, 85, 125, and 165) post-inoculation. A 1% tissue homogenate was prepared for biochemical assay and analysed using 96-well dot blot apparatus. (A) Membranes were probed with an anti-ubiquitin antibody (Santa Cruz) and analysed using the Li-cor Odyssey system. (B) Quantification demonstrates an accumulation of total ubiquitin in the brains of prion infected mice from day 125 to end stage disease. Data were normalised to β-actin levels in the same samples measured by Western blot and Li-cor analysis in **Figure 4.11**.

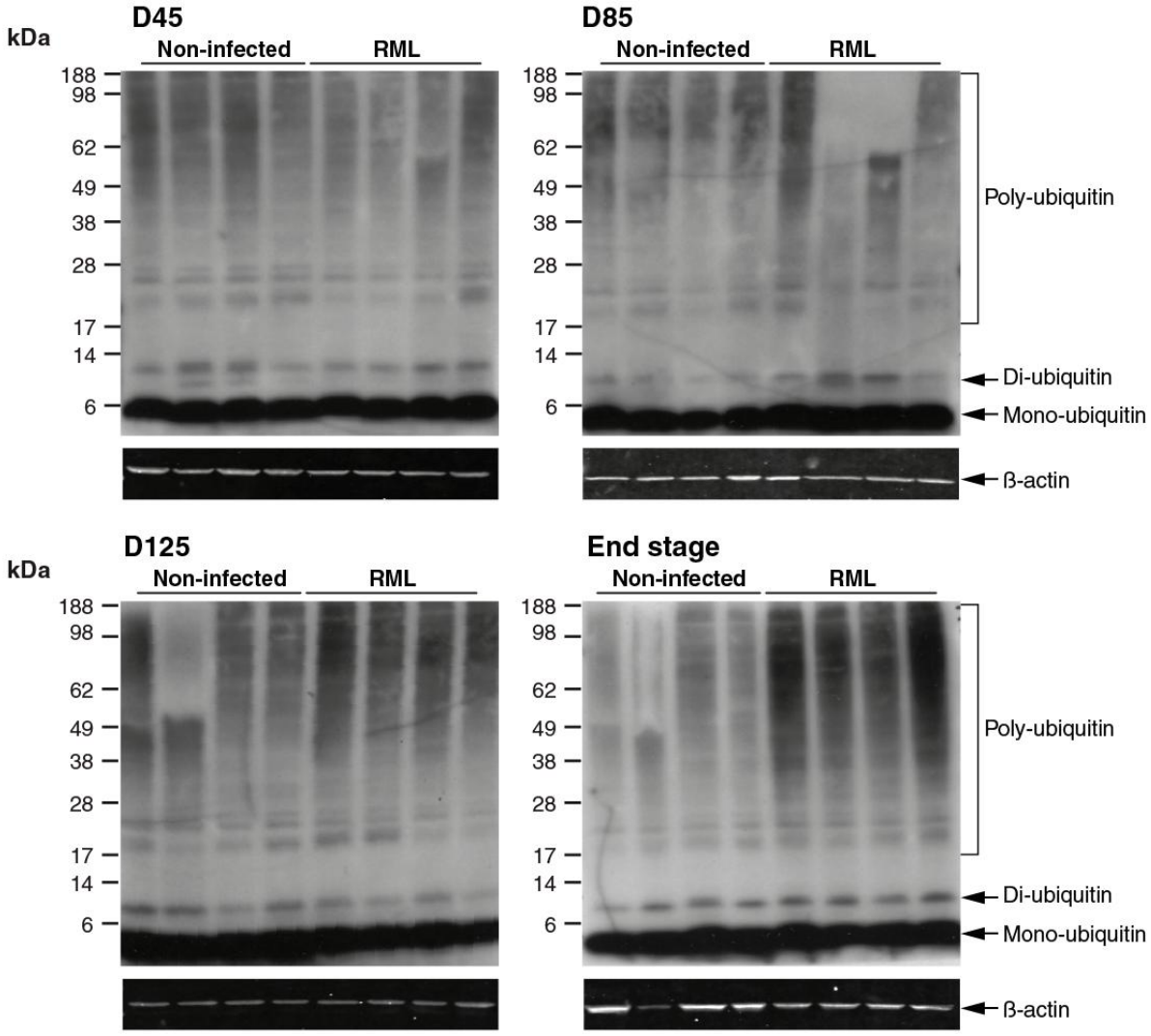

Figure 4.11 Accumulating ubiquitin in the brains of prion-infected Ub^{G76V}-GFP1 mice appears to consist of high molecular weight species.

Ub^{G76V}-GFP1 mice were inoculated with RML prions and culled at various time-points (days 45, 85, 125, and 165) post-inoculation. A 1% tissue homogenate was made for biochemical assay. Immunoblots were probed with anti-ubiquitin and anti β-actin antibodies. High molecular weight poly-ubiquitin species appear to accumulate in the brains of infected mice as disease progresses.

4.4.5 26S proteasome activity is impaired in the brains of prion-infected Ub^{G76V}-GFP1 mice

Given the observations made here that the UPS is impaired in the brains of RML-infected Ub^{G76V}-GFP1 mice during prion disease pathogenesis, and that a direct inhibitory effect of β-sheet-rich PrP species on 26S proteasomes has been reported by (Deriziotis et *al*., 2011), the activity of 26S proteasomes in the brains of the RML-infected Ub^{G76V}-GFP1 mice was assessed. The enzymatic function of the proteasomes in RML-infected Ub^{G76V} – GFP mice was analysed using fluorogenic peptide activity assays, as used routinely in our laboratory (Kristiansen et *al*., 2007). In particular, the chymotrypsin-like peptidase activity of the 26S proteasome was measured (**Figure 4.12**). The results demonstrate that 26S proteasomal activity was inhibited from day 145 post-inoculation onwards, correlating reasonably well with the deposition of poly-ubiquitinated substrates in the brain described above (**Figure 4.10**) at these time-points. Thus, the effect of prions to cause UPS dysfunction is associated with a functional loss of proteasome activity in the brains of these mice. Student t-test ***p<0.001, *p<0.05 (compared to uninfected control). See **Appendix IV for** statistics report.

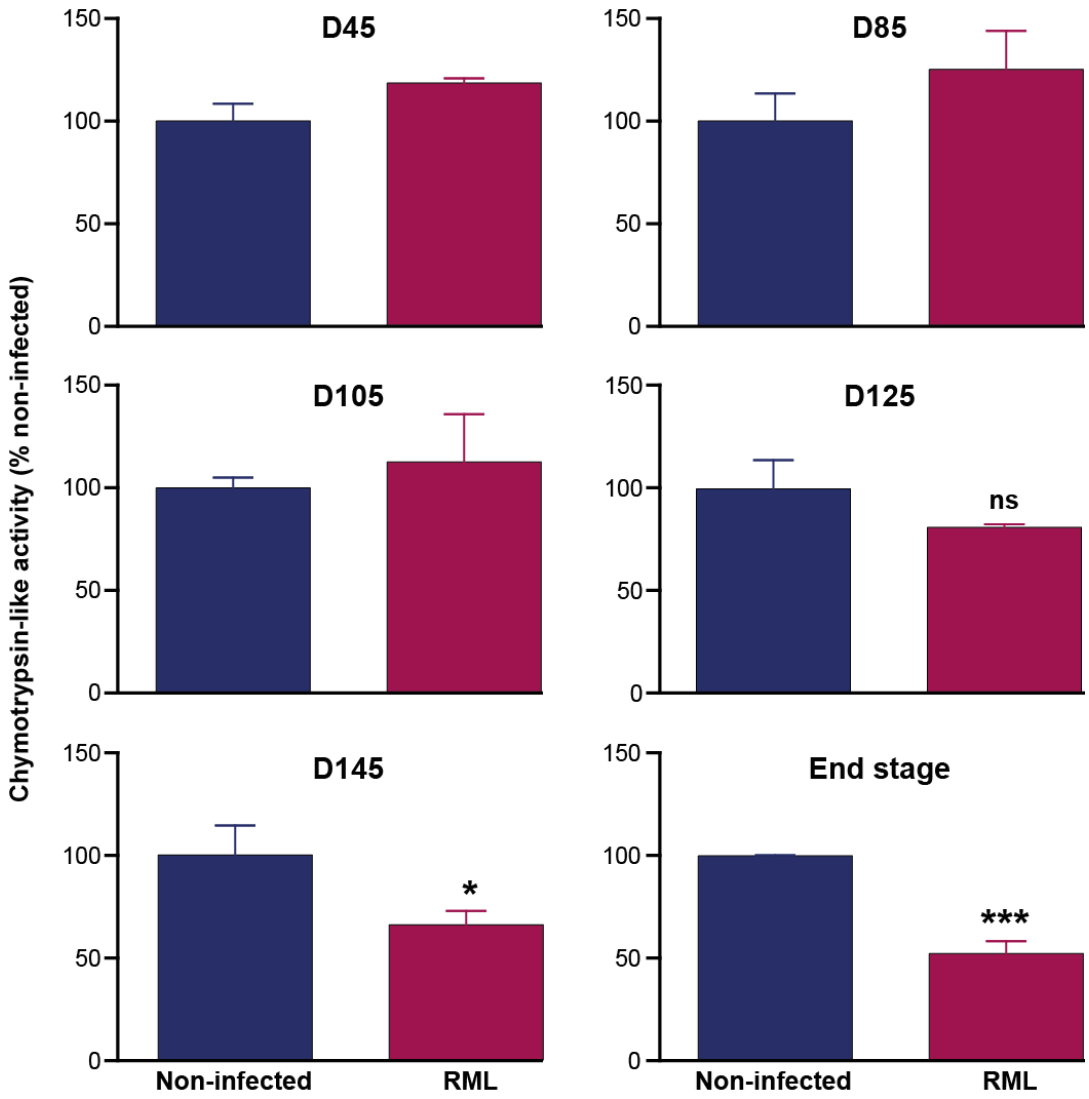

Figure 4.12 RML prion infection causes impairment of the proteolytic activity of the 26S proteasome in Ub^{G76V}-GFP1 mice.

26S proteasomes in the brains of RML prion-infected Ub^{G76V}-GFP1 mice showed a significant reduction in 20S proteasome chymotrypsin-like proteolytic activity as compared to control non-infected mice towards end stage disease. Data are means of three independent experiments. *This experiment was done by Dr. Ralph Andre.*

4.4.6 A marker of ER stress is observed at end stage disease in the brains of prion-infected Ub^{G76V}-GFP1 mice

Alteration of ER homeostasis by several forms of stress, such as heat shock, overexpression of mutant proteins, or alteration of proteasome activity can cause the accumulation of misfolded proteins in the ER (Ferri and Kroemer, 2001; Liu et *al*., 1997). These alterations trigger specific activation of a protective cellular response, leading to upregulation of ER chaperones and a general decrease in protein synthesis (Rao et *al*., 2002; Reddy et *al*., 1999). Increased expression of ER chaperones glucose-regulated protein (grp) such as; Grp78/BiP (immunoglobulin chain binding protein) can exert a pro-survival effect of the UPR (Reddy et *al*., 1999; Rao et *al*., 2002; Sitia and Braakman, 2003).

To investigate whether a relationship exists between RML prion infection and ER stress, Ub^{G76V}-GFP1 reporter mice brains were evaluated for the ER stress marker, Grp78/BiP. The Grp78/BiP protein was observed in a few dispersed cells at end stage disease in the thalamus of RML prion infected Ub^{G76V}-GFP mice brain, but not in non-infected controls (**Figure 4.13)**. The small pool of cells expressing Grp78/BiP indicates that ER stress may be a late event in the course prion disease. This observation suggests that prion-induced UPS dysfunction may precede disease-associated ER stress, and that prions may trigger a non-classical ER stress response.

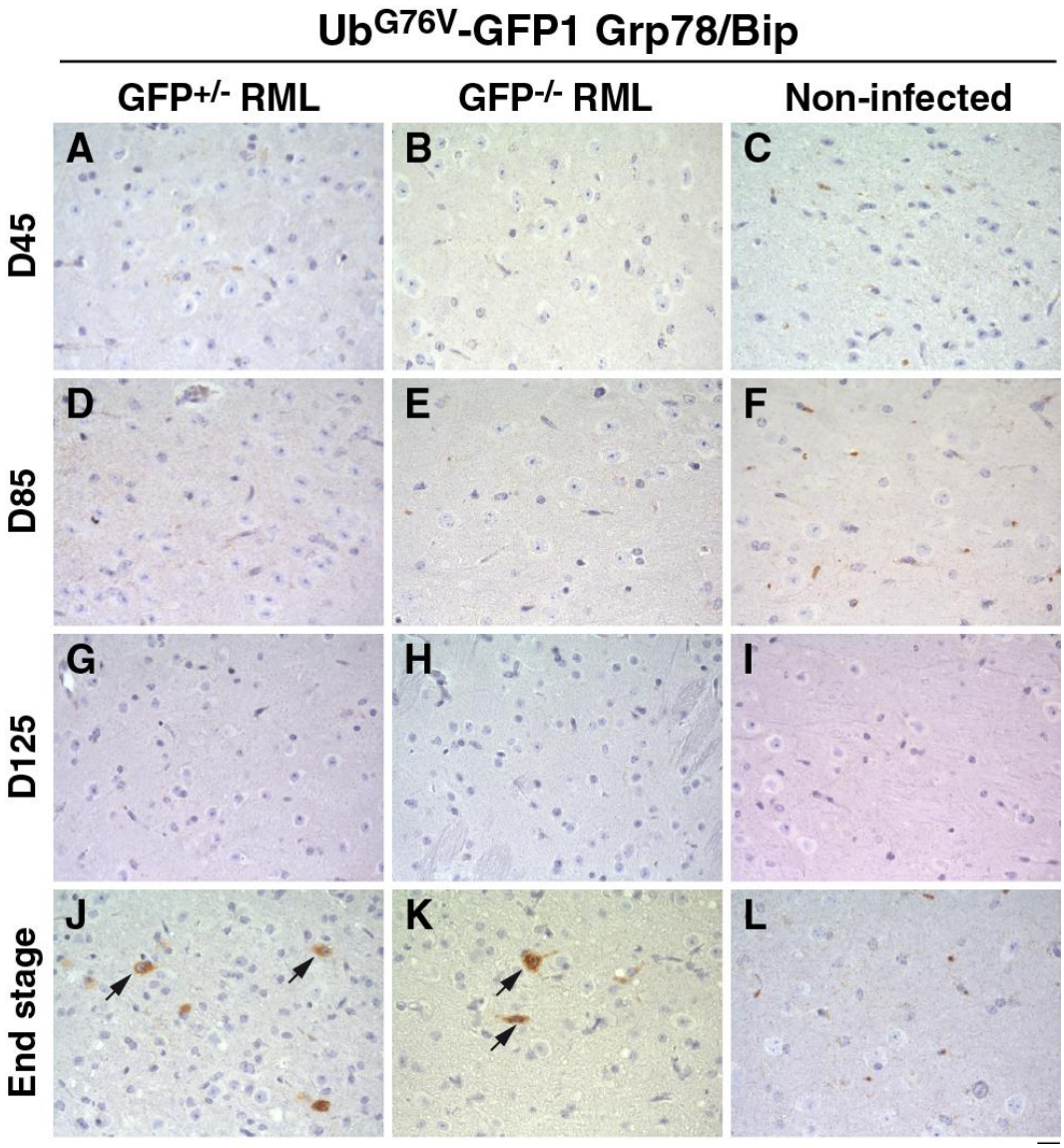

Figure 4.13 Prion infection increases the expression of Grp78/Bip, indicating ER stress, at end stage disease in the brains of Ub^{G76V}-GFP1 mice .

Ub^{G76V}-GFP1 mice (n=3) and non-transgenic controls (n=3) were inoculated i.c with 30 µl of 1% RML-infected mouse brain homogenates. Immunohistochemistry analysis was carried out on paraffin-embedded day 45, 85, 125 and 165 mouse brain tissue using an anti-Grp78/Bip antibody (Cell Signaling). Deposits, shown with arrows, were observed in the thalamus of RML prion infected brain at end stage disease (**J** and **K),** but not in the non-transgenic controls (**L**). Images are taken of the thalamus, scale bar = 20 µm.

4. 5 DISCUSSION

The data presented in this chapter indicate an impairment of the UPS machinery in the brains of Ub^{G76V}-GFP reporter mice infected with RML prion infection, as shown by the accumulation of the model substrate, Ub^{G76V}-GFP (Dantuma et *al*., 2000; Lindsten et *al*., 2003). Accumulation of the Ub^{G76V}-GFP reporter occurred only in the brains of prion-infected mice, with no Ub-GFP being observed in animals injected with non-prion control homogenate. The observed accumulation of Ub-GFP coincided with markers of prion disease neuropathology such as PrP^{Sc} deposition and extensive GFAP immunoreactivity. The accumulation of the Ub-GFP reporter was observed early in the disease time-course, at least at 85 days post-inoculation following infection with RML prions in a ~160 day disease time-course **(Figure 4.1)**. This was also the earliest time-point at which PrP^{Sc} and other neuropathological markers were observed. Moreover, these observations seemed to be restricted at these early time-points to certain regions of the brain such as the thalamus, suggesting some spatial as well as temporal correlation between UPS impairment and prion disease pathology. This supports the claim that impairment of the UPS may be an important contributor to prion disease pathogenesis (Kristiansen et *al*., 2007; Deriziotis and Tabrizi, 2008; Andre and Tabrizi, 2012).

During the experimental time-course, clinical symptoms of prion disease were monitored in both Ub^{G76V}-GFP transgenic mice until end-stage disease. The onset of disease pathology was confirmed by the presence of PrP^{Sc} deposits, gliosis and spongiosis in affected areas of the brain in the RML prion-infected mice, but not in non-infected littermate control animals (**Figure 4.3; Figure 4.6, Figure 4.7)**. Further confirmation of PrP^{Sc} deposits was provided by western blot analysis of proteinase K resistant material in the brains of these animals. PrP^{Sc} was not observable at day 45 post-inoculation, in agreement with the immunohistochemistry analysis. The onset of PrP^{Sc} was observed by Western blotting at day 85 post-inoculation, with a subsequent increase in PrP^{Sc} levels until end-

stage disease, is also consistent with the immunohistochemistry observations. There were no obvious differences in the appearance or time-course of prion disease pathology between either of the two Ub^{G76V}-GFP lines and their non-transgenic Ub^{G76V}-GFP^{neg} counterparts. This indicates that the expression of the Ub-GFP reporter itself does not influence the course of disease pathology in these animals.

Due to its apparent increased sensitivity to UPS impairment, the Ub^{G76V}-GFP1 line was chosen for use in the majority of the experiments described in this Chapter. Detection of the Ub-GFP reporter was observed only in the brains of RML-prion infected mice. No Ub-GFP reporter accumulation was seen in the brains of Ub^{G76V}-GFP inoculated with control normal brain homogenate, or in RML-prion infected Ub^{G76V}-GFP^{neg} littermates (**Figure 4.1).** This indicates that the effects observed are specific to both infection of animals with RML prions and to the detection of the Ub-GFP reporter itself. Similar results were obtained with the two available reporter mouse strains, Ub^{G76V}-GFP1 and Ub^{G76V}-GFP2, established from different founders (Dantuma et *al*., 2002; Lindsten et *al*., 2003). Taken together, these data show that UPS dysfunction occurs in the brains of prion-infected mice relatively early in disease progression, well before the onset of clinical signs.

The majority of the cells in which the Ub-GFP reporter was observed in the thalamus appeared to be astrocytes, although some neurons were observed throughout the time-course. Increasing evidence points towards reactive astrogliosis to play either a primary or a contributing role in neurodegeneration, either via a loss of normal astrocyte functions or a gain of abnormal effects (Eklund et *al*., 1967; Race et *al*., 1995; Raeber et *al*., 1997). Although diffuse reactive astrogliosis is one of the most prominent neuropathological features and most commonly observed in prion diseases (Scott and Fraser, 1984), it is not clear whether astrocytes play an active role in prion replication or disease pathogenesis, or whether astrogliosis is largely reactive to the disease process in other cell types (Kovacs and Budka, 2008). In Parkinson' s disease, astrocytes have been implicated as potentially

exerting both neurotoxic (Di Monte et *al*., 1996; Przedborski et *al*., 2000) and neuroprotective activities (Chen et *al*., 2009).

There is evidence to suggest two different potential roles for astrocytes in neurodegenerative diseases, through the loss of a neuroprotective function and a gain of a neurotoxic effect (Lepore et *al*., 2008; Rothstein et *al*., 2005). In Huntington's disease, astrocytes have been implicated in the disturbances of glutamate uptake that can alter synaptic function and lead to excitotoxicity, or in abnormal production of neurotoxic molecules (Lobsiger and Cleveland, 2007; Maragakis and Rothstein, 2006; Gil and Rego, 2008). In Alzheimer's disease, reactive astrogliosis tends to be focal such that they are intimately associated with amyloid plaques or diffuse deposits of amyloid and surround them with dense layers of processes (Nagele et *al*., 2004; Thal et *al*., 2000). It is also reported that reactive astrocytes can take up and degrade extracellular deposits of AB42 (Wyss-Coray et *al*., 2003), and this function is attenuated in ApoE-/- astrocytes (Koistinaho et *al*., 2004), suggesting that both the function and dysfunction of astrocytes could play a role in the progression and severity of Alzheimer's disease.

The occurrence of astrogliosis and impaired proteasome activity in neurodegenerative diseases has led to the speculation that the UPS might contribute to the regulation of astrogliosis (Midderldorp et *al*., 2009; Sabbatini et *al*., 1999; Yoshida et *al*., 1996). GFAP protein levels are generally up-regulated in reactive astrocytes in diseases, in which impaired proteasome activity is confirmed, (Tang et *al*., 2006; Maragakis et *al*., 2006). By contrast, it was shown that proteasome inhibition does not induce an accumulation of GFAP protein but rather induces a sharp decrease in the transcript levels of all expressed GFAP isoforms *in vitro* (Midderldorp et *al*., 2009). Furthermore, proteasome inhibition prevents GFAP accumulation in reactive astrocytes *in vivo,* thereby suppressing reactive astrocytes (Midderldorp et *al*., 2009). The decrease in proteasome activity described by others, however, was measured in whole brain homogenates without discriminating between different cell types (Keller et *al*., 2000; Lopez et *al*., 2000; Glenn et

al., 2004). Moreover, ubiquitin immunoreactivity was found mostly in inclusion bodies within neurons (Layfield et *al*., 2005; Lowe et *al*., 1988), but not astrocytes. Taken together, it could be argued that the proteasome is not inhibited in astrocytes but might rather be activated.

Intracellular cytosolic granular ubiquitinated deposits have been shown to accumulate in the brains of 22L prion-infected mice, accompanying with the appearance of the Ub-GFP reporter (Kristiansen et *al*., 2007). These deposits may represent ubiquitinated-protein conjugates that accumulate as they are not degraded by the failing proteasome. Although, similar intracellular cytosolic granular ubiquitinated deposits were observed by immunohistochemistry in the present study in the brains of RML prion-infected Ub^{G76V}-GFP1 mice, they were not observed at early time-points to coincide with the accumulation of the Ub-GFP reporter. Nevertheless, a slight increase of ubiquitinated-protein was observed towards end-stage disease in the thalamus of the RML prion-infected Ub^{G76V}-GFP1 mice (**Figure 4.8).** Interestingly, ubiquitin-protein conjugates within neurons have been reported in the brains of prion-infected mice, whereby intracellular ubiquitinated deposits were seen early and increased with disease progression (Lowe et *al*., 1992). In addition, the pathological accumulation of the intracellular ubiquitin-protein structures corresponded temporally with the earliest detection of PrP^{Sc} (Lowe et *al*., 1992).

To further assess differences in ubiquitin levels in the brains of RML prion-infected Ub^{G76V}-GFP1 mice, brain homogenates from these mice were analysed by immunoblotting. Using a quantitative dot-blotting assay, ubiquitin levels were significantly increased in the brains of RML-prion infected mice from day 125 post-inoculation to end stage disease, as compared to their non-infected controls (**Figure 4.10**). Such differences were not observed at earlier time-points post-RML infection. Furthermore, Western blots were carried out on the same samples to determine whether changes in total ubiquitin levels corresponded to differences in poly-ubiquitin associated with UPS substrates that may have failed to

degrade by the proteasome, (**Figure 4.11**). The results demonstrate that increase in total ubiquitin levels correlates with the appearance of high-molecular weight poly-ubiquitin conjugates. Collectively, these data suggest that the differences in total ubiquitin levels can be ascribed to an accumulation of poly-ubiquitin associated with UPS dysfunction, rather than differences in the expression level of non-conjugated monomeric ubiquitin.

Recent work done by our group described a novel mechanism of inhibition by PrP isoforms containing a β-sheet-rich structure similar to that of PrP^{Sc} (Deriziotis et *al*., 2011; Andre and Tabrizi, 2012). This occurs by a direct interaction between the 20S proteasome core particle and β-sheet-rich PrP isoforms, as demonstrated by immunoprecipitation both *in vitro* and *in vivo* (Deriziotis et *al*., 2011). The interaction causes an impairment of the opening of the gate of the 20S core particle through which substrates are able to pass into the catalytic core of the proteasome. Such impairment results in reduction in the rate of proteolytic cleavage by each of the peptidase sites; (chymotrypsin-like, trypsin-like and caspase-like) in the 20S proteasome (Deriziotis et *al*., 2011). Similar findings have been shown in Alzheimer's disease, where *in vitro* studies demonstrated a direct binding of Aβ protein to bovine 20S proteasomes, resulting in a reduction in chymotrypsin-like activity (Gregory et *al*., 1995, Gregory et *al*., 1997). Moreover, transgenic Alzheimer's disease mice have been shown to have impaired proteasome activity that correlates with an accumulation of intraneuronal Aβ oligomers (Tseng et *al*., 2008).

Direct interaction of PrP^{Sc} with the 20S core particle to mediate impairment of the 26S proteasome may be the cause of the accumulation of the Ub-GFP reporter in RML-prion infected Ub^{G76V}-GFP mice. If so, a reduction in the proteolytic activity of the 26S proteasome in brains extract from these mice would be expected. Therefore, to ascertain this inhibitory effect in the brains of RML-prion infected Ub^{G76V}-GFP mice, fluorogenic peptide activity assays were performed to assess proteasomal function (**Figure 4.12**). Indeed, the chymotrypsin-like activity measured in brain tissue lysates was significantly reduced from day 145 post-inoculation onwards. The data presented here correlate

reasonably well with the deposition of poly-ubiquitinated substrates described above (**Figure 4.11**). However, the proteasome inhibition described here is observed much later than the initial appearance of the Ub-GFP reporter in the brains of the RML-prion infected mice. Presumably, this discrepancy can be explained by the limited spatial distribution of UPS impairment at these earlier time-points, to an extent that fluorogenic peptide activity assays of whole brain tissue lysate would not be sensitive enough to detect such an impairment.

Accumulation of ubiquitin may be related to the activity of protein degradation machinery attempting to degrade aggregates of misfolded proteins, or misfolded proteins themselves have an inhibitory effect on the UPS (Bence et *al*., 2001; Glickman and Ciechanover, 2002). A large number of *in vitro* studies support the potential importance of UPS impairment in neurodegenerative diseases (Ciechanover and Brundin, 2003), but the precise role of the UPS and its mechanisms of action in disease remains unclear despite the huge increase of *in vivo* studies. Mass spectrometry-based method revealed that lysine 48-linked polyubiquitin chains, which is typically associated with proteasomal targeting, accumulate early in the pathogenesis of both transgenic Huntington's disease mice and in Huntington's disease patients (Bennett et *al*., 2007). In addition, *Psmc1*(Rpt2) knock-out mouse model with a neurodegenerative phenotype and ubiquitin-positive inclusions displayed 26S proteasomal dysfunction in neurons (Bedford et *al*., 2008), providing *in vivo* evidence for a direct role of the UPS in the pathogenesis of these neurodegenerative diseases. Taken together, the results presented here suggest that UPS dysfunction is associated with neurodegenerative diseases. However, the mechanism(s) of UPS impairment remain unclear.

ER stress is not only caused by disturbances in the ER structure and function, but also by accumulation of misfolded proteins, as well as alterations in calcium homeostasis (Ciechanover and Brundin, 2003; Imai et *al*., 2001; Korhonen and Lindholm, 2004). In case of prolonged or aggravated ER stress, cellular signals leading to cell death are activated.

Indeed, cell expressing mutant presenilin involved in familiar early-onset AD are more sensitive to ER stress compared to normal cells (Guo et *al*., 1999). ER resident chaperones involved in quality control play a major role in neurodegenerative disorders. High capacity and low affinity of calcium of Grp78/Bip and Grp94 has led to the suggestion that chaperones may act as a calcium buffer and are thus protective against alteration in calcium homeostasis (Michalak et *al*., 2002). Heat shock protein, Hsp90 and Hsp70 can inhibit Aß aggregation (Evans et *al*., 2006). One of the chaperones of the UPR, BiP/GRP78 has been found to be upregulated in AD brain (Hoozemans et *al*., 2005). In addition, increased levels of Bip/Grp78 and the protein kinase, perk have been shown in AD brain, suggesting neurotoxicity leading to cell death (Hoozemans et *al*., 2005). BiP (GrP78) binds regulating protein APP in AD and reduces the production of Aß aggregates (Kudo et *al*., 2006; Yang et *al*., 1998).

A frequently discussed hypothesis to explain the pathogenesis of neurodegenerative disorders involves chronic oxidative stress. Dysfunction of any of several interconnected cellular pathways is sufficient to cause oxidative stress in the brain, including defects in the ubiquitin-proteasome system and the presence of aggregated proteins (Halliwell, 2006; Menendez-Benito et *al*., 2005). Several lines of evidence suggest that PrP^{C} may play a role in protecting cells from oxidative stress (Milhavet and Lehmann, 2002; Brown et *al*., 1997; Brown et *al*., 2002). Perhaps the most compelling observation is that neurons cultured from cerebellar granular layer and neocortex from Prn-p0/0 mice are more susceptible than neurons from wild-type mice to treatment with agents that induce oxidative stress, including hydrogen peroxide and copper ions (Brown et *al*., 1997; Brown et *al*., 2002).

There is evidence to suggest that activation of ER stress genes are significantly upregulated in prion pathogenesis, suggesting that ER stress is linked to the disease. ER specific caspases, such as the caspase-12, are thought to directly induce cell death. The

correlation between caspase-12 activation and neuronal loss was confirmed in model of prion-infected mice as well as in CJD patients (Castilla and Soto, 2005). Previously, it was shown that prion replication is accompanied by increased expression of Grp58 in the brain regions showing extensive neuronal loss at terminal stage of the disease in both human affected with CJD and mouse models (Yoo et *al*., 2002; Hetz et *al*., 2003). In addition, downregulation of Grp58 at the terminal stage of the disease correlated with the occurrence of neuronal loss (Hetz et *al*., 2005; Hetz et *al*., 2003), suggesting a general mechanism of neuronal toxicity initiated by the accumulation of misfolded proteins in neurodegenerative diseases (Soto, 2003). Bip/Grp78 and Grp94 have been reported to have protective activity against ER stress-mediated apoptosis and control protein folding and components of the UPR (Liu et *al*., 1997; Reddy et *al*., 1999; Rao et *al*., 2002). Therefore, to investigate whether ER stress is implicated in the RML prion infection, Ub^{G76V}-GFP reporter mice brain, were assessed for Bip/Grp78 expression.

A small increase in Bip/Grp78 protein level was observed in the Ub^{G76V}-GFP mice brain infected with RML prion but not in non-infected controls (**Figure 4.13)**. It is important to note that this effect was seen only at the late stage of prion disease, indicating that ER stress may be a late event in the course of prion disease, occurring after the onset of UPS impairment. The question that remains, however, is whether cell death is caused by ER stress and not the result of other pathway malfunction. Indeed, very little is known about the importance of interaction in the control of cell death, and the proteins taken part in ER-cross pathways communication.

Collectively, data presented in this chapter support the hypothesis that relates prion infection with the impairment of the UPS machinery. Evidence for a direct relationship between neuropathology and the UPS impairment in the Ub^{G76V}-GFP reporter mice is presented. Together, results in this chapter support a potential role of the UPS in prion disease mediated neurodegeneration.

4.6 SUMMARY

The work in this chapter describes an early UPS impairment in the Ub^{G76V}-GFP reporter mice during the course of prion disease, following RML infection. The Ub-GFP reporter accumulates only in the brains of RML-prion infected mice and not in the brains of Ub^{G76V}-GFP inoculated with control normal brain homogenate, or in RML-prion infected Ub^{G76V}-GFP^{neg} littermates, indicative of a functional impairment in the UPS machinery. The observed accumulation of Ub-GFP coincides with markers of prion disease neuropathology such as PrP^{Sc} deposition and extensive GFAP immunoreactivity. The majority of the cells in which the Ub-GFP reporter was observed in the thalamus appeared to be astrocytes, suggesting that astrocyte pathology may contribute to disease pathophysiology. Additionally, ubiquitin levels were significantly increased in the brains of RML prion infected mice from day 125 post-inoculation to end stage disease, correlating with fluorogenic peptide assays data, which show prion infection inhibits the chymoptrypsin-like and 26S proteasomal activities in brain lysates of the Ub^{G76V}-GFP mice. An assessment of ER stress indicates that ER stress may be a late event in the course of prion disease. Together, these results provide evidence for a direct relationship between prion neuropathology and UPS impairment in Ub^{G76V}-GFP -reporter transgenic mice. Collectively, this chapter described UPS impairment as an early phenomenon in prion disease pathogenesis.

5 MOTOR SKILLS DEFICITS AND SYNAPTIC DYSFUNCTION IN Ub^{G76V}-GFP REPORTER MICE

5.1 BACKGROUND

The neuropathology of prion diseases is associated with a dysfunction and/or loss of neurons that contributes to the onset and progression of disease symptoms (Malucci et *al*., 2007). A combination of behavioural and neurophysiological analysis provides direct evidence for early neuronal dysfunction, which leads to cognitive impairment in prion infected mice (White et *al*., 2008; Mallucci et *al*., 2003). Furthermore, typical neuropathological features of prion infection and behavioural deficiencies are accompanied with a progressive cognitive dysfunction in prion diseases (Nazor et *al*., 2005; Nazor et *al*., 2007). Prion infected mice show changes in species-typical motivational behaviours long before emergence of motor signs (Guenther et *al*., 2001; Deacon et *al*., 2001), which correlate with early loss of presynaptic terminals in the dorsal hippocampus (Cunningham et *al*., 2003). Until recently, the majority of studies on prion disease have been focused on the terminal stages of the disease, and criteria for the onset of clinical prion disease in mice have relied on detecting changes in locomotor activities that appear within a few weeks of death (Hunter et *al*., 1986). However, the complexity of the spectrum of clinical symptoms and of the neuropathology at terminal disease has made it difficult to draw conclusions about these relationships and the underlying mechanisms of prion disease pathogenesis.

Based on the relationship between prion disease neuropathology and the UPS presented in **Chapters 3** and **4**, this present chapter attempts to determine whether the UPS dysfunction observed in the Ub^{G76V}-GFP reporter mice correlates with behavioural and

motor measures throughout the time-course of disease, and with markers of neuronal loss or dysfunction that may underlie them.

5.2 AIMS

- To monitor specific neuronal and synaptic markers in RML prion-infected Ub^{G76V}-GFP mice;

- To assess motor function and behavioural phenotypes in RML prion-infected Ub^{G76V}-GFP mice.

5.3 METHODS

All protocols using these mice were first approved by the MRC Prion Unit animal committee, and official approved procedures were followed for the care and use of these mice. The environment of the experimental room was kept consistent between test sessions with respect to temperature, humidity and light intensity (**Section 2.9**).

Mice were grouped together prior to individual experiments and were monitored daily. Behavioural testing was performed on groups of at least ten age-matched Ub^{G76V}-GFP1 mice, which had been inoculated i.c. with 30 µl of 1% RML-prion infected mouse brain or control homogenates (**Section 2.2.2**). Each mouse was given a unique identification number and all subsequent behavioural assessments were performed blinded as to which experimental group the animal belonged to. Testing was initiated from twenty days post-inoculation with RML prions. The animals were tested within a conserved ~3 hour time period in the morning.

For histological analysis, brains were dissected rapidly after sacrifice and immersed into a fixing formalin buffer solution. Half brain tissues were embedded in paraffin and 4

µm saggital sections were obtained and mounted onto positively charged glass slides for immunohistochemistry analysis (**Section 2.5**).

Data were expressed as standard deviation (SD) and analysed by two-way ANOVA with Bonferroni post-test. Significance was expressed as follows: *** p <0.001; ** p <0.01, * p <0.05. See **Appendix IV.**

5.4 RESULTS

5.4.1 Neuronal loss in the brains of RML prion infected Ub^{G76V}-GFP reporter mice

Previous work showed that neurons are lost during prion disease progression. For example, significant loss of cells from the CA1 region of the hippocampus has been reported in ME7 prion infected mice (Cunningham et *al*., 2003). Therefore, to determine whether the UPS dysfunction observed in prion-infected mice correlates either temporally and/or spatially with neuronal loss, RML prion-infected Ub^{G76V}-GFP1 mice were examined by immunohistochemistry for the neuronal marker, NeuN. In the thalamus of the prion-infected mice, little difference was seen in the pattern of NeuN staining at any stage of the disease course until end-stage disease at ~160 days post-inoculation (**Figure 5.1**). This contrasted with the evidence of UPS dysfunction observed early in this part of the brain described in Chapter 4. This may indicate that UPS dysfunction seen in certain areas of the brain in prion-infected mice does not necessarily lead to neuronal cell death. Nevertheless, these data demonstrate that UPS dysfunction in the brains of prion-infected mice precedes the onset of neuronal loss as the disease progresses.

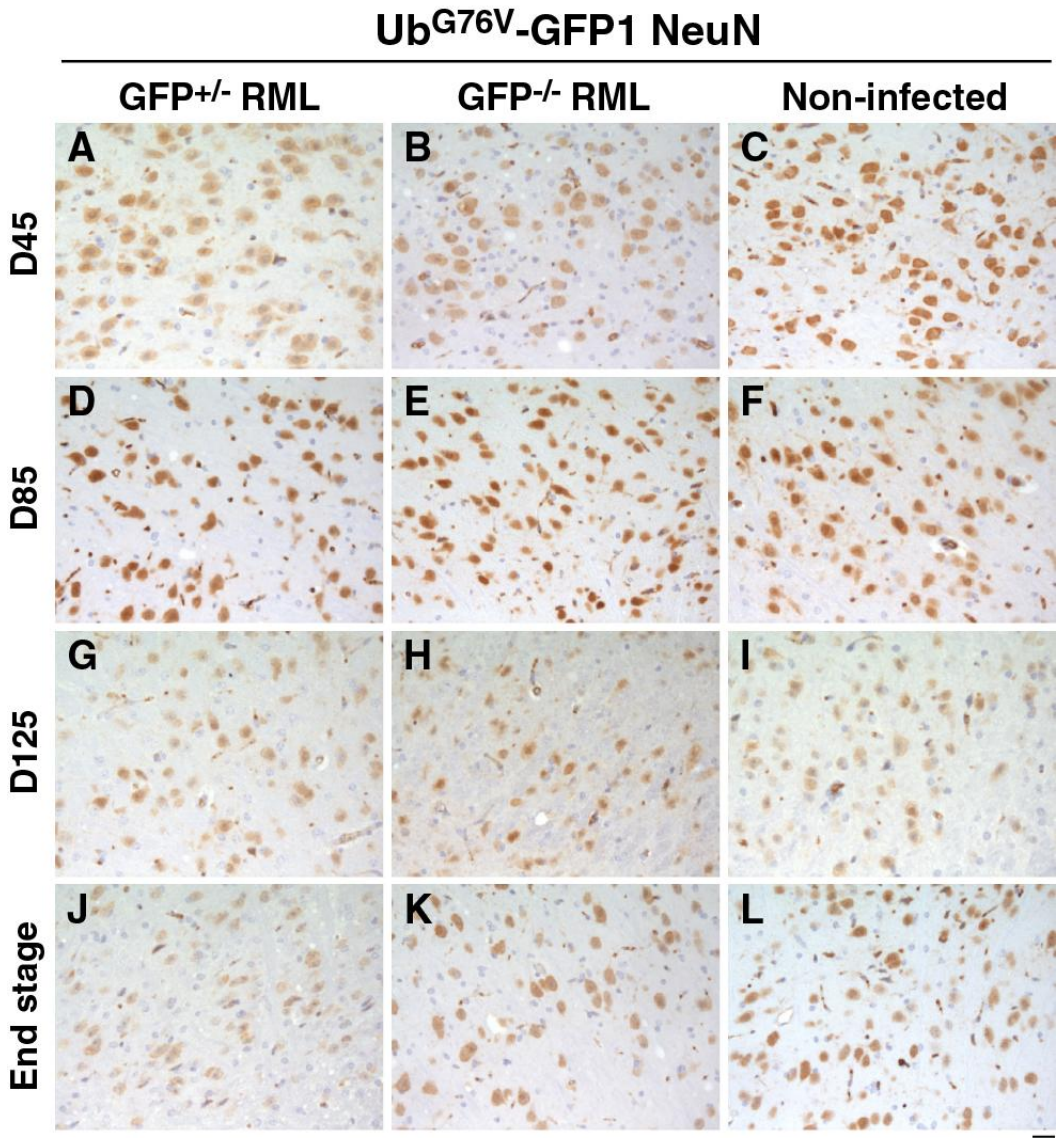

Figure 5.1 NeuN expression in the thalamus in the brain of RML prion-infected Ub^{G76V}-GFP mice.

Ub^{G76V}-GFP1 mice were inoculated i.c with 30 µl of 1% RML-prion infected mouse brain or control homogenates, and culled at days 45, 85 and 125 post-inoculation, and at end-stage disease. Immunohistochemistry analysis was carried out on paraffin-embedded brain tissue using an anti-NeuN antibody. Images are taken of the thalamus and, in this region, show similar levels of staining between the RML-prion infected mice and non-infected controls. Scale bar = 20 µm.

5.4.2 Neuronal loss in the CA1/CA3 region of the brains of Ub^{G76V}-GFP mice following RML prion infection

To assess whether neuronal loss could be detected in other neuropathological region of the brain, the hippocampus of the prion-infected mice was evaluated by immnohistochemistry. A noticeable loss of neurons was observed in the CA1/CA3 region at the later stages of the disease time-course, from day 125 post-inoculation with RML prions onwards (**Figure 5.2**). However, despite a widespread accumulation of PrP^{Sc}, these areas did not show consistent evidence of UPS dysfunction (see **Chapter 4**). Other prion strains have been shown to induce hippocampal pathology which gives rise to distinct phases of behavioural and anatomical abnormalities (Guenther et *al*., 2001; Jeffrey et *al*., 2000; Betmouni et *al*., 1999), and it has been demonstrated that early behavioural deficits correlate with a selective disorganization of the CA1 synapses that initially occurs in the absence of cell death (Cunningham et *al*., 2003).

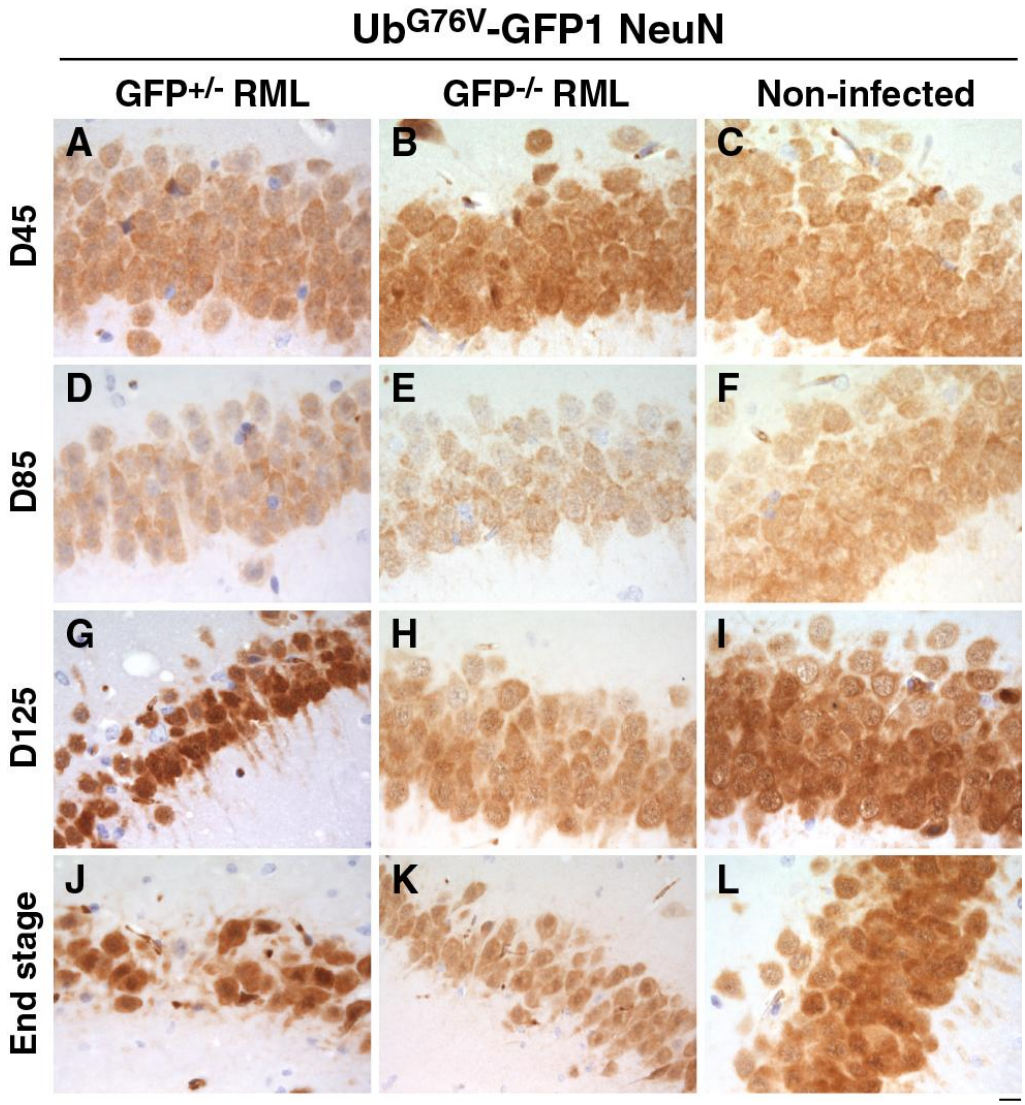

Figure 5.2 NeuN expression in the hippocampus in the brain of RML prion-infected Ub^{G76V}-GFP mice.

Ub^{G76V}-GFP1 mice were inoculated i.c with 30 µl of 1% RML-prion infected mouse brain or control homogenates, and culled at days 45, 85 and 125 post-inoculation, and at end-stage disease. Immunohistochemistry analysis was carried out on paraffin-embedded brain tissue using an anti-NeuN antibody. Images are taken of the hippocampus (CA1/CA3) and, in this region, show a loss of neurons in the RML-prion infected mice as compared to the non-infected controls. Scale bar = 20 µm.

5.4.3 Synaptic loss in the brains of Ub^{G76V}-GFP mice following RML prion infection

Dysfunction in synaptic function is thought to underlie the earliest symptoms in several neurodegenerative diseases, and loss of synapses is thought to precede the loss of neuronal cell bodies (Mallucci, 2009; Wishart et *al*., 2006). To assess any synaptic dysfunction Ub^{G76V}-GFP1 mice brain were analysed by immunohistochemistry.

In the thalamus of the prion-infected mice, small deposits of synaptophysin staining indicating dysfunction of synapses were observed towards end-stage disease at ~160 days post-inoculation (**Figure 5.3**). This subtle staining was not observed in other parts of the brain. The localisation of synaptic dysfunction in the thalamus is similar to where UPS dysfunction was most strongly observed in prion-infected Ub^{G76V}-GFP1 mice (see **Chapter 4**). This indicates that UPS dysfunction may precede some synaptic dysfunction during the time-course of prion disease progression.

In an attempt to quantify any loss of synapses during prion disease pathogenesis, brain homogenates of Ub^{G76V}-GFP1 mice were examined by Western blots using an anti-synaptophysin antibody. No differences were observed in comparing prion-infected Ub^{G76V}-GFP1 mice and their non-infected control counterparts (**Figure 5.4**). This observation may reflect a lack of sensitivity using this particular method to detect small or focal differences in certain parts of the brain.

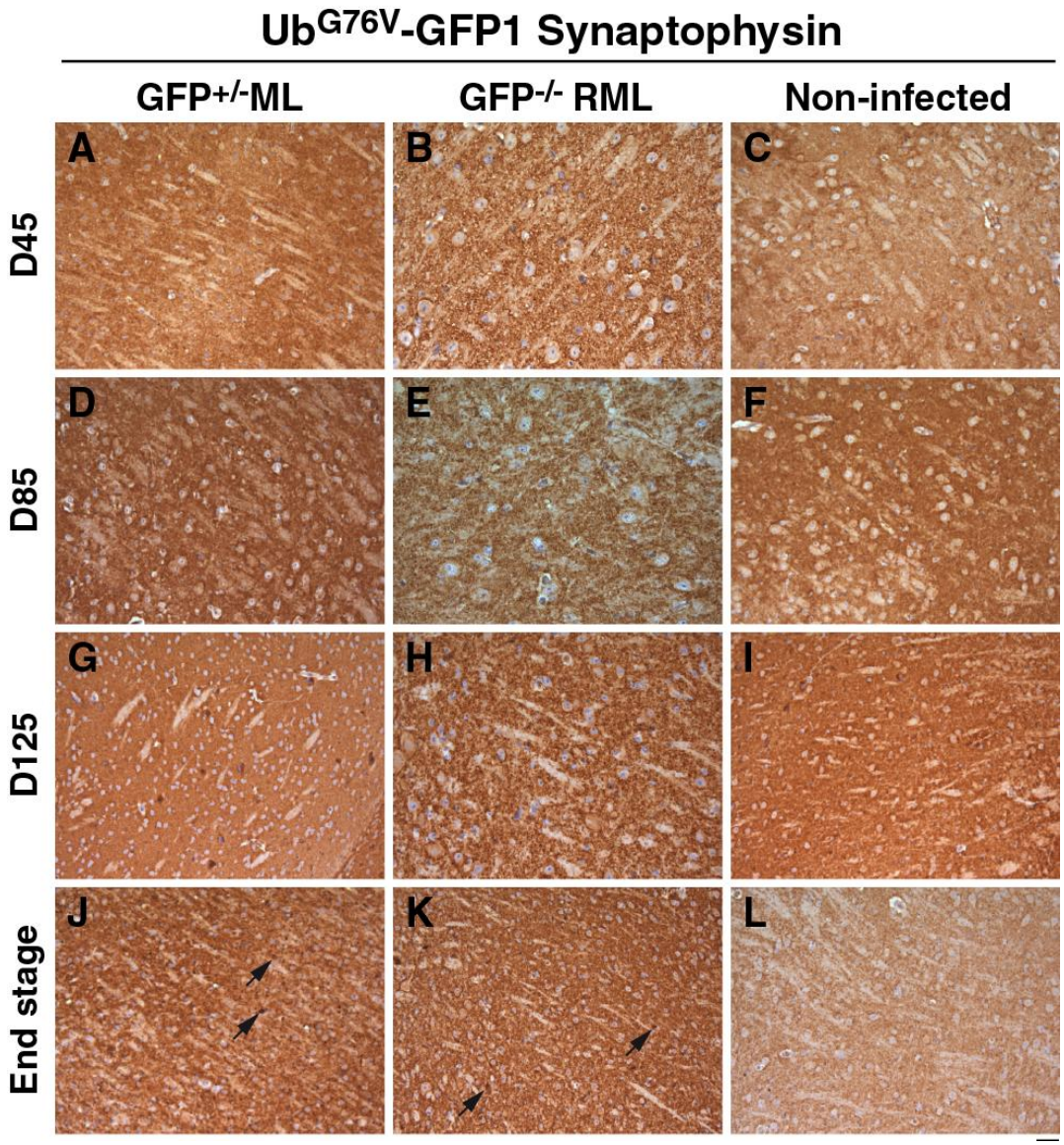

Figure 5.3 Synaptophysin expression in the thalamus of RML prion-infected Ub^{G76V}-GFP mice.

Ub^{G76V}-GFP1 mice were inoculated i.c with 30 µl of 1% RML-prion infected mouse brain or control homogenates, and culled at days 45, 85 and 125 post-inoculation, and at end-stage disease. Immunohistochemistry analysis was carried out on paraffin-embedded brain tissue using an anti-synaptophysin antibody. Deposits of synaptophysin are seen in the thalamus of RML-prion infected mice, as compared to the non-infected controls. Scale bar = 20 µm.

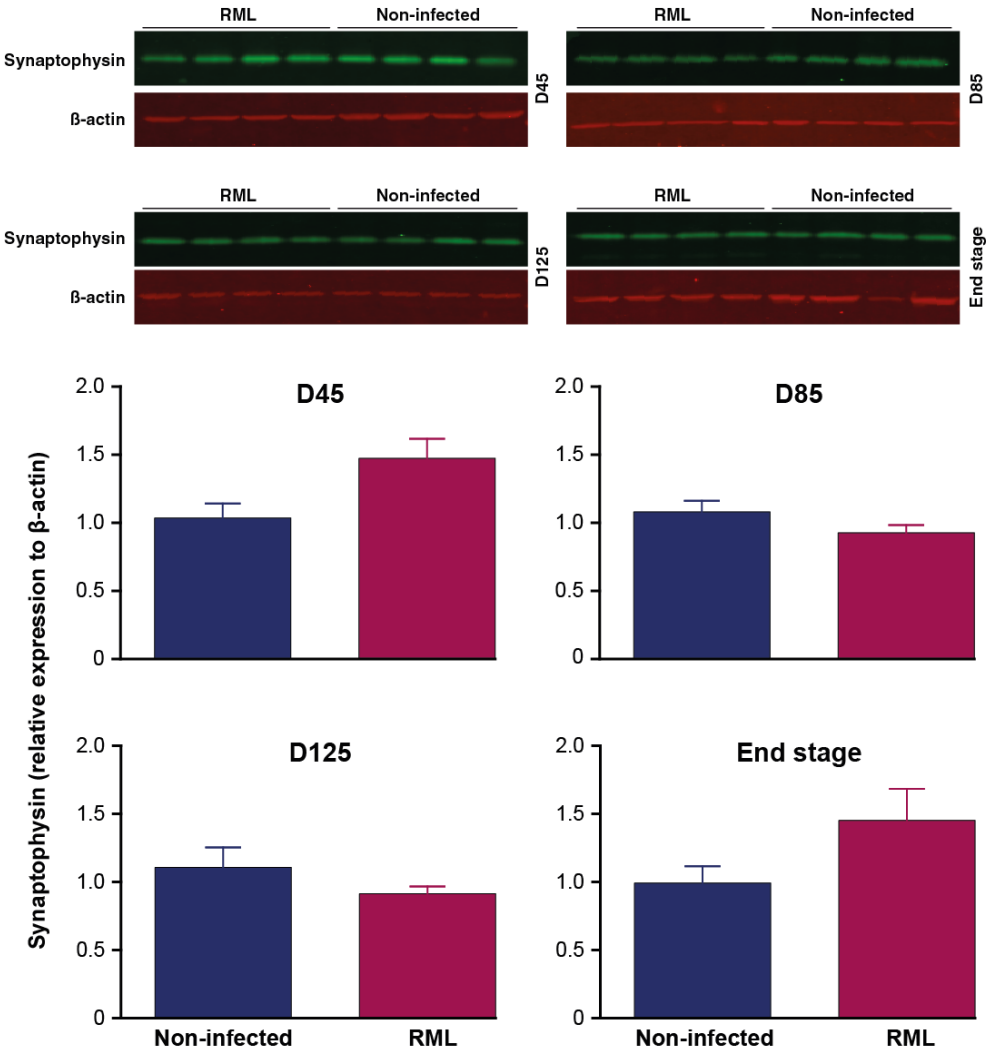

Figure 5.4 Immunoblot analysis of synaptophysin expression in the brains of RML prion-infected Ub^{G76V}-GFP mice.

Ub^{G76V}-GFP1 mice were inoculated i.c with 30 µl of 1% RML-prion infected mouse brain or control homogenates, and culled at days 45, 85 and 125 post-inoculation and at end-stage disease. A 1% tissue homogenate was made and immunoblotted with anti-synaptophysin or anti β-actin antibodies. Detection of Li-Cor secondary antibodies was done by scanning the membrane using the Odyssey Infrared Imaging System (Li-Cor Biosciences). No significant differences in synaptophysin in whole brain lysates was detected between RML-prion infected and control Ub^{G76V}-GFP1 mice.

5.4.4 Balance and coordination impairment in RML prion-infected Ub^{G76V}-GFP reporter mice

Previous work indicates that sensorimotor deficits precede the spontaneous onset of prion disease in Tg (GSS) mice, and behavioural abnormalities appear in prion-infected mice long before the manifestation of clinical signs (Nazor et *al*., 2007; Bertmouni et *al*., 1999). To evaluate whether prion infection causes a loss of balance and coordination in prion-infected Ub^{G76V}-GFP1 reporter mice, correlating with the onset of UPS dysfunction, assessments were made using rotarod apparatus. This comprises a well-characterised behavioural task designed to monitor motor function by requiring mice to ambulate on an accelerating rotating rod (Dunham and Miya, 1957; Jones and Roberts, 1968). Mice were tested at various time-points from day 45 until day 105 post-inoculation with RML-prions. A significant difference was observed in the performance of the Ub^{G76V}-GFP1 reporter mice, as compared to non-infected control animals, from the earliest post-inoculation time-point onwards (**Figure 5.5**). This indicates that deficits in this motor test are apparent early in the disease-course, well before the onset of disease pathology. Two-way ANOVA with Bonferroni post-test*** p <0.001. See **Appendix IV** for F values and *DF* or relevance.

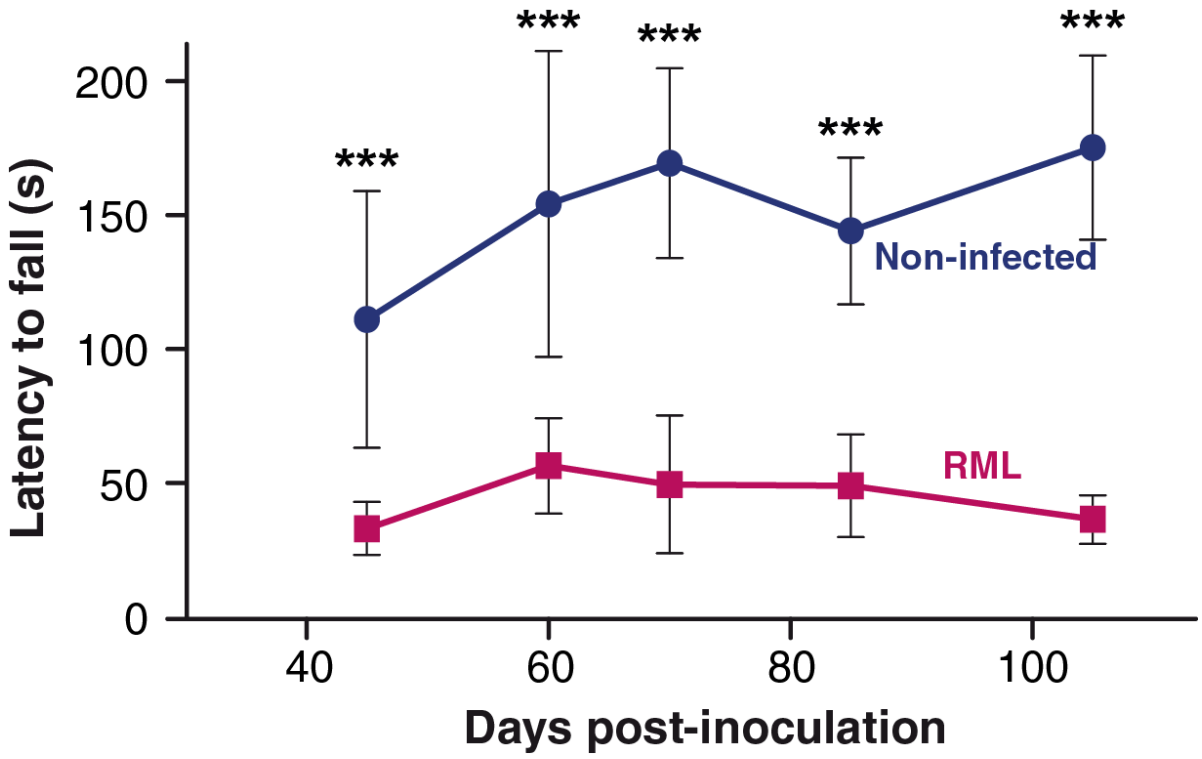

Figure 5.5 Early motor deficits in Ub^{G76V}-GFP mice following RML prion infection. Rotarod testing was performed on groups of ten RML prion-infected and ten non-infected Ub^{G76V}-GFP1 reporter mice. They were inoculated i.c with 30 µl of 1% RML-infected mouse brain or control homogenates. The mean latency to fall over two trials for each individual mouse was analysed. A significant difference was observed between the groups of RML prion-infected and control Ub^{G76V}-GFP1 mice at every time-point tested, including the earliest time-point at day 45 post-inoculation with RML prions.

5.4.5 Burrowing impairment in RML prion-infected Ub^{G76V}-GFP reporter mice.

Spontaneous burrowing behaviour by rodents has a robust association with early prion pathology (Mallucci et *al*., 2007; Deacon et *al*., 2001). Burrowing has been proposed as a powerful tool for elucidating brain function requiring a high degree of reorganisation and executive function that are thought to reflect motivational aspects of spontaneous behaviour in rodents (Deacon et *al*., 2001; Guenther et *al*., 2001). To investigate the ability of RML-prion infected Ub^{G76V}-GFP1 mice to burrow, a container filled with objects food pellets was placed into a clean cage and left overnight (**Appendix III**). Typically, non-infected mice actively burrowed to displace 70-80% of the pellets (**Figure 5.6**). This was also observed at the earliest time-point post-inoculation, at day 25, in the RML-prion infected Ub^{G76V}-GFP1 animals. Thereafter however, a progressive decrease in burrowing was recorded from day 45 post-inoculation onwards in the RML prion-infected mice. Two-way ANOVA with Bonferroni post-test*** p <0.001. See **Appendix IV** for F values and *DF* or relevance.

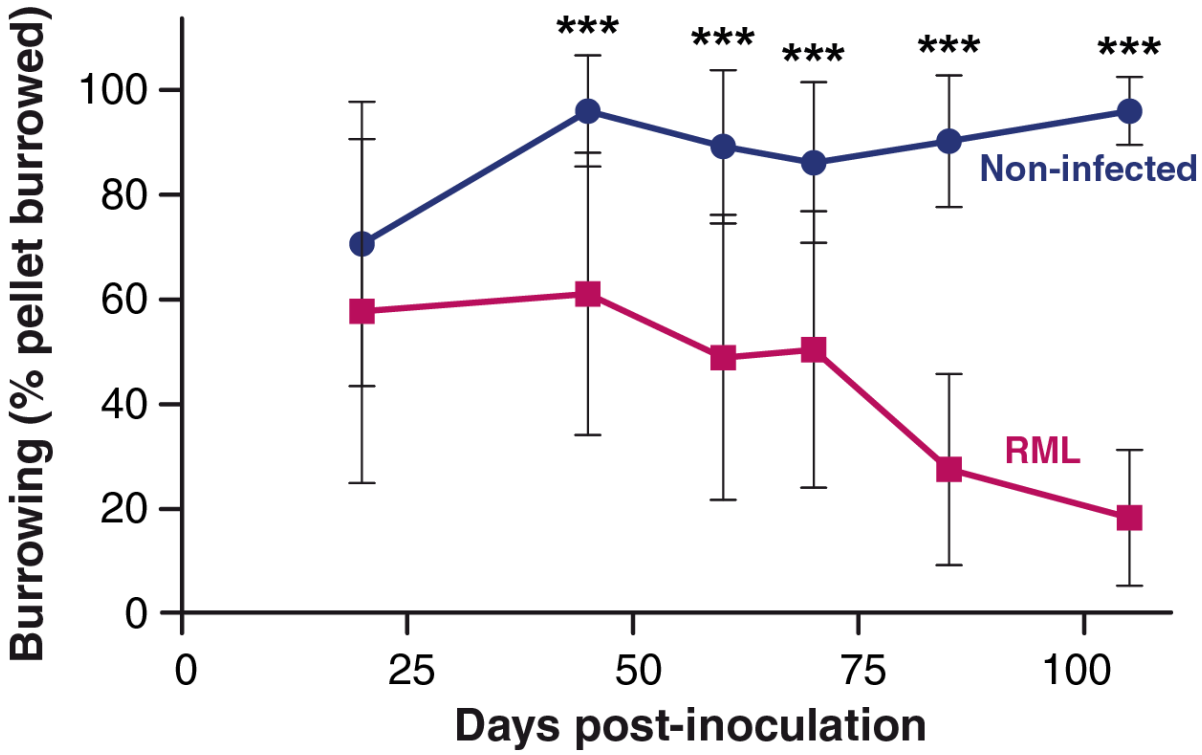

Figure 5.6 Burrowing behaviour is progressively lost in RML prion-infected Ub^{G76V}-GFP mice.

Burrowing was investigated in groups of fourteen prion-infected and fifteen non-infected Ub^{G76V}-GFP1 mice. They were inoculated i.c with 30 µl of 1% RML prion-infected mouse brain or control homogenate. The displacement of food pellets from a filled tube placed in the animal's cage was analysed. Whilst burrowing was similar at the earliest time-point tested, day 25 post-inoculation with RML prions, a significant difference was observed between the groups of RML prion-infected and control Ub^{G76V}-GFP1 mice at every time-point tested thereafter. This deficit progressively worsened as the disease progressed. See **Appendix IV.**

5.4.6 Nest building impairment in RML prion-infected Ub^{G76V}-GFP reporter mice.

Nest building in rodents is a natural behaviour that is important for heat conservation, as well as for reproduction and shelter. It is a task that requires an intact dorsal hippocampus (Deacon et *al*., 2002). To evaluate nest building, RML-prion infected Ub^{G76V}-GFP1 reporter mice were at various time-points post-inoculation left overnight with a nestlet placed into the home cage. The animals routinely shredded the tightly-packed material and arranged it into a nest. Qualitative assessments were made based on the neatness of the nest and the amount of un-shredded material left (see **Appendix III**). Mice were tested at various time-points from day 25 until day 105 post-inoculation with RML prions. A significant difference was observed in the performance of the prion-infected Ub^{G76V}-GFP1 reporter mice, as compared to non-infected control animals, from the earliest post-inoculation time-point onwards (**Figure 5.7**). This data indicates that deficits in this behavioural test are apparent early in the disease-course, well before the onset of disease pathology. Moreover, the deficit became progressively worse as the disease progressed. Two-way ANOVA with Bonferroni post-test*** p <0.001. See **Appendix IV** for F values and *DF* or relevance.

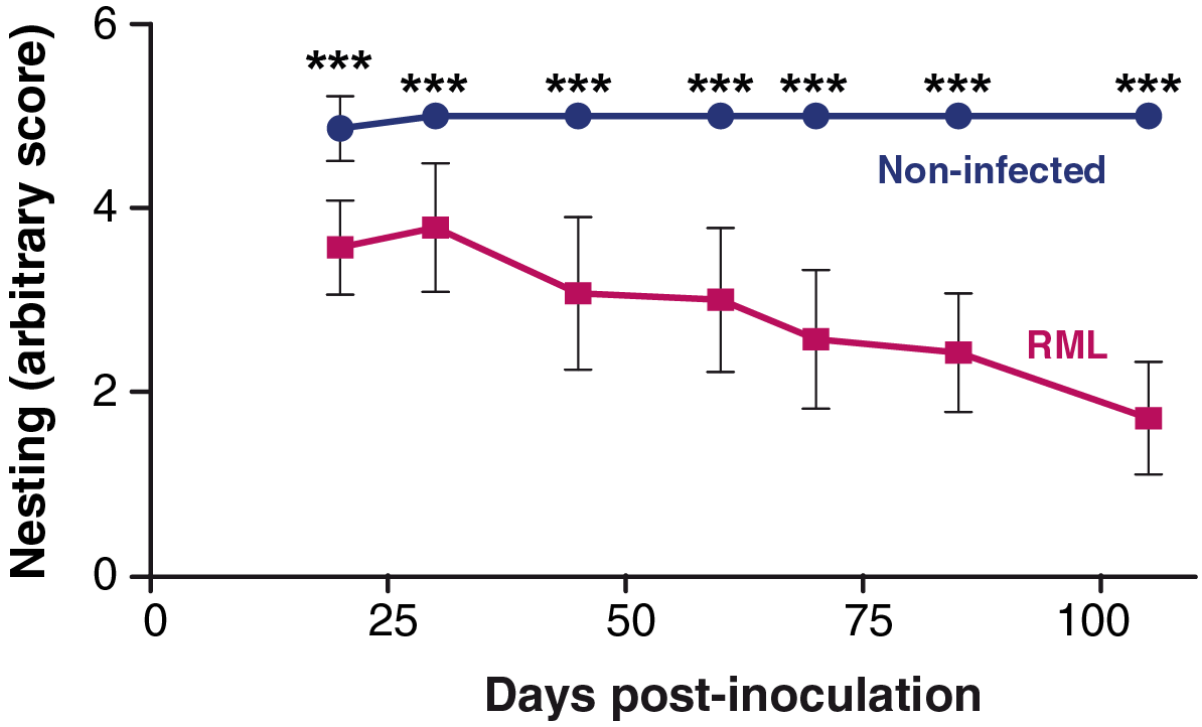

Figure 5.7 Nesting scores decline during disease progression in prion-infected Ub^{G76V}-GFP mice.

Nesting was investigated in groups of ten prion-infected and ten non-infected Ub^{G76V}-GFP1 mice. They were inoculated i.c with 30 µl of 1% RML-prion infected mouse brain or control homogenates. Scores of shredding of nesting material placed in the cage were analysed. Mice in all groups constructed nestlets. However, shredding was significantly lower in the RML prion-infected mice when compared to the non-infected groups. A moderate difference was observed at day 25 post-inoculation, which got progressively larger as the disease progressed thereafter. See **Appendix IV.**

5.4.7 RML Prion infection does not affect grip strength in Ub^{G76V}-GFP reporter mice

To investigate whether neuromuscular strength was impaired in prion-infected Ub^{G76V}-GFP reporter mice, a grip strength test was used to evaluate limb strength in both healthy and prion-infected mice. This method is used to measure disease progression and neurobehaviour, as well as to test specific therapeutic interventions in mouse models (Spurney et *al*., 2009; Rayavarapu et *al*., 2010). This test is based on the natural tendency of the mouse to grip a bar or grip when suspended by the tail. Mice were tested at various time-points from day 25 until day 105 post-inoculation with RML prions. There were no consistently significant differences in the performance of the RML prion infected Ub^{G76V}-GFP1 reporter mice, as compared to non-infected control animals (**Figure 5.8**). Two-way ANOVA with Bonferroni post-test. *** p <0.001; ** p <0.01, * p <0.05. See **Appendix IV** for F values and *DF* or relevance.

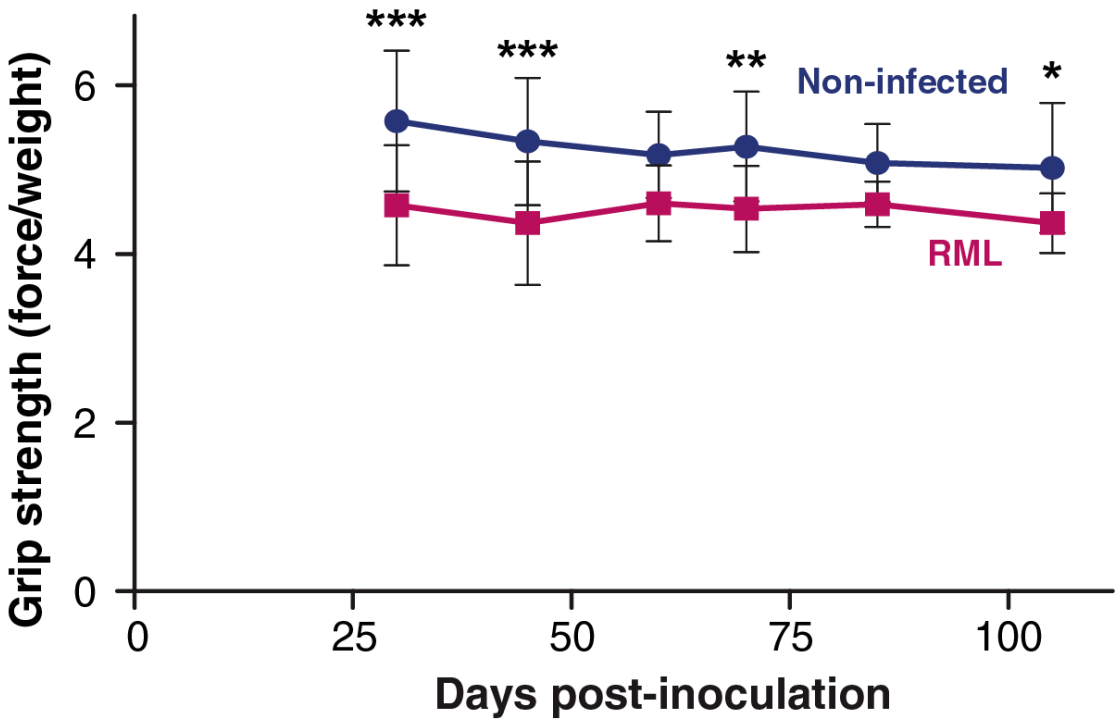

Figure 5.8 Grip strength in RML prion-infected Ub^{G76V}-GFP mice.

Grip strength was investigated in groups of fourteen prion-infected and fifteen control Ub^{G76V}-GFP1 mice. They were inoculated i.c with 30 µl of 1% RML-prion infected mouse brain or control homogenates. The mean peak force applied by the forelimbs of the mouse was analysed. Although grip strength appeared to be slightly reduced in the RML prion-infected mice at some time-points, a progressive deficit was not observed. See **Appendix IV.**

5. 5 DISCUSSION

Premature neuronal cell death is typical in prion disease (Collinge et *al*., 1995; Medori et *al*., 1992; Forloni et *al*., 1993). However, the underlying mechanisms that contribute to neuronal loss are far from being elucidated. As reported in **Chapters 3** and **4,** substantial PrP^{Sc} deposits accumulate in the brain of RML prion-infected mice during the disease time-course following prion infection. Whether PrP^{Sc} is the toxic component involved in the molecular mechanisms leading to neurodegeneration remains unclear. There are indications that neuronal cell death might be related to the altered function of several cellular processes, including cell signalling, intracellular trafficking and cellular proteostasis. Indeed, experimental evidence suggests that neuronal death is associated with UPS impairment (Goldberg, 2003; Tydlacka et *al*., 2008). However, it is not known if UPS dysfunction is the cause or the consequence of cellular damage. Impairment of the UPS has been shown to be important in prion disease (Ma et *al*., 2002; Ma and Lindquist, 2002; Kang et *al*., 2004; Deriziotis et *al*., 2011), as further evidenced by data presented in **Chapter 4** of the present thesis.

The data presented in this chapter attempts to determine whether aspects of prion neuropathology such as neuronal and synaptic integrity, and behaviour and motor function, are altered in prion-infected mice in a manner that relates to the UPS dysfunction reported in **Chapter 4**. The UPS was impaired in the thalamus of RML prion-infected Ub^{G76V}-GFP mice at day 85 post-inoculation of a ~160 day disease time-course, but in this region, overt loss of neurons was not observed (**Figure 5.1**). Notably, however, obvious neuronal loss was observed in the CA1 and CA3 regions of the hippocampus of the prion-infected mice (**Figure 5.2**), as well as to a lesser extent in some other areas. This neuronal loss in the hippocampus was observed from day 125 post-inoculation onwards. This coincided with widespread increases in markers of prion disease pathology such as extensive PrP^{Sc} deposition and GFAP immunoreactivity, and with the broadly increased ubiquitin levels and deficits in 26S proteasome peptidase activity first observed at this time-point (**Chapter 4**).

Nevertheless, whilst the temporal correlation of neuronal loss with some indicators of UPS dysfunction was clear, the overt impairment of the UPS in the thalamus was not particularly reflected by a loss of neurons in this area.

To further assess whether UPS dysfunction corresponded with any synaptic loss or dysfunction, the brains of prion-infected Ub^{G76V}-GFP1 mice brain were examined for the specific marker, synaptophysin. Some synaptic loss, in the form of small synaptophysin deposits indicating a retraction of functional synapses, was detected towards end-stage disease in the thalamus of prion-infected mice (**Figure 5.3**). Such differences were not observed at earlier time-points post-prion infection. These changes were particularly marked in the thalamus, the area of the brain in which UPS impairment was most obvious. The focal nature of the altered synaptophysin staining was reflected by Western blots of whole brain homogenates that did not show any differences in total synaptophysin levels as compared to non-infected controls (**Figure 5.4**). Clearly, the discrepancy in the data with the synaptophysin marker may be explained due to the sensitivity of the different detection methods. Nevertheless, that UPS dysfunction in the thalamus precedes a loss of synapse integrity seems to be clear.

During the experimental time-course, infected Ub^{G76V}-GFP transgenic mice showed the expected clinical symptoms of prion disease. This led to a closer assessment of behavioural and motor abnormalities, which might associate temporally with the onset of UPS dysfunction and other aspects of prion neuropathology. Therefore, a small behavioural study was designed such that clear behavioural phenotypes correlating to pathological features would be measurable. Behavioural testing can reveal effect in prion-infected mice long before the manifestation of clinical signs appears (Bertmouni et *al*., 1999). Indeed, it has been shown that sensorimotor deficits precede the spontaneous onset of prion disease in Tg(GSS) mice (Nazor et *al*., 2007).

Several well characterised behavioural tasks designed to assess performance in motor function and coordination were employed. One of them, burrowing, was used to measure motor coordination in prion-infected mice. Burrowing, as measured by the displacement of food pellets from a tube in the home cage, decreases in ME7 prion-infected mice early in disease at twelve weeks post-inoculation (Guenther et *al*., 2001). In the present study, the RML infected groups showed a progressive decrease in burrowing ability from day 45 post-inoculation onwards (**Figure 5.5**). This is notable in that it precedes markers of prion neuropathology, including UPS impairment, by up to forty days.

Nest construction, a species-typical behaviour test was also measured, starting at day 20 post-RML prion infection. Nesting ability was significantly impaired in the RML prion-infected group, as compared with non-infected animals. Taken together, these data support the claim that burrowing and nesting tests are sensitive, early indicators of behavioural impairment in prion infected mice (Deacon et *al*., 2001). Nesting and burrowing strengthens the preclinical changes seen in an earlier study (Bermouni et *al*., 1999). However, it is unclear whether the effects observed were due to motor rather than motivational impairments and further studies would be needed to resolve this question.

The rotarod task has been described as a sensitive indicator of motor skills impairment and cerebellar abnormalities (Hilber and Caston, 2001). It not only assesses motor coordination and balance, but also characterises the motor phenotype of transgenic and knockout mice. The latency to fall at a set speed was measured in both RML prion-infected and non-infected groups of mice. A significant difference was observed in the performance of the prion-infected Ub^{G76V}-GFP1 mice, as compared to non-infected control animals, from the earliest time-point at day 45 post-inoculation (**Figure 5.6**). This indicates that deficits in this motor test were apparent early in the disease-course, well before the onset of disease pathology. In contrast, a grip strength test was used to assess forelimb strength, which can also be influenced by co-ordination deficits. However, no difference

was detected in grip strength ability between RML prion-infected and the non-infected animal groups (**Figure 5.8**).

The main findings of the data presented here were that characteristic behavioural changes can be reliably detected in this model of prion disease. However, many pathways that underlie diverse clinical signs are complex and thus it is difficult to relate a particular clinical symptom to a specific neuropathological feature. It is not clear whether the behavioural phenotype and motor skills deficits observed in these mice can be correlated with particular aspects of loss of neurons or synapses in particular brain areas. Prion infected mice show changes in species-typical motivational behaviours before emergence of motor signs (Guenther et *al*., 2001; Deacon et *al*., 2001), which correlate with early loss of pre-synaptic terminals in the dorsal hippocampus (Cunningham et *al*., 2003). It should be recognised that several limitations to this study may have affected the data presented here. Validity of the results obtained from behavioural phenotyping is largely dependent on methods of animal husbandry, so physiological parameters were kept constant throughout the time of testing. The majority of mouse behavioural studies are dependent on age, sex and strain, and it was important to keep these parameters comparable throughout a single experiment. Environment factors contribute to the levels of anxiety within the mouse, so temperature, humidity, ventilation, noise and lighting intensity were kept at a constant level that is appropriate to the mice. Mice were also kept at a uniform environment before and after testing to avoid anomalous results.

The work presented here indicates that deficits in the behavioural tests are early in the disease-course, well before the onset of disease pathology. However, It is not clear that neuronal loss and alteration of synapses alone are sufficient to account for the behavioural deficiency observed. Previous studies give strong evidence that UPS impairment is linked to prion disease, and altered activities of the UPS are crucially involved in the pathophysiology of several other neurodegenerative diseases. This study clearly indicates an early effect of prion infection to behavioural function in the Ub^{G76V}-GFP1 mice.

However, a more in depth behavioural study is needed with a baseline set at pre-inoculation with RML prion to better understand the relationship between prion infection and behavioural abnormalities in these mice.

5.6 SUMMARY

The work in this chapter presents data which support previous report that neuronal and synaptic loss contribute to the pathological features that underlying early behavioural dysfunction in prion diseases. Significant impairment in motor functions was observed in Ub^{G76V}-GFP reporter mice infected with RML prion and a marked neuronal loss was observed in key neuropathological region of the hippocampus. In addition, some sign of synaptic loss was observed toward end stage of prion disease. Neuromotor deficits and prion disease-related neuropathology in the RML infected Ub^{G76V}-GFP reporter mice observed in this study suggest that prion disease mediates important pathological and behavioural changes during the course of disease. Taken together, the data in the present chapter demonstrate evidence of neuronal loss and synaptic dysfunction in the brains of prion-infected mice that may, especially the latter in the thalamus, correlate with UPS dysfunction. Collectively, these changes may underlie behavioural changes that are seen early disease in prion-infected mice, although some of these changes precede discernible alterations in neuropathology. The causative nature, however, of these different observations remains to be determined. Collectively, data presented in this chapter suggest a relationship, which correlates UPS dysfunction observed in the Ub^{G76V}-GFP reporter mice with behavioural and motor skills deficits and neuropathological features of prion disease. Although, the mechanisms/pathways contributing to this relationship are not well understood.

6 CONCLUSIONS AND FUTURE WORK

The work described in this thesis aimed to investigate impairment of the UPS *in vivo* in the pathogenesis of prion disease. Specifically, this thesis aimed to monitor the functional status of the UPS following RML prion infection using Ub^{G76V}-GFP reporter mice. Previous studies have suggested a role for the UPS in prion disease (Ma *et al.*, 2002; Kang *et al.*, 2004; Kristiansen *et al.*, 2007; Deriziotis et *al.*, 2011), but it is not known how early in disease progression that this phenomenon occurs and how it correlates with other aspects of disease pathogenesis. Determining those pathogenic events that are causative to disease progression and those that are secondary to other disease-associated events remains a difficult task. However, it may be expected that underlying causative events in disease pathogenesis should be observed relatively early in disease progression and in those areas of the brain that are considered most pathologically important. In the present studies, a temporal relationship with the onset of typical prion neuropathology and of impairment of the UPS was observed in prion-infected Ub^{G76V}-GFP mice. This onset was first detected at day 85 post-inoculation with RML prions, which was about halfway through a disease time-course of about 160 days.

The UPS dysfunction observed by accumulation of the Ub^{G76V}-GFP reporter was followed, as might be expected, by a measurable increase in total ubiquitin in the brains of prion-infected mice, which seemed to correspond to an increase in high-molecular weight poly-ubiquitin species. The UPS is associated with the degradation of substrates that are tagged by the addition of polyubiquitin that is lysine-48 linked. Most poly-ubiquitinated substrates targeted for proteasomal degradation are lysine-48 linked (Pickart and Fusman, 2004) and their steady-state cellular levels are expected to reflect proteasome function. If the UPS is impaired in prion-infected animals, it might be expected that lysine-48 linked poly-ubiquitin accumulates as disease progresses. Lysine 48-linked poly-ubiquitin is often used as an endogenous marker of UPS function, and its levels have been measured by UBA

pull-down and mass spectrometry analysis to assess UPS function in neurodegenerative disease (Bennett et *al*., 2007), and quantify poly-ubiquitin chains (Kirkpatrick et *al*., 2006). Moreover, if the substrate proteins to which accumulating lysine-48 linked polyubiquitin were linked could be identified, this would allow the identification of subsets of accumulating aberrant proteins accumulating as cells die during disease pathology. The underlying molecular mechanisms of the UPS impairment observed in prion-infected mice remain only partially understood. The underlying cause of this UPS dysfunction could lie in a recently described mechanism of proteasome inhibition by β-sheet-rich PrP species (Deriziotis et *al*., 2011). In that *in vivo* study, proteasome proteolytic activity as was measured by fluorogenic substrate assays shown to be impaired prior to end-stage disease. This impairment was observed much later than the Ub-GFP reporter UPS dysfunction. An explanation for this discrepancy could be due to a lack of sensitivity of these assays in a whole brain homogenates.

Given the potential limitations of the Ub^{G76V}-GFP mouse model, the data presented here could be validated further by use of alternative UPS reporter substrates. Since substrates carrying different degradation signals are likely to be handled differentially by the UPS, a different type of substrate to that used in Ub^{G76V} -GFP mice could be used (Menendez-Benito et *al*., 2005), which could potentially reflect how another class of substrate is handled by the UPS. Kumarapeli and colleagues generated a ubiquitously expressing GFPdgn transgene, modified GFP targeted for proteasome degradation (Kumarapeli et *al*., 2005). This model is comparable to the Ub^{G76V}-GFP model and has been shown to delineate dysfunction of the UPS in several disease models (Kumarapeli et *al*., 2005; Chen et *al*., 2005; Liu et *al*., 2006). Alternatively, specific aberrant ubiquitin substrates can be measured in relation to the UPS. For example, UBB^{+1} is a mutant form of ubiquitin that accumulates in cells in neurodegenerative diseases, and appears to be both a substrate and an inhibitor of the UPS (Lindsten et *al*., 2002; Verhoef et *al*., 2007). UBB^{+1} causes a general blockage of proteasomal degradation in neuronal cells, and that inhibitory

effect is dependent on ubiquitination of UBB^{+1}. UBB^{+1} has been found to play a role in Alzheimer's disease (Van Leeuwen et *al*., 2000), where it mediates Aβ toxicity via inhibition of the 26S proteasome (Song et *al*., 2003). It would be of interest to investigate whether UBB^{+1} accumulates during prion disease pathogenesis and, if so, is associated with inhibition of the 26S proteasome.

Beyond the use of monitoring UPS dysfunction, GFP reporter substrate models can be used as research tools in cell biology for the purpose of through screenings for small compound inhibitors of the UPS as well as the bioviability of compound in combination with therapeutic potential of proteasome inhibitors (Verdoes et *al*., 2006; Dantuma et *al*., 2000; Tsien, 1998). This is of great importance since it is well documented that proteasome inhibitors have many therapeutics purpose. However, limitations still exist within the model in detecting UPS impairment. Nevertheless, the Ub^{G76V}-GFP reporter mouse model provides a useful tool for monitoring the functional status of the UPS in the pathogenesis of prion disease and several other neurodegenerative diseases. This mouse model based on the ubiquitin-proteasomal reporter substrate opens new opportunities to gain insight into the global effect of pathological conditions on the UPS (Menendez-Benito et *al*., 2005; Bowman et *al*., 2005; Luker et *al*., 2003).

Experiments to examine the links between UPS dysfunction and prion disease pathogenesis could be undertaken using agents that activate or decrease UPS function. For example, it may be expected that compounds that increase activity of the UPS might be beneficial to the onset of pathology in prion-infected animals. Recently, a small molecular inhibitor of a proteasome-associated deubiquitinating enzyme called USP14 was shown to up-regulate activity of the UPS (Lee et *al*., 2010). USP14 dissembles the ubiquitin chain, thereby slowing down proteasome degradation (Lee et *al*., 2004), but its loss in mice leads to an ataxic neurological phenotype (Wilson et *al*., 2002; Anderson et *al*., 2005). However, IU1-mediated inhibition of USP14 indirectly accelerates proteasomal degradation of

proteins, including tau and ataxin-3, both of which are involved in neurodegenerative disease (Lee et *al*., 2010). Therefore, a similar approach could be explored in prion-infected cells and mice, in which USP14-inhibition might be expected to reduce levels of misfolded protein, possibly including disease-associated PrP.

Conversely, experiments could be done that monitor UPS dysfunction in animals in which the production of disease-associated PrP^{Sc} is altered. For example, lentivirus-mediated delivery of RNAi targeting PrP that would be expected to show a reduction in PrP^{Sc} production, may show a concurrent reversal in the UPS dysfunction observed in prion-infected mice. An RNAi-based approach such as this has been used previously, in which White and colleagues demonstrated the development of phenotypic deficits in parallel with the development of early spongiform changes, and the recovery of these deficits in mice in which PrP was depleted (White et *al*., 2008). It has been shown that transgenic mice generated by lentiviral transduction of embryos stably express anti-PrP shRNAs have increased resistance to prion infection because of RNAi –mediated reduced expression of endogenous PrP (Pfeifer et *al*., 2006). Injection of virus into the hippocampus after prion infection could prevent behavioural deficits associated with early pathology (Cunningham et *al*., 2003).

Astrocytes in the thalamus seemed to be particularly affected by prion-infection in terms of UPS dysfunction, as shown by accumulation of the Ub-GFP reporter in this thesis work. In many studies in which the UPS has been studied in brain tissue, proteasome activity has been measured in whole brain homogenates without discriminating between the different cell types present (Wang et *al*., 2008; Keller et *al*., 2000; Glenn et *al*., 2004; Lopez et *al*., 2000). This may to some degree reflect differences in the detection of the sensitivity of the Ub-GFP reporter in different cell types. For example, it may be that expression of sequence encoding the Ub^{G76V}-GFP reporter may be inherently higher in astrocytes rather than other neural cells. This could be tested in primary cultures of

different neural cells isolated from Ub^{G76V}-GFP mice, in which mRNA sequences encoded by the Ub^{G76V}-GFP transgene are quantified by real-time PCR. Alternatively, *in situ* hybridisation could be used to monitor Ub^{G76V}-GFP transgene expression in different cells in the brains of the mice. If expression of the transgene does differ between different cell types, it may be possible detect Ub-GFP in, for example, increased numbers of neurons using more sensitive detection techniques. Alternative methods of tissue processing, such as cryosections from frozen tissue, might be a better method of detecting the Ub-GFP reporter in neurons and other cells type. The use of fluorescent detection methods may increase detection sensitivity and would allow the co-localisation of Ub-GFP with specific cellular markers such as GFAP for astrocytes and NeuN for neurons. Fluorescence-based methods would facilitate visualisation using laser confocal microscopy, where more in-depth images could be obtained of various sub-cellular groups.

Nevertheless, astrocyte function is becoming increasingly recognised as important in the maintenance of the neuronal environment in neurodegenerative disease, and alterations in astrocyte function may be important in disease pathogenesis. If the UPS is particularly impaired in astrocytes in prion disease, then the reasons for this could be investigated further. A more detailed time-course experiment to monitor the functional relevance of astrocytes could be important. Specific aspects of UPS dysfunction in astrocytes could be investigated *in vitro*, but might be hampered by a lack of suitable astrocyte cell lines that are susceptible to prions.

Altered behavioural and motor phenotypes were observed in prion-infected Ub^{G76V}-GFP mice, but these preceded the onset of neuropathology, including measures of UPS dysfunction. This suggests that the very earliest underlying events of prion disease progression remain to be determined. Nevertheless, the UPS dysfunction observed in the thalamus of prion-infected mice corresponded with some later loss of synaptic integrity seen in this area, as shown using synaptophysin as a marker. Previous reports have shown

that prion disease pathogenesis is accompanied by neuronal and synaptic loss associated with early behavioural impairments. Mallucci and colleagues showed evidence for recovery of behavioural and synaptic impairments, as well as spongiosis when neuronal PrP^{C} was depleted in prion infected mice (White et *al*., 2008; Mallucci et *al*., 2007). Moreover, experiments in ME7 prion-infected mice show loss of synapses early, with a significant reduction in synaptophysin in the CA1 region of the hippocampus, thirteen weeks after the ME7 prions were injected in the hippocampus (Belinchenko et *al*., 2000; Cunningham et *al*., 2003). Synaptic loss was observed in my study in the same thalamic regions, albeit substantially later in the disease time-course, in which UPS dysfunction was most pronounced in the RML prion-infected Ub^{G76V}-GFP mice. Synaptic loss and dysfunction are well documented in several other neurodegenerative diseases (Wang et *al*., 2008; Klyubin et *al*., 2005; Ross and Pickart, 2004). Importantly, a study done by Wang and colleagues in Huntington's disease mice showed that mutant huntingtin causes a loss of proteasome activity in neurons that is specifically localised at the synapses (Wang et *al*., 2008). Such an observation has not yet been described in prion diseases, but it is possible that similar events take place. Localised UPS dysfunction in synapses could be investigated in purified synaptosome in which fluorogenic peptidase assays could be carried out to measure proteasome activity in the synapses of neurons from prion-infected mice.

Given the impairment of the UPS observed following prion-infection, it would be interesting to investigate whether other aspects of cellular proteostasis are altered as well. The other major intracellular degradation system is autophagy. Unlike the UPS, autophagy is mainly responsible for the degradation of long-lived proteins and large intracellular bodies, including organelles (Levine and Klionsky, 2004; Lum et *al*., 2005). At least twenty seven *ATG* genes have been defined to participate in autophagy or autophagy-related process (Klionsky et *al*., 2003). However, the functional connection of autophagy to the UPS is not well understood. Ding and colleagues demonstrated that the two cellular degradation systems are functionally coupled and suppression of the UPS can activate

autophagy (Ding et *al*., 2007, Ding et *al*., 2006). Simultaneous inhibition of autophagy promotes accumulation of ubiquitinated protein aggregates, ER stress and cell death. Whereas the evidence by Ding and colleagues that UPS and autophagy are functionally linked is derived from inhibiting proteasome function, evidence indicating such a connection has also emerged in other studies where autophagy machinery is disrupted. Mice deficient in key autophagy genes, atg5 or atg7, accumulate ubiquitinated protein aggregates in neurons at an early stage and develop symptoms of neurodegenerative diseases (Kotmatsu et *al*., 2006; Hara et *al*., 2006). Therefore, it is worth investigating whether the inhibition of the proteasome induces autophagy. The use of a proteasome inhibitor could reveal whether the two proteins degradation pathways are functionally coupled as inhibition of proteasome activates autophagy. Proteasome inhibition of MG132 for example, could elicit a time-dependent and dose-dependent accumulation of LC3II, a lipid form of LC3, which is localized on the autophagic vacuoles (Kabeya et *al*., 2000). It has become evident that the function of autophagy and UPS are coordinated in several neurodegenerative diseases, and the impairment of the UPS can result in the upregulation of autophagy.

During neurodegeneration ER stress may have a protective effect initially as expression levels of ER chaperones are increased, thus helping cell handle misfolded proteins. On the other hand, prolonged activation of the UPR pathways may lead to cell death and eventually neurodegeneration. Therefore, molecular mechanisms mediate the change in the UPR from being a beneficial to cell death-inducing response is worth investigating. It would be of a particular interest to study the vulnerability of the UPS towards proteotoxic stress conditions in the Ub^{G76V} –GFP reporter model and different cell types. Impairment of the UPS may also be linked to ER stress, which has been shown as PrP^{Sc} accumulates in cells (Budka, 2003; Menendez-Benito et *al*., 2005; Hetz and Soto, 2006).

Several studies indicate that ER resident chaperones involved in quality control play a major role in neurodegenerative disorders and there is evidence to suggest the activation of ER stress genes have been found to be significantly upregulated in prion pathogenesis, suggesting that ER stress is linked to the disease. Previous studies have shown that the expressions of Grp78 and Grp94 have protective effects against ER stress-mediated apoptosis (Liu et *al*., 1997; Reddy et *al*., 1999; Rao et *al*., 2002), and ER specific caspases, such as caspase-12 is thought to directly induce cell death. The correlation between caspase 12 activation and neuronal loss was confirmed in models of prion infected mice as well as in CJD patients (Castilla and Soto, 2005). Previously, it was shown in both human affected with CJD and mouse models that prion replication in brain is accompanied by increased expression of Grp58 in the terminal stage of the disease and in the brain regions showing extensive neuronal loss (Yoo et *al*., 2002; Hetz et *al*., 2003). However, it is not clear whether this alteration is early or late during disease progression. Although a small increase in Bip/Grp78 protein level was observed in the Ub^{G76V}-GFP mice brain, it is not clear whether upregulation of Bip/Grp78 and other binding partners influence the UPS. Therefore, a more detailed time-course experiment to monitor the expression levels of Grp58, Grp78 and Grp94 in different brain areas could be done by quantitative Western blotting.

In summary, work presented in this thesis indicates early UPS dysfunction in the brains of prion-infected Ub^{G76V}-GFP mice. In addition, neuropathological features of prion disease correlate with the accumulation of the Ub-GFP substrate. Taken together, this work supports the hypothesis that UPS dysfunction occurs relatively early and may play an important role in disease pathogenesis. Further studies to elucidate the mechanisms of UPS impairment in prion disease may be important in understanding the underlying processes of disease pathogenesis.

7 APPENDICES

Appendix I

Table 7.1 List of antibodies for immunocytochemistry

Antibody	Species	Company	Dilution
GFP	Rabbit polyclonal	Invitrogen	1 μg/ml
NF200	Mouse monoclonal	Insight genomics	1 μg/ml
AF 488	Goat anti-mouse	Life Technologies	1 μg/ml
AF 568	Goat anti-rabbit	Life Technologies	1 μg/ml

Table 7.2 List of primary antibodies used for immunohistochemistry

Antibody	Species	Company	Dilution
ICSM35	Mouse monoclonal	D-GEN	2 μg/ml
GFAP	Mouse monoclonal	Dako	1 μg/ml
GFP	Rabbit polyclonal	Invitrogen	1 μg/ml
Ubiquitin	Mouse monoclonal	Santa Cruz	1 μg/ml
Synaptophysin	Mouse monoclonal	Santa Cruz or Zymed	1 μg/ml
NeuN	Mouse monoclonal	Chemicon	1 μg/ml
GRP78 (Bip)	Mouse monoclonal	Cell Signalling	1 μg/ml

Table 7.3 List of primary antibodies used for immunoblotting

Antibody	Species	Company	Dilution
ICSM35	Mouse monoclonal	D-GEN	5 μg/ml
Ubiquitin	Mouse monoclonal	Santa Cruz	10 μg/ml
Synaptophysin	Mouse monoclonal	Santa Cruz or Zymed	5 μg/ml
β-actin	Mouse monoclonal	Sigma	.1 μg/ml

Appendix II

Primary cortical neuron culture medium

NeuroBasal medium

B27 supplement

L-glutamine (200 mM)

Penicillin (5000 U/ml)/ streptomycin (5000μg/ml)

Foetal bovine serum (FBS)

Homogenisation buffer solution

50mM Tris pH 7.5

5mM $MgCl_2$

250mM sucrose

1mM DTT

2mM ATP

Antigen retrieval buffer

Mild citrate (MCC1) Tris/citrate EDTA buffer pH 7.8

1.3 mM EDTA

2.1 mM Tris

1.1 mM citrate, pH 7.8

Ventana reagents

DAB Map Kit

Diaminobenzidine (DAB)

Horse radish peroxidise (HRP)

Copper sulphate

Inhibitor D

***i*View DAB Detection Kit**

Inhibitor (3 % hydrogen peroxide solution)

SA-HRP (Conjugated streptavidin horseradish peroxidase)

H_2O_2 (.04 %-.08% hydrogen peroxide in an phosphate buffer solution

Diaminobenzidine DAB substrate

Copper sulphate.

Lysis Buffer

100 mM Tris-HCl, pH 7.4

300 mM NaCl

4 mM EDTA

1 % Triton-X-100

1 % deoxycholate

8 mM AEBSF

2x reducing sample buffer

125 mM Tris, pH 6.8

20 % glycerol

0.05 % bromophenol blue

4 % SDS

Fluorogenic assay reagents

Homogenization buffer

50 mM Tris.HCl, pH 7.4,

2 mM ATP

5mM $MgCl_2$

250 mM sucrose

1 mM DTT

Assay buffer

50 mM Tris.HCl, pH 7.4

5 mM $MgCl_2$

2 mM ATP

1 mM DTT

Appendix III

Behavioural assessment

Nesting assessment

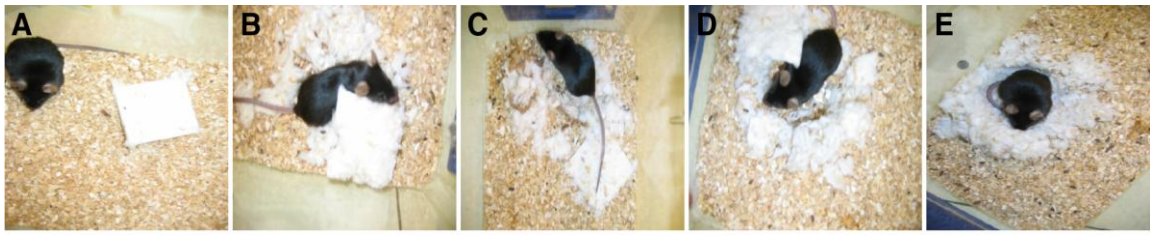

A. Grade (1) = nestlet not touched (more than 90% intact)

B. Grade (2) = nestlet partially torn (50-90% remain intact),

C. Grade (3) = nestlet mostly shredded (less than 50 % remain intact)

D. Grade (4) = nestlet mostly torn and the material gathered into a flat nest

E. Grade (5) = nestlet nearly perfect

Burrowing assessment

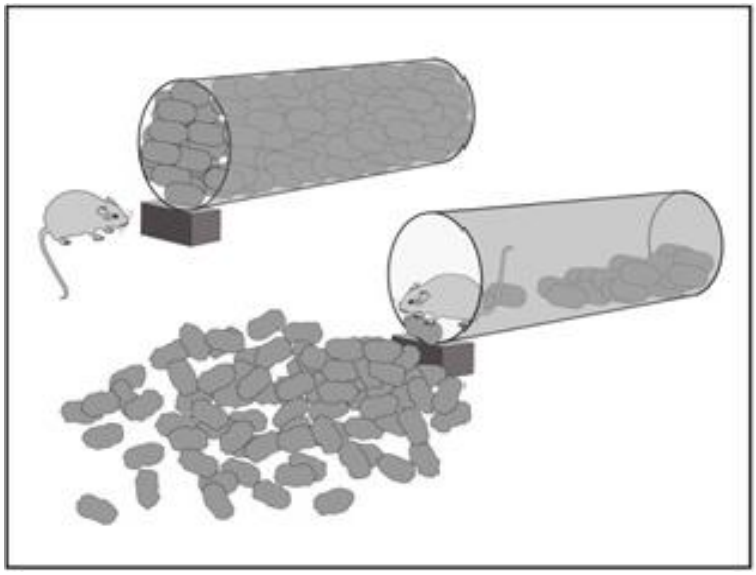

A one-end closed opaque plastic tube (250 x 55 mm, length x diameter) was filled with 200 g of normal food diet pellets were placed into a clean cage and left overnight for mice to burrow the pellet out.

Appendix IV

Statistical report

Survival curve

Log-rank (Mantel-Cox) Test	
Chi square	0.1572
df	2
P value	0.9244
P value summary	ns
Are the survival curves sig different?	No
Logrank test for trend	
Chi square	0.09846
df	1
P value	0.7537
P value summary	ns
Sig. trend?	No

Non-transgenic	GFP1	GFP2
159.1	161	160.8
9.478	3.464	1.643
3.351	2	0.7348

Ubiquitin dot blot

Table Analyzed	Data 1				
Two-way ANOVA					
Source of Variation	% of total variation	P value			
Interaction	7.16	0.0543			
Column Factor	30.46	< 0.0001			
Row Factor	42.8	< 0.0001			
Source of Variation	P value summary	Significant?			
Interaction	ns	No			
Column Factor	***	Yes			
Row Factor	***	Yes			
Source of Variation	Df	Sum-of-squares	Mean square	F	
Interaction	3	65.46	21.82	2.927	
Column Factor	1	278.4	278.4	37.35	
Row Factor	3	391.2	130.4	17.49	
Residual	24	178.9	7.454		
Number of missing values	0				
Bonferroni posttests					
Control vs RML					
Row Factor	Control	RML	Difference	95% CI of diff.	
45	7.105	10.97	3.863	-1.350 to 9.075	
85	9.88	12.39	2.507	-2.705 to 7.720	
125	12.35	19.88	7.533	2.320 to 12.75	
165	12.72	22.42	9.695	4.482 to 14.91	
Row Factor	Difference	t	P value	Summary	
45	3.863	2.001	P > 0.05	ns	
85	2.507	1.299	P > 0.05	ns	
125	7.533	3.902	P<0.01	**	
165	9.695	5.022	P<0.001	***	

Fluorogenic assay

Chymotrpysin D45

Table Analyzed	Data 1
Column A	control
vs	vs
Column B	RML
Unpaired t test	
P value	0.2879
P value summary	ns
Are means signif. different? (P < 0.05)	No
One- or two-tailed P value?	Two-tailed
t, df	t=1.225 df=4
How big is the difference?	
Mean ± SEM of column A	100.0 ± 2.887 N=3
Mean ± SEM of column B	105.00 ± 2.887 N=3
Difference between means	5.000 ± 4.082
95% confidence interval	-6.333 to 16.33
R square	0.2727
F test to compare variances	
F,DFn, Dfd	1.000, 2, 2
P value	1
P value summary	ns
Are variances significantly different?	No

Chymotrpysin D85

Table Analyzed	Data 1
Column A	control
vs	vs
Column B	RML
Unpaired t test	
P value	0.2379
P value summary	ns
Are means signif. different? (P < 0.05)	No
One- or two-tailed P value?	Two-tailed
t, df	t=1.470 df=3
How big is the difference?	
Mean ± SEM of column A	100.0 ± 7.782 N=3
Mean ± SEM of column B	125.2 ± 18.65 N=2
Difference between means	-25.22 ± 17.15
95% confidence interval	-79.80 to 29.36
R square	0.4188
F test to compare variances	
F,DFn, Dfd	3.830, 1, 2
P value	0.3789
P value summary	ns
Are variances significantly different?	No

Chymotrpysin D105

Table Analyzed	Data 1
Column A	control
vs	vs
Column B	RML
Unpaired t test	
P value	0.416
P value summary	ns
Are means signif. different? (P < 0.05)	No
One- or two-tailed P value?	Two-tailed
t, df	t=0.9064 df=4
How big is the difference?	
Mean ± SEM of column A	99.98 ± 2.994 N=3
Mean ± SEM of column B	112.5 ± 13.49 N=3
Difference between means	-12.52 ± 13.81
95% confidence interval	-50.87 to 25.83
R square	0.1704
F test to compare variances	
F,DFn, Dfd	20.29, 2, 2
P value	0.0939
P value summary	ns
Are variances significantly different?	No

Chymotrpysin D125

Table Analyzed	Data 1
Column A	control
vs	vs
Column B	RML
Unpaired t test	
P value	0.0755
P value summary	ns
Are means signif. different? (P < 0.05)	No
One- or two-tailed P value?	Two-tailed
t, df	t=2.386 df=4
How big is the difference?	
Mean ± SEM of column A	100.0 ± 7.741 N=3
Mean ± SEM of column B	81.18 ± 1.523 N=3
Difference between means	18.82 ± 7.890
95% confidence interval	-3.080 to 40.72
R square	0.5873
F test to compare variances	
F,DFn, Dfd	25.85, 2, 2
P value	0.0745
P value summary	ns
Are variances significantly different?	No

Chymotrpysin D145

Table Analyzed	Data 1
Column A	control
vs	vs
Column B	RML
Unpaired t test	
P value	0.019
P value summary	*
Are means signif. different? (P < 0.05)	Yes
One- or two-tailed P value?	Two-tailed
t, df	t=3.806 df=4
How big is the difference?	
Mean ± SEM of column A	100.0 ± 8.069 N=3
Mean ± SEM of column B	65.96 ± 3.858 N=3
Difference between means	34.04 ± 8.944
95% confidence interval	9.212 to 58.87
R square	0.7836
F test to compare variances	
F,DFn, Dfd	4.374, 2, 2
P value	0.3722
P value summary	ns
Are variances significantly different?	No

Chymotrpysin End stage

	Data 1
Table Analyzed	
Column A	control
vs	vs
Column B	RML
Unpaired t test	
P value	0.0002
P value summary	***
Are means signif. different? (P < 0.05)	Yes
One- or two-tailed P value?	Two-tailed
t, df	t=13.78 df=4
How big is the difference?	
Mean ± SEM of column A	99.99 ± 0.1898 N=3
Mean ± SEM of column B	52.37 ± 3.450 N=3
Difference between means	47.62 ± 3.455
95% confidence interval	38.03 to 57.21
R square	0.9794
F test to compare variances	
F,DFn, Dfd	330.4, 2, 2
P value	0.006
P value summary	**
Are variances significantly different?	Yes

Behavioural assessment statistics report

Rotarod

Table Analyzed	Total data bar chart				
Two-way RM ANOVA	Matching by cols				
Source of Variation	% of total variation	P value			
Interaction	2.75	0.006			
Time	4.55	0.0001			
Column Factor	69.2	< 0.0001			
Subjects (matching)	4.846	0.4263			
Source of Variation	P value summary	Significant?			
Interaction	**	Yes			
Time	***	Yes			
Column Factor	***	Yes			
Subjects (matching)	ns	No			
Source of Variation	Df	Sum-of-squares	Mean square	F	
Interaction	4	15614	3903	3.833	
Time	4	25835	6459	6.342	
Column Factor	1	392871	392871	371.3	
Subjects (matching)	26	27513	1058	1.039	
Residual	104	105912	1018		
Number of missing values	0				
Bonferroni posttests					
Control vs RML					
Column Factor	Control	RML	Difference	95% CI of diff.	
45	111.2	33.07	-78.1	-109.7 to -46.44	
60	154.3	56.55	-97.79	-129.4 to -66.13	
70	169.6	49.52	-120	-151.7 to -88.39	
85	144.2	49.07	-95.12	-126.8 to -63.46	

105	175.2	36.55	-138.7	-170.3 to -107.0	
Column Factor	Difference	t	P value	Summary	
45	-78.1	6.45	P<0.001	***	
60	-97.79	8.076	P<0.001	***	
70	-120	9.914	P<0.001	***	
85	-95.12	7.855	P<0.001	***	
105	-138.7	11.45	P<0.001	***	

Burrowing

Table Analyzed	Total data				
Two-way RM ANOVA	Matching by cols				
Source of Variation	% of total variation	P value			
Interaction	10.41	< 0.0001			
Time	4.82	0.0002			
Column Factor	46.14	< 0.0001			
Subjects (matching)	14.2731	< 0.0001			
Source of Variation	P value summary	Significant?			
Interaction	***	Yes			
Time	***	Yes			
Column Factor	***	Yes			
Subjects (matching)	***	Yes			
Source of Variation	Df	Sum-of-squares	Mean square	F	
Interaction	5	18148	3630	11.11	
Time	5	8409	1682	5.149	
Column Factor	1	80441	80441	84.05	
Subjects (matching)	26	24884	957.1	2.93	
Residual	130	42458	326.6		
Number of missing values	0				

Bonferroni posttests					
Control vs RML					
Column Factor	Control	RML	Difference	95% CI of diff.	
20.	70.51	57.79	-12.72	-33.71 to 8.264	
45.	95.8	61.06	-34.74	-55.72 to -13.75	
60.	89.02	48.97	-40.05	-61.03 to -19.06	
70.	85.98	50.48	-35.5	-56.49 to -14.51	
85.	90.07	27.73	-62.34	-83.32 to -41.35	
105.	95.79	18.55	-77.24	-98.22 to -56.25	
Column Factor	Difference	t	P value	Summary	
20.	-12.72	1.62	P > 0.05	ns	
45.	-34.74	4.424	P<0.001	***	
60.	-40.05	5.1	P<0.001	***	
70.	-35.5	4.521	P<0.001	***	
85.	-62.34	7.938	P<0.001	***	
105.	-77.24	9.835	P<0.001	***	

Nesting

Table Analyzed	Total data			
Two-way RM ANOVA	Matching by cols			
Source of Variation	% of total variation	P value		
Interaction	7.43	< 0.0001		
Time	6.57	< 0.0001		
Column Factor	71.71	< 0.0001		
Subjects (matching)	6.4608	< 0.0001		
Source of Variation	P value summary	Significant?		
Interaction	***	Yes		
Time	***	Yes		
Column Factor	***	Yes		
Subjects (matching)	***	Yes		
Source of Variation	Df	Sum-of-squares	Mean square	F
Interaction	6	23.23	3.871	24.16
Time	6	20.55	3.425	21.37
Column Factor	1	224.3	224.3	299.7
Subjects (matching)	27	20.21	0.7484	4.671
Residual	162	25.96	0.1602	
Number of missing values	0			
Bonferroni posttests				
Control vs RML				
Column Factor	Control	RML	Difference	95% CI of diff.
20.	4.867	3.571	-1.295	-1.795 to -0.7958
30.	5	3.786	-1.214	-1.714 to -0.7148
45.	5	3.071	-1.929	-2.428 to -1.429
60.	5	3	-2	-2.499 to -1.501
70.	5	2.571	-2.429	-2.928 to -1.929
85.	5	2.429	-2.571	-3.071 to -2.072
105.	5	1.714	-3.286	-3.785 to -2.786

Column Factor	Difference	t	P value	Summary
20.	-1.295	7.053	P<0.001	***
30.	-1.214	6.612	P<0.001	***
45.	-1.929	10.5	P<0.001	***
60.	-2	10.89	P<0.001	***
70.	-2.429	13.22	P<0.001	***
85.	-2.571	14	P<0.001	***
105.	-3.286	17.89	P<0.001	***

Grip strength

Table Analyzed	Total data edited				
Two-way RM ANOVA	Matching by cols				
Source of Variation	% of total variation	P value			
Interaction	1.86	0.2647			
Time	2.67	0.1016			
Column Factor	28.08	< 0.0001			
Subjects (matching)	28.9401	< 0.0001			
Source of Variation	P value summary	Significant?			
Interaction	ns	No			
Time	ns	No			
Column Factor	***	Yes			
Subjects (matching)	***	Yes			
Source of Variation	Df	Sum-of-squares	Mean square	F	
Interaction	5	1.562	0.3123	1.307	
Time	5	2.248	0.4495	1.881	
Column Factor	1	23.62	23.62	26.2	
Subjects (matching)	27	24.34	0.9015	3.772	
Residual	135	32.26	0.239		

Number of missing values	0				
Bonferroni posttests					
Control vs RML					
Column Factor	Control	RML	Difference	95% CI of diff.	
30.	5.573	4.577	-0.9964	-1.583 to -0.4097	
45.	5.333	4.364	-0.9697	-1.556 to -0.3830	
60.	5.173	4.6	-0.5733	-1.160 to 0.01337	
70.	5.273	4.533	-0.7399	-1.327 to -0.1532	
85.	5.077	4.586	-0.4912	-1.078 to 0.09549	
105.	5.017	4.364	-0.6533	-1.240 to -0.06662	
Column Factor	Difference	t	P value	Summary	
30.	-0.9964	4.536	P<0.001	***	
45.	-0.9697	4.415	P<0.001	***	
60.	-0.5733	2.61	P > 0.05	ns	
70.	-0.7399	3.369	P<0.01	**	
85.	-0.4912	2.236	P > 0.05	ns	
105.	-0.6533	2.974	P < 0.05	*	

8 REFERENCE LIST

Abid K., Soto C. (2006). Biomedicine and diseases: Review the intriguing prion disorders. Cell Mol Life Sci. 63: 2342-2351.

Aguzzi, A., and Calella AM. (2009). Prions: Protein Aggregation and Infectious Diseases. Physiol Rev 89: 1105–1152.

Aguzzi A., Heikenwalder M, Polymenidou M. (2007). Insights into prion strains and neurotoxicity. Nat Rev Mol Cell Biol. 8:552-61.

Aguzzi A. and Polymenidou M., (2004). Mammalian prion biology. One century of evolving concepts. Cell. 116: 313-327.

Aguzzi A., Glatzel M., Montrasio F., Prinz M., and Heppner FL., (2001). Interventional strategies against prion diseases. Nat. Rev. Neurosci. 2: 745-749.

Alper T., Haig DA., and Clarke MC. (1978). The scrapie agent: evidence against its dependence for replication on intrinsic nucleic acid. J Gen. Virol. 41: 503-516.

Alpers M. (1987). Epidemiology and Clinical Aspects of Kuru. In Prions: Novel infectious pathogens causing scrapie and Creutzfeldt-Jakob disease., S.B.Prusiner and M.P.McKinley, eds. (San Diego: Academic Press), pp. 451-465.

Alper T., Cramp WA., Haig DA., and Clarke MC. (1967). Does the agent of scrapie replicate without nucleic acid? Nature. 214: 764-766.

Anderson C., Crimmins S., Wilson JA., Korbel GA., Ploegh HL., Wilson SM. (2005). Loss of Usp14 results in reduced levels of ubiquitin in ataxia mice. Journal of Neurochemistry 95: 724-731.

Anderson R.M., Donnelly,C.A., Ferguson NM., Woolhouse MJ., Watt C.J., Udy HJ., MaWhinney S., Dunstan SP., Southwood TE., Wilesmith JW., Ryan JM., Hoinville LJ., Hillerton JE., Austin AR., and Wells GA. (1996). Transmission dynamics and epidemiology of BSE in British cattle. Nature. 382: 779-788.

Andre R and Tabrizi SJ. (2012). Misfolded PrP and a novel mechanism of proteasome inhibition. Prion. 6:32-6.

Aravind L and Koonin E.V. (2000). The U box is a modified RING finger- a common domain in ubiquitination. Curr. Biol. 10:132-134.

Archer CT., Delahodde A., Gonzalez F., Johnston SA., Kodadek T. Activation domain-dependent monoubiquitylation of Gal4 protein is essential for promoter binding in vivo. J Biol Chem. 2008 May 2;283(18):12614-23.

Arendt CS and Hochstrasser M. (1997). Identification of the yeast 20S proteasome catalytic centers and subunit interactions required for active-site formation. Proc. Natl. Acad. Sci. USA. 94:7156-7161.

Arnason T and Ellison, MJ. (1994). Stress resistance in Saccharomyces cerevisiae is strongly correlated with assembly of a novel type of monoubiquitin chain. Mol. Cell. Biol. 14:7876-7883.

Arrigo AP., Tanaka K., Goldberg A and W. J. Welch. (1988). Identity of the 19S 'prosome' particle with the large multifunctional protease complex of mammalian cells (the proteasome). Nature. 331:192-4.

Asante E., Linehan J., Desbruslais M., Joiner S., Gowland I., Wood A., Welch J., Hill AF., Lloyd S., Wadsworth J., and Collinge J. (2002). BSE prions propagate as either variant CJD-like or sporadic CJD-like prion strains in transgenic mice expressing human prion protein. EMBO J. *21 (23)*, 6358-6366.

Barbanti P., Fabbrini G., Salvatore M., Petraroli R., Cardone F., Maras B., Equestre M., Macchi G., Lenzi GL., and Pocchiari,M. (1996). Polymorphism at codon 129 or codon 219 of *PRNP* and clinical heterogeneity in a previously unreported family with Gerstmann-Straussler-Scheinker disease (PrP-P102L mutation). Neurol *47*, 734-741.

Baron T., Bencsik A., Biacabe AG., Morignat E., and Bessen,R.A. (2007). Phenotypic Similarity of Transmissible Mink Encephalopathy in Cattle and L-type Bovine Spongiform Encephalopathy in a Mouse Model. Emerg. Infect. Dis. *13*, 1887-1894.

Barry RA., Kent SB., McKinley MP., Meyer RK., DeArmond SJ., Hood LE., and Prusiner SB. (1986). Scrapie and cellular prion proteins share polypeptide epitopes. J Infect. Dis. *153*, 848-854.

Bartz JC., Bessen RA., McKenzie D., Marsh RF., and Aiken JM. (2000). Adaptation and selection of prion protein strain conformations following interspecies transmission of transmissible mink encephalopathy. J. Virol. *74*, 5542-5547.

Baskakov IV., Legname G., Baldwin MA., Prusiner SB., and Cohen FE. (2002). Pathway complexity of prion protein assembly into amyloid. J. Biol. Chem. *277*, 21140-21148.

Basler K., Oesch B., Scott M., Westaway D., Walchli M., Groth DF., McKinley MP., Prusiner SB., and Weissmann C. (1986). Scrapie and cellular PrP isoforms are encoded by the same chromosomal gene. Cell *46*, 417-428.

Baumeister WB., Dahlmann R., Hegerl F., Kopp L. (1998). Electron microscopy and image analysis of the multicatalytic proteinase. FEBS Lett. 241:239-45

Bedford L., Hay D., Devoy A., Paine S., Powe DG., Seth R., Gray T., Topham I., Fone K., Rezvani N., Mee M., Soane T., Layfield R., Sheppard PW., Ebendal T., Usoskin D., Lowe J., Mayer RJ. (2008). Depletion of 26S proteasomes in mouse brain neurons causes neurodegeneration and Lewy-like inclusions resembling human pale bodies. J Neurosci 28:

8189–8198.

Bendheim PE., Barry RA., DeArmond SJ., Stites DP., and Prusiner SB. (1984). Antibodies to a scrapie prion protein. Nature *310*, 418-421.

Bence NF., Bennett EJ., Kopito RR., (2005). Application and analysis of the GFPu family of ubiquitin-proteasome system reporters. Methods Enzymol. 399:481-90.

Bence NF., Sampat RM., Kopito RR.. (2001). Impairment of the Ubiquitin-Proteasome System by Protein Aggregation. Science 292: 1552-1555.

Bennett EJ., Bence NF., Jayakumar R., Kopito RR. (2005). "Global impairment of the ubiquitin-proteasome system by nuclear or cytoplasmic protein aggregates precedes inclusion body formation." Mol Cell 17: 351-365.

Berkers CR., Verdoes M., Lichtman E., Fiebiger E., Kessler BM., Anderson KC., Ploeg HL., Ovaa H., Galardy PJ. (2005). Activity probe for in vivo profiling of the specificity of proteasome inhibitor bortezomib. Nat Methods. *2*, 357-362.

Bessen RA. and Marsh RF. (1992). Biochemical and physical properties of the prion protein from two strains of the transmissible mink encephalopathy agent. J. Virol. *66*, 2096-2101.

Bessen RA. and Marsh RF. (1994). Distinct PrP properties suggest the molecular basis of strain variation in transmissible mink encephalopathy. J Virol:*68*, 7859-7868.

Betmouni S., Deacon RM., Rawlins JP., Ferry VH. (1999). Behavioral consequences of prion disease targeted to the hippocampus in a mouse model of scrapie. Psychobiology 27:63–71.

Bett JS., Benn CL., Ryu KY., Kopito RR., Bates GP. (2009). The polyubiquitin Ubc gene modulates histone H2A monoubiquitylation in the R6/2 mouse model of Huntington's disease. J Cell Mol Med. 13:2645-57.

Bodner RA., Outeiro TF., Altmann S., Maxwell MM., Cho SH., Hyman BT., McLean PJ., Young AB., Housman DE., Kazantsev AG. (2006). Pharmacological promotion of inclusion formation: a therapeutic approach for Huntington's and Parkinson's diseases. Proc Natl Acad Sci U S A. 103:4246-51.

Bolton DC., McKinley MP., Prusiner SB. (1982). Identification of a protein that purifies with the scrapie prion. Science *218*: 1309-1311.

Borchelt DR., Rogers M., Stahl N., Telling G., Prusiner SB. (1993). Release of the cellular prion protein from cultured cells after loss of its glycoinositol phospholipid anchor. Glycobiol. *3:* 319-329.

Bounhar Y., Zhang Y., Goodyer CG., LeBlanc A. (2001). Prion protein protects human neurons against Bax-mediated apoptosis. J. Biol. Chem. *276*, 39145-39149.

Bowman AB., Yoo SY., Dantuma NP., Zoghbi HY. (2005). Neuronal dysfunction in a polyglutamine disease model occurs in the absence of ubiquitin-proteasome system impairment and inversely correlates with the degree of nuclear inclusion formation. Hum. Mol. Genet. *14*, 679-691.

Brandner S., Klein MA., Aguzzi A. (1999). A crucial role for B cells in neuroinvasive scrapie. Transfus Clin Biol.6:17-23.

Brandner S., Isenmann S., Raeber A., Fischer M., Sailer, A.. (1996). Normal host prion protein necessary for scrapie-induced neurotoxicity. Nature 379: 339.

Braun BC., Glickman M., Kraft R., Dahlmann B., Kloetzel M., Finley D., Schmidt M. (1999). The base of the proteasome regulatory particle exhibits chaperone-like activity. Nat Cell Biol 1:221-6.

Braun BC., Glickman M., Kraft R., Dahlmann B., Kloetzel M., Finley D., Schmidt, M. (1999). The base of the proteasome regulatory particle exhibits chaperone-like activity. Nat. Cell. Biol. 1:221-226.

Bronson RT., Donahue LR., Samples R., Kim JH., Naggert JK. (2001). Mice with mutations in the mahogany gene Atrn have cerebral spongiform changes. J Neuropathol Exp Neurol;60:724–730.

Brown DR., Nicholas RS., Canevari L. (2002). Lack of prion protein expression results in a neuronal phenotype sensitive to stress. J Neurosci Res ;67:211–224.

Brown P., Preece M., Brandel JP., Sato T., McShane L., Zerr I., Fletcher A., Will RG., Pocchiari M., Cashman NR., D'Aignaux JH., Cervenáková L., Fradkin J., Schonberger LB., and Collins SJ. (2000). Iatrogenic Creutzfeldt-Jakob disease at the millennium. Neurology *55*, 1075-1081.

Brown P. and Bradley R. (1998). 1755 and all that: a historical primer of transmissible spongiform encephalopathy. BMJ. *317*, 1688-1692.

Brown DR., Schulzschaeffer WJ., Schmidt B., Kretzschmar HA. (1997). Prion protein-deficient cells show altered response to oxidative stress due to decreased SOD-1 activity. Exp Neurol; 146:104–112.

Brown DR., Schmidt B., and Kretzschmar HA. (1996). Role of microglia and host prion protein in neurotoxicity of a prion protein fragment. Nature *380*, 345-347.

Brown DR., Herms J., and Kretzschmar HA. (1994). Mouse cortical cells lacking cellular PrP survive in culture with a neurotoxic PrP fragment. Neuroreport *5*, 2057-2060.

Brown P., Gibbs CJ.Jr., Rodgers Johnson P., Asher,D.M., Sulima,M.P., Bacote,A., Goldfarb,L.G., and Gajdusek,D.C. (1994). Human spongiform encephalopathy: the National

Institutes of Health series of 300 cases of experimentally transmitted disease. Ann Neurol. 35: 513-529.

Brown P., Preece MA., and Will RG. (1992). "Friendly fire" in medicine: hormones, homografts, and Creutzfeldt-Jakob disease. Lancet. 340: 24-27.

Brown P., Cathala F., Raubertas RF., Gajdusek DC., and Castaigne P. (1987). The epidemiology of Creutzfeldt-Jakob disease: conclusion of a 15-year investigation in France and review of the world literature. Neurol. *37*:895-904.

Brown P., Rodgers-Johnson P., Cathala F., Gibbs CJJr., and Gajdusek DC. (1984). Creutzfeldt-Jakob disease of long duration: clinicopathological characteristics, transmissibility, and differential diagnosis. Annals of Neurol. 16: 295-304.

Brown P., Green EM., and Gajdusek DC. (1978). Effect of different gradient solutions on the buoyant density of scrapie infectivity. Proc. Soc. Exp. Biol. Med. 158:513-516.

Browning SR., Mason GL., Seward T., Green M., Eliason GA., Mathiason C., Miller MW., Williams ES., Hoover E., Telling GC. (2004). Transmission of Prions from Mule Deer and Elk with Chronic Wasting Disease to Transgenic Mice Expressing Cervid PrP. J Virol *78*: 13345-13350.

Bruce M., Chree A., McConnell I., Foster J., Pearson G., Fraser H. (1994). Transmission of bovine spongiform encephalopathy and scrapie to mice: Strain variation and the species barrier. Philos. Trans. R. Soc. Lond. [Biol] 343:405-411.

Bruce ME., Will RG., Ironside JW., McConnell I., Drummond D., Suttie A., McCardle L., Chree A., Hope J., Birkett C., Cousens S., Fraser H., and Bostock CJ. (1997). Transmissions to mice indicate that 'new variant' CJD is caused by the BSE agent. Nature *389*:498-501.

Bueler H., Aguzzi A., Sailer A., Greiner RA., Autenried P., Aguet M., and Weissmann C.

(1993). Mice devoid of PrP are resistant to scrapie. Cell. *73*:1339-1347.

Bueler H., Fischer M., Lang Y., Bluethmann H., Lipp H.-P., DeArmond SJ., Prusiner SB., Aguet M., and Weissmann C. (1992). Normal development and behaviour of mice lacking the neuronal cell-surface PrP protein. Nature. 356:577-582.

Budka H. (2003). Neuropathology of prion diseases. Br. Med. Bull. 66: 121-130.

Campana V., Sarnataro D., and Zurzolo C. (2005). The highways and byways of prion protein trafficking. Trends Cell Biol. 15: 102-111.

Cardozo C., Michaud C and Orlowski M. (1999). Components of the bovine pituitary multicatalytic proteinase complex (proteasome) cleaving bonds after hydrophobic residues. Biochem. 38:9768-77.

Caramelli M., Ru G., Acutis P., and Forloni G. (2006). Prion diseases : current understanding of epidemiology and pathogenesis, and therapeutic advances. CNS Drugs. 20: 15-28.

Carlson GA., Kingsbury DT., Goodman PA., Coleman, S., Marshall, ST., DeArmond, SJ., Westaway D and Prusiner SB. (1986). Linkage of prion protein and scrapie incubation time genes. Cell. 46: 503–511.

Cascio P., Call M., Petre BM., Walz T., Golberg A. (2002). "Properties of the hybrid form of the 26S proteasome containing both 19S and PA28 complexes." EMBO J. 21: 2636-2645.

Cashman NR. (1997). A prion primer. CMAJ.157:1381-5.

Cashman NR., Loertscher R., Nalbantoglu J., Shaw I., Kascsak RJ., Bolton,DC. and Bendheim PE. (1990) Cellular isoform of the scrapie agent protein participates in lymphocyte activation. Cell: 61, 185–192.

Castilla J., Saa P., Hetz C., and Soto C. (2005). In vitro generation of infectious scrapie

prions. Cell 121: 195-206.

Castilla J., Soto C. (2003). Caspase-12 and endoplasmic reticulum stress mediate neurotoxicity of pathological prion protein, EMBO J. 22:5435–5445.

Castilla J., Hetz C., Soto C., (2004). Molecular mechanisms of neurotoxicity of pathological prion protein, Curr. Mol. Med. 4:397–403. of inducible cell lines independently of its nuclear localization signals and is not cytotoxic, Mol. Cell. 4:397-403.

Corsaro A., Thellung S., Villa V., Nizzari M., Aceto A., Florio T. (2012). Recombinant human prion protein fragment 90-231, a useful model to study prion neurotoxicity. OMICS. 2:50-9.

Caughey B., Baron GS. (2006). Prions and their partners in crime. Nature 443: 803–810.

Caughey B., Lansbury PT. (2003). Protofibrils, pores, fibrils and neurodegeneration: separating the responsible protein aggregates from the innocent bystanders. Annu Rev Neurosci 26: 267–298.

Chapman J., Brown P., Goldfarb LG., Arlazoroff A., Gajdusek DC., and Korczyn AD. (1993). Clinical heterogeneity and unusual presentations of Creutzfeldt- Jakob disease in Jewish patients with the PRNP codon 200 mutation. J Neurol Neurosurg Psych *56:*, 1109-1112.

Chen SG. and Gambetti P. (2002). A Journey through the Species Barrie. Neuron *34*, 854-856.

Chesebro B. (1998). Prion diseases - BSE and prions: Uncertainties about the agent. Science 279: 42-43.

Chesebro B., Trifilo M., Race R., Meade-White K., Teng,C., LaCasse R., Raymond L., Favara C., Baron G., Priola S., Caughey B., Masliah E., and Oldstone M. (2005). Anchorless prion protein results in infectious amyloid disease without clinical scrapie. Science *308*: 1435-1439.

Chiesa R., Piccardo P., Quaglio E., Drisaldi B., Si-Hoe SL., Takao M,. Ghetti B., Harris DA. (2003). Molecular distinction between pathogenic and infectious properties of the prion protein. J Virol 77: 7611–7622.

Ciechanover A. (2006). The ubiquitin proteolytic system: from an idea to the patient bed. Proc Am Thorac Soc. 3:21-31.

Ciechanover A., Schwartz AL. (2004). The ubiquitin system: pathogenesis of human diseases and drug targeting. Biochim Biophys Acta. 1695:3-17.

Ciechanover A and Brundin P. (2003). The ubiquitin proteasome system in neurodegenerative diseases. Sometimes the chicken, sometimes the egg. Neuron *40*: 427-446.

Ciechanover A., Orian A., and Schwartz,A.L. (2000). Ubiquitin-mediated proteolysis: biological regulation via destruction. Bioessays *22*:442-451.

Ciechanover A. (1994). The ubiquitin-proteasome proteolytic pathway. Cell 79: 13–21.

Ciechanover A., Elias S., Heller H., Ferber S and Hershko A. (1980). Characterization of the heat-stable polypeptide of the ATP-dependent proteolytic system from reticulocytes. J Biol Chem. 255:7525-8.

Chau V., Tobias W., Bachmair A., Marriott D., Ecker J., Gonda K., Varshavsky A. (1989). A multiubiquitin chain is confined to specific lysine in a targeted short-lived protein. Science 243:1576-1583.

Chen Q., Liu JB., Horak, KM., Zheng H., Kumarapeli AR, Li J., Li F., Gerdes, A M., Wawrousek, EF., and Wang X. (2005). Intrasarcoplasmic amyloidosis impairs proteolytic function of proteasomes in cardiomyocytes by compromising sub-strate uptake. Circ Res. 97:1018 –26

Chen HK., Fernandez-Funez SF., Acevedo YC., Lam MD., Kaytor MH., Fernandez A. Aitken

EM., Skoulakis H., Orr T., Botas J., Zoghbi HY. (2003). Interaction of Akt-phosphorylated ataxin-1 with 14-3-3 mediates neurodegeneration in spinocerebellar ataxia type 1. Cell. 113:457-68.

Chen P., and Hochstrasser M. (1996). Autocatalytic subunit processing couples active site formation in the 20S proteasome to completion of assembly. Cell. 86:961-72.

Cheroni C., Marino M., Tortarolo M., Veglianese P., De Biasi S., Fontana E. (2009). Functional alterations of the ubiquitin-proteasome system in motor neurons of a mouse model of familial amyotrophic lateral sclerosis. Hum Mol Genet 18: 82-96.

Cohen E and Taraboulos A. (2003). Scrapie-like prion protein accumulates in aggresomes of cyclosporin A-treated cells. EMBO J. 22: 404-417.

Cohen FE., Pan KM., Huang Z., Baldwin M., Fletterick RJ., and Prusiner SB. (1994). Structural clues to prion replication. Science 264:530-531.

Colby DW and Prusiner SV. (2011). Cold Spring Harb Perspect Biol. 3(1):a006833

Chung CH and Baek SH. (1999). Deubiquitinating enzymes: their diversity and emerging roles. Biochem. Biophys. Res. Commun. 266:633-640.

Collinge J and Clarke AR. (2007). A general model of prion strains and their pathogenicity. Science 318: 930–936.

Collinge J., Whitfield J., McKintosh E., Beck J., Mead S., Thomas DJ., and Alpers M. (2006). Kuru in the 21st century--an acquired human prion disease with very long incubation periods. Lancet *367*, 2068-2074.

Collinge J. (2005). Molecular neurology of prion disease. Journal of Neurology Neurosurgery and Psychiatry *76*, 906-919.

Collinge J. (2001). Prion diseases of humans and animals: their causes and molecular basis. Annu. Rev. Neurosci. *24*, 519-550.

Collinge J. (1999). Variant Creutzfeldt-Jakob disease. Lancet *354*, 317-323.

Collinge J. (1997). Human prion diseases and bovine spongiform encephalopathy (BSE). Hum Mol Genetics *6*, 1699-1705.

Collinge J., Beck J., Campbell T., Estibeiro K., and Will RG. (1996a). Prion protein gene analysis in new variant cases of Creutzfeldt-Jakob disease. Lancet *348*: 56.

Collinge J., Sidle KC., Meads S., Ironside J., and Hill AF. (1996b). Molecular analysis of prion strain variation and the aetiology of 'new variant' CJD. Nature 383: 685-690.

Collinge J., Palmer MS., Gowland I., Sidle KC., Hill AF, and Meads S. (1995a). Transmission of human prion disease to transgenic mice expressing human prion protein. Quarterly Journal of Medicine *88*: 839-840.

Collinge J., Palmer MS., Sidle KC., Gowland I., Medori R., Ironside J., and Lantos PL. (1995b). Transmission of fatal familial insomnia to laboratory animals. Lancet 346: 569-570.

Collinge J., Whittingto ,MA., Sidle KL., Smith CJ., Palmer MS., Clarke A, and Jefferys JR. (1994). Prion protein is necessary for normal synaptic function. Nature *370*, 295-297.

Collins S., Law MG., Fletcher A., Boyd A., Kaldor J., and Masters CL. (1999). Surgical treatment and risk of sporadic Creutzfeldt-jakob disease: a case-control study. Lancet 353:693-697.

Collins SJ., Sanchez-Juan P., Masters CL., Klug GM., van Duijn C., Poleggi A., Pocchiari M., Almonti S., Cuadrado-Corrales N., Pedro-Cuesta J., Budka H., Gelpi E., Glatzel M., Tolnay M., Hewer,E., Zerr,I., Heinemann,U., Kretszchmar,H.A., Jansen,G.H., Olsen,E., Mitrova,E., Alperovitch A., Brandel JP., Mackenzie J., Murray K., and Will RG. (2006). Determinants of

diagnostic investigation sensitivities across the clinical spectrum of sporadic Creutzfeldt-Jakob disease. Brain 129, 2278-2287.

Combs CK., Johnson DE., Cannady SB., Lehman TM., and Landreth,G.E. (1999). Identification of microglial signal transduction pathways mediating a neurotoxic response to amyloidogenic fragments of b-amyloid and prion proteins. J. Neurosci. *19*, 928-939.

Cronier S., Laude H., and Peyrin JM. (2004). Prions can infect primary cultured neurons and astrocytes and promote neuronal cell death. Proc. Natl. Acad. Sci. U. S. A 101: 12271-12276.

Crozet C., Beranger F., Lehmann S. (2008). Cellular pathogenesis in prion diseases Vet. Res. 39:44-61.

Cuillé J and Chelle PL. (1936). La maladie dite tremblante du mouton est-elle inocuable? C. R. Acad. Sci. 203: 1552-1554.

Cunningham C., Deacon R., Wells H., Boche D., Waters S., Diniz CP., (2003). Synaptic changes characterize early behavioural signs in the ME7 model of murine prion disease, Eur. J. Neurosci. 17:2147–2155.

Damberger FF., Christen B., Pérez DR., Hornemann S., Wüthrich K.. (2011). Cellular prion protein conformation and function. Proc. Natl. Acad. Sci. U.S.A. 108 (42): 17308–13.

Dantuma NP., and Masucci MG. (2002). Stabilization signals: a novel regulatory mechanism in the ubiquitin/proteasome system. FEBS Lett 529:22-6.

Dantuma NP., Lindsten K., Glas R., Jellne M., Masucci MG. (2000). Short-lived green fluorescent proteins for quantifying ubiquitin/proteasome-dependent proteolysis in living cells. Nat Biotech 18: 538-543.

Dantuma NP., Heessen S., K. Lindsten K., Jellne M, Masucci MG (2000). Inhibition of

proteasomal degradation by the gly-Ala repeat of Epstein-Barr virus is influenced by the length of the repeat and the strength of the degradation signal. Proc Natl Acad Sci U S A 97:8381-5.

Daude N., Marella M., and Chabry J. (2003). Specific inhibition of pathological prion protein accumulation by small interfering RNAs. J Cell Sci 116: 2775-2779.

Dawson TM., Dawson, VL. (2003). Molecular pathways neurodegeneration in Parkinson's disease. Science: 302:819-22.

Deacon RM., Croucher A., Rawlins., JN. (2002). Hippocampal cytotoxic lesion effects on species-typical behaviours in mice. Behav Brain Res. 132:203-13.

Deacon RM., Raley JM., Perry VH., Rawlins JN. (2001). Burrowing into prion disease. NeuroReport 12:2053–2057.

DeArmond SJ. (2004) Discovering the mechanisms of neurodegeneration in prion diseases. Neurochem Res.29:1979-98.

DeArmond SJ., and Ironside, JW. (1999). Neuropathology of prion diseases. In: *Prion Biology and Diseases* (S. B. Prusiner, Ed.), pp. 585– 652. Cold Spring Harbor Laboratory Press, Cold Spring Harbor, NY.

DeArmond SJ., Qiu Y., Wong K., Nixon R., Hyun W., Prusiner SB., Mobley WC. (1996). Abnormal plasma membrane properties and functions in prion-infected cell lines. Cold Spring Harb Symp. Quant. Biol. 61:531-40.

Deriziotis P., Andre R., Smith DM., Goold R., Kinghorn KJ., Kristiansen M., Nathan JA., Rosenzweig R., Krutauz D., Glickman MH., Collinge J., Goldberg, AL.,Tabrizi, SJ. (2011). Misfolded PrP impairs the UPS by interaction with the 20S proteasome and inhibition of substrate entry. EMBO J 30: 3065–3077.

Deriziotis P., Tabrizi SJ. (2008). Prions and the proteasome. Biochim Biophys Acta 1782: 713–722.

Dick T P., A. K. Nussbaum, M. Deeg, W. Heinemeyer, M. Groll, M. Schirle, W. Keilholz, S. Stevanovic, D. H. Wolf, R. Huber, H. G. Rammensee, and H. Schild. (1998). Contribution of proteasomal beta-subunits to the cleavage of peptide substrates analyzed with yeast mutants. J Bio Chem. 273:25637-46.

Dimcheff DE., Askovic S., Baker AH., Johnson-Fowler C., and Portis,J.L. (2003). Endoplasmic reticulum stress is a determinant of retrovirus-induced spongiform neurodegeneration. J Virol. 77:12617-12629.

Di Monte DA., Royland JE., Irwin I., Langston JW. (1996). Astrocytes as the site for bioactivation of neurotoxins. Neuro- toxicology 17:697–703.

Di Giorgio FP., Carrasco MA., Siao MC., Maniatis T., Eggan K. (2007). Non-cell autonomous effect of glia on motor neurons in an embryonic stem cell-based ALS model. Nat Neurosci 10:608–614.

Ding WX., Ni HM., Gao M., Yoshimori T., Stolz DB., Ron D., Yi XM. (2007). Linking of autophagy to ubiquitin-proteasome system is important for the regulation of endoplasmic reticulum stress and cell viability. Am J Pathol. 171:513-24.

Ding Q., Dimayuga E., and Keller JN. (2006). Proteasome regulation of oxidative stress in aging and age-related diseases of the CNS. Antioxid. Redox. Signal. *8*:163-172.

Ding Q., Dimayuga E., Martin S., Bruce-Keller AJ., Nukala V., Cuervo AM., and KellerJN. (2003). Characterization of chronic low-level proteasome inhibition on neural homeostasis. J. Neurochem. 86:489-497.

Di Rocco A., Molinari S., Stollman AL., Decker A., Yahr MD. (1993). MRI abnormalities in

Creutzfeldt-Jakob disease. Neuroradiol. 35:584-5.

Dodelet VC and Cashman NR. (1998). Prion protein expression in human leukocyte differentiation. Blood. 91: 1556-61.

Drisaldi B., Stewart RS., Adles C., Stewart LR., Quaglio E., Biasini E., Fioriti L., Chiesa R., and Harris DA. (2003). Mutant PrP is delayed in its exit from the endoplasmic reticulum, but neither wild-type nor mutant PrP undergoes retrotranslocation prior to proteasomal degradation. J. Biol. Chem. 278: 21732-21743.

Dunham., NW and Miya TS. (1957). A note on a simple apparatus for detecting neurological deficit in rats and mice. *J*. Am. Pharmac. Assoc. Sci. Ed*.* 46:208-209.

Edgworth JA., Farmer M., Sicilia A., Tavares P., Beck, J., Campbell, T., Lowe, J., Mead, S., Rudge, P., Collinge, J., Jackson, GS. (2010). Detection of prion infection in variant Creutzfeldt-Jakob disease: a blood-base assay. Lancet. 377:487-93.

Eghiaian F., Grosclaude J., Lesceu S., Debey P., Doublet B., Treguer E., Rezaei H., and Knossow M. (2004). Insight into the PrPC -> PrPSc conversion from the structures of antibody-bound ovine prion scrapie-susceptibility variants. Proc. Natl. Acad Sci U. S. A *101*: 10254-10259.

Eklun CM., Kennedy RC., and Hadlow WJ. (1967). Pathogenesis of scrapie virus infection in the mouse. *J.* Infect. Dis*.* 117: 15–22.

Elsasser S., Schmidt M., and Finley,D. (2005). Characterization of the proteasome using native gel electrophoresis. In Methods in Enzymology, Elsevier Academic Press), pp. 353-363.

Elsasser S., and Finley D. (2005). Delivery of ubiquitinated substrates to protein-unfolding machines. Nat Cell Biol 7:742-9.

Elasser S., Gali R., Schwickart, C., Larsen, N., Leggett, B., Muller, M., Feng, T., Tubing, F., Dittmar, A., Finley, D. (2002). Proteasome subunit Rpn1 binds ubiquitin-like protein domains. Nat. cell. Biol. 4:725-730.

Enari M., Flechsig E., and Weissmann C. (2001). Scrapie prion protein accumulation by scrapie-infected neuroblastoma cells abrogated by exposure to a prion protein antibody. Proc. Natl. Acad. Sci. USA. 98:9295-9299.

Enenke C., Lehmann A., and Kloetzel, PM. (1998). Subcellular distribution of proteasomes implicates a major location of protein degradation in the nuclear envelope-ER network in yeast. EMBO. J. 17:6144-6154.

Escartin C., Bonvento G. (2008). Targeted activation of astrocytes: a potential neuroprotective strategy. Mol Neurobiol. 38:231–241.

Ettaiche M., Pichot R., Vincent JP., and Chabry J. (2000). *In vivo* cytotoxicity of the prion protein fragment 106-126. Journal of Biological Chem. 275: 36487-36490.

Evans CG., Wisen S. and Gestwicki JE. (2006). Heat shock proteins 70 and 90 inhibit early stages of amyloid beta-(1-42) aggregation in vitro. J Biol Chem. 281: 33182-33191.

Ferdous A., D. Sikder, et al. (2007). "The role of the proteasomal ATPases and activator monoubiquitylation in regulating Gal4 binding to promoters." Genes Dev. 21: 112-123.

Ferdous A., Gonzalez F., Sun L., Kodadek T., Johnston SA. (2001). The 19S regulatory particle of the proteasome is required for efficient transcription elongation by RNA polymerase II. Mol Cell. 7:981-91.

Ferri KF and Kroemer, G. (2001). Organelle-specific initiation of cell death pathways. *Nat* Cell Biol 3: E255-E263.

Finle D., Sadis S., Monia B., Boucher P., Ecker DJ., Crooke ST., Chau V. (1994). Inhibition of

proteolysis and cell cycle progression in a multiubiquitination-deficient yeast mutant. Mol Cell Biol. 14:5501-9.

Finley D., Ciechanover A., and A. Varshavsky. (1984). Thermolability of ubiquitin-activating enzyme from the mammalian cell cycle mutant ts85. Cell. 37:43-55.

Fioriti L., Dossena S., Stewart LR., Stewart,R.S., Harris,D.A., Forloni,G., and Chiesa,R. (2005). Cytosolic prion protein (PrP) is not toxic in N2a cells and primary neurons expressing pathogenic PrP mutations. J. Biol. Chem. *280*, 11320-11328.

Forloni G., Angeretti N., Chiesa R., Monzani E., Salmona M., Bugiani O., and Tagliavini,F. (1993). Neurotoxicity of a prion protein fragment. Nature *362*, 543-546.

Forman MS., Lal D., Zhang B., Dabir DV., Swanson E., Lee VM., Trojanowski JQ. (2005) Transgenic mouse model of tau pathology in astrocytes leading to nervous system degeneration. J Neurosci 25:3539–3550.

French B., Van Leeuwen F., Riley E., Yuan X., Bardag-Gorce K., Gaal Y., Lue H., Marceau N., French W. (2001). Aggreasome formation in liver cells in response to different toxic mechanisms: role of the ubiquitin-proteasome pathway and the frameshift mutant of ubiquitin. Exp. Mol. Pathol. 71:241-246.

Gaczynska M., Golberg A., Tanaka K., Hendil B., Rock KL. (1996). Proteasome subunits X and Y alter peptidase activities in opposite ways to the interferon-gamma-induced subunits LMP2 and LMP7. J. Biol. Chem. 271:17275-17280.

Gajdusek DC., Gibbs CJ.Jr., and Alpers M (1966). Experimental transmission of a kuru-like syndrome to chimpanzees. Nature *209*: 794-796.

Gajdusek DC., and Zigas V. (1957) Degenerative disease of the central nervous system in New Guinea: The endemic occurrence of “kuru” in the native population. N. Engl. J. Med.

257:974 –978.

Gambetti P., Parchi P., Petersen., RB., Chen SG., Lugaresi E. (1995). Fatal familial insomnia and familial Creutzfeldt-Jakob disease: Clinical, pathological and molecular features. Brain Pathol. 5: 43-51.

Gambetti P., Kong Q., Zou W., Parchi P., Chen SG. (2003). Sporadic and familial CJD: classification and characterisation. Br.Med Bull. 66, 213-239.

Gasset M., Baldwin MA., Fletterick RJ., and Prusiner,S.B. (1993). Perturbation of the secondary structure of the scrapie prion protein under conditions that alter infectivity. Proc. Natl. Acad. Sci. U. S A. *90*, 1-5.

Geier E., PfeiferG., Wilm M., Lucchiari-Hartz M., Baumeister W., Eichmann K., Niedermann G. (1999). A giant protease with potential to substitute for some functions of the proteasome. Science 283:978-81.

Gerber R., Tahiri-Alaoui A, Hore PJ., James W. (2007). Oligomerization of the human prion protein proceeds via a molten globule intermediate. J Biol Chem 282: 6300–6307.

Ghani AC., Ferguson NM., Donnelly, CA., Hagenaars TJ., and Anderson RM. (1999). Epidemiological determinants of the pattern and magnitude of the vCJD epidemic in Great Britain. Proc R Soc Lond B. 265: 2443-2452.

Gibbs CJJr., Gajdusek DC., Asher DM., Alpers M., Beck E., Daniel PM., Matthews, B. (1968). Creutzfeldt-Jakob Disease (Spongiform Encephalopathy): Transmission to the Chimpanzee. Science *161*: 388-389.

Gil JM., Rego AC. (2008). Mechanisms of neurodegeneration in Huntington's disease. Eur J Neurosci 27:2803–2820.

Gilon T., Chomsky O and Kulka GR. (1998). Degradation signals for ubiquitin system

proteolysis in Saccharomyces cerevisiae. Embo J 17:2759-66.

Glenn RJ., Pemberton AJ., Royle HJ., Spackman RW., Smith E., Jennifer, RA., Steverding D. (2004). Trypanocidal effect of α′,β′-epoxyketones indicates that trypanosomes are particularly sensitive to inhibitors of proteasome trypsin-like activity. Int. J. Antimicrob. Agents 24,286-289.

Glickman MH and Ciechanover A. (2002). The ubiquitin-proteasome proteolytic pathway: destruction for the sake of construction. Physiol Rev 82: 373–428.

Glickman MH., Finley D. (2000). A gated channel into the proteasome core particle. Nat Struct Biol 7: 1062–1067.

Glickman MH., Rubin DM., Coux O., Wefes I., Pfeifer G., Cjeka Z., Baumeister W., Fried VA., and FinleyD. (1998). A subcomplex of the proteasome regulatory particle required for ubiquitin-conjugate degradation and related to the COP9-signalosome and eIF3. Cell *94*: 615-623.

Glover KJ., Whiles JA., Wood M.J., Melacini G., Komives EA., and Vold RR. (2001). Conformational dimorphism and transmembrane orientation of prion protein residues 110-136 in bicelles. Biochemistry *40*: 13137-13142.

Glover JR., Kowal AS., Schirmer EC., Patino MM., Liu JJ., Lindquist S. (1997). Self-seeded fibers formed by Sup35, the protein determinant of [PSI+], a heritable prion-like factor of S. cerevisiae. Cell. 89:811-9.

Goldberg AL. (2003). Protein degradation and protection against misfolded or damaged proteins. Nature *426*, 895-899.

Goldfarb LG., BrownP., HaltiaM., Ghiso J., Frangione B., and Gajdusek DC. (1993). Synthetic peptides corresponding to different mutated regions of the amyloid gene in familial

Creutzfeldt-Jakob disease show enhanced *in vitro* formation of morphologically different amyloid fibrils. Proc Natl Acad Sci USA. *90*: 4451-4454.

Gonzalez F., Delahodde A., Kodadek T., Johnsto S.A. (2002). "Recruitment of a 19S proteasome subcomplex to an activated promoter." Science 296: 548-550.

Goold R., Rabbanian S., Sutton, L., Andre R., Arora P., Moonga J., Clarke, AR., Schiavo G., Jat, P., Collinge J., Tabrizi, SJ. (2011). Highly rapid cell surface prion protein conversion revealed using a novel cell system. Nat commun. 2:281.

Gordon WS (1946). Advances in veterinary research. Louping-ill, tick-borne fever and scrapie. Veterinary Record *58*, 516-520.

Graham RW., Jones D and Candido EP. (1989). UbiA, the major polyubiquitin locus in Caenorhabditis elegans, has unusual structural features and is constitutively expressed. Mol Cell Biol. 9:268-77.

Gregori L., Hainfeld JF., Simon MN., Goldgaber D.. (1997). Binding of amyloid beta protein to the 20S proteasome. J Biol Chem 272: 58–62.

Gregori L., Fuchs C., Figueiredo-Pereira ME., Van Nostrand WE., Goldgaber D. (1995). Amyloid beta-protein inhibits ubiquitin- dependent protein degradation in vitro. J Biol Chem 270: 19702–19708.

Gregori L., Poosch MS., Cousins G., and Chau V. (1990). A uniform isopeptide multiubiquitin chain is sufficient to target substrate for degradation in ubiquitin-mediated proteolysis. J. Bio Chem. 265:8354-8357.

Griffith JS. (1967). Self Replication and Scrapie. Nature *215*, 1043-1044.

Groll M and Huber R. (2004). "Inhibitors of the eukaryotic 20S proteasome core particle: a structural approach." Biochim Biophys Acta 1695(1-3): 33-44.

Groll M and Huber R. (2003). Substrate access and processing by the 20S proteasome core particle. Int. J. Biochem. Cell Biol. *35*: 606-616.

Groll M., Bajorek M., Kohler A., Moroder L., Rubin DM., Huber R., Glickman MH., Finley D. (2000). A gated channel into the proteasome core particle. Nat Struct Biol 7: 1062–1067.

Groll M., Heinemeyer W., Jager S., Ullrich T., Bochtler M., Wolf DH., and Huber R. (1999). The catalytic sites of 20S proteasomes and their role in subunit maturation: a mutational and crystallographic study. Proc. Natl. Acad. Sci. U. S. A *96*, 10976-10983.

Groll M., Ditzel J. Lowe., D. Stock, M. Bochtler, H. D. Bartunik, and R. Huber. (1997). Structure of 20S pro,teasome from yeast at 2.4 A resolution. Nature. 386:463-71.

Guenther K., Deacon, RM., Perry VH., Rawlins JN. (2001). Early behavioural changes in scrapie-affected mice and the influence of dapsone. Eur J Neurosci. 14:401-9.

Guo Q., Fu W., Sopher BL., Miller MW., Ware C B., Martin GM. and Mattson MP. (1999) Increased vulnerability of hippocampal neurons to excitotoxic necrosis in presenilin-1 mutant knock-in mice. Nat Med, 5:101-106.

Guo Q., Sebastian L., Sopher BL., Miller MW., Ware CB., Martin GM. and Mattson MP. (1999). Increased vulnerability of hippocampal neurons from presenilin-1 mutant knock-in mice to amyloid beta-peptide toxicity: central roles of superoxide production and caspase activation. J Neurochem, 72: 1019- 1029.

Haass C., Selkoe DJ. (2007) Soluble protein oligomers in neurodegeneration: lessons from the Alzheimer's amyloid beta-peptide. Nat Rev Mol Cell. Biol 8: 101–112.

Haigh CL., Marom SY., Collins SJ. (2010). Copper, endoproteolytic processing of the prion protein and cell signaling Front Biosci. 15:1086-104.

Haire F., Whyte SM., Vasisht N., Gill AC., Verma C., Dodson EJ., Dodson GG., and Bayley

PM. (2004). The crystal structure of the globular domain of sheep prion protein. J Mol. Biol. *336*:1175-1183.

Halliwell B. (2006). Oxidative stress and neurodegeneration: where are we now? J Neurochem. 97:1634– 1658.

Hatakeyama S., Yada M., Matsumoto N., Ishida K., , and Nakayama I. (2001). U box proteins as a new family of ubiquitin-protein ligases. J Biol Chem. 276:33111-20.

Hampton RY. (2002). ER-associated degradation in protein quality control and cellular regulation. Curr Opin Cell Biol. 14:476-82.

Hampton RY. (2002). Proteolysis and sterol regulation. Annu Rev Cell Dev Biol 18:345-78.

Hara T., Nakamura K., Matsui M., Yamamoto A., Nakahara Y., Suzuki-Migishima R., Yokoyama M., Mishima K., Saito I., Okano H., and Mizushima N. (2006). Suppression of basal autophagy in neural cells causes neurodegenerative disease in mice. Nature 441: 885-889.

Harris DA. (1999). Cellular biology of prion diseases. Clin. Microbiol. Rev. *12*: 429-444.

Harper JD., Lieber CM. , Lansbury PT. (1997). Atomic force microscopic imaging of seeded fibril formation and fibril branching by the Alzheimer's disease amyloid-beta protein. Chem Biol. 4:951-9.

Harper JD., and Lansbury PT. (1997). Models of amyloid seeding in Alzheimer's disease and scrapie: mechanistic truths and physiological consequences of the time-dependent solubility of amyloid proteins. Annu. Rev. Biochem. 66:385-407.

Hegde AN. (2004). "Ubiquitin-proteasome-mediated local protein degradation and synaptic plasticity." Prog Neurobiol 73(5): 311-357.

Hegde RS., Tremblay P., Groth D., DeArmond S., Prusiner SB., and Lingappa VR. (1999). Transmissible and genetic prion diseases share a common pathway of neurodegeneration. Nature *402*: 822-826.

Hegde RS., Mastrianni JA., Scott MR., DeFea KA., Tremblay P., Torchia M., DeArmond SJ., Prusiner SB., and Lingappa,V.R. (1998). A transmembrane from of the prion protein in neurodegenerative disease. Science *279*: 827-834.

Heller U., Winklhofer KF., Heske J., Reintjes A., and Tatzelt J. (2003). Post-translational import of the prion protein into the endoplasmic reticulum interferes with cell viability: A critical role for the putative transmembrane domain. J Biol. Chem. 27:36139-47.

Heppner FL., Aguzzi A (2004). Recent developments in prion immunotherapy. Curr Opin Immunol. 5:594-8.

Hershko A. and Ciechanover A. (1998). "The ubiquitin system." Annu Rev Biochem 67: 425-479.

Hershko A., Heller H., Elias S., and Ciechanover A. (1983). Components of ubiquitin-protein ligase system. Resolution, affinity purification, and the role in protein breakdown. J. Biol. Chem. 258:8206-8214.

Heessen S., Dantuma NP., Tessarz P., Jellne M., Masucci MG. (2003). Inhibition of ubiquitin/proteasome-dependent proteolysis in Saccharomyces cerevisiae by a Gly-Ala repeat. FEBS Lett. 555:397-404.

Heessen S., Leonchiks A., Issaeva N., Sharipo A., Selivanova G., Dantuma NP. (2002). Functuntional P53 chimeras containing the Epstein-Barr virus are protected from Mdm2- and HPV-E6-induced proteolysis. Proc. Natl. Acad. Sci. USA. 99:1532-1537.

Hetz C., Castilla J., Soto C., (2007) Perturbation of endo- plasmic reticulum homeostasis

facilitates prion replication, J. Biol. Chem. 282:12725–12733.

Hetz CA., Soto C. (2006). Stressing out the ER: a role of the unfolded protein response in prion-related disorders, Curr. Mol. Med. 6:37–43.

Hetz C., Russelakis-Carneiro M., Walchli S., Carboni S., Vial-Knecht E., Maundrell K., Castilla J and Soto C. (2005). The disulfide isomerase Grp58 is a protective factor against prion neurotoxicity. J. Neurosci. 25: 2793–2802.

Hetz C., Russelakis-Carneiro M., Maundrell K., Castilla J and Soto C. (2003). Caspase-12 and endoplasmic reticulum stress mediate neurotoxicity of pathological prion protein. EMBO J. 22: 5435–5445.

Hicke L. (2001). Protein regulation by monoubiquitin. Nat Rev Mol Cell Biol. 2:195- 201.

Hicke L. (2001). "A new ticket for entry into budding vesicles-ubiquitin." Cell. 106: 527-530.

Hicke L. (1999). Gettin' down with ubiquitin: turning off cell-surface receptors, transporters and channels. Trends Cell Biol. 9:107-12.

Hilber P., Caston J. (2001) Motor skills and motor learning in Lurcher mutant mice during aging. Neuroscience 102:615-623.

Hill AF., Joiner S., Beck J., Campbell T.A., Dickinson A., Poulter M., Wadsworth J., and Collinge J. (2006). Distinct glycoform ratios of protease resistant prion protein associated with *PRNP* point mutations. Brain. 129: 676-685.

Hill AF., Joiner S., Wadsworth J., Sidle KC., Bell JE., Budka H., Ironside JW., and Collinge J. (2003). Molecular classification of sporadic Creutzfeldt-Jakob disease. Brain. 126: 1333-1346.

Hill AF and Collinge J. (2003). Subclinical prion infection. Trends Microbiology. 11: 578-584.

Hill AF and Collinge J (2003). Subclinical prion infection in humans and animals. Brit Med Bulletin. 66: 161-170.

Hill AF., Joiner S., Linehan J., Desbruslais M., Lantos PL., and Collinge J. (2000). Species barrier independent prion replication in apparently resistant species. Proc Natl Acad Sci USA. *97*: 10248-10253.

Hill AF., Desbruslais,M., Joiner S., Sidle KC., Gowland I., and Collinge J. (1997). The same prion strain causes vCJD and BSE. Nature *389*: 448-450.

Hilton DA., Ghani AC., Conyers L., Edwards P., McCardle L., Penney M., Ritchie D., and Ironside JW. (2002). Accumulation of prion protein in tonsil and appendix: review of tissue samples. BMJ. *325*: 633-634.

Hilton DA., Ghani AC., Conyers L., Edwards P., McCardle L., Ritchie D., Penney M., Hegazy D., and Ironside JW. (2004). Prevalence of lymphoreticular prion protein accumulation in UK tissue samples. J Pathol. 203: 733-739.

Hoozemans JJ., Veerhuis R., Van Haastert ES., Rozemuller JM., Baas F., Eikelenboom P and Scheper W. (2005). The unfolded protein response is activated in Alzheimer's disease. *Acta* Neuropathol. 110: 165–172.

Hope T., Matuschewski K., Rape M., Schlenker S., Ulrich H., Jentsch D. (2000). Activatiation of a membrane bound transcription factor by regulated ubiquitin/proteasome-dependent processing. Cell 102:577-586.

Hope J., Morton LJ., Farquhar CF., Multhaup G., Beyreuther K., and Kimberlin RH. (1986). The major polypeptide of scrapie-associated fibrils (SAF) has the same size, charge distribution and N-terminal protein sequence as predicted for the normal brain protein (PrP). EMBO J. *5*: 2591-2597.

Hosszu LP., BaxterNJ., Jackson GS., Power A., Clarke AR., Waltho JP., CravenCJ and Collinge J. (1999). Structural mobility of the human prion protein probed by backbone hydrogen exchange. Nature Struct. Biol. *6*: 740-743.

Hsiao K., Baker HF., Crow TJ., Poulter M., Owen F., Terwilliger JD., Westaway D., Ott J., and Prusiner SB. (1989). Linkage of a prion protein missense variant to Gerstmann- Straussler syndrome. Nature *338*:342-345.

Hunter AJ., Caulfield MP., Kimberin RH.(1986). Learning ability of mice infected with different strains of scrapie. Physiol. Behav. 36:1089-1092.

Illing ME., Rajan RS., Bence NF. and Kopito, RR. (2002). A rhodopsin mutant linked to autosomal dominant retinitis pigmentosa is prone to aggregate and interacts with the ubiquitin proteasome system. J. Biol. Chem., 277: 34150 – 34160.

Imai Y., Soda M., Hatakeyama S., Akagi T., Hashikawa T., Nakayama I., and Takahashi R. (2002). CHIP is associated with Parkin, a gene responsible for famililal Parkinson's disease, and enhances its ubiquitin ligase activity. Mol. Cell 10:55-67.

Imai Y., Soda M., Inoue H., Hattori N., Mizuno Y and Takahashi R. (2001). An unfolded putative transmembrane polypeptide, which can lead to endoplasmic reticulum stress, is a substrate of Parkin. Cell 105: 891–902.

Imai Y., Soda M., and Takahashi R. (2000). Parkin suppresses unfolded protein stress-induced cell death through its E3 ubiquitin-protein ligase activity. J Biol Chem. 275:35661-4.

Jackson GS., Murray I., Hosszu LL., Gibbs N., Waltho JP., Clarke AR., and Collinge J. (2001). Location and properties of metal-binding sites on the human prion protein. Proc. Natl. Acad. Sci. U. S. A *98*: 8531-8535.

Jeffrey M., Halliday WG., Bell J., Johnston AR., Macleod NK., Ingham C., Sayers AR., Brown

DA., Fraser JR. (2000). Synapse loss associated with abnormal PrP precedes neuronal degeneration in the scrapie-infected murine hippocampus. Neuropath. Appl. Neurobiol., 26:41-54.

Jeffrey M., Goodsir CM., Bruce M., McBride PA., Scott JR. and Halliday WG. (1994) Correlative light and electron microscopy studies of PrP localisation in 87V scrapie. *Brain Res*., 656: 329–343.

Jeffrey M., Scott JR., Williams A., and Fraser H. (1992). Ultrastructural features of spongiform encephalopathy transmitted to mice from three species of bovidae. Acta Neuropathol (Berl) *84*: 559-569.

Jentsch S and Pyrowolakis. (2000). Ubiquitin and its Kin: how close are the family ties. Trends Cell. 10:335-342.

Jentsch S., Seufert W and Hauser HP. (1991). Genetic analysis of the ubiquitin system. Biochim Biophys Acta. 1089:127-39.

Jentsch S., McGrath JP., et al. (1987). "The yeast DNA repair gene RAD6 encodes a ubiquitin- conjugating enzyme." Nature 329(6135): 131-134.

Joazeiro CA., and Weissman AM. (2000). Ring finger proteins: Mediators of ubiquitin ligase activity. Cell 102:549-552.

Johnson RT., Gibbs CJ. (1998). Creutzfeldt-Jakob disease and related transmissible spongiform encephalopathies. N Engl J Med. 339:1994-2004.

Johnson ES., Ma, PC., Ota IM. and Varshavsky A. (1995) A proteolytic pathway that recognizes ubiquitin as a degradation signal. J Biol Chem, 270, 17442- 17456.

Jones DE., Crowe T., Stevens A and Candido EP. (2002). Functional and phylogenetic analysis of the ubiquitylation system in Caenorhabditis elegans: ubiquitin-conjugating

enzymes, ubiquitin-acitivating enzymes, and ubiquitin-like proteins. Genome Biol. 3 RESEARCH0002.

Jones BJ and Roberts DJ. (1968). The quantitative measurement of motor inco-ordination in naive mice using an accelerating rotarod. J. Pharm. Pharmacol. 20:302-304.

Jung T., Catalgol B., Grune, T. (2009). "The proteasomal system." Molecular Aspects of Medicine 30(4): 191-296.

Kabeya Y., Mizushima N., Ueno T., Yamamoto A., Kirisako T., Noda T., Kominami E., Ohsumi Y., and Yoshimori T. (2000). LC3, a mammalian homologue of yeast Apg8p, is localized in autophagosome membranes after processing. EMBO J. *19*: 5720-5728.

Kang SC., Brown DR., Whiteman M., Li R., Pan T., Perry G., Wisniewski T., Sy,M S., and Wong BS. (2004). Prion protein is ubiquitinated after developing protease resistance in the brains of scrapie-infected mice. J Pathol. 203: 603-608.

Kaski D., Mead S., Hyare H., Cooper S., Jampana R., Overell J., Knight, R., Collinge J., Rudge, P. (2009). Variant CJD in an individual heterozygous for PRNP codon 129. *Lancet* . 374, 2128.

Keller JN., Hanni KB., and Markesbery, WR. (2000). Impaired proteasome function in Alzheimer's disease. J. Neu- rochem. 75:436 – 439.

Keller JN., Huang, FF. and Markesbery WR. (2000). Decreased levels of proteasome activity and proteasome expression in aging spinal cord. Neuroscience, 98, 149-156.

Khalili-Shirazi A., Summers L., Linehan J., Mallinson G., Anstee D., Hawke,S., Jackson GS, and Collinge J. (2005). PrP glycoforms are associated in a strain-specific ratio in native PrPSc. J. Gen. Virol. 86: 2635-2644.

Kimberlin RH and Marsh RF. (1975). Comparison of scrapie and transmissible mink

encephalopathy in hamsters. I. Biochemical studies of brain during development of disease. J Infect. Dis. 131: 97-103.

King CY and Diaz-Avalos R. (2004). Protein-only transmission of three yeast prion strains. Nature. 428: 319–323.

Kisselev AF., Akopian TN., and Goldberg AL. (1998). Range of sizes of peptide products generated during degradation of different proteins by archaeal proteasomes. J. Biol. Chem. *273*: 1982-1989.

Kisselev AF., Akopian TN., Woo KM., and Goldberg AL. (1999). The sizes of peptides generated from protein by mammalian 26 and 20 S proteasomes. Implications for understanding the degradative mechanism and antigen presentation. J. Biol. Chem. 27*4*: 3363-3371.

Kisselev AF., Callard A., and Goldberg AL. (2006). Importance of the proteasome's different proteolytic sites and the efficacy of inhibitors varies with the protein substrate. J Biol. Chem. 281:8582-90

Kisselev AF., and Goldberg AL. (2005). Monitoring activity and inhibition of 26S proteasomes with fluorogenic peptide substrates. Methods Enzymol. 398: 364-378.

Kisselev AF., Kaganovich D., and Goldberg AL. (2002). Binding of hydrophobic peptides to several non-catalytic sites promotes peptide hydrolysis by all active sites of 20 S proteasomes - Evidence for peptide-induced channel opening in the alpha-rings. J Biol. Chem. 277:22260-22270.

Klein MA., Frigg R., RAeber AJ., Flechsig E., Hegyi I., Zinkermagel RM., Weissmann C., Aguzzi A. (1998). PrP expression in B lymphocytes is not required for prion neuroinvasion. Nature Med.4, 1429–1433.

Klyubin I., Walsh DM., Lemere CA., Cullen WK., Shankar GM., BettsV., Spooner ET., JiangL., Anwyl R., Selkoe DJ., and Rowan MJ. (2005). Amyloid beta protein immunotherapy neutralizes Abeta oligomers that disrupt synaptic plasticity in vivo. Nat. Med. 11*:* 556-561.

Kirkpatrick DS., Hathaway NA., Hanna J., Elsasser S., Rush J., Finley D., King RW., and Gygi SP. (2006). Quantitative analysis of in vitro ubiquitinated cyclin B1 reveals complex chain topology. Nat. Cell Biol. *8*: 700-710.

Kisselev AF., Callard A., and Goldberg AL. (2006). Importance of the proteasome's different proteolytic sites and the efficacy of inhibitors varies with the protein substrate. J Biol. Chem. 281:8582-90.

Klionsky DJ., Cregg JM., Dunn WA., Emr SD., Sakai Y., Sandoval IV., Sibirny A., Subramani S., Thumm M., Veenhuis M., Ohsumi Y. (2003). A unified nomenclature for yeast autophagy-related genes. Dev Cell. 5:539 –545.

Knaus KJ., Morillas M., Swietnicki W., Malone M., Surewicz WK., and Yee VC. (2001). Crystal structure of the human prion protein reveals a mechanism for oligomerization. Nat. Struct. Biol. *8*: 770-774.

Kocisko DA., Come JH., Priola SA., Chesebro B., Raymond G.J., Lansbury PT., and Caughey B. (1994). Cell-free formation of protease-resistant prion protein. Nature. 370: 471-474.

Koegl M., Hoppe T., Schlenker S., Ulrich DH., Mayer TU., Jentsch S. (1999). A novel ubiquitination factor, E4, is involved in multiubiquitin chain assembly. Cell. 96:635-44.

Kohler AP., Cascio DS., Leggett K., Woo M.,Goldberg AL., Finley D. (2001). The axial channel of the proteasome core particle is gated by the Rpt2 ATPase and controls both substrate entry and product release. Mol Cell 7:1143-52.

Kovacs GG., Preusser M., Strohschneider M., and Budka H. (2005). Subcellular localization of disease-associated prion protein in the human brain. Am J Pathol. *166*:287-294.

Kovacs GG., Budka H. (2008) Prion Diseases: From Protein to Cell Pathology. Am J Pathol 172: 555-565.

Koistinaho M., Lin S., Wu X., Esterman M., Koger D., Hanson J., Higgs R., Liu F., Malkani S., Bales KR., Paul SM. (2004). Apoli- poprotein E promotes astrocyte colocalization and degradation of deposited amyloid-beta peptides. Nat Med 10:719–726.

Komatsu M., Waguri S., Chiba,T., Murata,S., Iwata,J., Tanida,I., Ueno,T., Koike,M., Uchiyama,Y., Kominami,E., and Tanaka,K. (2006). Loss of autophagy in the central nervous system causes neurodegeneration in mice. Nature 441, 880-884.

Korhonen L and Lindholm D. (2004). The ubiquitin proteasome system in synaptic and axonal degeneration: a new twist to an old cycle. J Cell Biol. 165: 27–30

Kretzschmar HA., Kufer P., Riethmuller G et al. (1992). Prion protein mutation at codon 102 in an Italian family with Gerstmann-Straussler-Scheinker syndrome. Neurology. 42:809-10.

Kristiansen M., Deriziotis P., Dimcheff DE., Jackson GS., Ovaa H., Naumann H., Clarke AR., van Leeuwen FWB., Menqndez-Benito V., Dantuma NP., Portis JL., Collinge J., Tabrizi SJ. (2007). Disease-Associated Prion Protein Oligomers Inhibit the 26S Proteasome. Molecular Cell 26: 175-188.

Kristiansen M., Messenger MJ., Klohn PC., Brandner S., Wadsworth J D., Collinge J., and Tabrizi,S.J. (2005). Disease-related prion protein forms aggresomes in neuronal cells leading to caspase activation and apoptosis. J. Biol. Chem. 280: 38851-38861.

Kubler E., Oesch B., and Raeber AJ. (2003). Diagnosis of prion diseases. Br. Med. Bull. *66*: 267-279.

Kudo T., Okumura M., Imaizumi K., Araki W., Morihara T., Tanimuka, H., Kamagata E., Tabuchi N., Kimura R., Kanayama D., Fukumori A., Tagami S., Okochi M., Kubo M., Tanii H., Tohyama M., Tabira T., Takeda M. (2006). Altered localization of amyloid precursor protein under endoplasmic reticulum stress. Biochem Biophys Res Commun. 344:525-30.

Kumarapeli AR., Horak KM., Glasford JW., Li J., Chen Q., Liu J., Zheng H., and Wang X. (2005). A novel transgenic mouse model reveals deregulation of the ubiquitin-proteasome system in the heart by doxorubicin. FASEB J. 19(14):2051-3.

Kuroda Y., Gibbs CJ Jr., Amyx HL., Gajdusek DC. (1983). Creutzfeldt-Jakob disease in mice: persistent viremia and preferential replication of virus in low-density lymphocytes. Infect Immun. 41:154-61.

Lam YA., Lawson GT., Velayutham, M., Zweier JL., and Pickart CM. (2002). A proteasomal ATPasedegradation signal. Nature 416:763-7.

Lasmezas CI., Deslys JP., Robain O., Jaegly A., Beringue V., Peyrin JM., Fournier JG., Hauw JJ., Rossier J., and Dormont D. (1997). Transmission of the BSE agent to mice in the absence of detectable abnormal prion protein. Science *275*, 402-405.

Lauwers E., Jacob C et al. (2009). "K63-linked ubiquitin chains as a specific signal for protein sorting into the multivesicular body pathway." J Cell Biol 185: 493-502.

Layfield R., Lowe J., Bedford L. (2005). The ubiquitin-proteasome system and neurodegenerative disorders. Essays Biochem. 41:157-171.

Layfield R., Lowe J., Tang G., Xu, Z., Goldman JE. (2006) Synergistic effects of the SAPK/JNK and the proteasome pathway on glial fibrillary acidic protein (GFAP) accumulation in Alexander disease. J. Biol. Chem. 281:38634-38643.

Lecker SH., Golberg AL., Mitch WE. (2006). Protein degradation by the ubiquitin-

proteasome pathway in normal and disease states. J Am. Soc. Nephrol. 17:1807-1819.

Levine B., Klionsky DJ. (2004). Development by self-digestion: molecular mechanisms and biological functions of autophagy. Dev Cell, 6:463– 477.

Lee BH., Lee MJ, Park S., Oh DC., Elsasser S., Chen PC.,Gartner C., Dimova N., Hanna J., Gygi SP.,Wilson SM., King RW, and Finley, D. (2010). Enhancement of proteasome activity by a small-molecule inhibitor of USP14. Nature 467, 179-184.

Lee HS., Brown P., Cervenáková L., Garruto RM., Alpers M., Gajdusek DC., and Goldfarb LG. (2001). Increased susceptibility to Kuru of carriers of the *PRNP* 129 methionine/methionine genotype. Journal of Infectious Diseases. *183*:192-196.

Leggett DS., Hanna J., Borodovsky A., Crosas B., Schmidt M., Baker RT., Walz T., Ploegh H., and Finley D.. (2002). Multiple associated proteins regulate proteasome structure and function. Mol Cell 10:495-507.

Leggett MM., Dukes J., and Pirie HM. (1990). A spongiform encephalopathy in a cat. Vet. Rec. 127:586-588.

Legname G., Baskakov IV., Nguyen HO., Riesner D., Cohen FE., DeArmond SJ., and Prusiner SB. (2004). Synthetic mammalian prions. Science *305*: 673-676.

Lepore AC., Rauck B., Dejea C., Pardo AC., Rao MS., Rothstein JD., Maragakis NJ. (2008). Focal transplantation-based astrocyte replacement is neuroprotective in a model of motor neuron disease. Nat Neurosci 11:1294–1301.

Lewis PA., Properzi F., Prodromidou K., Clarke A., Collinge J, and Jackson GS. (2006). Removal of the glycosylphosphatidylinositol anchor from PrP(Sc) by cathepsin D does not reduce prion infectivity. Biochemical Journal *395*:443-448.

Li A., Barmada SJ., Roth KA., and Harris DA. (2007). N-terminally deleted forms of the prion

protein activate both Bax-dependent and Bax-independent neurotoxic pathways. J Neurosci. 27: 852-859.

Liberski PP., Brown DR., Sikorska,B., Caughey,B., and Brown,P. (2008). Cell death and autophagy in prion diseases (transmissible spongiform encephalopathies). Folia Neuropathol. 46:1-25.

Liberski PP., Streichenberger N., Giraud P., Soutrenon M., Meyronnet D., Sikorska B., and Kopp N. (2005). Ultrastructural pathology of prion diseases revisited: brain biopsy studies. Neuropathol. Appl. Neurobiol. 31: 88-96.

Liberski PP., Gajdusek DC., and Brown P. (2002). How do neurons degenerate in prion diseases or transmissible spongiform encephalopathies (TSEs): neuronal autophagy revisited. Acta Neurobiol. Exp. 62:141-147.

Lindenbaum S. (1979). Kuru Sorcery: Disease and Danger in the New Guinea Highlands. Palo Alto: Mayfield.

Lindholm D., Wootz H., Korhonen L. (2006). ER stress and neurodegenerative diseases. Cell Death and Differentiation 13**:**385–392.

Lindsten K., and. Dantuma NP. (2003). Monitoring the ubiquitin/proteasome system in conformational diseases. Ageing Res Rev 2:433-49.

Lindsten K., Menendez-Benito V., Masucci MG., and Dantuma NP. (2003). A transgenic mouse model of the ubiquitin/proteasome system. Nat. Biotechnol. *21*, 897-902.

Lindsten K., de Vrij F., Verhoef L., Fischer DF., van Leeuwen FW. (2002). Mutant ubiquitin found in neurodegenerative disorders is a ubiquitin fusion degradation substrate that blocks proteasomal degradation. J Cell Biol 157: 417-427.

Llyod S., Mead S., Collinge, J. (2011). Genetics of prion disease. Top Curr Chem. 305:1-22.

Lloyd S., Onwuazor ON., Beck J., Mallinson G., Farrall M., Targonski P., Collinge J, and Fisher E. (2001). Identification of multiple quantitative trait loci linked to prion disease incubation period in mice. Proc. Natl. Acad. Sci. USA. 98: 6279-6283.

Li J., and Rechsteiner. (2001). Molecular dissection of the 11 S REG (PA28) proteasome activators. Biochimic. 83:373-383.

Liu J., Chen Q., Huang, W., Horak, K. M., Zheng, H., Mestril, R., and Wang, X. (2006) Impairment of the ubiquitin-proteasome system in desminopathy mouse hearts. FASEB J. 20, 362– 4.

Liu H., Bowes III RC., van de Water B., Sillence C., Nagelkerke JF., Stevens JL. (1997). Endoplasmic reticulum chaperones GRP78 and calreticulin prevent oxidative stress, Ca^{2+} disturbances, and cell death in renal epithelial cells. J Biol Chem. 272: 21751-21759.

Lobsiger CS Cleveland DW. (2007). Glial cells as intrinsic components of non-cell-autonomous neurodegenerative disease. Nat Neurosci 10:1355–1360.

Lopez SM., Morelli L., Castano EM., Soto EF., and Pasquini JM. (2000). Defective ubiquitination of cerebral proteins in Alzheimer's disease. J. Neurosci. Res. 62: 302–310.

Lorenzo ME., Ploegh HL and Tirabassi RS. (2001). Viral immune evasion strategies and the underlying cell biology. Semin. Immunol. 13:1-9.

Lowe J., Stock D., Jap B., Zwickl P., Baumeister W., and Huber R. (1995). Crystal structure of the 20S proteasome from the archaeon T. acidophilum at 3.4 A resolution. Science. 268: 533-539.

Lowe J., Fergusson J., Kenward N., Laszlo L., Landon M., Farquhar C., Brown,J., Hope,J., and Mayer,R.J. (1992). Immunoreactivity to ubiquitin-protein conjugates is present early in the disease process in the brains of scrapie-infected mice. J Pathol. 168: 169-177.

Lowe J., Blanchard, A., Morrell, K., Lennox, G., Reynolds, L., Billett, M., Landon, M., Mayer, R. J. (1988). Ubiquitin is a common factor in intermediate filament inclusion bodies of diverse type in man, including those of Parkinson's disease, Pick's disease, and. Alzheimer's disease, as well as Rosenthal fibres in cerebellar astrocytomas, cytoplasmic bodies in muscle, and Mallory bodies in alcoholic liver disease. J. Pathol. 155, 9-15.

Luker GD., Pica CM., Song J., Luke KE., Piwnica-Worms D. (2003). Imaging 26S proteasome activity and inhibition in living mice. Nat Med. 9:969-73.

Lum JJ., DeBerardinis RJ., Thompson CB. (2005). Autophagy in metazoans: cell survival in the land of plenty. Nat Rev Mol Cell Biol. 6:439 – 448.

Lundgren J., Masson P., Realini CA., Young P. (2003). Use of RNA interference and complementation to study the function of the Drosophila and human 26S proteasome subunit S13. Mol Cell Biol.23:5320-30.

Ma J., Wollmann R., Lindquist S. (2002). Neurotoxicity and Neurodegeneration When PrP Accumulates in the Cytosol. Science 298: 1781-1785.

Ma J and Lindquist S. (2002). Conversion of PrP to a Self-Perpetuating PrPSc-like Conformation in the Cytosol Science 298: 1785-1788.

Mallucci G. (2009). Prion neurodegeneration: starts and stops at the synapse. Prion. 3:195-201.

Mallucci G., White MD., Farmer M., Dickinson A., Khatun H., Powell AD., Brandner S., Jefferys JG., and Collinge J. (2007). Targeting cellular prion protein reverses early cognitive deficits and neurophysiological dysfunction in prion-infected mice. Neuron. *53*: 325-335.

Mallucci G., Dickinson A., Linehan J., Klohn PC., Brandner S., Collinge J. (2003). Depleting Neuronal PrP in Prion Infection Prevents Disease and Reverses Spongiosis. Science 302:

871-874.

Mallucci G., Ratte S., Asante EA., Linehan J., Gowland I., Jefferys JG., Collinge J. (2002). Post-natal knockout of prion protein alters hippocampal CA1 properties but does not result in neurodegeneration. EMBO J 21: 202–210.

McCormack TA., Cruikshank AA., Grenier L., Melandri S., Nunes L., Plamondon R., Stein L., Dick LR. (1998). Kinetic studies of the branched chain amino acid preferring peptidase activity of the 20S proteasome: development of a continuous assay and inhibition by tripeptide aldehydes and clasto-lactacystin beta-lactone. Biochemistry 37:7792-800.

McGrath J., Jentsch S., Varshavsky A. (1991). UBA 1: an essential yeast gene encoding ubiquitin-activating enzyme. Embo J. 10:227-36.

Manson JC., Clarke A., Hooper ML., Aitchison L., McConnell I., and Hope J. (1994). 129/Ola mice carrying a null mutation in PrP that abolishes mRNA production are developmentally normal. Mol. Neurobiol. *8*: 121-127.

Masson P., Anderson U., Petersen M. and Young P. (2001). Characterization of a drosophila nuclear proteasome regulator. A homolog of human 11 S REGgamma(PA28gamma). J. Biol. Chem. 276:1383-1390.

Maragakis NJ amd Rothstein JD. (2006) Mechanisms of Disease: astrocytes in neurodegenerative disease. Nat Clin Pract Neurol 2:679–689.

Marsh RF. (1992). Transmissible Mink Encephalopathy. In Prion Diseases of Humans and Animals, S.B.Prusiner, Collinge J, J.Powell, and B.Anderton, eds. (London: Ellis Horwood).

Marsh RF., Bessen RA., Lehmann S., and Hartsough GR. (1991). Epidemiological and experimental studies on a new incident of transmissible mink encephalopathy. J Gen. Virol. 72: 589-594.

Martins SM., Frosoni DJ., Martinez AM., De Felice FG., Ferreira ST. (2006). Formation of soluble oligomers and amyloid fibrils with physical properties of the scrapie isoform of the prion protein from the C-terminal domain of recombinant murine prion protein mPrP-(121-231). J Biol Chem. 281: 26121–26128.

Masters CL., Gajdusek DC., and Gibbs CJ.Jr. (1981). Creutzfeldt-Jakob disease virus isolations from the Gerstmann- Straussler syndrome with an analysis of the various forms of amyloid plaque deposition in the virus-induced spongiform encephalopathies. Brain. 104: 559-588.

Masters CL., Gajdusek DC., and Gibbs CJJr. (1981). The familial occurrence of Creutzfeldt-Jakob disease and Alzheimer's disease. Brain. 104: 535-558.

Mathiason CK., Powers JG., Dahmes SJ., Osborn DA., Miller KV., Warren RJ., Mason GL., Hays SA., Hayes-Klug J., Seelig DM., Wild MA., Wolfe LL., Spraker TR., Miller MW., Sigurdson CJ., Telling GC., and Hoove EA. (2006). Infectious prions in the saliva and blood of deer with chronic wasting disease. Science. 314: 133-136.

Mead S., Poulter M., Uphill J., Beck J., Whitfield J., Webb TE., Campbell T., Adamson G., Deriziotis P., Tabrizi SJ., Hummerich H., Verzilli C., Alpers MP., Whittaker JC and Collinge J. (2009). Genetic risk factors for variant Creutzfeldt-Jakob disease: a genome-wide association study. Lancet Neurol. *8*: 57-66.

Mead S. (2006). Prion disease genetics. European Journal of Human Genetics. 14*:*273-281.

Mead S., Poulter M., Beck J., Webb T., Campbell T., Linehan J., Desbruslais M, Joiner S, Wadsworth J, King A, Lantos P, and Collinge J. (2006). Inherited prion disease with six octapeptide repeat insertional mutation--molecular analysis of phenotypic heterogeneity. Brain. 129: 2297-2317.

Mead S., Stumpf MP., Whitfield J., Beck J., Poulter M., Campbell T., Uphill J., Goldstein D.,

Alpers M., Fisher E., and Collinge J. (2003). Balancing selection at the prion protein gene consistent with prehistoric kuru-like epidemics. Science *300*, 640-643.

Mead S., Mahal SP., Beck J., Campbell T., Farrall M., Fisher E., and Collinge J. (2001). Sporadic - but not variant - Creutzfeldt-Jakob disease is associated with polymorphisms upstream of *PRNP* Exon 1. Am. J. Hum. Genet. 69, 1225-1235.

Medori R., Montagna P., Tritschler HJ., LeBlanc A., Cortelli P., Tinuper P., Lugaresi E., Gambetti P. (1992). Fatal familial insomnia: a second kindred with mutation of prion protein gene at codon 178. Neurology. 42:669–670.

Mehmet H. (2000). Caspases find a new place to hide. Nature 403: 29-30.

Mendez E., Harris DA., Ironside J., Tagliavini F., Carp RI,. Frangione B. (2000). Reversion of prion protein conformational changes by synthetic beta-sheet breaker peptides. Lancet 355: 192-197.

Menendez-Benito V., Verhoef LG., Masucci MG., Dantuma NP. (2005). Endoplasmic reticulum stress compromises the ubiquitin-proteasome system. Hum Mol Genet. 14:2787-99.

Meng L., Mohan R., Kwok BH., Elofsson M., Sin N., Crews CM.. (1999). Epoxomicin, a potent and selective proteasome inhibitor, exhibits in vivo anti-inflammatory activity. Proc Natl Acad Sci USA. 96:10403-8.

Meng L., Kwok BH., Sin N., and Crews CM. (1999). Eponemycin exerts its antitumor effect through the inhibition of proteasome function. Cancer Res 59:2798-801.

Meusser B., Hirsch C., Jarosch E., and Sommer T. (2005). ERAD: the long road to destruction. Nat. Cell Biol. *7*:766-772.

Merz PA., Somerville RA., Wisniewski HM., and Iqbal K. (1981). Abnormal fibrils from

scrapie-infected brain. Acta Neuropathol (Berl) *54*:63-74.

Michalak M., Robert Parker JM., Opas M. (2002). Ca^{2+} signaling and calcium binding chaperones of the endoplasmic reticulum. Cell Calcium 32: 269-278.

Middeldorp J., Kamphuis W., Sluijs JA., Achoui D., Leenaars HC., Feenstra GP., van Tijn P., Fischer DF., Celia Berkers C., Ovaa H., Quinlan RA., and Hol EM. (2009). Intermediate filament transcription in astrocytes is repressed by proteasome inhibition. FASEB. 23: 2710-2716.

Milhavet O and Lehmann S. (2002). Oxidative stress and the prion protein in transmissible spongiform encephalopathies. Brain Res Rev. 38:328–339.

Milhavet O., McMahon HE., Rachidi W., Nishida N., Katamine S., Mangé A., Arlotto M., Casanova D., Riondel J., Favier A., and Lehmann S. (2000). Prion infection impairs the cellular response to oxidative stress. Proc. Natl. Acad. Sci. USA. 97: 13937-13942.

Miller MW and Williams ES. (2003). Prion disease: horizontal prion transmission in mule deer. Nature. 425: 35-36.

Mironov A., Latawiec D., Wille H., Bouzamondo-Bernstein E., Legname G., Williamson RA., Burton D., DeArmond SJ., Prusiner SB., and Peters PJ. (2003). Cytosolic prion protein in neurons. J Neurosci. 23: 7183-7193.

Moore RA., Vorberg I., and Priola SA. (2005). Species barriers in prion diseases--brief review. Arch Virol Suppl. 187-202.

Moore RC, Lee IY, Silverman GL, Harrison PM, Strome R, Heinrich C, Karunaratne A, Pasternak SH, Chishti MA, Liang Y, Mastrangelo P, Wang K, Smit AFA, Katamine S, Carlson GA, Cohen FE, Prusiner SB, Melton DW, Tremblay P, Hood LE, Westaway D. (1999). Ataxia in prion protein (PrP) deficient mice is associated with upregulation of the novel PrP-like

protein doppel. J Mol Biol. 292:797–817.

Morales R., Abid K., and Soto C. (2006). The prion strain phenomenon: Molecular basis and unprecedented features. Biochim. Biophys. Acta. 1772: 681-691.

Muller S., Hoege C., Pyrowolakis G., and Jentsch S. (2001). SUMO, ubiquitin's mysterious cousin. Nat. Rev. Mol. Cell. Biol. 2:202-210.

Murata S., Kawahara H., Tohma S., Yamamoto K., Kasahara M., Nabeshima Y., Tanaka K., and Chiba T. (1999). Growth retardation in mice lacking the proteasome activator PA28gamma. J Biol Chem. 274:38211-5.

Muramoto T., DeArmond S., Scott M., Telling GC., Cohen FE., and Prusiner SB. (1997). Heritable disorder reseming neuronal storage disease in mice expressing prion protein with deletion of an alpha-helix. Nature Med. *3*: 750-755.

Muramoto T., Kitamoto T., Koga H., Tateishi J. (1992). The coexistence of Alzheimer's disease and Creutzfeldt-Jakob disease in a patient with dementia of long duration. Acta Neuropathol. 84:686-9.

Myung J., K. B. Kim KB.,. Crews CM. (2001). The ubiquitin-proteasome pathway and proteasome inhibitors. Med Res Rev. 21:245-73.

Nagele RG., Wegiel J., Venkataraman V., Imaki H., Wang KC. (2004) Contribution of glial cells to the development of amyloid plaques in Alzheimer's disease. Neurobiol Aging 25:663–674 179.

Nagai M., Re DB., Nagata T., Chalazonitis A., Jessell TM., Wichterle H., Przedborski S. (2007) Astrocytes expressing ALS- linked mutated SOD1 release factors selectively toxic to motor neurons. Nat Neurosci 10:615–622.

Naslavsky N., Shmeeda,H., Friedlander G., Yanai A., Futerman AH., Barenholz Y., and

Taraboulos A. (1999). Sphingolipid depletion increases formation of the scrapie prion protein in neuroblastoma cells infected with prions. J. Biol. Chem. 274: 20763-20771.

Naslavsky N., Stein R., Yanai A., Friedlander G., and Taraboulos A. (1997). Characterization of detergent-insoluble complexes containing the cellular prion protein and its scrapie isoform. J. Biol. Chem. 272:6324-6331.

Nazor KE., Seward T., and Telling GC. (2007) Motor behavioral and neuropathological deficits in mice deficient for normal prion protein expression Biochim Biophys Acta. 1772: 645–653.

Nazor KE., Kuhn F., Seward T., Green M., Zwald D., Purro M., Schmid J., Biffiger K., Power AM., Oesch B., Raeber AJ., Telling GC. (2005). Immunodetection of disease-associated mutant PrP, which accelerates disease in GSS transgenic mice. Embo J. 24:2472–2480.

Nicoll AJ., Trevitt CR., Tattum MH., Risse E., Quarterman E., Ibarra AA., Wright C., Jackson GS., Sessions RB., Farrow M., Waltho JP., Clarke AR., Collinge J. (2010). Pharmacological chaperone for the structured domain of human prion protein. Proc Natl Acad Sci U S A. 107:17610-5.

Nicoll AJ and Collinge J. (2009). Preventing prion pathogenecity by targeting the cellular prion protein. Infect. Disord. Drug. Targets. 9:48-57.

Oesch B., Westaway D., Walchli M., McKinley MP., Kent SB., Aebersold R., Barry RA., Tempst P., Teplow DB., Hood LE., Prusiner SB., and Weissmann C. (1985). A Cellular Gene Encodes Scrapie Prp 27-30 Protein. Cell. 40: 735-746.

Okabe M., Ikawa M., Kominami K., Nakanishi T., Nishimune Y. (1997). 'Green mice' as a source of ubiquitous green cells. FEBS Lett 407:313-9.

Orlowski M and Wilk S. (2003). Ubiquitin-independent proteolytic functions of the

proteasome. Arch. Biochem. Biophys. 415: 1-5.

Orlowski M., Cardozo C., and Michaud C. (1993). Evidence for the presence of five distinct proteolytic component in the pituitary multicatalytic proteinase complex. Properties of two components cleaving on the carboxyl side of branched chain and small neutral amino acids. Biochem. 32: 1563-1572.

Ortega Z., Dıaz-Hernandez M., Maynard CJ., Hernandez F., Dantuna NP., Lucas JJ. (2010) Acute polyglutamine expression in inducible mouse model unravels ubiquitin/proteasome system impairment and permanent recovery attributable to aggregate formation. J Neurosci 30: 3675–3688.

Owen F., Poulter M., Lofthouse R., Collinge J., Crow TJ., Risby D., Baker HF., Ridley RM., Hsiao K., and Prusiner SB. (1989). Insertion in prion protein gene in familial Creutzfeldt-Jakob disease. Lancet. 1:51-52.

Palmer MS., Dryden AJ., Hughes JT., and Collinge J. (1991). Homozygous prion protein genotype predisposes to sporadic Creutzfeldt-Jakob disease. Nature. 352: 340-342.

Pan KM., Baldwin MA., Nguyen J., Gasset M., Serban A., Groth D., Mehlhorn I., Huang Z., Fletterick RJ., Cohen FE., and Prusiner SB. (1993). Conversion of a-helices into b-sheets features in the formation of the scrapie prion proteins. Proc Natl Acad Sci USA. *90*: 10962-10966.

Parchi P., Giese A., Capellari S., Brown P., Schulz-Schaeffer W., Windl O., Zerr I., Budka H., Kopp N., Piccardo P., Poser S., Rojiani A., Streichenberger N., Julien J., Vital C., Ghetti B., Gambetti P., and Kretzschmar H. (1999). Classification of sporadic Creutzfeldt-Jakob Disease based on molecular and phenotypic analysis of 300 subjects. Annals of Neurol. 46: 224-233.

Parchi P., Castellani R., Capellari S., Ghetti B., Young K., Chen SG., Farlow M., Dickson DW., Sims AF., Trojanowski JQ., Petersen RB., and Gambetti P. (1996). Molecular Basis of

Phenotypic Variability in Sporadic Creutzfeldt-Jakob Disease. Annals of Neurol. *39*: 669-680.

Parry HB. (1979). Elimination of natural scrapie in sheep by sire genotype selection. Nature 277: 127-129.

Pattison IH. (1965). NINDB Monograph No. 2, Slow, Latent and Temperate Virus Infections (eds Gajdusek, D. C., Gibbs, C. J. & Alpers, M.) 249–257.

Peden AH., Head MW., Ritchie DL., Bell JE., and Ironside JW. (2004). Preclinical vCJD after blood transfusion in a PRNP codon 129 heterozygous patient. Lancet. 364: 527-529.

Peden AH., Ritchie DL., Head MW., and Ironside JW. (2006). Detection and Localization of PrPSc in the Skeletal Muscle of Patients with Variant, Iatrogenic, and Sporadic Forms of Creutzfeldt-Jakob Disease. Am J Pathol. 168:927-935.

Peden AH., Ritchie DL., and Ironside JW. (2005). Risks of transmission of variant Creutzfeldt-Jakob disease by blood transfusion. Folia Neuropathol. *43*:271-278.

Pedersen MØ., Mikkelsen K., Behrens MA., Pedersen JS., Enghild JJ., Skrydstrup T., Malmendal A., Nielsen NC. (2010). NMR reveals two-step association of Congo Red to amyloid β in low-molecular-weight aggregates. J Phys Chem B. 114:16003-10.

Peretz D., Scott MR., Groth D., Williamson RA., Burton DR., Cohen FE., and Prusiner SB. (2001). Strain-specified relative conformational stability of the scrapie prion protein. Prot. Sci. 10:854-863.

Peretz D., Williamson RA., Kaneko K., Vergara J., Leclerc E., Schmitt-Ulms G., Mehlhorn IR., Legname G., Wormald MR., Rudd PM., Dwek RA., Burton DR., and Prusiner SB. (2001). Antibodies inhibit prion propagation and clear cell cultures of prion infectivity. Nature. 412: 739-743.

Petrucelli L., O'Farrell C., Lockhart PJ., Baptista M., Kehoe K., Vink L., Choi P., Wolozin B., Farrer M., Hardy, J. et al. (2002) Parkin protects against the toxicity associated with mutant a-synuclein: proteasome dysfunction selectively affects catecholaminergic neurons. Neuron. 36:1007 – 1019.

Pickart CM and Fushman D. (2004). Polyubiquitin chains: polymeric protein signals. Curr Opin Chem Biol. 8:610-6.

Pickart CM and Eddins MJ. (2004). Ubiquitin: structures, functions, mechanisms. Biochim Biophys Acta. 1695:55-72.

Pickart CM and Cohen RE. (2004). Proteasomes and their kin: proteases in the machine age. Nat Rev. Mol Cell Biol. *5*: 177-187.

Pickart CM. (2001). Mechanisns underlying ubiquitination. Annu. Rev Biochem. 70:503-533.

Pickart CM. (2000). Ubiquitin chains. Trends Biochem. Sci. 25:544-548.

Pfeifer A., Eigenbrod S, Al-Khadra S, Hofmann A, Mitteregger G, Moser M, Bertsch U, Kretzschmar H. (2006) Lentivector-mediated RNAi efficiently suppresses prion protein and prolongs survival of scrapie-infected mice. J Clin Invest 116:3204 –3210.

Poser S., Mollenhauer B., Krauss A, et al. (1999). How to improve the clinical diagnosis of Creutzfeldt- Jakob disease. Brain. 122:2345-51

Przedborski S., Jackson-Lewis V., Djaldetti R., Liberatore G., Vila M, Vukosavic S, Almer G (2000) The parkinsonian toxin MPTP: action and mechanism. Restor Neurol Neurosci. 16:135– 142.

Prusiner SB. (1998). Prions. Proc Natl Acad Sci U. S. A. 95: 13363-13383.

Prusiner SB., Torchia M., Westaway D. (1991). Molecular biology and genetics of prions--implications for sheep scrapie, "mad cows" and the BSE epidemic. Historical background. Cornell.Vet. 81: 85-101.

Prusiner SB., Scott M., Foster D., Pan KM., Groth D., Mirenda C., Torchia M., Yang SL., Serban D., Carlson GA., Hoppe PC., Westaway D., & DeArmond SJ. (1990) Transgenetic studies implicate interactions between homologous PrP isoforms in scrapie prion replication. Cell. 63: 673– 686.

Prusiner SB., McKinley MP., BowmanK., Bolton DC., Bendheim,P.E., Groth,D.F., and Glenner,G.G. (1983). Scrapie prions aggregate to form amyloid-like birefringent rods. Cell *35*: 349-358.

Prusiner SB. (1982). Novel proteinaceous infectious particles cause scrapie. Science. 216: 136-144.

Prusiner SB., Bolton DC., Groth DF., Bowman K., Cochran SP., and Mc Kinley MP. (1982). Further purification and characterization of scrapie prions. Biochem. 21: 6942-6950.

Prusiner SB., Cochran SP., Groth DF., Downey DE., Bowman K., and Martinez,H.M. (1982). Measurement of the scrapie agent using an incubation time interval assay. Ann Neurol. 11: 353-38.

Prusiner SB., Groth, DF., Bolton, DC., Kent, SB., & Hood, LE. (1984) Purification and structural properties of a major scrapie prion protein. Cell. 38: 127–134.

Prusiner SB., McKinley MP., Bowman K., Bolton DC., Bendheim PE., Groth DF., and Glenner GG. (1983). Scrapie prions aggregate to form amyloid-like birefringent rods. Cell. 35: 349-358.

Prusiner SB., McKinley MP., Groth DF., Bowman K., Mock NI., Cochran SP., and Masiarz FR.

(1981). Scrapie agent contains a hydrophobic protein. Proc. Natl. Acad. Sci. USA. 78 *:* 6675-6679.

Prusiner SB., Groth DF., Cochran SP., Masiarz FR., McKinley MP., and Martinez HM. (1980). Molecular properties, partial purification, and assay by incubation period measurements of the hamster scrapie agent. Biochem. 19: 4883-4891.

Prusiner SB., Groth DF., Cochran SP., McKinley MP., and Masiarz FR. (1980). Gel electrophoresis and glass permeation chromatography of the hamster scrapie agent after enzymatic digestion and detergent extraction. Biochem. 19: 4892-4898.

Prusiner SB., Garfin DE., Cochran SP., McKinley MP., Groth,D.F., Hadlow,W.J., Race,R.E., and Eklund,C.M. (1980). Experimental scrapie in the mouse: electrophoretic and sedimentation properties of the partially purified agent. J Neurochem. 35: 574-582.

Prusiner SB., Hadlow WJ., Eklund CM., Race RE., and Cochran SP. (1978). Sedimentation characteristics of the scrapie agent from murine spleen and brain. Biochem. 17: 4987-4992.

Quaglio E., Restelli E., Garofoli A., Dossena S., De Luigi A., Tagliavacca L., Imperiale D, Migheli A, Salmona M, Sitia R, Forloni G, Chiesa R. (2011). Expression of mutant or cytosolic PrP in transgenic mice and cells is not associated with endoplasmic reticulum stress or proteasome dysfunction. PLoS One 6: e19339.

Race R., Meade-White K., Raines A., Raymond GJ., Caughey B., and Chesebro B. (2002). Subclinical Scrapie Infection in a Resistant Species: Persistence, Replication, and Adaptation of Infectivity during Four Passages. J. Infect. Dis. 186 Suppl *2*, S166-S170.

Race R., Raines A., Raymond GJ., CaugheyB., and Chesebro B. (2001). Long-term subclinical carrier state precedes scrapie replication and adaptation in a resistant species: Analogies to bovine spongiform encephalopathy and variant Creutzfeldt-Jakob disease in humans. Journal of Virol. *75*:10106-10112.

Race RE., Priola SA., Besse, RA., Ernst D., Dockter J., Ral, GF., Mucke L., Chesebro B. & Oldstone, MB.(1995) Neuron-specific expression of a hamster prion protein minigene in transgenic mice induces susceptibility to hamster scrapie agent. Neuron. 15: 1183–1191.

Raiborg C and Stenmark H. (2009). "The ESCRT machinery in endosomal sorting of ubiquitylated membrane proteins." Nature. 458: 445-452.

Rambold AS., Miesbauer M., Rapaport D., Bartke T., Baier M., Winklhofer KF., and Tatzelt J. (2006). Association of Bcl-2 with misfolded prion protein is linked to the toxic potential of cytosolic PrP. Molecular Biology of the Cell. 17: 3356-3368.

Rane NS., Kang SW., Chakrabarti O., Feigenbaum L., and Hegde RS. (2008). Reduced translocation of nascent prion protein during ER stress contributes to neurodegeneration. Dev. Cell 15: 359-370.

Rao RV., Peel A., Logvinova A., del Rio G., Hermel E., Yokota T., Goldsmith PC., Ellerby LM., Ellerby HM., Bredesen DE. (2002) Coupling endoplasmic reticulum stress to the cell death program: role of the ER chaperone GRP78. FEBS Lett. 514: 122-128.

Rayavarapu S., Van der meulen JH., Gordish-Dressman H., Hoffman EP., Nagaraju K., Knoblach SM. (2010). Characterization of Dysferlin Deficient SJL/J Mice to Assess Preclinical Drug Efficacy: Fasudil Exacerbates Muscle Disease Phenotype. PLoS ONE. 5(9):e12981.

Raymond GJ., Hope J., Kocisko DA., Priola SA., Raymond LD., Bossers A., Ironside J., Will RG., Chen SG., Petersen RB., Gambetti P., Rubenstein R., Smits MA., Lansbury PT., and Caughey B. (1997). Molecular assessment of the potential transmissibilities of BSE and scrapie to humans. Nature. 388: 285-288.

Reddy RK., Lu J., Lee AS. (1999). The endoplasmic reticulum chaperone glycoprotein GRP94 with Ca^{2+}-binding and antiapoptotic properties is a novel proteolytic target of calpain during etoposide-induced apoptosis. J Biol Chem. 274: 28476-28483.

Richardson., PG. Barlogie., J. Berenson, S. Singhal, S. Jagannath, D. Irwin, S. V. Rajkumar, G. Srkalovic, M. Alsina, R. Alexanian, D. Siegel, R. Z. Orlowski, D. Kuter, S. A. Limentani, S. Lee, T. Hideshima, D. L. Esseltine, M. Kauffman, J. Adams, D. P. Schenkein, and K. C. Anderson. (2003). A phase 2 study of bortezomib in relapsed, refractory myeloma. N Engl J Med 348:2609-17.

Riek R., Wide ,G., Billeter M., Hornemann S., Glockshuber R., and Wuthrich K. (1998). Prion protein NMR structure and familial human spongiform encephalopathies. Proc Natl Acad Sci U. S. A. *95*, 11667-11672.

Riek R., Hornemann S., Wider G., Glockshuber R., Wüthrich K. (1997). NMR characterization of the full-length recombinant murine prion protein, mPrP(23-231). FEBS Lett. 413: 282-288.

Riek R., Hornemann S., Wider G., Billeter M., Glockshuber R., and Wuthrich K. (1996). NMR structure of the mouse prion protein domain PrP (121-231). Nature. 382:180-182.

Reinstein, E. and Ciechanover, A. (2006). Narrative review: protein degradation and human diseases: the ubiquitin connection. Ann Intern Med. 145:676-684.

Reits EA., Benham M., Plougastel B., Neefjes J., Trowsdale J. (1997). Dynamics of proteasome distribution in living cells. Embo J. 16:6087-94.

Riesner D. (2003). Biochemistry and structure of PrP(C) and PrP(Sc). Br. Med. Bull. *66*: 21-33.

Rock KL and Golberg AL. (1999). Degradation of cell proteins and the generation of MHC class I-presented peptides. Annu. Rev. Immunl. 17:739-779.

Ross CA and Poirier MA. (2004). Protein aggregation and neurodegenerative disease. Nat Med 10 Suppl 1, S10-S17.

Rothstein JD., Patel S., Regan MR., Haenggeli C., Huang YH., Bergles DE., Jin L., Dykes Hoberg M., Vidensky S., Chung DS., Toan SV., Bruijn LI., Su ZZ., Gupta P., Fisher PB. (2005). Beta- lactam antibiotics offer neuroprotection by increasing glutamate transporter expression. Nature. 433:73–77.

Roucou X., Giannopoulos PN., Zhang Y., Jodoin J., Goodyer CG., LeBlanc A. (2005). Cellular prion protein inhibits proapoptotic Bax conformational change in human neurons and in breast carcinoma MCF-7 cells. Cell Death Differ. 12:783–795.

Roucou X., Gains M., LeBlanc AC. (2004). Neuroprotective functions of prion protein. *J* Neurosci Res. 75:153–161.

Roucou X., Gu Q., Zhang Y., Goodyer CG., and LeBlanc AC. (2003). Cytosolic prion protein is not toxic and protects against Bax-mediated cell death in human primary neurons. J Biol. Chem. 278:40877-81.

Rubinsztein DC. (2006). The roles of intracellular protein-degradation pathways in neurodegeneration. Nature. 443: 780-786.

Russell SJ., Reed SH., Huang W., Friedberg, EC., Johnston SA. (1999.) The 19S regulatory complex of the proteasome functions independently of proteolysis in nucleotide excision repair. Mol Cell. 3:687-95.

Sabbatini M., Baldoni E., Cadoni A., Vitaioli L., Zicca A., Amenta F. (1999). Forebrain white matter in spontaneously hypertensive rats: a quantitative image analysis study. Neurosci Lett. 265:5-8.

Safar J., Wang W., Padgett MP., Ceroni M., Piccardo P., Zopf D., Gajdusek DC., and Gibbs CJJr. (1990). Molecular mass, biochemical composition, and physicochemical behavior of the infectious form of the scrapie precursor protein monomer. Proc. Natl. Acad. Sci. USA. 87: 6373-6377.

Sailer A., Büeler H., Fischer M., Aguzzi A., Weissmann C. (1994). No propagation of prions in mice devoid of PrP. Cell. 77:967-8.

Salomons FA., Verhoef LG., Dantuma NP. (2005). Fluorescent reporters for the ubiquitin-proteasome system. Essays Biochem 41:113-28.

Schatzl HM., Laszlo L., Holtzman DM., Tatzelt J., DeArmond SJ., Weiner RI., Mobley WC., and Prusiner SB. (1997). A hypothalamic neuronal cell line persistently infected with scrapie prions exhibits apoptosis. J. Virol. 71: 8821-8831.

Scott JR and Fraser H. (1984) Degenerative hippocampal pathology in mice infected with scrapie. Acta Neuropathol. *(Berl)*, 65:62–68.

Sandberg MK., Al-Doujaily H., Sharps B., Clarke AR., Collinge J (2011). Prion propagation and toxicity in vivo occur in two distinct mechanistic phases. Nature. 470: 540–2.

Schmid HP., Akhayat O., Martin De Sa, C., Puvion, F., Koehler, K., Scherrer, K. (1984). The proteasome: an ubiquitous morphologically distinct RNP particle associated with repressed mRNPs and containing specific ScRNA and a characteristic set of proteins. EMBO J. 3:29-34.

Schreuder BE., van Keulen LJ., Vromans ME., Langeveld JP., Smits MA. (1996). Preclinical test for prion diseases. Nature. 381:563.

Schwarz K., de Giuli R., Schmidtke G., Kostka S., van den Broek M., Kim KB., Crews CM ., Kraft R., Groettrupn M. (2000). The selective proteasome inhibitors lactacystin and epoxomicin can be used to either up- or down-regulate antigen presentation at nontoxic doses. J Immunol. 164**:**6147-57.

Scott MR., Groth D., Tatzelt J., Torchia M., Tremblay P., DeArmond SJ., and Prusiner SB. (1997). Propagation of prion strains through specific conformers of the prion protein. J. Virol. 71:9032-9044.

Seidel R., Engelhard M. (2011). Chemical biology of prion protein: tools to bridge the in vitro/vivo interface. Top Curr Chem. 305:199-223.

Serio TR and Lindquist SL. (2000). Protein-only inheritance in yeast: something to get [PSI+]-ched about. Trends Cell Biol. 10: 98-105.

Serwold T., Gonzale F., Kim J., Jacob R., Shastri N. (2002). ERAAP customizes peptides for MHC class I molecules in the endoplasmic reticulum. Nature. 419:480-483.

Shmerling D., Hegyi I., Fischer M., Blättler T., Brandner S., Götz J., Rülicke T., Flechsig E., Cozzio A., von Mering C., Hangartner C., Aguzzi A., and Weissmann C. (1998). Expression of amino-terminally truncated PrP in the mouse leading to ataxia and specific cerebellar lesions. Cell. *93*: 203-214.

Shyng SL., Huber MT., and Harris DA. (1993). A prion protein cycles between the cell surface and an endocytic compartment in cultured neuroblastoma cells. J. Biol. Chem. 268: 15922-15928.

Shyng SL., Heuser JE., and Harris DA. (1994). A glycolipid-anchored prion protein is endocytosed via clathrin- coated pits. J. Cell Biol. 125: 1239-1250.

Sigurdson CJ. and Aguzzi A. (2006). Chronic wasting disease. Biochim. Biophys. Acta 1772: 610-618.

Sigurdsson., EM., Brown DR., Daniels M., Kascsak, R.J., Kascsak R., Carp R., Meeker HC., Frangione B., Wisniewski T. (2002). Immunization delays the onset of prion disease in mice. Am.J.Pathol. 161: 13-17.

Silveira JR., Raymond GJ., Hughson AG., Race RE., Sim VL., Hayes SF., and Caughey B. (2005). The most infectious prion protein particles. Nature. 437:257-261.

Simoneau S., Rezaei H., Salès N., Kaiser-Schulz G., Lefebvre-Roque M., Vidal C., Fournier JG.,

Comte J., Wopfner F., Grosclaude J., Schätzl H., Lasmézas CI. (2007). In vitro and in vivo neurotoxicity of prion protein oligomers. PLoS Patho. 3(8):e125.

Sitia R., Braakman I. (2003). Quality control in the endoplasmic reticulum protein factory. Nature. 426: 891-894.

Smith PG., and Bradley R. (2003). Bovine spongiform encephalopathy (BSE) and its epidemiology. Br. Med. Bull. *66*: 185-198.

Spence J., Sadis AS., Haas L., Finley D. (1995). A ubiquitin mutant with specific defects in DNA repair and multiubiquitination. Mol Cell Biol. 15:1265-73.

Stahl N., Borchelt DR., and Prusiner SB. (1990). Differential release of cellular and scrapie prion proteins from cellular membranes by phosphatidylinositol-specific phospholipase. Biochem. 29: 5405-5412.

Stahl N., Borchelt DR., Hsiao K., and Prusiner SB. (1987). Scrapie prion protein contains a phosphatidylinositol glycolipid. Cell. 51: 229-240.

Steinhoff BJ., Zerr I., Glatting M., et al. (2004). Diagnostic value of periodic complexes in Creutzfeldt-Jakob disease. Ann Neurol. 56:702-8.

Stewart RS., Piccardo,P., Ghetti,B., and Harris,D.A. (2005). Neurodegenerative illness in transgenic mice expressing a transmembrane form of the prion protein. J. Neurosci. 25: 3469-3477.

Sofroniew MV., Vinters, HV. (2010). Astrocytes: biology and pathology. Acta Neuropathol. 119:7–35.

Sofroniew MV. (2009). Molecular dissection of reactive astrogliosis and glial scar formation. Trends Neurosci. 32:638–647.

Song S., Kim Y., Hong M., Jo D., Lee Y., Shim M., Chung W., Seo S.,Yoo J., Koh MC. Lee., Yates AJ., Ichijo H.,. Jung YK. (2003). Essential role of E2-25K/Hip-2 in mediating amyloid-beta neurotoxicity. Mol Cell. 12:553-63.

Soto C and Castilla J. (2004). The controversial protein-only hypothesis of prion propagation. Nat. Med. 10: S63–S67.

Soto C. (2003) Unfolding the role of protein misfolding in neurodegenerative diseases. Nat Rev Neurosci 4: 49-60.

Spencer MD., Knight RS., and Will RG. (2002). First hundred cases of variant Creutzfeldt-Jakob disease: retrospective case note review of early psychiatric and neurological features 51. BMJ. 324:1479-1482.

Spurney CF., Gordish-Dressman H., Guerron AD, Sali A., Pandey GS, et al. (2009). Preclinical drug trials in the mdx mouse: assessment of reliable and sensitive outcome measures. Muscle Nerve 39: 591–602.

Sunyach C., Jen A., Deng J., Fitzgerald KT., Frobert Y., Grassi J., McCaffrey MW., and Morris R. (2003). The mechanism of internalization of glycosylphosphatidylinositol- anchored prion protein. EMBO J. *22*:3591-3601.

Supattapone S. (2004). Prion protein conversion in vitro. J. Mol. Med. *8:* 348-356.

Swietnicki W., Petersen RB., Gambetti P., and Surewicz WK. (1998). Familial mutations and the thermodynamic stability of the recombinant human prion protein. Journal of Biological Chemistry. 273: 31048-31052.

Tanahashi N., Murakami Y., Nimani Y., Shimbara N., Hendil KB., Tanaka K. (2000). "Hybrid proteasomes. Induction by interferon-gamma and contribution to ATP-dependent proteolysis." J Biol Chem 275: 14336-14345.

Tang G., Xu Z., Goldman JE. (2006) Synergistic effects of the SAPK/JNK and the proteasome pathway on glial fibrillary acidic protein (GFAP) accumulation in Alexander disease. J. Biol. Chem. 281:38634-38643.

Tattum MH., Cohen-Krausz S., Thumanu K., Wharton CW., Khalili-Shirazi A., Jackson GS, Orlova EV., Collinge J., Clarke A, and Saibil,H.R. (2006). Elongated oligomers assemble into mammalian PrP amyloid fibrils. Journal of Molecular Biology 357:975-985.

Tatzelt J and Schatzl HM. (2007). Molecular basis of cerebral neurodegeneration in prion diseases. FEBS J. 274:606-11.

Taylor DR., Hooper NM. (2006). The prion protein and lipid rafts. Mol Membr Biol. 23:89–99.

Taylor DR., Watt NT., Perera WS., and Hooper NM. (2005). Assigning functions to distinct regions of the N-terminus of the prion protein that are involved in its copper- stimulated, clathrin-dependent endocytosis. J. Cell Sci. *118*, 5141-5153.

Taylor JP., Hardy J., and Fischbeck KH. (2002). Toxic proteins in neurodegenerative disease. Science. *296*: 1991-1995.

Taylor DR and Hooper NM. (2007). The low-density lipoprotein receptor-related protein 1 (LRP1) mediates the endocytosis of the cellular prion protein. Biochem. J. *402*: 17-23.

Telling GC., Trembla P., Torchia M., DeArmond SJ., Cohen FE., and Prusiner SB. (1997). N-terminally tagged prion protein supports prion propagation in transgenic mice. Protein Science. 6:825-833.

Thal DR., Schultz C., Dehghani F., Yamaguchi H., Braak H., Braak E. (2000). Amyloid beta-protein (Abeta)-containing astrocytes are located preferentially near N-terminal-truncated Abeta deposits in the human entorhinal cortex. Acta Neuropathol 100:608–617properties. J

Neurochem 101:555–565.

Thellung S., Florio T., Corsaro A., Arena S., Merlino M., Salmona M., Tagliavini F., Bugiani O., Forloni G., and Schettini G. (2000). Intracellular mechanisms mediating the neuronal death and astrogliosis induced by the prion protein fragment 106-126. Int. J. Dev. Neurosci. *18*:481-492.

Thrower JS., Hoffman L.,Rechsteiner M., Pickart CM. (2000). Recognition of the polyubiquitin proteolytic signal. Embo J. 19:94-102.

Trevitt C and Collinge J. (2006). A systematic review of prion therapeutics in experimental models. Brain. 129: 2241-2265.

Tschampa HJ., Kallenberg K., Kretzschmar HA, et al. (2007). Pattern of Cortical Changes in Sporadic Creutzfeldt-Jakob Disease. AJNR Am J Neuroradiol;28:1114-18.

Tsien RY. (1998). The green fluorescent protein. Annu Rev Biochem. 67:509-44.

Tseng BP., Green KN., Chan JL., Blurton-Jones M., LaFerla FM (2008) Abeta inhibits the proteasome and enhances amyloid and tau accumulation. Neurobiol Aging 29: 1607–1618.

Tsui-Pierchala BA., Encinas M., Milbrandt J., Johnson EM. (2002). Lipid rafts in neuronal signaling and function. Trends Neurosci.25:412–417.

Turk E., Teplow DB., Hood LE., and Prusiner SB. (1988). Purification and properties of the cellular and scrapie hamster prion proteins. Eur. J Biochem. 176: 21-30.

Tydlacka S., Wang CE., Wang X., Li S., Li XJ. (2008). Differential activities of the ubiquitin-proteasome system in neurons versus glia may account for the preferential accumulation of misfolded proteins in neurons. J Neurosci. 28:13285-95.

Vanderlugt CL., Rahbe SM., Elliott PJ., Dal Canto MC., and Miller SD. (2000). Treatment of

established relapsing experimental autoimmune encephalomyelitis with the proteasome inhibitor PS-519. J Autoimmun. 14:205- 11.

Vanik DL., Surewicz KA., and Surewicz WK. (2004). Molecular basis of barriers for interspecies transmissibility of mammalian prions. Mol. Cell. 14: 139-145.

Van Keulen LJ., Schreuder BE., Meloen RH., Mooij-Harkes G., Vromans ME., Langeveld JP. (1996). Immunohistochemical detection of prion protein in lymphoid tissues of sheep with natural scrapie. J Clin Microbiol. 34:1228-31.

Van Leeuwen FW., Hol EM., Hermanussen RW., Sonnemans MA., Moraal E., Fisher DF., Evans DA., Chooi KF., Burbach JP and Murphy D. (2000). Molecular misreading in non-neuronal cells. FASEB J. 14:1595-1602.

Verdoes M., Florea BI., Menendez-Benito V., Maynard CJ., Witte, MD., Van Der Linden W. A., Van Den Nieuwendijk AM., Hofmann HC., Berkers R., Van Leeuwen F.W., Groothuis T. A., Leeuwenburgh MA., Ovaa H., Neefjes JJ., Filippov DV., Van Der Marel GA., Dantuma N. P., Overkleeft HS. (2006). A fluorescent broad-spectrum proteasome inhibitor for labeling proteasomes *in vitro* and *in vivo*. Chem & Biol. 13: 1217-1226.

Verhoef LG., Lindsten K., Masucci MG., and Dantuma NP. (2002). Aggregate formation inhibits proteasomal degradation of polyglutamine proteins. Hum Mol Genet. 11:2689-2700.

Verma R., Aravind L.,. Oania R., McDonald WH., Yates JR., Koonin EV and Deshaies RJ. (2002). Role of Rpn11 metalloprotease in deubiquitination and degradation by the 26S proteasome. Science. 298:611-5.

Vollmert C., Windl O., Xiang,W., Rosenberger A., Zerr I., Wichmann H.E., Bickeboller H., Illig T., and Kretzschmar H.A. (2006). Significant association of a M129V independent polymorphism in the 5' UTR of the PRNP gene with sporadic Creutzfeldt-Jakob disease in a

large German case-control study. J Med Genet. 43, e53.

Wadsworth JD and Collinge J. (2011). Molecular pathology of human prion disease. Acta Neuropathol. 121:69-77.

Wadsworth JD., Asante EA., Collinge J. (2010). Contribution of transgenic models to understanding human prion disease. 36:576-97.

Wadsworth JD., Joiner S., Linehan JM., Asante EA., Brandner S., Collinge, J. (2008). The origin of the prion agent of kuru: molecular and biological strain typing. Philos Trans R Soc Lond B Biol Sci. 363: 3747-3753.

Wadsworth J and Collinge J. (2007). Update on human prion disease. Biochimica et Biophysica Acta. 1772:598-609.

Wadsworth J., Joiner S., Fox K., Linehan J., Desbruslais M., Brandner S., Asante E., and Collinge J. (2007). Prion infectivity in variant Creutzfeldt-Jakob disease rectum. Gut. 56: 90-94.

Wadsworth J., Joiner S., Hill AF., Campbell TA., Desbruslais.,M., Luthert PJ., and Collinge J (2001). Tissue distribution of protease resistant prion protein in variant CJD using a highly sensitive immuno-blotting assay. Lancet. 358:171-180.

Wadsworth J., Joiner S., Linehan J., Cooper S., Powell C., Mallinson G., Buckell J., Gowland I., Asante E, Budka H., Brandner S, and Collinge J. (2006). Phenotypic heterogeneity in inherited prion disease (P102L) is associated with differential propagation of protease-resistant wild-type and mutant prion protein. Brain. 129: 1557-1569.

Walz J., Erdmann A., Kania M., Typke D., Koster AJ., Baumeister W. (1998). 26S proteasome structure revealed by three-dimensional electron microscopy. J Struct Biol. 121:19-29.

Wang J., Wang CE., Orr A., Tydlacka S., Li SH., and Li XJ. (2008). Impaired ubiquitin-

proteasome system activity in the synapses of Huntington's disease mice. J. Cell Biol. 180: 1177-1189.

Ward H.J., Everington D., Croes EA., Alperovitch A., Delasnerie-Laupretre N., Zerr,I., Poser S., and van Duijn CM. (2002). Sporadic Creutzfeldt-Jakob disease and surgery: a case-control study using community controls. Neurol. 59*:* 543-548.

Weissmann C and Aguzzi A. (1997). Bovine spongiform encephalopathy and early onset variant Creutzfeldt-Jakob disease. Curr Opin Neurobiol. *7*:695-700.

Weissmann C. (1994). Molecular biology of prion diseases. Trends Cell Biol*.* 4: 10- 14.

Wells GA., Scott, AC., Johnson CT., Gunning RF., Hancock RD., Jeffrey M., Dawson M., Bradley R. (1987). A novel progressive spongiform encephalopathy in cattle. Vet.Rec*.* 31, 419-420.

Wenzel T., and Baumeister W. (1995). Conformational constraints in protein degradation by the 20S proteasome. Nat. Struct. Biol. 2:199-204.

Westergard L., Christensen HM., and Harris,DA. (2007). The cellular prion protein (PrP(C)): Its physiological function and role in disease. Biochim. Biophys Acta. 1772:629-44.

Westaway D., Goodman PA., Mirenda C A., McKinley, MP., Carlson,GA., & Prusiner SB. (1987). Distinct prion proteins in short and long scrapie incubation period mice. Cell. 51: 651– 662.

Wishart TM., Parson SH., Gillingwater TH. (2006). Synaptic vulnerability in neurodegenerative disease. J Neuropathol Exp Neurol. 65:733-9.

White MD., Farmer M., Mirabile I., Brandner S., Collinge J., and Mallucci,GR. (2008). Single treatment with RNAi against prion protein rescues early neuronal dysfunction and prolongs survival in mice with prion disease. PNAS. 105:10238-43

White AR., Enever P., Tayebi M., Mushens R., Linehan J., Brandner S., Anstee D., Collinge J., and Hawke S. (2003). Monoclonal antibodies inhibit prion replication and delay the development of prion disease. Nature. 422: 80-83.

Wickner RB., Edskes HK., Shewmaker F., and Nakayashiki T. (2007). Prions of fungi: inherited structures and biological roles. Nat Rev Microbiol. 5:611-618.

Wickner RB., Edskes HK., Maddelein ML., Taylor KL., and Moriyama H. (1999) Prions of yeast and fungi: Proteins as genetic material. J. Biol. Chem. 274:555–558.

Wickner RB. (1997). A new prion controls fungal cell fusion incompatibility. Proc. Natl. Acad. Sci. USA. 94:10012-10014.

Wilkinson CR., Seeger M., Hartmann-Petersen R., Stone M., Wallace M., Semple C., Gordon C. (2001). Proteins containing the UBA domain are able to bind to multi-ubiquitin chains. Nat Cell Biol. 3:939-43.

Wilkinson CR., Ferrell K., Penney M., Wallace M., Dubiel W., and Gordon C. (2000). Analysis of a gene encoding Rpn10 of the fission yeast proteasome reveals that the polyubiquitin-binding site of this subunit is ewhen Rpn12/Mts3 activity is compromised. J Biol Chem. 275:15182-92.

Wilesmith JW., Ryan JB., and Atkinson MJ. (1991). Bovine spongiform encephalopathy: epidemiological studies on the origin. Vet. Rec. 128: 199-203.

Wilesmith JW., Wells GA., Cranwell MP., and Ryan JB. (1988). Bovine spongiform encephalopathy: epidemiological studies. Vet Rec. 123: 638-644.

Will RG., Ironside JW., Zeidler M., Cousens SN., Estibeiro K., Alperovitch A., Poser S., Pocchiari,M., Hofman,A., and Smith,P.G. (1996). A new variant of Creutzfeldt-Jakob disease in the UK. Lancet. 347: 921-925.

Will RG., Matthews WB. (1982). Evidence for case-to-case transmission of Creutzfeldt-Jakob disease.J Neurol Neurosurg Psychiatry. 45:235-8.

Williams ES. (2005). Chronic wasting disease. Vet Pathol. *42*: 530-549.

Williams ES and Miller MW. (2002). Chronic wasting disease in deer and elk in North America. Rev. Sci. Tech. 21: 305-316.

Williams ES and Young S. (1980). Chronic wasting disease of captive mule deer: a spongiform encephalopathy. J Wildl. Dis. 16: 89-98.

Wilson SM., Bhattacharyya B., Rachel RA., Coppola V., Tessarollo L., Householder DB., Fletcher CF., Miller RJ., Copeland NG., Jenkins NA. (2002) Synaptic defects in ataxia mice result from a mutation in Usp14, encoding a ubiquitin-specific protease. Nature Genetics. 32: 420-425.

Windl O., Giese A., Schulz-Schaeffer W., Zerr I., Skworc K., Arendt S., Oberdieck C., Bodemer M., Poser S., and Kretzschmar HA. (1999). Molecular genetics of human prion diseases in Germany. Hum. Genet. 105: 244-252.

Wroe SJ., Pal S., Siddique D., Hyare H., Macfarlane R., Joiner S., Linehan J., Brandner S., Wadsworth J., Hewitt P., and Collinge J. (2006). Clinical presentation and pre-mortem diagnosis of variant Creutzfeldt-Jakob disease associated with blood transfusion: a case report. Lancet. 368: 2061-2067.

Wu Y., Han B.,Luo H., Shi G., Wu J. (2004). Dipeptide boronic acid, a novel proteasome inhibitor, prevents islet-allograft rejection. Transplant. 78:360-6.

Wyss-Coray T., Loike JD., Brionne TC., Lu E., Anankov R., Yan F., Silverstein SC., Husemann J. (2003) Adult mouse astrocytes degrade amyloid-beta in vitro and in situ. Nat Med 9:453–457.

Yang M., Omura S., Bonifacino JS. and Weissman AM. (1998) Novel aspects of degradation of T cell receptor subunits from the endoplasmic reticulum (ER) in T cells: importance of oligosaccharide processing, ubiquitination, and proteasome-dependent removal from ER membranes. J. Exp. Med. 187:835 – 846.

Yao T., and Cohen RE. (2002). A cryptic protease couples deubiquitination and degradation by the proteasome. Nature. 419:403-7.

Yedidia Y., Horonchik L., Tzaban S., Yanai A., and Taraboulos A. (2001). Proteasomes and ubiquitin are involved in the turnover of the wild-type prion protein. EMBO J. *20*:5383-5391.

Yoo BC., Krapfenbauer K., Cairns N., Belay G., Bajo M., Lubec G. (2002) Overexpressed protein disulfide isomerase in brains of patients with sporadic Creutzfeldt-Jakob disease. Neurosci Lett. 334: 196-200.

Yoshida T., Goldsmith SK., Morgan TE., Stone DJ., Finch CE. (1996) Transcription supports age-related increases of GFAP gene expression in the male rat brain. Neurosci Lett. 215:107-110.

Young GS., Geschwind MD., Fischbein NJ., et al. (2005). Diffusion-weighted and fluid-attenuated inversion recovery imaging in Creutzfeldt-Jakob disease: high sensitivity and specificity for diagnosis. AJNR Am J Neuroradiol. 26:1551-62.

Zanusso G., Petersen RB., Jin T., Jing Y., Kanoush R., Ferrari S., Gambetti P., and Singh N. (1999). Proteasomal degradation and N-terminal protease resistance of the codon 145 mutant prion protein. J. Biol. Chem. 274: 23396-23404.

Zerr I., Giese A., Windl O., Kropp S., Schulz-Schaeffer W., Riedemann C., Skworc K., Bodemer M., Kretzschmar HA., Poser S. (1998). Phenotypic variability in fatal familial insomnia (D178N-129M) genotype. Neurol 51: 1398-1405.

Zollner TM., Podda M., Pien, C., Elliott PJ., Kaufmann R and Boehncke WH. (2002). Proteasome inhibition reduces superantigen-mediated T cell activation and the severity of psoriasis in a SCID-hu model. J Clin Invest. 109:671-9.

9 PUBLICATION, POSTER PRESENTATIONS AND CONFERENCES

Goold R., Rabbanian S., Sutton L., Andre R., Arora P., Moonga J., Clarke AR., Schiavo G., Jat P., Collinge J., Tabrizi SJ. (2011). Rapid cell-surface prion protein conversion revealed using a novel cell system. Nat Commun. 2:281.

Published conference abstracts from this thesis

In vivo dissection of the role of ubiquitin proteasome system in the pathogenesis of prion disease. Julie Moonga, Ralph Andre, Nico Dantuma, Sebastian Brandner, John Collinge and Sarah J. Tabrizi. American Association for the Advancement of Scienc (AAAS) 117th Annual Meeting. Book of abstracts P 540. Washington D.C. February 17-21, 2011.

Early impairment in the ubiquitin proteasome system in prion disease pathogenesis.
Julie Moonga, Ralph Andre, Nico Dantuma, Sebastian Brandner, John Collinge, Sarah J. Tabrizi. Society for Neuroscience (SFN) 40th Annual Neuroscience Meeting 2010. Book of abstracts P 865.4/V8. San Diego, California, November 13-17 2010.

Impairment of the ubiqutin proteasome system occurs early in prion disease pathogenesis *in vivo*. Julie Moonga, Ralph Andre, Nico Dantuma, Sebastian Brandner, John Collinge, Sarah J. Tabrizi. European Molecular Biology Organization (EMBO), 5th IN Proteolysis Annual Meeting. Proteolysis and neurodegeneration. Book of abstracts P 66. Madrid, Spain.
May 5-11, 2010.